January 7, 2008

Modeling Dynamic System in Finance with Applications

Takashi Yamashita

PhD. Thesis

Department of Statistical Science
School of Multidisciplinary Sciences
The graduate University for Advanced Studies

2 0 0 7

This work was carried out under the supervision of

Professor Tohru Ozaki

Contents

List of Tables

List of Figures

Abstract

This thesis summarizes a dynamic modeling approach for financial topics. Practitioners often use mathematical approaches for solving financial issues using statistical models, however, these models are almost always static.

The aim of this thesis is to consider model requirements for practical dynamic models with academic and practical applications. To this end, I studied the statistical nature of actual market data. Next, I constructed models for practical financial issues and applied these to actual market data.

The main contribution of this thesis is that I point out conditions for the use of dynamic models for practitioners, and study statistical methods. One necessary condition is the time-varying volatility of an asset. The other is Poisson jumps of states. I use the conventional GARCH model and the market microstructure model for estimating the former. I devise a new model from a market microstructure model the latter. I provide the statistical methods for dealing with Poisson jumps in these models. I model typical behavior patterns of market traders and construct a delay van der Pol type price model. This model can explain price jumps.

Another contribution of the thesis is that I point out the limitations of the solving frame work used by conventional static models. For this purpose, estimating the style drift of investment managers is employed as a practical problem. The time-varying exposure of managers can be estimated by this *simple* dynamic model. The results suggest that dynamic models have significant potential for practical use. I believe that the development of a dynamic modeling approach can lead to innovative changes in finance.

1 Introduction

The purpose of investment is to increase asset value. However, asset price fluctuations can not be avoided. Unexpected changes in asset value, specially falls, have a significant negative impact. Hence the need to effectively manage assets.

Recent interest in investment management has spurred a great deal of research. Financial engineering (also known as computational finance) is the scientific tool for this. Financial engineering tries to solve financial issues using a variety of mathematical models. For the purpose of asset management, appropriate investment decisions are needed, taking into account dynamic market changes. I believe dynamic models are needed for this purpose. However, dynamic modeling has not yet entered the mainstream business world. There are a number of reasons why this is the case. Financial engineering uses mathematical models for two purposes. One purpose is pricing, the other is for decisions related to investment action. One of the best-known models for pricing is the Black-Scholes model, which is the basic theory of an option contract. An option contract is an agreement in which the buyer (holder) has the right (but not the obligation) to exercise buying or selling of an asset at a set price (strike price) on (European style option) or before (American style option) a future date (the exercise date or expiration); and the seller (writer) has the obligation to honor the terms of the contract. Since the option gives the buyer a right and the writer an obligation, the buyer pays an option premium to the writer. Empirical research has shown that the Black-Scholes model is inadequate for actual price dynamics [29, 22, 56, 55].

The primary limitation of the model is that it assumes price volatility is constant. Many researchers have suggested that the volatility of many asset prices fluctuates [44]. The pricing theory is based on the equilibrium of supply and demand in economics. This is based on the theory of arbitrage-free in financial engineering. Some assumptions are needed when using this theory for pricing. The most important is "replicability". We can replicate financial instruments through a combination of other instruments. However, it is extremely difficult to replicate the effect of time-varying volatility. This is because the price of an instrument is assumed to be dependent on its risk. The risk is the price variability in financial engineering. These time-varying volatility models are virtually impossible to use in the practical world. Thus it is difficult to use empirical research of price fluctuation in dynamic models for the purpose of pricing.

In contrast, it is comparatively easy to use time-varying volatility for the purpose of making investment decisions. This is because it does not require the "replicability". There are many kinds of investment actions, i.e. corporate finance problem, standard portfolio problem, option pricing, duration and immunization problem. In recent years, research in these fields has gained considerable attention in the financial business world. Because scientific approaches became essential in the financial field, the field now requires a sophistication of intuition that only comes from experience. One of the best-known theories for this purpose is the MPT (modern portfolio theory) based on the ideas of H. Markowitz [46], W. Sharpe [60] and J. Lintner [41]. This theory is used to solve optimum asset allocation problems. However, we can not solve issues for multi-term allocations using this theory, because it is based on a single term price model. The theory assumes that an asset price fluctuates according to normal distribution.

Many researchers have developed theories based on this assumption. Optimum

asset allocation is one of the most important issues when taking investment action. It is expensive for pension funds to keep a department of investment in their organizations. It is normally impossible for the average personal investor to make quick decisions regarding investments. Thus, they often outsource the task of investment management to qualified professionals. The optimal mix of investment managers rather than asset allocations has become the major issue in recent years. "Conventional" MPT recommends that investors mix managers of heterogeneous styles to address this problem. This strategy is called "diversification investment" in MPT. Thus, a multi regression analysis has been used to solve this problem with a non-dynamic model [61]. However, it is natural to think that the skill of rotating (the investment style under a market environment change) is one of the most important factors. Therefore, I think it is worthwhile to estimate investment style dynamically.

Financial risk management is the practice of creating economic value in a firm by using financial instruments to manage exposure to risk. It focuses on when and how to hedge capital using financial instruments to allocate costly exposure to risk. Therefore, we should evaluate the risk, which is an estimation of the volatility of assets. Static models are often used to evaluate these risks in business world. However, as mentioned above, many researchers have suggested that the asset price volatility fluctuates, thus, it is important to research a dynamic system for estimating time-varying volatility.

Price jump is an important topic for financial risk management. Asset management risk gains attraction when asset prices change abruptly. The VaR (Value at Risk), the most popular method of financial risk management, is a measure of how the market value of an asset (or a portfolio of assets) is likely to decrease over a certain time period (usually 1 day or 10 days) under usual conditions. The common VaR method assumes that an asset price fluctuates following stable log-normal distribution without price jumps. However, many financial data analyzed exhibit fat tails relative to the log-normal distribution. Many practitioners know this point empirically, therefore they often triple or double the VaR in practice [12, 18].

I believe modeling dynamic systems with jumps is extremely useful, not only for estimating time-varying volatility, but also for analyzing investment manager's styles. This is because a manager's investment actions depend on actual price fluctuations including price jumps.

For this purpose, two areas of research were undertaken. First, I surveyed some conventional studies on dynamic price models and examined the statistical nature of market price data using return distribution analysis and time series analysis. Next, I evaluated three financial issues by modeling a dynamic system based on the results of the research. The first issue is the modeling for estimating time-varying investment style drift of fund managers. The second is the modeling for estimating time-varying volatility for a stock using conventional price models. The third is the modeling of physical structures such as the trading mechanism.

I estimated and identified for the three areas with jumps using actual market data. For these steps, I used the innovation approach. The Kalman filtering technique was applied for obtaining innovations. Some continuous-time models were used as physical structure models, thus the local linearization scheme is used because actual market data is discrete in time. Following this step, modeling evolved for the same issues considering jumps in the system noise, and identified using market data. Ozaki and Iino provided a computationally simple method based on the

innovation approach for the filtering of non-linear state space models with a mixed Gaussian-Poisson type short noise [52]. Models were evaluated using the Akaike information criteria (AIC).

This work confirmed the usefulness of the dynamic model for the financial issues discussed above. It became apparent that modeling the jump-diffusion model (with Poisson noise plus Gaussian noise) was necessary. It was also evident that it is essential to consider the physical structure of such a trading mechanism.

In the Section 2 I do a survey and examine the statistical nature of actual asset price data by taking particular note of the price jump. In Section 3 I do a modeling and identification for three financial issues (i.e. estimating an investment style fluctuation, conventional modeling for estimating time-varying volatility and physical structure modeling with trading mechanism) without any jump. Finally I apply this dynamic modeling with jump for the above three issues and identify them in Section 4. Also I apply the physical modeling based on the trading mechanism of a market and try to qualitatively explain price jumps.

2 Statistical Nature of Market Data

A number of researches about statistical nature of actual asset price have been reported. The purpose of my work is building dynamic models for financial topics and applies the model to actual market data and check the performance. Hence main interests in this Section are the behavior f time series price fluctuation and existence of the price jump.

In this section, I survey and examine the statistical nature of market data by analysis of actual asset price data. For the analysis I adopted historical data of NYSE, NASDAQ and other countries listed stock exchanges. A stock exchange has a significant role to play in a capital market. A stock exchange is a corporation or mutual organization which provides facilities for stock brokers and traders, to trade company stock. To be able to trade a stock on a stock exchange, it is listed there. Stocks are traded intensively and the trading volume is recorded with the price. Thus we can obtain high objectivity data from listed markets. The price of the stock is adjusted by "stock split" and "dividends", because such corporate action changes the stock price in a discontinuous manner. Stock split refers to a corporate action that increases the number of shares in a public company. Dividends are payments made by a company to its stockholders. When a company earns a profit, it can be put the money to two uses: it can either be re-invested in the business (called retained earnings), or it can be paid to the stockholders of the company as a dividend. Capitalization events such as split or dividends fluctuate stock price discontinuously. These fluctuations are not intrinsic value changes, thus listed price must be adjusted in consideration of the capitalizations.

Some researchers report that the distribution of returns in financial markets does not follow a Gaussian distribution. Mandelbrot analyzed a relatively short time series of cotton prices and observed that returns had a Lévy stable symmetric distribution with a Pareto fat tail [43]. He also found a power-law behavior of the probability density function (pdf) of returns, with the heavy tail exceeding the Lévy stable distribution. When high frequency data became easy to obtain after 1990', many researchers have discussed return tail-behavior. Now, (ultra) high frequency data analysis is important in the field of *econophysics* [65].

FIGs.1 $\sim$ 4 show typical time series stock data, the Standard & Poor's 500 stock index (31-Dec-1998 to 12-Dec-2006), the Dow Jones stock index (31-Dec-1998 to 12-Dec-2006), TOYOTA Motors (23-Dec-1998 to 13-Dec-2006) and Microsoft Corp. (31-Dec-1998 to 12-Dec-2006) are shown in FIG. 1, FIG. 2, FIG. 3 and FIG. 4 respectively. Graph (a) indicates the daily closing log-price, (b) indicates the daily trading log-volume, (c) indicates the daily log-returns and (d) indicates the normal-quantile log-returns plot. The most distinguishing feature of these data is that stock log-prices do not fluctuate following Gaussian process. The time-varying volatility and infrequent spikes are seen graphically from the time series log-returns on graph(c). The number of return spikes of individual stocks seems to be larger than indexes such as S&P500.

Table 1 shows summary statistics of log-returns and Table 2 shows the top and bottom 5 of them. The most characteristic feature of Table 2 is that all samples have large kurtosis, compared to normal distribution case 3. This fact indicates that their distributions have greater than normal heavy-tail distributions. Given the constant and the normal distribution to log-returns, magnitudes of their spikes are too large. In the case of IBM, minimum log-return is 16.8%, which is over 8

times the standard deviation, and occurrence probability is almost 1.5×10^{-16}. It is virtually non-existent. However, as over 16% of disastrous devaluation occurs one more time in this measurement period, we cannot say with confidence that it is "first and probably the last" phenomena. Even though the spikes are not so much upward as downward, the maximum rise up is +12.3%, which is over 6 times standard deviation. In spite of the occurrence probability of almost 1×10^{-9}, we can observe a few points of nearly 12% in this observation period. These spikes are particularly noticeable in Microsoft on graph(c) in FIG.4 and other individual stocks compared to indexes. Most of the spikes occur around the same time as the company's announcement of quarterly earnings (QE). It is natural to consider that the stock price fluctuates in response to QE, because stock price reflects its prospect of revenue. Aside from the case of individual stocks, S&P500 index returns reflect macroeconomic information such as change of policy rate and mass terrors such as *Sep. 11 terrorist attacks.* However, there are situations in which there are no identifiable causes.

One cause for excess kurtosis of asset returns is a spike. However the kurtosis shows larger than 3 even though there is no spike. If return volatility fluctuates, the kurtosis is over 3. Let $X_t = \{x_1, x_2, x_3 \cdots\}$ be random variables and defined following equation,

$$x_t = \sigma_t w_t \tag{1a}$$

where $\sigma \geq 0$, $w_t \sim N(0,1), Cov[\sigma_t, w_t] = 0$. By Eq.(1a) and Jensen's inequality, we get expectation of x_t^4,

$$\begin{aligned} E[x_t^4] &= E[\sigma_t^4 w_t^4] \\ &= E[\sigma_t^4] E[w_t^4] \\ &\geq (E[\sigma_t])^2 E[w_t^4]. \end{aligned} \tag{1b}$$

And we get expectation of x_t^2 on condition σ_t^2,

$$E[x_t^2|\sigma_t^2] = E[\sigma_t^2 w_t^2|\sigma_t^2] = \sigma_t^2 E[w_t^2] = \sigma_t^2,$$

thus

$$E[\sigma_t^2] = E[E[x_t^2|\sigma_t^2]] = E[x_t^2] \tag{1c}$$

Eq.(1a) and Eq.(1c), we get

$$E[x_t^4] \geq E[\sigma_t^2]^2 E[w_t^4] = E[x_t^2]^2 E[w_t^4]. \tag{1d}$$

Both side of Eq.(1d) are divided $E[x_t^2]^2$, then

$$\begin{aligned} \frac{E[x_t^4]}{E[x_t^2]^2} &\geq \frac{E[x_t^2]^2 E[w_t^4]}{E[x_t^2]^2} \\ &= E[w_t^4] = \frac{E[w_t^4]}{E[w_t^2]^2}. \end{aligned}$$

From the definition of kurtosis, $E[w_t^4]/E[w_t^2]^2$ indicates normal distribution, that is 3, and $E[x_t^4]/E[x_t^2]^2$ indicates nonconstant volatility, thus is over 3. Therefore, I would suggest the following three hypothesizes as causes of non-Gaussian process,

A :the deviation of the price fluctuates and could become large instantaneously,

B :the price jumps infrequently by another mechanism different from the normal deviations,

C :both A and B.

Plots of log-returns in graph (c) in FIGs.1 $\sim$ 4 suggest that the hypothesis (A) is true. This is because volatilities appear to fluctuate(Compare range of log-returns the latter half to the first half).

FIG.5 shows (a):the time series chart of high frequency (5min.) price data of S&P500 and (b):semi-log probability distribution plot of this for $\tau = 5$ min, $\tau = 1$ hour and $\tau = 1$ day. The each return probabilities are normalized by their standard deviations and for comparative purpose, expected distribution for the Gaussian process and the symmetric α-Lévy process are plotted. As the results, it is reasonable to suppose that the distribution of a stock returns does not depend on observation time scale and does not obey normal distribution but Lévy distribution.

Fig.6 shows (a):autocorrelation function of log-returns of S&P500 index, τ=5min., 30min., 60min. and 1 day over the period 1-Apr-2006 to 31-Aug-2006. Graph (b) illustrates autocorrelation function of squared log-returns. From the graph (a) in FIG. 6, the autocorrelation function of log-returns is typically insignificant at lags between a few minutes and a month. On the other hand it is clear that the autocorrelation function of square log-returns decreases gradually, and is evidence for the existence of *volatility clustering*. The important point to note is that square return autocorrelation plots of $\tau = 30$ min and $\tau = 60$ min have periodical pulsing. This periodical patterns may be caused by an "U-shaped pattern" over the course of the day. McInish and Wood analyzed NYSE trading data and showed that the number of stocks traded following this pattern over the trading day [47]. Volatility is systematically higher near the open and generally just prior to the close. Trading volume has a similar pattern. The time between trades, or durations, tend to be shortest near the open and just prior to the close [23]. I would suggest that these observations may appear by the market *microstructure noise*. The market microstructure noise, a noise process, may be due to market microstructure effects such as bid-ask bounces and trading regulations such as trading units and trading intervals. Any observed intraday price does not correspond to a unique market price at a precise point in time but instead represents the underlying ideal theoretical price confounded by an error term reflecting the impact market microstructure friction, or *noise* [4]. FIG.7 shows (a) the 5 min. high frequency price chart and (b) daily closing price chart of S&P500 index over the period 31-Dec-1998 to 12-Dec-2006. Due to trading hours of stock exchange markets(Since September 30, 1985 the NYSE trading hours have been 9:30 - 16:00), the intraday-data has deficit time, thus this chart has diagonal lines from closing prices to next opening prices. During intervals between open and close, events that drive market occur, the opening prices jump from just before closing price, thus square return autocorrelation shows periodicity in the case of $\tau = 30$ min and $\tau = 60$ min.

The question we must consider here is the hypothesis (B), that is the exact mechanism of price jumps. Chuan[13] used the intra-day stock price for IBM and

obtained empirical implementation about the market microstructure noise with price jumps. The observed prices are contaminated by microstructure noises naturally arising from trading based on information and/or liquidity [57]. He suggests that frequent small jumps may be disguised as large infrequent jumps if the sampling frequency is low, a result that is intuitively plausible, and that at the 5-minute or 10-minute sampling frequency, the jump intensity can be overestimated by more than 50% if one ignores microstructure noises. Hence spikes of returns are observed in high frequency data such as 5 min.

These results mean that the trading structure is closely linked to the dynamics of price fluctuation. Admittedly jumps occur between trading intervals, nonetheless I would suggest that jumps occur independently of trading intervals. It is not reasonable to suppose trading intervals as a cause of return spikes of daily data such as FIG.1, because I couldn't confirm that the differences of pdf between $\tau = 5$ min and $\tau = 1$ day from FIG.5(b). It is natural to think that the big news which drives the market occurs depending on the *point process*. Hence I adopt hypothesis (C), and develop following argument on the assumption of the existence of price jumps.

A method so called *chart analysis* is used to predict the future stock price by finding patterns in the time series of a stock price. Chart analysis assumes that non-random price patterns and trends exist in markets, and that these patterns can be identified and exploited. Chart analysts search for current price activity resembling archetypal patterns, such as the well-known head and shoulders reversal pattern (this is a chart pattern with three peaks, the middle peak being higher than the other two, and is considered a bearish signal), Double Top/Bottom (when price peaks after a rise, and the decline that follows leads to another rise in prices to form a second peak at or about the level of the first peak, a double peak is said to have formed) and also study the graphs of mathematical "indicators" derived from price and/or volume action, such as the popular moving average.

From the graph (a) in FIGs.1 $\sim$ 4, we have some archetypal patterns about the stock price fluctuation, as follows;

1. The stock price has an upward or downward trend.
2. The stock price has a struggle period. The amplitude of the price is decreased gradually in this period.
3. After a struggle period, the price jumps suddenly.

The pattern 2 makes a wedge-like chart. This form is called "triangle chart" in chart analysis. The chart analysis is an empirical approach, which is not clearly explained theoretically. However, these behaviors of the price fluctuation are unexplained features given the perfect random walk of the price. I suggest that these features must be considered for modeling which will be studied on Subsection 4.3.2 in Section 4.

3 A Dynamic Approach to Modeling Systems for Financial topics

In this section, applying potentiality of dynamic models for finance is examined by some issues. Statistical dynamic models need some system noise, it is assumed to be Gaussian noise on the standard case. I concluded that an asset price jumps in section 2, however, in this section models are described assuming Gaussian system noise. Assuming Gaussian plus Poisson noise will be considered in next section.

In this section, three financial topics are examined. First topic is the modeling for time-varying style estimation of fund managers. Next topic is the modeling for estimating of time-varying volatility using conventional price models. Third topic is the physical structure modeling for it considering trading mechanism.

3.1 Style Analysis of Mutual Funds by Dynamic Models

Common investors use "diversification"; spreading their investments around into many assets. "Diversification" reduces the risk of portfolio. If investor diversify his asset infinitely, the portfolio becomes a "market portfolio". A market portfolio is a portfolio consisting of a weighted sum of every asset in the market, with weights in the proportions that they exist in the market. A market portfolio is only a theoretical concept, it exists in virtually. However, a market index such as the S&P500 in USA and the TOPIX in Japan (the average of whole stock market) is used as proxy. Active managers are evaluated using that market index as a performance criterion. Investors use "excess return" for evaluating an active manager's performance as it is the return in excess of a stock market index as a *benchmark*.

It has been recognized that performance of the equity fund is depending on its investment style. In finance, the most significant influence factor for equity funds is the market beta (β_M), the performance coefficient between the fund and the market portfolio. A stock that has a $\beta_M = 2$ follows the market in an overall decline or growth, but does so by a factor of 2; meaning when the market has an overall decline of 4% a stock with β_M of 2 will fall 8%. (β_M can also be negative, meaning the stock moves in the opposite direction of the market: a stock with β of -3 would decline 9% when the market goes up 3% and conversely would climb 9% if the market fell by 3%.) Investors can control β_M of the fund by mixing cash or high volatility stocks into the fund. However, it is well known that using the β_M strategy is too difficult to get high performance. This strategy requires a stock price forecasting, is ultimate dream for all investors. Whether true or not, some equity fund managers advocate keeping their funds neutral for β_M and use other non-β_M strategies. I think that it is too difficult to get reliance of the clients only using β_M strategy.

"Value" or *"growth"* styles are widely used investment styles for equity funds. We can separate between value and growth styles using fundamental analysis. Value style managers generally buy companies whose stocks appear under priced; these may include stocks that are trading at, for example, high dividend yields or low price-to-earning or price-to-book ratios. In contrast, growth style managers invest in companies that exhibit signs of above-average growth, even if the stock price appears expensive in terms of metrics such as price-to-earning or price-to-book ratios. There is another criterion in investment style management. Equity investment styles are often grouped by the size of the companies. By size we mean a company's value on the stock market: the number of outstanding stock multiplied by the stock price.

This is known as market capitalization, or cap size. *"Large"* companies tend to be less risky than *"small"* ones, however *"small"* ones can often offer more growth potential.

Therefore, a stock benchmark index is divided into these four sectors. Many consultants classify equity funds in four styles based on above idea, i.e. large value(LV), large growth(LG), small value(SV) and small growth(SG).

W. F. Sharpe proposed the simple classification method for this using linear regression model [61].

$$r_{F,t} = \alpha + \beta_{LV} r_{LV,t} + \beta_{LG} r_{LG,t} + \beta_{SV} r_{SV,t} + \beta_{SG} r_{SG,t}, \tag{2}$$

where,

$$\begin{aligned} \beta &\geq 0, \\ \sum \beta &= 1, \end{aligned}$$

where α is a constant parameter and β is the coefficient parameter represented style exposure weight. $r_{F,t}$ is the fund return and $r_{LV,t} \cdots r_{SG,t}$ are four sectors index return at t. Suffixes LV, LG, SV, and SG represent four sectors named "large value", "large growth", "small value" and "small growth" respectively. A fund's return is represented by linear coupling four sector returns and the coefficients β by Eq.(2). Four coefficients are obtained by some optimization methods under the condition $\beta \geq 0$ and $\sum \beta = 1$. This return based method is widely used because of its easy-to-use approach.

The equity style management using Sharpe's method and "diversification" is adopted by institutional investors such as pension funds. This style management is based on the assumption that fund managers fix their strategy. Some fund managers fix their strategy, however, other managers change it depending on their predictions [42]. This is because It is well known that a superiority period for each of the four strategies appears alternately. In addition to that, the factor most affecting fund performance is β_M (already mentioned above), it is difficult to build this factor into Eq.(2), because of strong possibility of *multicollinearity* problems. Four sector returns (the independent variables in Eq.(2), $r_{LV,t}$, $r_{LG,t}$ $r_{SV,t}$ and $r_{SG,t}$) are highly correlated with each other. If we add $r_{M,t}$ to Eq.(2), multicollinearity becomes more serious.

$$r_{F,t} = \alpha + \beta_M r_{M,t} + \beta_{LV} r_{LV,t} + \beta_{LG} r_{LG,t} + \beta_{SV} r_{SV,t} + \beta_{SG} r_{SG,t} \tag{3}$$

For example, following shows the VIF(Variance Inflation Factor) for four and five sectors of monthly returns of the Russell/Nomura Japan sector Indexes(described below) over the period Feb. 1989 to Apr 2007.

$$\begin{aligned} [VIF_{LV}, VIF_{LG}, VIF_{SV}, VIF_{SG}] &= [6.34, 4.29, 7.30, 5.89] \\ [VIF_{LV}, VIF_{LG}, VIF_{SV}, VIF_{SG}, \beta_M] &= [25.52, 35.13, 7.75, 6.41, 109.38] \end{aligned}$$

From this result, it may be suspected that we can not believe the solution by this five factor model. The VIFs by Eq.(2) are under 10, however the results obtained by Eq.(2) have low reliability. This is because this model assumes two constraint conditions such as $\beta \geq 0$ and $\sum \beta = 1$. The multicollinearity problem can be reduced

using the return in excess of a benchmark as dependent and independent variables. Moreover, using excess returns reduces independent variables of these models. This is because a benchmark is a sum of 4 sectors (large-value, large-growth, small-value and small-growth), and the value of each strategy is represented by the value on the straight line around zero. However, it is inappropriate for β to represent the coefficients because β has a special meaning in finance. β is a measure of a stock (or portfolio)'s volatility in relation to the rest of the market. Thus γ is used instead of β except market beta in this paper. Therefore, Eq.(3) is rewritten,

$$\begin{aligned} r_{F,t} - r_{M,t} &= \gamma_{VG}(r_{V,t} - r_{M,t}) - \gamma_{VG}(r_{G,t} - r_{M,t}) \\ &\quad + \gamma_{LS}(r_{L,t} - r_{M,t}) - \gamma_{LS}(r_{S,t} - r_{M,t}) + \beta_M r_{M,t} + \alpha \\ &= \gamma_{VG}(r_{V,t} - r_{G,t}) + \gamma_{LS}(r_{L,t} - r_{S,t}) + \beta_M r_{M,t} + \alpha \end{aligned} \tag{4}$$

Eq.(4) means that the fund excess returns are represented sum of each products of the factor and factor excess returns. The VIFs of Eq.(4) is listed below.

$$[VIF_{VG}, VIF_{LS}, VIF_{\beta_M}] = [1.07, 1.84, 1.87]$$

Most equity fund managers make their investment decisions based on the financial analysis of the firm. Therefore, they advocate that source of the excess return is based on the skill of individual stock selection [15]. It can be interpreted in the business world that α in Eq.(2) represents contribution of this individual stock selection skill. In fact, many equity funds show large contribution by α in this model. However, it may be suspected that this is divided into contributing factors of individual stock selection strategy and β_M strategy. This is because the most simple strategy to get excess return is controlling the β_M, albeit its difficulty. It is a worthwhile topic to estimate and divide them. Regarding the individual stock selection strategy, I think that this strategy depends on following three factors,

A Skill of the fund manager.

B The market environment; exactly correlative relationship between return of stocks.

C Fund size.

I think that it is difficult to build A and B into the model, then use C for this purpose. If the fund size becomes large, it is decreasingly able to concentrate investment individual stocks. This is because the number of a stock is not infinity. Therefore, it can be assumed that the exposure is in inverse proportion to the log-volume ratio of the fund for the whole market. The contribution of that strategy is represented,

$$\gamma_{I,t} \log(\frac{U_{F,t}}{U_{M,t}}), \tag{5}$$

where, $\gamma_{I,t}$ is a time-varying parameter representing individual stock selection strategy of the fund, and $U_{F,t}$ and $U_{M,t}$ are the volume of the fund and whole market respectively. Since the value obtained by this is time-varying, it is necessary to consider changing the static model into a dynamic one, because this value depends on t.

Up to now I have given the following five models. Two models are static and three models are dynamic. Each models show that the fund excess returns are represented as the sum of each product of the factor and factor excess returns. These two static models are often used for return contribution analysis. Regarding the three dynamic models, let's assume exposures β and γ have a dynamic structure driven by a random Gaussian noise in each dynamic models.

It should be noted that it is inappropriate for β to represent the coefficients for VG and LS strategies. This is because β has a special meaning in finance, that of a measure of a stock (or portfolio)'s volatility in relation to the rest of the market. Thus γ is used instead of β except market beta in this work.

model VG-LS static

$$\begin{aligned} r_{F,t} - r_{M,t} = \alpha \\ + \gamma_{VG}(r_{V,t} - r_{G,t}) \\ + \gamma_{LS}(r_{L,t} - r_{S,t}) \end{aligned} \tag{6}$$

model VG-LS dynamic

$$\begin{aligned} r_{F,t} - r_{M,t} = \gamma_{VG,t}(r_{V,t} - r_{G,t}) \\ + \gamma_{LS,t}(r_{L,t} - r_{S,t}) \end{aligned} \tag{7a}$$

where,

$$\gamma_{VG,t} = \gamma_{VG,t-1} + q_{VG}W_{VG,t} \tag{7b}$$
$$\gamma_{LS,t} = \gamma_{LS,t-1} + q_{LS}W_{LS,t} \tag{7c}$$
(7d)

model VG-LS-M static

$$\begin{aligned} r_{F,t} - r_{M,t} = \alpha \\ + \gamma_{VG}(r_{V,t} - r_{G,t}) \\ + \gamma_{LS}(r_{L,t} - r_{S,t}) \\ + \beta_M r_{M,t} \end{aligned} \tag{8}$$

model VG-LS-M dynamic

$$\begin{aligned} r_{F,t} - r_{M,t} = \gamma_{VG,t}(r_{V,t} - r_{G,t}) \\ + \gamma_{LS,t}(r_{L,t} - r_{S,t}) \\ + \beta_{M,t} r_{M,t} \end{aligned} \tag{9a}$$

where,

$$\gamma_{VG,t} = \gamma_{VG,t-1} + q_{VG}W_{VG,t} \tag{9b}$$
$$\gamma_{LS,t} = \gamma_{LS,t-1} + q_{LS}W_{LS,t} \tag{9c}$$
$$\beta_{M,t} = \beta_{M,t-1} + q_M W_{M,t} \tag{9d}$$

model VG-LS-M-I dynamic

$$\begin{aligned} r_{F,t} - r_{M,t} &= \gamma_{VG,t}(r_{V,t} - r_{G,t}) \\ &+ \gamma_{LS,t}(r_{L,t} - r_{S,t}) \\ &+ \beta_{M,t} r_{M,t} \\ &+ \gamma_{I,t} \log(U_{F,t}/U_{M,t}) \end{aligned} \tag{10a}$$

where,

$$\gamma_{VG,t} = \gamma_{VG,t-1} + q_{VG} W_{VG,t} \tag{10b}$$
$$\gamma_{LS,t} = \gamma_{LS,t-1} + q_{LS} W_{LS,t} \tag{10c}$$
$$\beta_{M,t} = \beta_{M,t-1} + q_{M} W_{M,t} \tag{10d}$$
$$\gamma_{I,t} = \gamma_{I,t-1} + q_{I} W_{I,t} \tag{10e}$$

where q of all models are a positive constant parameter and $W \sim N(0,1)$.

For example, from model (10), we obtain the following discrete time state space representation, let consider $\boldsymbol{X}_t$ is the vector of conditional mean of the state and $\boldsymbol{Z}_t$ is the observation data vector at t, we obtain

$$\boldsymbol{X}_t = \boldsymbol{F}\boldsymbol{X}_{t-1} + \boldsymbol{G}\boldsymbol{W}_t \tag{11a}$$
$$\boldsymbol{Z}_t = \boldsymbol{H}_t \boldsymbol{X}_t \tag{11b}$$

where $\boldsymbol{F} = 4 \times 4$ singular matrix,

$$\boldsymbol{X}_t = \begin{bmatrix} \gamma_{VG,t} & \gamma_{LS,t} & \beta_{M,t} & \gamma_{I,t} \end{bmatrix}^T, \tag{12}$$

$$\boldsymbol{G} = \begin{bmatrix} q_{VG} & 0 & 0 & 0 \\ 0 & q_{LS} & 0 & 0 \\ 0 & 0 & q_{M} & 0 \\ 0 & 0 & 0 & q_{I} \end{bmatrix}, \tag{13}$$

$$\boldsymbol{H_t} = \begin{bmatrix} r_{V,t} - r_{G,t} & r_{L,t} - r_{S,t} & r_{M,t} & \gamma_{I,t} \log(\frac{U_{F,t}}{U_{M,t}}) \end{bmatrix}, \tag{14}$$

and

$$\boldsymbol{Z_t} = r_{F,t} - r_{M,t}, \tag{15}$$

with $\boldsymbol{V}_t$ as prediction error variance and ν_t as prediction error at t, we obtain *log-likelihood function* of the state space model,

$$\begin{aligned} -2 \log p(z_1, \cdots z_N | \boldsymbol{\Omega}) &= \sum_{t=1}^{N} \log p(\nu_t | z_{t-1}, \cdots, z_1, \boldsymbol{\Omega}) \\ &= \sum_{t=1}^{N} (\log |\nu_t| + \nu_t^2 / V_t) + N \log 2\pi. \end{aligned} \tag{16}$$

Ω is a parameter vector of the model, V_t and ν_t are obtained by a recursive filtering technique. ν_t is called "innovations", otherwise known as prediction error, named by Wiener, who noticed that we can improve the model using innovations. Prediction error has improvement information because it is the difference between observation and estimation. Historically this theory was developed by Wold, Kolmogorov and Wiener [74, 39, 73]. Wiener proposed the solution method of the prediction problem using the spectral function of the time series, and to estimate the spectrum from the past observations so that it leads to the best predictor of future observations. Akaike [1] changed the trend of Wiener's frequency domain approach to the time domain approach for predictions in statistical time series analysis. He noticed that the spectrum estimation problem is solved by finding the best AR predictor, using a statistical criterion FPE (final prediction error). This idea, which later culminated in Akaike's Information Criterion (AIC) as a more general statistical model selection criterion, including some state space representation models, using Boltzmann's probabilistic interpretation of entropy.

Wiener proposed the idea of "whitening" in his innovation approach, and introduced the Wiener-Hopf equation, which supplies the solution method called the Wiener filter. Wiener filter minimizes the mean-square estimation error to whitening; however, it has the disadvantage that it requires infinity observation data. R. Kalman suggested a solution about it, called Kalman filter [38]. (see Appendix A) The state of the system is represented as a vector of real numbers. At each discrete time increment, a linear operator is applied to the state to generate the new state, with some noise mixed in, and optionally some information from the controls on the system if they are known. Then, another linear operator mixed with more noise generates the visible outputs from the hidden state. The Kalman filter may be regarded as analogous to the hidden Markov model, with the key difference that the hidden state variables are continuous (as opposed to being discrete in the hidden Markov model). Additionally, the hidden Markov model can represent an arbitrary distribution for the next value of the state variables, in contrast to the Gaussian noise model that is used for the Kalman filter. After the recursive filter introduction, several interesting works followed. A recursive smoother based on the Kalman filter [8], Bayesian interpretation smoother [48]. An unified explanation of Bayesian interpretation about the Kalman filter was given by Harrison et al. [28].

The optimum parameters of Ω and initial conditions may be obtained by minimizing the likelihood function Eq.(16) as follows

$$\hat{\Omega}, \hat{\boldsymbol{X}}_0, \hat{\boldsymbol{P}}_0 = arg \min_{\Omega, \boldsymbol{X}_0, \boldsymbol{P}_0} \sum_{t=1}^{N} (\log |\nu_t| + \nu_t^2 / V_t) + N \log 2\pi. \tag{17}$$

Six Japanese long life (investing over ten years) and big size (total assets over 30 billion yen) mutual funds at Apr 2007 are used to identify models(7) $\sim$ (10) by Kalman filtering technique and models(6) and (8) by multiple regression method for comparison. All these funds use the TOPIX index (most popular stock market index in Japan, tracking all domestic companies of the exchange's First Section, almost 1700 major companies in Japan) as a benchmark. However, because the Tokyo stock exchange does not make public TOPIX sector information such as value and growth, we need to use an alternative index. Therefore, the Russell/Nomura Japan sector indexes are used. This indexes are another Japanese stock market index. This is produced by Nomura Securities Co., Ltd. and the Frank Russell Company, classified

into several styles. The component parts are approximately consistent with TOPIX, with the monthly return correlation coefficient at 0.996 over the period Dec. 1998 to Apr 2007.

FIG.8 shows time series of cumulative each factor returns over the period Feb. 1994 to Nov. 2006, (a) VG, (b) LS, (c) TOPIX and (d) the market(TOPIX) volume. It is obvious that market trend of each factors shift from "bull" to "bear" or "bear" to "bull" (e.g. see the trajectory of cumulative VG factor return before and after 2000 in graph (a) in FIG.8). Thus a superior strategy swaps. FIGs.9 $\sim$ 14 show (a) Net Asset Value(NAV; price of the fund), (b) excess returns and (c) log-volume of six datasets for analysis. FJO *sim* AVO are condensation codes of the fund name. FJO, NJO, VRG, HJF, FBR and AVO represent "Fidelity Japan Open"(Jan-1996 to Apr-2007), "Nomura Japan Open"(Mar-1996 to Apr-2007), "Value Regress Open"(May-1994 to Apr-2007), "Heisei Japan Fund"(May-1994 to Apr-2007), "Fidelity Japan Growth Open"(Jul-1998 to Apr-2007) and "Active Value Open"(Mar-1996 to Apr-2007) respectively. Some funds seem to indicate a spike-like excess return(e.g. see HJF and VRG around year 2000).

Table 3 shows fitting performance, and tables 4 and 5 show estimated parameters by the static models(6),(8) analyzed by multiple regression method. From the AICs in table 3, three factors model(8) shows better fitting performance than two factors model(6) except the cases of HJF($-708.8 \rightarrow -707.0$) and AVO($-657.7 \rightarrow -655.8$). The R-square values of NJO and FBR by model(6) indicate poor fitting performance. Adding β_M factor to this model improved fitting performance(NJO:0.0771 $\rightarrow$ 0.5009, FBR:0.1540 $\rightarrow$ 0.5769) These results suggest that β_M strategy have a possibility of improvement fitting performance, however, this is depending on manager's strategy. The t-values of parameter β_M in table 5 indicate low reliability in HJF(-0.50) and AVO(-0.26), and high reliability in NJO(-10.59) and FBR(-10.20), so it is believed that these are consistent with above results.

Table 6 shows fitting performance and Tables 7,8,9 show estimated parameters by the dynamic models(7),(9),(10) analyzed by the scheme above mentioned. Compare AICs between VG-LS Model static and dynamic, Model VG-LS-M static and dynamic. The dynamic models show better fitting performance than the static models (for example; FJO by VG-LS model:$-726.8 \rightarrow -1572.3$, FJO by VG-LS-M model:$-740.7 \rightarrow 1612.9$). A comparison of AIC values from static and dynamic models strongly suggested that factors exposure of each fund are time-varying. Therefore, the static model such as Sharpe's model is insufficient for analyzing manager's investment style.

The most least AICs were obtained by model(10) in all six funds. This result suggests that the skill of individual stock selection is necessary for this style analysis. By comparing the AIC values of VRG, model (10) indicated poor improvement than model (9). It can be interpreted that this fund does not use the skill of individual stock selection as main strategy. FIGs.15 $\sim$ 20 show (a) innovations and (b) normalized innovations. Graph (c), (d), (e) and (f) indicates $\gamma_{VG,t|t-1}$, $\gamma_{LS,t|t-1}$, $\beta_{M,t|t-1}$ and $\gamma_{I,t|t-1}$ respectively. The dotted line indicates ± 1 standard deviation around each states. From graph (a) and (b), there are some spike-like innovations (e.g. see Feb-2000 in NJO and HJF), however there is no spike-like return at corresponding time in factor returns (see FIG.8). This suggests that style exposure does not fluctuate not only following Gaussian. It may have an adverse effect on estimation by Kalman filtering technique. This point is elaborated in the following sections 4.1.

Table 4 and 5 show estimated parameters by two static models. It should be noted that the static model estimate negative (short) β_M for all six fund by comparison of graph(e) in FIGs.15 $\sim$ 20. From graphs (c) and (d), γ_{VG} and γ_{LS} obviously change corresponding to the market trend. Some funds reverse their strategy(e.g. see γ_{VG} of AVO; before and after 2004). Graph (f) indicates exposure of individual stock selection γ_I. It vibrates short period around zero. This suggests that predominance of a specific stock does not sustain. Connolly et al. reported characteristic patterns in the dynamics between stocks returns and trading volume. They found substantial momentum (reversals) in consecutive week returns when the latter week has unexpectedly high (low) turnover [16]. γ_I may indicate this reversal pattern of excess return of individual stock.

FIGs.21 $\sim$ 26 show investment style maps by the dynamic model and the static model, graph (a) is the original "VGLS Sharpe map" obtained by the model (2), graph (b) is the VG-LS strategy style map by the model (10), graph (c) is the β_M-VG strategy map and graph (d) is the LS-β_M strategy map. In order to be able to compare between Sharpe method and the dynamic model (10), each exposure by the dynamic model is normalized by the standard deviation of their factor returns. The graph corresponding original Sharpe map is (b). These maps exhibit unlike investment style as compared to the Sharpe map. For example, Sharpe method indicates that NJO fund have no "small" exposure, however the dynamic model (10) indicates that this fund shift its L-S strategy into "small" . It is observed that β_M exposure of some fund fluctuates more greatly than VG-LS This could be due to the low reliability of the Sharpe method.

This static model is often used in practice to evaluate for manager's performance, however it suggests that the static model may provide an erroneous conclusion.

From above analysis, I conclude following three points;

1. The exposure of each strategy fluctuates, thus the fund manager changes his investment style.

2. It is necessary to use dynamic modeling for managers performance evaluation.

3. The investment style does not fluctuate in Gaussian, it may have an adverse effect on estimation by Kalman filtering technique.

3.2 Estimation of Time-varying Volatility by GARCH Model

The Black-Sholes model is the most widespread dynamic price model in business. This classical model is assumed to be a constant volatility independent of the asset price, and the stochastic term is driven by an additional Brownian motion. All of cumulants of the Brownian distribution beyond the second are zero, thus Black-Scholes option model was constructed with this property as crucial advantage. However, a constant volatility assumption obviously conflicts with actual market nature mentioned Section 2.

Stochastic volatility (SV) models have some random process volatility. In section 2, I showed the kurtosis of an asset returns is over 3, it was possible to be interpreted that this was due to the time-varying volatility. A natural generalization to Black-Scholes model is changing volatility some stochastic processes. For a SV model, replace the constant volatility σ; in Black-Scholes model for some stochastic process,

most common model is the following one as proposed by Merton et al. [49].

$$dS_t = (\alpha + \beta S_t)dt + \sqrt{\sigma_t} dw_t, \tag{18}$$

where $w \sim N(0, \sigma)$, σ_t is a non-negative and mean-reverting time-varying parameter as observed in the market. Hence Stein and Stein [66] consider it,

$$d\sigma_t = -a(\sigma_t - b)dt + cdw_t \tag{19}$$

In this model, the volatility is driven by Gaussian process. Volatility tends to decrease slowly after being raised suddenly, thus this property is represented with autoregression (AR) structure. The Black-Scholes price model does not explain skew and heavy tail of an asset return because its volatility is assumed constant and driven by Gaussian noise. While in contrast, this autoregressive-SV (ARSV) model describes that property by time-varying volatility even if it is driven by Gaussian noise. In order to identify the continuous time model using market data, some kind of discrete approximation method is necessary. Hull and White obtained the discretization model by Euler method. That is the most simplest approximation method [30].

$$r_t = \beta r_{t-1} + e_t \tag{20a}$$

$$e_t = \sigma_t z_t, \tag{20b}$$

where r_t is log-return of a asset at t, β is a constant parameter $[-1, 1]$, z_t is Gaussian process $\sim N(0, 1)$,and σ must above zero because volatility is non-negative, hence in order to use model(20) we square both sides of Eq.(20b) to transform a linear function using $y_t^* = \log e_t^2$ and $e_t^* = \log z_t^2$ then

$$y_t^* = \sigma_t^2 + e_t^* \tag{21}$$

We cannot use conventional maximum-likelihood approach in order to identify a model because the stochastic term e_t^* is not Gaussian but chi-square distribution. For this reason, the estimation performance by this approach is insufficient, thus this ARSV model is not mainstream trend.

The general autoregressive conditional heteroscedasticity (GARCH) model is a special case of SV models, which was introduced by Engle [23]. This is known as generalizing an autoregressive conditional heteroscedasticity (ARCH) model, is widely discussed model in the econometrics literature. These models can represent time-varying volatility as well as SV model. Basically, the SV model assumes two dimensional error processes, while the GARCH model allows for only a single dimensional error process. The ARSV model parameters are not always easy to estimate, while GARCH parameters can easily be estimated using maximum likelihood. In the limits of continuous time, the GARCH and ARSV models bear strong similarities ([50], [20]), but when fitting these models to discretely-observed, say daily data, the models look rather distinct ([25]).

For constructing a discrete time ARSV model, the Euler approximations scheme is used. Euler approximations are found using a recursive formula that uses slope information. Given by the derivative, approximated a value on a solution close to an initial point. Let assume the following a differential equation.

$$\frac{dP}{dt} = f(P)$$

Since $\frac{dP}{dt} \approx \frac{\Delta P}{\Delta t}$, one may write

$$\begin{aligned}\frac{\Delta P}{\Delta t} &= \frac{P(t_n + \Delta t) - P(t_n)}{\Delta t} \\ &= \frac{P_{n+1} - P_n}{\Delta t} \\ &\approx \frac{dP}{dt} \\ &= f(P_n)\end{aligned}$$

Solving this expression P_{n+1} we end up with a discrete equation which predicts a future value of P_n, P_{n+1}, in terms of a past value:

$$P_{n+1} = P_n + \Delta t f(P_n).$$

Now considering following continuous time ARSV model which has exponential volatility term for non-negative condition,

$$dS_t = (\alpha + \beta S_t)dt + \theta_1 \exp(\eta_t/2)dw_{1,t}, \tag{23a}$$
$$d\eta_t = \gamma\eta_t dt + \theta_2 dw_{2,t}. \tag{23b}$$

The model (23) is discretized by above Euler approximations scheme, then we obtain

$$S_t = \alpha + (1+\beta)S_{t-1} + \theta_1 \exp(\eta_{t-1}/2)w_{1,t} \tag{24a}$$
$$\eta_t = \gamma + (1+\delta)\eta_{t-1} + \theta_2 w_{2,t}, \tag{24b}$$

here $w_{1,t}$ and $w_{2,t} \sim N(0,1)$. However, it is difficult for this model to estimate directly [69]. Hence the deterministic approximation [50, 26] is adopted, thus Eq.(24b) is

$$\eta_t = \gamma + (1+\delta)\eta_{t-1} + \theta_2 \frac{\xi_{t-1}^2 - 1}{\sqrt{2}}. \tag{25}$$

ξ_t is a normalized estimation error at t.

From Eqs.(24a) and (25), we obtain the following discrete time state space representation,

$$\boldsymbol{X}_t = \boldsymbol{F}_{t-1}\boldsymbol{X}_{t-1} + \boldsymbol{G}_{t-1}\boldsymbol{W}_t \tag{26a}$$
$$\boldsymbol{Z}_t = \boldsymbol{H}\boldsymbol{X}_t. \tag{26b}$$

Let's consider logarithm as an asset price is $S_t = \log(P_t)$,

$$\boldsymbol{X}_t = \begin{bmatrix} S_t & \eta_t & 1 \end{bmatrix}^T,$$
$$\boldsymbol{F}_t = \begin{bmatrix} 1+\beta & 0 & \alpha \\ 0 & 1+\gamma & \theta_2 \frac{\xi_t^2}{\sqrt{2}} \\ 0 & 0 & 1 \end{bmatrix},$$

where ξ_t is a normalized prediction error at t,

$$\boldsymbol{G}_t = \left[\theta_1 \exp(\eta_t/2) \quad 0 \quad 0\right]^T,$$
$$\boldsymbol{W}_t = \left[w_t\right],$$
$$w \sim N(0,1), \text{and}$$
$$\boldsymbol{H}_t = \left[1 \quad 0 \quad 0\right].$$

Then, $-2LLF$ is represented the same equation as Eq. (16), thus optimum parameters of $\boldsymbol{\Omega}$ and initial conditions may be obtained by minimizing this. $\boldsymbol{\Omega}$, $\boldsymbol{V}_t$, ν_t and ξ_t are obtained by recursive Kalman filtering technique same as Subsection 3.1 (see Appendix A).

The daily time series of closing price datasets using in section 2 were analyzed by the model (24). FIGs.27 $\sim$ 36 show results by this analysis, (a) estimated first sate prediction $P_{t|t-1}$, (b) estimated second state prediction $\eta_{t|t-1}$, (c) innovations and (d) estimated volatility. The dotted line in graph(a) indicates ± 1 standard deviation around $P_{t|t-1}$.

As is evident from graph (d), this model estimates volatility clustering mentioned in section 2 (e.g. compare the volatility level between $t = 200 - 600$ and $t = 1200 - 200$ in TOYOTA). From graph (c), spike-like innovations are observed, there are corresponding to the return jumps of same data (e.g. see graph (c) in FIGs.33 around $t = 1500$), it can be clearly seen from these that this model can not predict occurrence of the jumps. Rapid rise in volatilities are observed corresponding to these jumps. From trajectory observations of returns as graph (c) in FIGs.1$\sim$4, this model estimated that volatility rose just with jumps and decreased gradually. As a result, the volatility level is observed sustaining high level soon after jump. However, it not seems to be not so high volatility level from the daily log-returns (e.g. compare the graph (c) in FIG.4 and the graph (d) in FIG.32). This results suggest that this model has the tendency to overestimate volatility immediately after the jumps. This point is elaborated in the following sections 4.2.

Table 10 shows fitting performance and estimated parameters by this model.Each results in this table will be discussed in Subsection 4.2 by comparing with GARCH-jump model.

From above analysis, I conclude following two points;

1. an asset price volatility fluctuates, and we can estimate it by the conventional dynamic model(24).

2. an asset price jumps have adverse affects on the estimation by this model.

3.3 Estimation of Time-varying Volatility by a Dynamic Market Model

The conventional price models (e.g. SV model and GARCH model) are unconsidered pricing mechanism. From the researches of Section 2, the behavior of actual price fluctuation seems to be random. *The random walk hypothesis* is a financial theory. This is a variant of the *efficient market hypothesis*, it is one of the most important hypothesis in the MPT. It holds that stock prices follow a random walk pattern and, consequently, historic prices are of no value in forecasting future prices. However, many researchers do not believe it. This hypothesis has been tested; it is still competing with one another [45, 3].

In the recent years, the Market Microstructure (MMS) (a branch of economics concerned with the functional setup of a market) have gained considerable attention in market dynamics and modeling is attempted. M. O'Hara defines market microstructure as "the study of the process and outcomes of exchanging assets under a specific set of rules. While much of economics abstracts from the mechanics of trading, microstructure theory focuses on how specific trading mechanisms affect the price formation process" ([51]).

Microstructure focuses on a market pricing mechanism. A matter related price formation directly is *price discovery* and *price formation.* Price formation for an asset is based on the supply and demand conditions. Investors have different views on the future price of an asset. They trade assets at different prices. Price discovery happens when these prices match and a trade is executed. There are different mechanisms through which the price for an asset is determined. Call auction is one of the mechanisms followed by marketplaces for determining the asset price traded in that market. In stock exchange market, continuous auction is a mechanism where the orders are checked for possible match as and when it is received and is executed at the price available on the counter side of the order book. The process of price discovery also depends on the pre-trade transparency of the order book. An opaque order book makes investors to search for price information by calling the markets to give their quotes. Thus the investors spend more time in getting exact price information from multiple market makers than actually executing the trade. This will slow down the price discovery.

The price formation of the market is one of the Walrasian auction systems. A Walrasian auction is a type of simultaneous auction where each agent calculates its demand for the good at every possible price and submits this to an auctioneer. The price is then set so that the total demands across all agents equals the total amount of the good. Thus, a Walrasian auction perfectly matches the supply and the demand. In fact, there is no "Walrasian auctioneer" in the real stock market. However, traders of stockbrokers who offer bid or ask and short term traders (i.e. Day traders) operate similarly to "Walrasian auctioneer". They play an extremely important role as supplier of "market liquidity".

Market liquidity is a investment term that references an assets ability to quickly be liquidated or converted through an action of buying or selling without causing a significant movement in the price and with minimum loss of value. A liquid asset has some or more of the following features. It can be sold 1) rapidly, 2) with minimum loss of value, 3) anytime within market hours. The essential characteristic of a liquid market is that there are ready and willing buyers and sellers at all times. A market may be considered deeply liquid if there are ready and willing buyers and sellers in large quantities. This is related to a "market depth", where sometimes orders cannot strongly influence prices. A price forecast of market player vary from hour to hour depend on their time evolution mechanism and external information. Excess demand that arise from a mismatch between supply and demand vary with it.

Liquidity is the ability to meet obligations when market player come due without incurring unacceptable losses. Transaction cost is an important parameter with liquidity in Market microstructure. Studies have shown that for a given liquidity condition. Investors executing a transaction for larger volume end up incurring larger market impact cost compared to the investor executing a transaction for smaller volume. But market impact cost is more dependent on the liquidity condition of the market rather than the size of the transaction. If the market is more liquid even a

large volume transaction can be easily executed with less market impact cost as the spreads are narrowed down in a highly liquid market.

For simplifying the market microstructure model, Bouchaud and Cont ignore the cost and heterogeneity of market players [11]. They obtain following simple equation for price change ΔS, inverse of liquidity (market depth) λ and excess demand of k trader ω_k.

$$\Delta S_t = \frac{1}{\lambda_t} \sum_{k=1}^{N} \omega_{k,t}, \tag{27}$$

where N is number of market players. According to Eq.(27), the liquidity is larger, the price change becomes smaller. Hence the inverse of liquidity (market depth) is considered as price volatility. According to this idea, Iino and Ozaki [31] construct the dynamic system of price fluctuation.

$$dS_t = \phi_t \lambda_t dt + \theta_1 e^{\frac{\lambda_t}{2}} dw_{1,t} \tag{28a}$$
$$d\phi_t = (\alpha + \beta\phi_t)dt + \theta_2 dw_{2,t} \tag{28b}$$
$$d\lambda_t = (\gamma\lambda_t)dt + \theta_3 dw_{3,t} \tag{28c}$$

The continuous time model (28) can be written as a continuous time state space representation given by

$$d\boldsymbol{x}(t) = \boldsymbol{f}(\boldsymbol{x}(t))dt + \boldsymbol{g}(\boldsymbol{x}(t))d\boldsymbol{w}(t) \tag{29a}$$
$$dz(t) = \boldsymbol{H}\boldsymbol{x}(t) + \epsilon(t), \quad \epsilon(t) \sim N(0, \sigma^2) \tag{29b}$$

where

$$\begin{aligned}
\boldsymbol{x}(t) &= \begin{bmatrix} S_t & \phi_t & \lambda_t \end{bmatrix}^T, \\
\boldsymbol{f}(\boldsymbol{x}(t)) &= \begin{bmatrix} \phi_t\lambda_t & \alpha + \beta\phi_t & \gamma\lambda_t \end{bmatrix}^T, \\
\boldsymbol{g}(\boldsymbol{x}(t)) &= \begin{bmatrix} \theta_1 e^{\frac{\lambda_t}{2}} & 0 & 0 \\ 0 & \theta_2 & 0 \\ 0 & 0 & \theta_3 \end{bmatrix}, \\
d\boldsymbol{w}(t) &= \begin{bmatrix} dw_{1,t} & dw_{2,t} & dw_{3,t} \end{bmatrix}^T, \\
\boldsymbol{H} &= \begin{bmatrix} 1 & 0 & 0 \end{bmatrix}.
\end{aligned}$$

To apply the Kalman filtering technique and innovation approach to estimate model (28), some discrete approximation have to be derived. One of the most simple discretized approximation method is the Euler approximations.

This approximation method is simple and easy to solve, however, it can not accurately approximate nonlinearity functions. When we discrete the model (28), this approximation method indicates large approximation error. To apply the innovation approach to estimate state space models, we used the "*Local linearization method*" as approximation method, which was proposed by Ozaki et al. [53] first, and developed by Shoji [64] and Jimenez [35, 36]. In this work, this method was used for estimating by model (28)(see Appendix B).

Basic Kalman filtering approach is used within the framework of the linear model. Hence nonlinear Kalman filtering scheme shall be applied for nonlinear model such

as model Eq.(28). On the basis of the linear Kalman filtering approach, local linearization method calculates the conditional mean of state estimator, the conditional variance and innovations.

From continuous state space representation such as model(29), using non linear Kalman filtering technique (see Appendix C), innovations ν_k and conditional variance $\rho(t_k)$ are obtained, then the joint conditional density of $\nu(t_k)$ can be written as

$$P(\nu(t_k)|z(t_{k-1})\dots z(t_1),\boldsymbol{\theta},\boldsymbol{x}_0) = \frac{1}{2\pi|\rho(t_k)|^{(1/2)}}\exp\left(-\frac{1}{2}\nu^T(t_k)\rho^{-1}(t_k)\nu(t_k)\right) \quad (30)$$

Here $\boldsymbol{\theta}$ is constant parameters to be estimated. Therefore, (-2) log-likelihood function of the model is given by

$$\begin{aligned}(-2)\log p(z(t_N),\dots,z(t_1)|\boldsymbol{\theta},\boldsymbol{x}_0) &= \sum_{k=1}^{N}\log p(z(t_k)|z(t_{k-1}),\dots,z(t_1),\boldsymbol{\theta},\boldsymbol{x}_0)\\ &= \sum_{k=1}^{N}\log p(\nu(t_k)|z(t_{k-1}),\dots,z(t_1),\boldsymbol{\theta},\boldsymbol{x}_0)\\ &= \sum_{k=1}^{N}\{\log|\rho(t_k)| + \nu^T(t_k)\rho^{-1}(t_k)\nu(t_k)\} + N\log 2\pi.\end{aligned} \quad (31)$$

Based on the estimated innovation $\nu(\hat{t}_k)$ and its covariance $\rho(\hat{t}_k)$ with respect to the given parameters $\boldsymbol{\theta}$ and initial conditions, the optimum parameters and initial conditions may be obtained by minimizing the likelihood function Eq.(31) as follows,

$$\{\hat{\boldsymbol{\theta}},\hat{\boldsymbol{x}}_0,\hat{Q}_0\} = arg\min_{\theta,x_0,Q_0}\sum_{k=1}^{N}\{\log|\hat{\rho}(t_k)| + \hat{\nu}^T(t_k)\hat{\rho}^{-1}(t_k)\hat{\nu}(t_k)\} + N\log 2\pi, \quad (32)$$

where $Q_0 = Q(t_0)$ is also regarded as parameters to be estimated.

The model (28) was difficult to solve because of its nonlinearity and complexity . In general, nonlinear optimization problems depend on initial parameters. Setting inappropriate initial values have an optimizer put local-optimum solution. We must search acceptable approximation by trial and error approach with comparing LLF and behavior of error of the states. I used the "FMINCON" program (nonlinear optimization function) in MATLAB to estimate parameters. It is extremely-difficult to search the global optimum solution with this tool. In this work, I tried to solve about 10 datasets analyzed in section (2) over a prolonged period of time. I applied some functional techniques to the program, however, I had not obtained satisfying results. To easy to estimate, I reduced the parameter α in Eq.(28b), it means the trend of excess demand. Therefore, I obtained acceptable approximate solutions as best of a bad lot, S&P500 and TOYOTA.

Table 11 shows fitting performance and estimated parameters by this model. The AIC values obtained by model (28) present poor fitting performance by comparison with the GARCH model (24) in Table 10 (S& P500:-6323.4 v.s. -6200, TOYOTA:-5294.9 v.s. -5221.7). FIGs.37 and 38 show (a) estimated first state prediction $S_{t|t-1}$, (b) second state prediction $\phi_{t|t-1}$, (c) third state prediction $\lambda_{t|t-1}$, (d) innovations and (e) estimated volatility. The error of $\phi_{t|t-1}$ and $\lambda_{t|t-1}$ in FIG.37

are larger than fluctuations size of $\phi_{t|t-1}$ and $\lambda_{t|t-1}$. This means that estimated $\phi_{t|t-1}$ and $\lambda_{t|t-1}$ possess poor reliability.

From the standpoint of modeling procedure, it is reasonable to suppose that MMS model are one of stochastic volatility models, were evolved using the concepts of market microstructure. However, I obtained under fitting results compared to GARCH in Subsection 3.2. These results may suggest that GARCH model (ignored considerations of market mechanism) superior to more complex model such as this MMS model. Whereas I think that there are another two reasons for these poor results;

i) model (28) is unsuitable for describing of a stock price fluctuation.

ii) insufficient optimization.

The presumption [i] means that it is difficult for a stock price to analyze by this MMS model. It is well known that a stock price indicates an uncertainty trend relative to a currency rate. This is because an exchange rate such as Yen/Dollar fluctuates reflecting "national monetary policy" strongly. In contrast, a stock market has much more variety than currency. Thus disproportion between supply and demand does not tend to enlarge, and it is eliminated at short times in the high liquidity market. The fact suggests that it is harder to estimate an excess demand of a stock than that of a currency. Other models may be constructed for estimating excess demand of a stock.

The presumption [ii] means the lack of optimization skill. It should be mentioned here that I obtained another optimization results which have more large LLF than in table 11. Although I did not adopt these result because I decided that they possessed lower reliability. In order to estimate parameters of this model, the set of parameters are searched along with the objective function $-2LLF$ to be maximized, using searching calculator. In the case of nonlinear problems such as model (28), many set of initial parameters must be tested because nonlinear problems' results strongly depend on initial parameters. In my work, it was observed that high propensity to turn up the AR parameter of excess demand β, turn down the system noise parameter θ_2. The maximum LLF was obtained when the order of β is 10^3. This result suggested rising up over fitting. In order to eliminate the difficulty, I represented β as hyperbolic tangent. This functional technique gives numerical constraint $[-1, 1]$ on β. This over fitting was able to known by the behavior of prediction error. I rejected the result which is larger than size of fluctuation of ϕ. I think that it was likely to be caused by the presumption [ii].

From above analysis, I conclude following two points;

1. considering physical structure of a trading design in a market, i.e. market microstructure, makes dynamic modeling for asset price fluctuation.

2. this MMS model has technology problem regarding the estimation.

4 A Dynamic Modeling Approach to Financial Topics with Jumps

As mentioned in section 2, I suggested that an asset price jumps and its volatility fluctuate. The dynamic modeling for two financial topics, style analysis of mutual fund and estimating time-varying volatility of a stock price are considered in section 3. These approaches use a classical model with Gaussian system noise. These conventional models can not predict the jumps occurrence, thus it is likely that the jumps deteriorate fitting performance. Likewise, this deterioration appears in style analysis mentioned in Subsection 3.1. In this section, the models with jump are investigated.

4.1 Style Analysis of Mutual Funds by Dynamic Models with Jumps

Some spike-like innovations (these are prediction errors obtained by dynamic models) were observed in Subsection 3.1. These are believed to be due to the changeover of investment strategy of the fund, that is corresponding with changing positive and negative sign of style exposure. This is because dynamically changing of investment strategy is one of the most important skill of fund managers.

The selection of investment strategies for getting excess return is depend on the fund manager. It is obvious that the "bull' or "bear" market trends of each factors return, V-G L-S and β_M change (see FIG.8). Thus a superior strategy swaps, as mentioned in Subsection 3.1. Change over the trend cycle is roughly one year $\sim$ multiple years. Thus it is natural to think that changing frequency of main strategies are low. This suggests that a manager shifts the exposure infrequently; however the amount of change is large. Therefore, the exposure fluctuates following Gaussian plus Poisson process. In order to improve the fitting performance for this style analysis, it is necessary for the modeling to consider building into jump diffusion process.

The model 10 is assumed to four investment strategies. Considering addition of Poisson noise, assuming Poisson rate λ is sufficient low, into each states, we obtain following model;

$$\begin{aligned} r_{F,t} - r_{M,t} = \gamma_{VG,t}(r_{V,t} - r_{G,t}) + \gamma_{LS,t}(r_{L,t} - r_{S,t}) \\ + \beta_{M,t} r_{M,t} + \gamma_{I,t} \log(\frac{U_{F,t}}{U_{M,t}}) \end{aligned} \tag{33a}$$

where

$$\gamma_{VG,t} = \gamma_{VG,t-1} + q_{VG} W_{VG,t} + \kappa_{VG,t} \iota_{\kappa_{VG,t}}, \tag{33b}$$

$$\gamma_{LS,t} = \gamma_{LS,t-1} + q_{LS} W_{LS,t} + \kappa_{LS,t} \iota_{\kappa_{LS,t}}, \tag{33c}$$

$$\beta_{M,t} = \beta_{M,t-1} + q_M W_{M,t} + \kappa_{M,t} \iota_{\kappa_{M,t}}, \tag{33d}$$

$$\gamma_{I,t} = \gamma_{I,t-1} + q_I W_{I,t} + \kappa_{I,t} \iota_{\kappa_{I,t}}, \tag{33e}$$

where $q \geq 0$, $\kappa_t \sim N(0, \delta_\kappa^2)$ and $E(\iota_{\kappa,t}) = \lambda$. We can not identify using this model by conventional Kalman filtering technique as mentioned in section 3. This is

because model (33) does not have Gaussian system noise. Thus some jump detection techniques is required.

One of another method for estimating parameters in jump-diffusion model is based on Markov-chain Monte Carlo (MCMC) simulation [24]. This method can estimate under various stochastic processes, such as Gaussian plus Poisson. However, it should be impractical approach. This is because it requires hungry-computation power. On my work, other technique was applied. The basic idea of this technique is based on Ozaki[52]. It is assuming that the system noise is mixed Gaussian and compound Poisson processes. To get the maximum likelihood of the model with shot noise in N observation data, 2^N possible cases likelihood function must been calculate. This is because the observations z_s $(s > t)$ depend on the past states M_t, however the effect decreases exponentially for its Markov property. Hence they assumed that we ignore the effect of M_t with z_s $(s > t)$, proposed the detection method(see Appendix D).

The combination number of states with Poisson jump in the model 33 is 18, as following;

$$ {}_4C_0 + {}_4C_1 + {}_4C_2 + {}_4C_3 + {}_4C_4 = 18. $$

There are the 18 models to estimate. A large amount of computation power was required to estimate by the 18 models. Thus I picked only 4 models which have three Gaussian system noises and one Gaussian and Poisson system noise. Then I calculated by these 4 models, and adopted the maximum LLF model as final result from these.

Ozaki and Iino reported that the sensitivity of jump detection strongly depends on the jump probability ϑ in Appendix D [52]. If ϑ is turned into vary parameters, there is no end in optimization calculation. Therefor I assumed jump probability ϑ is 0.01 constant parameter.

Tables 12and 13 show fitting performance and estimated parameters by the model (33). "Strategy" in table 12 indicates the state which shows the best fitting (lowest AIC) model with Poisson jumps as system noise. The "improvement" in this table indicates comparison the AIC value with the model (10) in Subsection 3.1. These values suggest that the jump diffusion model is not always effective in this case (FJO:+18, AVO:+0.1). However, other funds indicated improvement in this scheme. Each parameters q_M, q_{VG}, q_{LS} and q_I representing constant volatility, estimated by this model, are smaller than estimated by classical Gaussian noise model (10). The estimated fluctuation of each time-varying exposures were smaller than the results obtained by Gaussian noise model. These suggested that detecting changeover of each strategies improve the fitting performance excepting at that time.

The graph(a) and (b) in FIGs.39 $\sim$ 44 show (a) innovations and (b) normalized innovations by this system. "D" indicates detecting points by the jump detection scheme in graph(b). This jump detecting model is effectively for estimation. For example, compare the graph (b) in FIG.16 to the graph (b) in FIG.40. We can observe more Gaussian-like normalized innovations by detecting jumps. Graph (c), (d), (e) and (f) indicates $\gamma_{VG,t|t-1}$, $\gamma_{LS,t|t-1}$, $\beta_{M,t|t-1}$ and $\gamma_{I,t|t-1}$ respectively. The dotted line indicates ± 1 standard deviation around each states, estimated states obtained by using the model (10) are plotted by red solid line for comparison. The model with jump estimated about the same results comparing with no-jump detection model. However, some results indicated relatively-large differences (see graph (d) in NJO

around 1997 and graph (c) in VRG around 1997).

The graph(e) and (f) in FIGs.45 $\sim$ 50 show cumulative returns of each strategies by this model and model(8). Many practitioners calculate cumulative returns for evaluating managers' investment skill using static models. For example, an investor measures investment skill of FJO fund from each strategies cumulative return (see graph (f) in FIG.21). He determines that the best skill of this fund was individual stock selection strategy and this fund did not use other strategies. However, from comparison with the results by obtained between dynamic model (graph(e)) and static model(graph (f)), a significant difference between two models. FJO fund used LS strategy as well as individual stock selection strategy, and it applied good performances. Therefore, we must not ignore the skill of this strategy. Comparing fitting performance between the static model (8) and this dynamic model (33) (see table 3 and 12), I conclude that conventional performance analysis for funds return by static models provide less-accurate decisions. I recommend that practitioners should use dynamic models instead of conventional static models for performance analysis.

From above analysis, I conclude following two point;

1. the investment style change suddenly, the jump detection technique is effective for estimating this dynamic model with jump.

2. practitioners should use the dynamic models for measuring investment skill of funds.

4.2 Estimation of Time-varying Volatility by GARCH Model with Jumps

In Section 2, I pointed out that the kurtosis of a stock returns has over 3. I suggested that one of the cause of this is time-varying volatility and the distribution not depending on Gaussian but α-Lévy process. Regarding former phenomenon, in Subsection 3.2, the time-varying volatility was estimated by the conventional GARCH model. α-stable model is well known for considering latter phenomenon, which follows α-Lévy noise process. This model is assumed a constant volatility independent of the asset price as well as Black-Scholes model.

α-stable price model is described by the following equation;

$$dS_t = (\alpha + \beta S_t)dt + \sigma dL_t, \tag{34}$$

where α, β and σ are constant parameters, and dL_t is α-stable process. This model was proposed by Mandelbrot who determined volatility clustering of the stock price fluctuation [43]. He adopted Lévy skew process in order to explain heavy-tail nature of asset price fluctuations. Stable processes owe their importance in both theory and practice to the generalization of the Central Limit Theorem to random variables without second order moments and the concomitant self-similarity of the stable family. An important property of Lévy process is the role that they play in the generalized central limit theorem. The central limit theorem states that the sum of a number of random variables with finite variances, it will tend to a normal distribution as the number of variables grows. A generalization due to Gnedenko and Kolmogorov [27] states that the sum of a number of random variables with power-law tail distributions will tend to a stable Lévy distribution. The stable process has the

important property of stability: If a number of independent identically distributed (i.i.d.) random variables have a stable distribution, then a linear combination of these variables will have the same distribution. Since the Gaussian process, the Cauchy process, and the Lévy process all have the above property. It follows that they are special cases of the stable process. The characteristic function of its process is defined as

$$\hat{\mu}(z) = \exp[i\gamma z - c|z|^{\alpha}\{1 - i\beta[sign(z)]\omega(z,\alpha)\}, \tag{35}$$

where,

$$\omega(z,\alpha) = \begin{cases} \tan\frac{\pi\alpha}{2} & \text{if } \alpha \neq 1\ , \\ \frac{2}{\pi}\log|z| & \text{if } \alpha = 1. \end{cases} \tag{36}$$

A Lévy skew stable distribution is specified by scale c, exponent α, shift μ and skewness parameter β. The skewness parameter must lie in the range $[-1, 1]$ and when it is zero, the distribution is symmetric and is referred to as a Lévy symmetric α-stable distribution. This "heavy tail" behavior causes the variance of Lévy distributions to be infinite for all $\alpha < 2$. Heavy tail behavior of this distribution depends on α.

- For $\alpha = 2$ the distribution reduces to a Gaussian distribution with variance $\sigma^2 = 2c$ and finite mean.

- For $1 < \alpha < 2$ the mean is finite but the variance is infinite.

- For $\alpha = 1$ and $\beta = 0$ the distribution reduces to a Cauchy distribution with infinite mean and variance.

- For $0 < \alpha < 1$ the mean and variance are infinite.

Eq.(35) is represented following simple equation by assuming symmetrical distributions ($\beta = 0$).

$$\hat{\mu}(z) = \exp[i\gamma z - c|z|^{\alpha}]. \tag{37}$$

This probability distribution function is defined by the Fourier transform of its characteristic function Eq.(37).

$$\mu_{\alpha} = \frac{1}{2\pi} Re[\int_{-\infty}^{\infty} \hat{\mu}_{\alpha} e^{-izx} dz].$$

For $\mu_\alpha(z) = e^{-a_\alpha|z|^\alpha} = \sum_{n=0}^{\infty} \frac{(-1)^n}{n!}$,

$$\begin{aligned}
\mu_\alpha(x) &= \frac{1}{2\pi}\sum_{n=0}^{\infty}\frac{(-1)^n}{n!}a_\alpha^n Re[\int_{-\infty}^{\infty}|z|^{n\alpha}e^{-izx}dz] \\
&= \frac{1}{2\pi}\sum_{n=0}^{\infty}\frac{(-1)^n}{n!}a_\alpha^n\int_{-\infty}^{\infty}|z|^{n\alpha}\cos zxdz \\
&= \frac{1}{\pi}\sum_{n=0}^{\infty}\frac{(-1)^n}{n!}a_\alpha^n\sum_{n=0}^{\infty}\frac{(-1)^n}{n!}a_\alpha^n \\
&= \frac{1}{\pi}\sum_{n=1}^{\infty}\frac{(-1)^{n+1}}{n!}a_\alpha^n\frac{\Gamma(n\alpha+1)}{x^{n\alpha+1}}\sin\frac{n\alpha}{2}\pi. \qquad (38)
\end{aligned}$$

Here, when x sufficiently large we can ignore the terms over $n = 2$ and obtain

$$\mu_\alpha(x) \propto x^{-1-\alpha} \qquad (39)$$

Eq.(39) represents that stable distribution following a power law.

A power law is any polynomial relationship that exhibits the property of scale invariance. This is a feature of objects that do not change if length scales are multiplied by a common factor. We can see this feature on graph(b) in FIG.5. This is consistent with multi-scale property that is advocated by Mandelbrot [44]. This model can explain that an asset price fluctuates with jumps. Lévy distribution is decomposed compound Poisson and Gaussian process by Lévy-Ito decomposition. Consider a triplet (b, c, ν) where $b \in \mathbb{R}$, $c \in \mathbb{R}_+$ and ν is a measure satisfying $\nu(0) = 0$ and $\int_{\mathbb{R}}(1 \wedge |x|^2)\nu(dx) < \infty$. Then, there exists a probability space $(\Omega, \mathcal{F}, P)$ on which four independent Lévy processes exist, $L^{(1)}$, $L^{(2)}$, $L^{(3)}$ and $L^{(4)}$, where $L^{(1)}$ is a constant drift, $L^{(2)}$ is a Brownian motion, $L^{(3)}$ is a compound Poisson process and $L^{(4)}$ is a square integrable pure jump martingale. countable number of jumps on each finite time interval of magnitude less that 1. Taking $L = L^{(1)} + L^{(2)} + L^{(3)} + L^{(4)}$, we have that there exists a probability space on which a Lévy process $L = (L_t)_{t\geq 0}$ with characteristic exponent as

$$\psi = iub - \frac{u^2c}{2} + \int_{\mathbb{R}}(e^{iux} - 1 - iux\mathbf{1}_{|x|<1})\nu(dx), \qquad (40)$$

for all $u \in \mathbb{R}$, is defined. Split the Lévy exponent Eq.(40) into four parts

$$\psi = \psi^{(1)} + \psi^{(2)} + \psi^{(3)} + \psi^{(4)} \qquad (41)$$

where

$$\begin{aligned}
\psi^{(1)}(u) &= iub, \\
\psi^{(2)}(u) &= \frac{u^2c}{2}, \\
\psi^{(3)}(u) &= \int_{|x|\geq 1}(e^{iux} - 1)\nu(dx), \\
\psi^{(4)}(u) &= \int_{|x|<1}(e^{iux} - 1 - iux)\nu(dx).
\end{aligned}$$

The first part corresponds to a linear drift with parameter b, the second one to a Brownian motion with coefficient c and the third part to a compound Poisson process with arrival rate $\lambda := \nu(\mathbb{R}\,(-1,1))$ and jump magnitude $F(dx) := \dfrac{\nu(dx)}{\nu(\mathbb{R}(-1,1))}\mathbf{1}_{|x|\geq 1}$.

As the result, Lévy process is able to be described as sum of Gaussian process and compound Poisson process. This property is a big advantage, because this model can explain heavy-tail behavior of return distribution and price jumps. It is natural to think that considering Poisson jump process into the conventional the ARSV model discussed in Subsection 3.2.

Iino and Ozaki studied based on this idea. Thy detected jumps from price fluctuations using maximum likelihood method[31]. They modified the model (24) into following,

$$S_t = \alpha + (1+\beta)S_{t-1} + \theta_1 \exp(\eta_{t-1}/2)w_{1,t} + \zeta_t q_t \tag{42a}$$
$$\eta_t = \gamma + (1+\delta)\eta_{t-1} + \theta_2 w_{2,t}, \tag{42b}$$

where $q_{1,t}$ is a Poisson process with intensity ι, and
$zeta_t$ is the size of the jump at t. From model.(42), we obtain the discrete time state space representation described in (26). Let consider logarithm an asset price is $S_k = log(P_k)$ at k,

$$\boldsymbol{X}_t = \begin{bmatrix} S_t & \eta_t & 1 \end{bmatrix}^T,$$
$$\boldsymbol{F}_t = \begin{bmatrix} 1+\beta & 0 & \alpha \\ 0 & 1+\gamma & \theta_2 \frac{\xi_t^2}{\sqrt{2}} \\ 0 & 0 & 1 \end{bmatrix},$$

where ξ_k is a normalized innovation at k,

$$\boldsymbol{G}_t = \begin{bmatrix} \theta_1 \exp((\eta_t + \kappa_t \iota_{\kappa,t})/2) & 0 & 0 \end{bmatrix}^T,$$
$$\boldsymbol{W}_t = \begin{bmatrix} w_t \end{bmatrix},$$
$w \sim N(0,1)$, and
$$\boldsymbol{H}_t = \begin{bmatrix} 1 & 0 & 0 \end{bmatrix}.$$

where, $\kappa_t \sim N(0, \delta_\kappa^2)$ and $\iota_{\kappa,t}$ is a Bernoulli number with $E(\iota_{\kappa,t}) = \lambda$.

Then, $-2LLF$ is represented the same equation as Eq. (16), thus optimum parameters of $\boldsymbol{\Omega}$ and initial conditions may be obtained by minimizing this. $\boldsymbol{\Omega}$, $\boldsymbol{V}_t$, ν_t and ξ_t are obtained by recursive Kalman filtering technique, see Appendix A. For using that model, separating Poisson jumps from Lévy noise is necessary. I used the jump detection scheme discussed in Subsection 4.1. The daily time series of closing price datasets discussed in Subsection 4.1 were analyzed. For reducing difficulties in estimation, I assumed jump probability ϑ is 0.03 constant parameter.

Table 14 shows fitting performance and estimated parameters by this model. The "improvement" in this table indicates comparison with the model(24) without jumps in Subsection 3.1. From comparison the results by two models, in spite of increasing number of parameters, all AIC values obtained by the model(42) with jumps are lower than the model(42) without jumps. Improvement degree of the AIC value tends to be larger in individual stocks than indexes (e.g. compare -21.3 of S&P500 as index to -133.4 of Microsoft as individual stock).

FIGs.51 $\sim$ 60 show results by this analysis, (a) estimated first sate $P_{t|t-1}$, (b) estimated second state $\eta_{t|t-1}$, (c) innovations and (d) conditional variances. "D" indicates detecting points by the jump detection scheme in graph(d). Compare the innovations (graph (c)) obtained by with jumps and without jumps model. We observe small differences between two models. This is because both models can not predict Poisson price jumps.

We see significant spikes in graph(d) (e.g. see three spikes between $t = 300 - 500$ of Microsoft in FIG.58), they are corresponding to the detection points of price jumps. Normalized innovation is obtained by normalized by corresponding conditional variance. FIGs.61 $\sim$ 70 show (a) histograms of normalized innovations obtained by the model (24) and (b) obtained by the jump detection model (42). The tails of graph (b) is thinner and the kurtosis seems to be smaller than that of (a). Compare the graph (a) to (b) in FIG.68). Some outliers (indicating arrows) are observed in graph (a). On the other hand, few outliers are observed in graph (b), and shape of the histogram become to like a normal distribution. This result shows that jump detection scheme have an efficacy for whitening normalized innovations. Graph (c) indicates estimated volatility by two models and (d) indicates the time series chart of daily log-returns for visual recognition. "D" indicates detecting points by the jump detection scheme in graph(d). Note that I eliminated the volatility spikes detecting this scheme from graph (c). This is because volatility spikes are too large to plot eye-friendly scale.

From the time series chart of (d) for S&P500 as shown in FIG.61 and log-returns (see graph (d) in FIG.61), the volatility seems to be relatively high in the first half and low in the second half. The solid lines indicate the volatility estimated by the jump detection model(42), and the dotted lines indicate it estimated by the model(24) without jump detection. Two lines show slight differences, however, the dotted line volatility is higher than solid line volatility at "b". This is because the price jump at "α" was identified as a volatility uprush by the model(24). It is seen from the graph(d) that the most volatile period is roughly in the $t = 900 - 1100$ range. By comparing the volatility level at that time, it seems reasonable that the volatility at "b" is more possible than at "a". In the case of Dow Jones as shown in FIG.62, the same overestimation occurred (see "a" and "α" on graph (c) and (d)). From the graph(c) in FIG.63, the model(24) estimated two peaks of volatility at "a" and "b" in the observations for Nikkei225. However, it seems to be natural that the most volatile range was $t = 600 - 1000$ by graph (d). Same overestimation by a price jump occurred in this case. The important noting point is that the return jump size of "α". The volatility peak corresponding "b" is not so large like as "β" corresponding "a". The difference between "a" and "b" (observed between the volatility by two models) is the pre-state of the volatility. It seems to be most low volatility around "β" all over the period. This observation leads to my presumption that the degree of overestimation depends on the pre-state of the volatility. This is because this GARCH model uses its estimation error at $t-1$ as the system noise of the volatility at t.

We can see the large overestimation for Seoul composite on graph (c) in FIG.64. The model (24) estimated high volatility around $t = 700$ (See "a"). However, we can not so volatile returns around $t = 700$ except for the return spike at "α". I would suggest that this result is consistent with above reason.

We can not obviously see differences between the dotted line and solid one for TOYOTA from the graph(c) in FIG.65. Similarity patterns were observed in Wal-

Mart; the reason for these may be that there are few jumps, which are infrequent and large in size. In the case of IBM, we can observe some infrequent and large jump from graph(d) in FIG.66, thus articulate differences appear between the trajectories by two models. The similarity of estimation pattern is observed at Pfizer and Microsoft (see FIGs.67 and 68), and the model(24) could not distinguish minute fluctuations of volatility. From the graph (c) in FIG.67, two volatility peaks estimated by model (24) decrease "a" to "b" and "c" to "d" by jump detections at "α" and "β" respectively. The model(42) did not detect the spike at "γ", thus it estimated the volatility uprush indicated by "e". The exact cause is not well understood. This could be due to the large of jump probability (ϑ was assumed 0.03).

A little differences are observed between dotted lines (model(24)) and solid lines (model(42)) in graph(c) in FIG.69 like as the case of TOYOTA. We can not observe outstanding jumps in these cases. In contrast, we can observe significant difference for the volatility around $t = 1500 - 1600$ on graph (c) in FIG.70. The model (24) estimated highest volatility "a" corresponding with the return spike at "α". However, we can not see so volatile returns around $t = 1500 - 1600$ except for the return spikes at "α" and "β". The model (42) detected these return spikes, and estimated the low volatility (compare dotted line "a" to solid line "b"). We observe the return spike around $t = 500$ as well as at "α". However, the model(24) did not over estimate the volatility as well as "a". The returns pre "α" were more volatile than that around $t = 500$. This observation suggests that the cause of this is same as the case of Nikkei225.

The following can be understood from above results:

(1) This GARCH model overestimates the volatility because of a price jump without its detection.

(2) The degree of overestimation depends on pre-state of the volatility, if it is low, the GRACH model overestimate significantly without jump detection.

4.3 Physical Dynamic Models for Market

4.3.1 Heterogeneous Market Players Market Microstructure Model

The model (28) is a simplified system. Original market microstructure model has various assumptions. The "Information asymmetry" assumption is one of them. It means heterogeneity of market players. Investment decisions depend on information. This is an important concept in the market microstructure theory. Information plays a significant role in determining the behavior and strategies that market players adopt to create or take liquidity. A better-informed trader is more likely to mitigate the risk involved in the trading compared to less informed trader. Although the Efficient Market Hypothesis (EMH) that is one of the important assumptions in MPT, assumes that market is anonymous and all the players in the market are equally informed about the trading. According to this idea, the market players are assumed to be homogeneous.

Market players are divided into following three types in market microstructure.

1. More informed traders: They access to the information, which affects the market value of the asset and make decision of investment. They tend to take the liquidity from the market by executing trades at the available prices, as they know that the spread will narrow down once the information is available

publicly. Hence better-informed traders tend to place more market orders before the information is actually broadcasted to the market as a whole.

2. Less informed traders: They don't have access to the information, which affects the market value of the asset, tend to adopt a different trading strategy compared to informed traders. These traders are exposed to more risk in the initial hours of trading, as the spread is wider in the market. These traders tend to place more limit orders and on the same side of the book as placing a market order or a limit order to pick up the quantity on the counter side will result in a trade at adverse price.

3. Liquidity traders: These traders represent the trading desk of an institutional investor who has given them a target of stocks to buy/sell during the trading session at best price possible for the day. These traders are open to more risk in the initial trading hours as the spread is too high and any trade executed during the initial hours of trading may result in adverse price as a result of which the average traded price of these traders at the end of the trading session may not be close to the day s average trade price.

The Walrasian auctioneer is the hypothetical auctioneer that matches supply and demand in a market of "perfect" competition [51]. The auctioneer provides for the features of perfect competition. "Perfect" in this definition means full information and no transaction costs. The process is relating to finding the market-clearing price for all commodities and giving rise to general equilibrium. There is no Walrasian auctioneer in real market, traders of stockbroker called "market maker" play a role similar to the auctioneer. Market makers quote both a buy and a sell price in a stock, hoping to make a profit on the turn or the bid/offer spread. For this reason, they are not interested in long-term fundamental information of the stock but short-term supply and demand on it. Market makers are distributors of stocks; they can't hold stocks too long. Day traders (who buy and sell stocks within the same trading day) will usually close their positions before the market close of the trading day. Thus they play a role similar to stock distributors. They withdraw from the market when it becomes illiquidity condition, in many cases it is market crush. This investment strategy of them makes the market more volatile.

According to this idea, Shiller et al. [62, 40] called this volatility as "excessive volatility". In 1981, Shiller compared actual stock price behavior over a century to the present discounted value of dividends. Then he found actual stock price is too volatile than the present value of them. Subsequent dividends at each point in time are not known and its terminal price contains some risk. Therefore, the actual price may fluctuate. However, that explanation would be insufficient, by orders of magnitude, to explain the degree of fluctuation of the actual price. Dumas et al. [21] advocated that volatility was decomposed to "excessive volatility" and "fundamental volatility". Dumas noticed that one of the possible occasions of assuming the excessive volatility is irrational traders in the market. "Irrational" does not mean a random strategy. It means an "atheoretical" strategy, does not based on forecasting fundamentals information.

Rational investors make their investment decision based on fundamental views of the stock. They are called "fundamentalists" or "informed traders". Other investors are called "noise trader". Noise traders do not have any specific information of the stock.

There are many criticisms about the EMH described above. "Stiglitz Paradox" is one of them. Based on the EMH, if markets are perfectly efficient, the return to gathering information is nil, in which case there would be little reason to trade and markets would eventually collapse [67]. Given the EMH, fundamentalists will not enter a market without noises, because it is impossible to profit from trading. They need the noise traders to "hide" their trades and by trading on their private information. Noise traders play an important role in the market as liquidity suppliers. Financial authorities of each country (which emphasize the market stability for sustainable growth) have a vested interest with them as occasion of market crush. To estimate excessive volatility is highly significant from the perspective of this point for them. I tried to customize the MMS model in order to estimate the excessive volatility.

From above idea, it is natural to think that there is different strategy between noise traders and fundamentalists. Fundamentalists take an interest in the corporate performance of the target stock, information of this fluctuate. There is no observable variables about them, however, it is natural to think that news related with them happen randomly and following on Gaussian process. On the contrast, noise traders take an interest in supply and demand. There are no observable variable represented fluctuation of supply and demand.However, it is natural to think that trading volume reflects fluctuation of supply and demand. Thus the information of trading volume is able to play as proxy variable of fluctuation of supply and demand. Assumed that noise traders are driven by information of the changing volume, I customized the original MMS model(28) to following model,

$$dS_t = \phi_t \exp(\lambda_{F,t} + \lambda_{N,t})dt + \theta_1 \exp^{\frac{\lambda_{N,t}+\lambda_{F,t}}{2}} dw_{1,t} \tag{43a}$$

$$d\phi_t = (\alpha + \beta\phi_t)dt + \theta_2 dw_{2,t} \tag{43b}$$

$$d\lambda_{F,t} = \gamma_F \lambda_{F,t} dt + \theta_3 dw_{3,t} \tag{43c}$$

$$d\lambda_{N,t} = \gamma_N \lambda_{N,t} dt + \theta_4 d\log(V_t), \tag{43d}$$

where the suffix F and N denote fundamentalist and noise trader respectively, $d\log(V)$ is normalized instantaneous log-return of trading volume. The market-wide liquidity consists of fundamentalist's and noise trader's by the model (43). Noise trader's liquidity has deterministic structure driven by fluctuation of normalized trading volume. We can separate liquidity fundamentalist's and noise trader's using this model. However, it was difficult to identify using this model, I considered to more simplifying this model.

Many researchers suggested that the stock price volatility is positively correlated with its trading volume [68, 4]. Clark [14] interpreted this phenomenon by following the "mixture of distributions hypothesis". He assumed each intraday return is identically and independently distributed (i.i.d.) with zero mean and variance σ^2, the joint distribution of daily returns and trading volume is a bivariate normal conditional on the daily number of information arrivals,

$$r_t | I_t \sim N(0, \sigma^2 I_t) \tag{44a}$$

$$V_t | I_t \sim N(a + bI_t, cI_t) \tag{44b}$$

where, r_t is stock return on the t day, V_t is trading volume, I_t is information, a, b and c are constant parameters. It follows from Eq.(44a) and Eq.(44b) that the dynamics of the volatility process of returns are depending on the time series

behavior of information which also affects the dynamics of trading volume. Based on this assumption, the timing of a return uprush is depending on outbreak of trading volume. It can be expected that considering a trading volume into the model has improved for identification same as the jump detection. However, this model can not use for prediction because we can not know the trading volume V_t at $t-1$.

All Market players are consisting of fundamentalists and noise traders. Thus composition ratio of noise trader is ψ, the inverse of liquidity of all market is defined using Eq.(43d) as

$$\lambda_t = \lambda_{F,t} + \psi \log(V_t) \tag{45}$$

Hence the model (43) becomes

$$dS_t = \phi_t \exp(\lambda_{F,t} + \lambda_{N,t})dt + \theta_1 \exp(\frac{\lambda_{F,t} + \lambda_{N,t}}{2})dw_{1,t} \tag{46a}$$

$$d\phi_t = (\alpha + \beta\phi_t)dt + \theta_2 dw_{2,t} \tag{46b}$$

$$d\lambda_{F,t} = \gamma_F \lambda_{F,t} dt + \theta_3 dw_{3,t} \tag{46c}$$

$$\lambda_t = \lambda_{F,t} + \psi \log(V_t) \tag{46d}$$

From the model (46), we obtain the state space representation described in (29). Where,

$$\begin{aligned}
\boldsymbol{x}(t) &= \begin{bmatrix} S_t & \phi_t & \lambda_{F,t} \end{bmatrix}^T, \\
\boldsymbol{f}(\boldsymbol{x}(t)) &= \begin{bmatrix} \phi_t \lambda_t & \alpha + \beta\phi_t & \gamma\lambda_{F,t} \end{bmatrix}^T, \\
\boldsymbol{g}(\boldsymbol{x}(t)) &= \begin{bmatrix} \theta_1 e^{\frac{\lambda_{F,t}+\lambda_{N,t}}{2}} & 0 & 0 \\ 0 & \theta_2 & 0 \\ 0 & 0 & \theta_3 \end{bmatrix}, \\
d\boldsymbol{w}(t) &= \begin{bmatrix} dw_{1,t} & dw_{2,t} & dw_{3,t} \end{bmatrix}^T, \\
\boldsymbol{H} &= \begin{bmatrix} 1 & 0 & 0 \end{bmatrix}.
\end{aligned}$$

The model (46) is imputed a external force into the model (28). The log likelihood function can be represented same as the model (28), because the external force is independent with the states.

This model is more complex more than original MMS model (28), it is more difficult to estimate by this model. To easy to estimate, I reduced the parameter α in Eq.(28b). I analyzed S&P500 and TOYOTA again.

Table 15 shows fitting performance and estimated parameters by this model. The "improvement" in this table indicates comparison the AIC values with the model (28). Comparison AIC values between two models, the HPMMS model shows better fitting performance than the MMS model (S&P500: -33.9, TOYOTA: -39.9). These fitting performances by the HPMMS model are better than MMS one, however not better than GARCH model.

FIGs.71 and 72 show results of this model; (a):$S_{t|t-1}$, (b):$\phi_{t|t-1}$, (c):$\lambda_{N,t|t-1}$, (d):$\lambda_{N,t|t-1}$, (e):innovations and (f):volatility. By comparison MMS model (28), it was difficult to observe distinct differences between two models. Distinguishing feature is microscopic fluctuation on trajectories of total liquidity $\lambda_{t|t-1}$ (see graph (d) in FIGs. 71 and 72). The inverse of the market liquidity equals to the sum of fundamentalist's $\lambda_{F,t}$ and Noise trader's $\psi \log(V_t)$. Thus λ_N seems to contribute only

adding microscopically fluctuations into the market liquidity. Theses microscopic fluctuation put on the estimated volatility.

This HPMMS model was constructed based on the idea that heterogeneous market players in market microstructure theory. This model is more complicated than MMS model, thus the fact suggests that it is more difficult to solve than MMS ones. Inverse of liquidity of noise traders λ_N is defined $\psi \log(V_t)$ as a deterministic function. Fluctuation of a trading volume depends on not only the price volatility but seasonal influence. The trading volume jumps up sharply at the expire day of the option contract which is arranged quarterly, decreases suddenly on the off-season as the year change period(see graph (b) in FIG.1). It was observed that microscopic fluctuations of volatility by HPMMS on graph(f) in FIGs.71 and 72. I suggest that the information of the volume fluctuation is effective in estimating volatility because the volatility depends on the trading volume. However, the information may deteriorate the estimating performance of HPMMS. This is because the volume follows non-Gaussian strange process (see graph (b) in FIG.1). For solving this problem, it is recommended that the stochastic model such as the model (43) is used.

From above analysis, I conclude following two points;

1. It is natural to assume that a market consists of heterogeneous market players. The HPMMS model is based on this assumption.

2. The HPMMS model can estimate the inverse of noise traders liquidity $\lambda_{N,t}$, however, it was difficult to estimate.

4.3.2 The Delay Van der Pol model; an agent model approach

Using the Ising model, the analysis of the market has been discussed in [5, 71]; besides, modeling the financial market by a certain form of Ising structure of the interactions of agents seems to be successfully achieved in several studies such as Bouchaud et. al. [17, 32]. It is think that most traders are influenced by rumors, excessively or under excessively react to the information, and like the subjective desirability more than the objective probability [19, 63]. The minority traders of a market, who are diffident to their investment position in many cases, are going to follow the decision of the majority. Because they tend to think that the majority of the traders have more accurate information than themselves. A majority orienting model [33] is introduced, which is composed of three elements: the mutation of dealers, the majority rule and the feedback by the price, as basic elements for the change of a stock price in a real market. This model is a ternary interaction model of a finite particle, which makes excursions that are similar to the Ising model [7], assuming a mutation to the other type for each particle. The van der Pol equation is obtained as a deterministic approximation, which seems to explain the oscillation of a stock price.

Traders make use of information from the history of a stock price in order to gain profits by dealing stocks. I develop the majority orienting model taking into account of the feedback rule considering the history of buying then I selling of traders and introduce a delayed van der Pol equation. The majority orienting model more realistic and helps to understand the dynamics for the change of the stock price.

The majority orienting model

The van der Pol equation is obtained from the majority orienting model for the change of a stock price [33]. In the model there are two types of particles in a box plus (+) and minus (−), whose numbers are N_+ and N_- respectively with $N = N_+ + N_-$. Let each trader be considered to be a particle in the box and change his position at random by the following step, with three substeps 1), 2) and 3), which are successively applied to the particles in the box. Here a + particle represents a bullish (feeling confident about the future stock price) trader, while a − particle represents a bearish (feeling pessimistic about the future stock price) trader.

1 *Mutation rule*: One particle out of N particles is chosen at random. It changes its sign to the opposite sign with probability m and does not change with probability $1 - m$, $(0 \leq m \leq 1)$.

2 *Majority rule*: Three particles are taken at random. If two of the particles taken have the sign + and one has the sign −, the one with − changes its sign to + and the price S increases by 1, while, if two of the particles have the sign − and one has +, the one with + changes to − and the price S decreases by 1. If the three particles have the sign +, no change of sign occurs for the three particles and the price S increases by 3, while, if the three particles have −, no change of sign occurs for the three particles and the price S decreases by 3.

3 *Feedback rule*: If S is positive, N_+ is decreased by 1 with probability S/N, while, if S is negative, N_+ is increased by 1 with probability $-S/N$. The absolute value of S can be larger than N when m is small. We only discuss the case of $|S| \leq N$ in this section. This condition is almost valid when $m \geq 0.75$.

Let us represent N_+ and S at step s as $N_+(s)$ and $S(s)$ respectively. Assuming that the duration of a step is τ, and the values of $N_+(s)$, $N_-(s)$ and $S(s)$ are given, we have the following expected values:

$$\begin{aligned} & E\left[\frac{N_+(s+1) - N_+(s)}{\tau N}\right] \\ = \; & m\left\{-\frac{N_+(s)}{N} + \frac{N_-(s)}{N}\right\} + 3\frac{N_+(s)\,(N_+(s)-1)\,N_-(s)}{N(N-1)(N-2)} \\ - \; & 3\frac{N_+(s)N_-(s)\,(N_-(s)-1)}{N(N-1)(N-2)} - \nu\frac{S(s)}{N} \end{aligned} \tag{47}$$

$$\begin{aligned} & E\left[\frac{S(s+1) - S(s)}{\tau N}\right] \\ = \; & 3\frac{N_+(s)(N_+(s)-1)(N_+(s)-2)}{N(N-1)(N-2)} + 3\frac{N_+(s)(N_+(s)-1)N_-(s)}{N(N-1)(N-2)} \\ - \; & 3\frac{N_-(s)(N_-(s)-1)N_+(s)}{N(N-1)(N-2)} - \frac{N_-(s)(N_-(s)-1)(N_-(s)-2)}{N(N-1)(N-2)} \end{aligned} \tag{48}$$

When N is sufficiently large, we obtain the deterministic approximation Eq.(49a)and Eq.(49b), putting $\dfrac{N_+(s) - N/2}{N}$ as x_t and $S(s)/N$ as y_t, taking an appropriate time

scale τ as,

$$\frac{d}{dt}x_t = -2mx_t + 6x_t\left(\frac{1}{2}+x_t\right)\left(\frac{1}{2}-x_t\right) - \nu y_t \tag{49a}$$

$$= -2\left(m-\frac{3}{4}\right)x_t - 6x_t^3 - \nu y_t,$$

$$\frac{d}{dt}y_t = 6x_t. \tag{49b}$$

Assuming the number of the particles N is large enough, we can neglect the random sampling effect of particles, while in the real market the stock price y_t is perturbed by random noise. Hence we have the following model of stochastic differential equations

$$dx_t = \{-2\left(m-\frac{3}{4}\right)x_t - 6x_t^3 - \nu y_t\}dt, \tag{50a}$$

$$dy_t = 6x_t\,dt + \theta dw_t, \tag{50b}$$

where w_t is the standard Brownian motion.

Delayed van der Pol equation

The rule 1 in the previous section models the trader's random change of his investment attitude "bullish" or "bearish". The rule 2 models traders' majority orienting behavior. Each trader makes effort to get good data or information in order to predict the stock price. But the information on a stock is heterogeneously distributed among traders in a real market. For example, it is natural to think that a holder of a stock has more accurate information on the stock than a non-holder of the stock. The minority traders of a market, who are diffident to their investment position in many cases, are going to follow the decision of the majority, because they tend to think that the majority of the traders have more accurate information than themselves. The majority orienting behavior of traders is called "herding" and "information cascade" phenomenon is referred to as one of the structural factors of the collapse (crash) of the price often observed in the stock market [72]. Let us consider on the feed back force of the rule 3. The term $-\nu\frac{S(s)}{N}$ of Eq.(47) represents the rule 3, which means the stock price gets the feedback force proportional to the excess over the standard price which is assumed to be 0 in the model given in [33], where the excess takes positive or negative real value. The rule 3 assumes that traders have the consensus of the standard price of a stock and have a tendency to sell and buy to compensate the excess. Even if the standard price exists, it is almost impossible to assume that all traders know it.

It is natural to think that the price, which each trader refers to, should be the price, which calculates the gain-or-loss of the position instead of zero. I assume that the book value of a stock to be the reference price, and that the power of pull back is proportional to the difference of book value and current price. Assume each trader refer the price of a stock of the time at $s-u$ at time s, namely the holding period (investment period) of each trader of a stock to be u. Consider the case of a book value is higher than a current price, a trader with buy-position tends to change his position to "bearish" and going to sell to take a profit. In the case of a book value is lower than a current price, he maintains "bullish". When a trader has the sell position, this relation becomes to reverse. Hence the stock price receives the pull

back pressure caused by the book value of the position at time $s-u$ of each trader. A trader changes their holding position on the basis of the book value at $s-u$. The following rule 3' is rewritten as follows;

3' *Feedback rule*: If $S(s)-S(s-u)$ is positive, then N_+ is decreased by 1 with probability $\mid (S(s)-S(s-u))/N \mid$, while, if $S(s)-S(s-u)$ is negative, then N_+ is increased by 1 with probability $\mid (S(s)-S(s-u))/N \mid$.

Assuming that the holding period (investment period) of each trader stock to be u, $-\nu\frac{S(s)}{N}$ in Eq.(47) is changed to;

$$\nu\frac{S(s)-S(s-u)}{N} \tag{51}$$

where $S(s-u)$ is the price t at time $s-u$, which is referred by each trader. Hence it seems to be natural to consider a delayed differential equation as,

$$\begin{aligned}\frac{d}{dt}x_t &= -2mx_t+6x_t(\frac{1}{2}+x_t)(\frac{1}{2}-x_t)-\nu(y_t-y_{t-u}),\\ &= -2(m-\frac{3}{4})x_t-6x_t^3-\nu(y_t-y_{t-u}), \qquad (52)\\ \frac{d}{dt}y_t &= 6x_t \qquad (53)\end{aligned}$$

where y_{t-u} is the price (the reference price) at $t-u$. From the system, unless y_{t-u} is constant, the argument for the van der Pol equation is not applied. The van der Pol equation of (49a) and (49b) has the Hopf bifurcation at $m=0.75$. The orbit and the flow for the equation are illustrated in FIG.73 of the phase plane, where the sign of y-component of the flow of the van der Pol equation is antisymmetric with respect to the y-axis. The set defined by the equation $\frac{d}{dt}x_t=0$ is the curve given by the equation;

$$y_t=-\frac{1}{\nu}\left\{2\left(m-\frac{3}{4}\right)x_t-6x_t^3\right\}. \tag{54}$$

The Eq.(54) has a local maximum and a local minimum when $m<0.75$ (shown by a dotted curve in FIG.73-(a)), which do not exist in $m>0.75$. The sign of x-component of the flow is changed in the curve given by Eq.(54). When $m>0.75$, each orbit is attracted to the fixed point $(0,0)$ drawing a spiral curve and then the price orbit becomes flat. In the case when $m<0.75$, the van der Pol equation has a limit cycle by the Poincare-Bendixson theorem [34]. Here we observe that the behavior of the solution of the delayed van der Pol equation considering the solution of the original van der Pol equation. In order to compare the delayed van der Pol equation with the equation without delay, taking the same values for all parameters other than the delay. A numerical study is shown in FIG.74. Assuming the price on the time interval $[-u,0]$ is a constant, say α, and take an initial function on the time interval $[-u,0]$ to be constant for the delayed van der Pol equation.

In this DVDP model, the stock price get the feedback force proportional to the excess over the past price to which each trader refers. In $m>0.75$, this system has a limit cycle as well as the system without delay and the orbit tend to expand out of the limit cycle. When $m<0.75$, the solution of this system makes the convergence patterns repeatedly as shown in FIG.73 or is similar to a limit cycle as shown FIG.74

depending on parameters, the orbit is not flat contrariwise with the case without delay. It is natural to think that, the reference point should be increased gradually with the time because of the demand cost for the risk of the investment. This cost is called "cost of capital" [9]. Let the rate of increase of this cost be g. The reference point price of the trader should be multiplied by e^{ug} by the rate g. Hence Eq.(51) becomes

$$-\nu\frac{S(s)-S(s-u)\times e^{ug}}{N} \tag{55}$$

Hence we have;

$$\frac{d}{dt}x_t = -2\left(m-\frac{3}{4}\right)x_t - 6x_t^3 - \nu(y_t - y_{t-u}\times e^{ug}), \tag{56}$$

$$\frac{d}{dt}y_t = 6x_t. \tag{57}$$

It is shown a typical numerical solution of this equation in FIG.75, where the initial function of on $[-u, 0]$ is assumed to be a constant. This corresponds to the case in which each trader made their position when the price fluctuation is small.

Delay van der Pol stock price model Systems of delay differential equations now occupy a place of importance in some areas of science and engineering, for example, epidemiology, population dynamics and neuron dynamics. Interest in such systems often arises when traditional pointwise modeling assumptions are replaced by more realistic distributed assumptions. The manner in which the properties of systems of delay differential equations differ from those of systems of ordinary differential equations has been and remains an active area of research.

From Eq.(52), the set of points $\frac{d}{dt}x_t = 0$ is given by

$$y_t - y_{t-u} = -\frac{1}{\nu}\left\{2\left(m-\frac{3}{4}\right)x_t - 6x_t^3\right\}. \tag{58}$$

From Eq.(58), we see that there is a *dynamical hysteresis effect* [34]. The orbit depends on its past history of the price y_{t-u}. This hysteresis effect is summarized as follows.

A: The case where $m > 0.75$, there is no negative resistance region (the solution flow is attracted to the fixed point), and the amplitude of the price fluctuation decreases gradually because the solution flow is attracted toward the reference point. However, by a big fluctuation of the past price given to the system, the current price is excited again.

B: The case where $m < 0.75$, the amplitude of the price increases compared with the van der Pol equation without delay because the negative resistance region vibrates on y according to a past price change.

When a past price fluctuation is relatively small, for the case of A, i.e. $m > 0.75$, the orbit is attracted to the reference point, which is enveloped by a triangle form like a wedge. As it can be observed from FIG.73-(a), the magnitude of flow of the solution flow near $(0, y_{t-u})$ is small. The change of the stock price at $t-u$ makes the sudden increase of magnitude of the solution flow at t. This argument is applied also

to the system Eq.(56) and Eq.(57), in which the system gets a continuous external force caused by the demand cost. When an initial function is constant and u is long enough, it makes a limit cycle of the original van der Pol equation. Therefore, although the stock price does not show a trend in the struggle period, the price jumps by the sudden change caused by the change of past price, the price struggles again and the amplitude becomes small gradually. In this condition, it is probable that a relatively large news steps in for the shock of past price change. Thereby, the change of a stock price sometimes shows a stairs-like trend given as in FIG.75. Considering the process, DVDP model can explain the volatility jumps and their successive damping.

In addition the trend depends on the sign of the price of the reference point. The minus sign of the price at the reference point, namely the minus sign of y_{t-u} in Eq.(56) makes a downward trend, while the plus sign of it makes an upward trend.

When u is relatively small with $m < 0.75$ as in the case B, the jump of a stock price tends to be hidden by the amplitude of a struggle. For this reason, a stock price does not show a stair-like trend but a smooth trend (See FIG.75). In a real market, these two cases may be combined. The parameter m shows the measure of conviction of trader's prediction for the market. A trader does't mutate when his conviction is strong, and mutate easily when it is week. Stock prices will be struggle, in which the buying and the selling almost evenly take place, when the traders think that the future of the corporate performance is unpredictable. When most of traders think that present stock prices are cheap (or expensive), the stock prices will show the trend because they do not hesitate to buy (or to sell) the stock. It is natural to think that conviction of traders is week in the former case and is strong in the latter case.

The solution flow of the delayed van der Pol equation on a phase plane depends on t not just on x, and y, while it is independent on time for the case of the van der Pol equation, Eq.(49a) and Eq.(49b). Up to previous argument, as a simple case, the holding period u of a position did not depend on a trader, but assumed that it was fixed. This seems to be a little strong assumption. Let us assume that the holding period of N traders are $u_1, u_2, \cdots, u_N$ respectively. The sum of each pull back power generated from the positions of all traders makes the feedback force as

$$-\nu \frac{S(s) - \frac{1}{N}\sum_{i=1}^{N} S(s-u_i)}{N}. \tag{59}$$

Assume the number of particles N is sufficiently large, and $v(q) = 0$ for $q \geq s$ and $0 \leq v(q)$ for $0 \leq q \leq s$ with $\int_{t-s}^{t} v(q)dq = 1$, the feedback force is given by

$$-\nu\{y_t - \int_{t-u}^{t} v(q)y_q dq\}. \tag{60}$$

The following stochastic equations will be reasonable to analyze real data of time series of a stock price:

$$dx_t = \{-2\left(m - \frac{3}{4}\right)x_t - 6x_t^3 - \nu(y_t - \int_{t-u}^{t} v(q)y_q dq)\}dt, \tag{61}$$

$$dy_t = 6x_t dt + \theta dw_t. \tag{62}$$

It will give a good short time prediction if we take $v(q)$ at time q ($v(q) = V(q)/\int_{t-u}^{t} V(q)dq$, $V(q)$:trading volume), normalized by $\int_{t-u}^{t} v(q)dq = 1$. From Eq.(61) and Eq.(62),

the reference price is the past price transition weighted average by trading volume. We often observe the phenomenon in which a price struggles, near the price at the time of a big trading volume in the past, which may be explained by this model.

I suggest that one of the advantage of DVDP model is constructed based on three simple rules(mutation, majority and feedback rules of market players. The feedback rule has close relation to The Prospect Theory by Kahneman and Tversky, which is a theory about decision making of the human being in an atmosphere of uncertainty. They says that human uses the "value function", as a measure of decision making instead of the linear function, whose conceptual figure of the value function is shown in FIG.76 [37]. By using the non-linear function, the delayed van der Pol equation shows more intricate orbit, which is an interesting subjects. FIG.77 shows an example of numerical simulation using a non-linear value function. This value function, similar in form FIG.76 described by connecting two log functions.

The Prospect theory is one section of the "Behavioral Finance", which is a new finance theory conditioning on the action of the investor who is not necessarily rational under such uncertain environment [19, 63]. It includes the above-mentioned "information cascade" in many cases.

Next advantage is that DVDP model is a self-excited system, a price fluctuate without sequential system noise input, an impulse such as a big news plays a role of "trigger". The degree of sensitivity to external shocks depend on state of the system. Thus we may be able to determinate the market stability based on this idea.

On the contrary, DVDP model has a material disadvantage. The delay differential equation system such as this DVDP model is not able to solve by a method by state space representation. This is because dimension of the state space representation is infinity for this system. The identification methods for delayed system require further study. From above analysis, I conclude following three points;

i). Base on the agent approach for a market trading structure, by assuming only three rules of a trader, the DVDP price model is obtained.

ii). This is one of the dynamic model containing a deterministic price jump generation mechanism.

iii). It is not able to solve by this model because of a problem in the estimation method.

5 Conclusion

The aim of this thesis is to consider model requirements for practical use of dynamic models in the academic and practical world. First, I studied the statistical nature of actual market data. Next, I constructed models for practical financial issues, and used these models with actual market data.

I developed three dynamic models for analyzing the investment style of mutual funds from the conventional static model; enabling the estimation of time-varying style drift of funds. This model is easy to use in practice, and may provide innovative change in style management in finance. I showed that Nelson-Foster's GARCH model has certain drawbacks, primarily that it overestimates volatility by price jumps. We can overcome this problem using the jump detection scheme.

I constructed a dynamic model based on the market trading mechanism, and so obtained the DVDP price model. This model provides qualitative explanations for typical price fluctuations, such as triangle patterns, decreasing volatility and price jumps.

From these results, I conclude that it is necessary to consider time-varying volatility and jumps of states (e.g. price and exposure) for dynamic modeling in finance. I think that this study has the potential to contribute to the development of dynamic models for finance.

6 Acknowledgment

The help of Tohru Ozaki and Yoshiaki Itoh, PhD of The graduate University for Advanced Studies in preparation of this manuscript is gratefully acknowledged. I acknowledge the support of J.C. Jimenez PhD of Instituto de Cibernetica, Matematica y Fisica. I wish to thank PhD Shoji and PhD Iino for their qualities and useful support.

References

[1] H. Akaike, *A new look at the statistical model identification.*, IEEE Transactions on Automatic Control, **19** (6), 716-723, (1974)

[2] T. Angelidis, A. Benos and S. Degiannakis, *The use of GARCH models in VaR estimation.*, Statistical Methodology, **1** Issues 1-2, 105-128, (2004)

[3] W. Andrew and C. Mackinlay, *A Non-Random Walk Down Wall Street* Princeton Univ Pr Published, (2002)

[4] G.T. Andersen, *Return Volatility and Trading Volume : An Information Flow Interpretation of Stochastic Volatility.*, Journal of Finance, **81**, 637-659, (1996)

[5] M. Aoki, *New Approaches to Macroeconomic Modeling.*, Cambridge University Press, New York,(1996).

[6] D. Bates, *Post-'87 Crash fears in S&P500 Futures Options.*, Jounal of Financial Economics, **94**, 181-238, (2000)

[7] K. Binder and D. W. Heermann, *Monte Carlo Simulation in Statistical Physics, 2nd ed.*, (1997).

[8] A.E. Bryson and M. Grazie, *Smoothing for liner and nonlinear dynamic system.*, In Proc. Optimum System Synthesis Conf., 354-364, (1977).

[9] R. A. Brealey and S. Myers, *Principals of Corporate Finance.* Mac.Grow-Hill, (2000)

[10] R. Biscay, J.C. Jimenez J. Riera and P. Valdes, *Local linearization method for the numerical solution of stochastic differential equations.*, Ann. Inst. Statist. Math., **48**, 631-644, (1996)

[11] J.P. Bouchaud and R. Cont, *A langevin approach to stock market fluctuations and crashes.*, European Physical Journal, **B6**, 543-550, (1998)

[12] P. Christoffersen and D. Pellerier *Backtesting Value-at-Risk: A Duration-Based Approach.*, Journal of Financial Econometrics, **2**, 84-108, (2004)

[13] J.C. Chuan and A. Fulop, *Estimating the Structural Credit Risk Model When Equity Prices Are Contaminated by Trading Noises.*, University of Toronto working paper, (2006)

[14] J.K. Clark, *A Subordinated Stochastic Process Model with Finite Variance for Speculative Prices.*, Econometrica, **41**, 135-155, (1973)

[15] T.D. Coggin, F.J.Fabozzi and S. Rahman, *The Investment Performance of U.S. Equity Pension Fund Managers: An Empirical Investigation.*, The Journal of Finance, **48** No.3, 1039-1055, (1993)

[16] R. Connolly and C. stivers, *Momentum and Reversals in Equity-Index Returns during Periods of Abnormal Turnover and Return Dispersion.*, The Journal of Finance, **58** No.4, 1521-1555, (2003)

[17] R. Cont and J. P. Bouchaud, *Macroeconomic Dynamics.* **4**, 170-196, (2000)

[18] J. Cotter, *Downside Risk for European Equity Markets.*, MPRA paper **3537**, University Library of Munich, (2004)

[19] W. DeBondt and R. H. Thaler, *Does the Stock Market Overreact?*, J. of Finance, **40**, 793(1996)

[20] J.C. Duan, *Augmented GARCH(p,q) process and its diffusion limit.*, Journal of Econometrics, **79**, 97-127, (1998)

[21] B.J. Dumas, A. Kurshev and R. Uppal, *What Can Rational Investors Do About Excessive Volatility and Sentiment Fuctuations?*, CEPR Discussion Papers, (2005)

[22] E. Eberlein, U. Keller and K. Prause, *New Insights into Smile, Mispricing and Value at Risk: The Hyperbolic Model*, Journal of Business, **71**, 371-405, (1998)

[23] R. Engle and J. Russell, *Autoregressive Conditional Duration: A New Model for Irregularly Space Data.* , Econometrica **66**, 1127-1162, (1998)

[24] B. Eraker, *Do Stock Prices and Volatility Jump? Reconciling Evidence from Spot and Option Prices.*, J. of Finance **3**, 1367(2004)

[25] J. Fleming and C. Kirby, *A closer look at the relation between GARCH and stochastic autoregressive volatility.*, Journal of Financial Econometrics, **1**, 365-419, (2003)

[26] D.B. Nelson and D.B. Foster, *Asymptopic filtering theory for univariate arch models.*, Econometrica, **62**, 1-41, (1994)

[27] B.V. Genedenko and Kolmogorov, *Limit distributions for sums of independent random variables,* (translated by K.L. Chung), Addison-Wesley, (1954)

[28] P.J. Harrison and C.F. Stevens, *Baysian forecasting(with discussion).*,] J. Roy. Statist. Soc. Ser. B., **38**, 205-247, (1976)

[29] J.C. Hull and A. White, *The Pricing of Options on Assets with Stochastic Volatilities.*, Journal of Finance, **42**, 281-300, (1987)

[30] J.C. Hull and A. White, *An Analysis of the Bias in Option Pricing Caused by a Stochastic Volatility.*, Advances in Futures and Options Research, **3**, 27-61, (1988)

[31] M. Iino and T. Ozaki, *A Nonlinear Model for Financial Dynamics, in Proceeding of the International Symposium on Frontiers of Time Series Modeling.*, ISM Tokyo Japan, Feb, 334-335, (2000)

[32] G. Iori, *J. of Economic behavior & Org.*, **49**, 269-285, (2002).

[33] H. Takahashi and Y. Itoh, *Majority orienting model for the oscillation of market price.*, Eur. Phys. J. B **37**, 271(2004)

[34] E. A. Jackson, *Perspectives of nonlinear dynamics.* (1989)

[35] J.C. Jimenez and T. Ozaki, *Linear estimation of continuous-discrete state space models with multiplicative noise.*, Systems and Control Letters., **47**, 91-100, (2002)

[36] J.C. Jimenez and T.Ozaki, *Local linearization filters for non-linear continuous-discrete state space models with multiplicative noise.*, Int. J. Control, **76**, 1159-1170, (2003)

[37] D. Kahneman and A. Tversky, *Prospect theory: An analysis of decisions under risk.*, Econometrica, **47**, 313(1979)

[38] R.E. Kalman, *A new approach to linear filtering and prediction probabilities.*, Trans. ASME jounal of Basic Engineering, **82**, 35-45, (1960)

[39] A.N. Kolmogorov, *International and extrapolation of stationary random sequences.*, USSR Mathematics Series, **5**, 3-14, (1962)

[40] S.F. LeRoy and R.D. Porter, *The Present-Value Relation: Tests Based on Implied Variance Bounds.*, Econometrica, **49**, 555-574, (1981)

[41] J. Lintner, *The valuation of risk assets and the selection of risky investments in stock portfolios and capital budgets.*, Review of Economics and Statistics, **47**, 13-37, (1965)

[42] A. Lucas R. Dijk and T. Kloek, *Stock selection, style rotation, and risk.*, Journal of Empirical Finance, **9**-1, 1-34, (2002)

[43] B. Mandelbrot, *The variation of certain speculative prices.*, Journal of Business, **36**, 418-419, (1963)

[44] B. Mandelbrot, *fractals and Scaling in Finance.*, Springer, New York, (1997)

[45] B.G. Malkiel *A Random Walk Down Wall Street.*, W.W. Norton & Company, Inc., (1973)

[46] H. Markowitz, *Portfolio Selection.*, Journal of Finance, **7**, 77-91, (1952)

[47] T.H. McInish and R.A. Wood, *An Analysis of Intraday Patterns in Bid/Ask Spreads for NYSE Stocks.*, Journal of Finance, **47**, 753-764, (1992)

[48] J.S. Meditch, *On optimal linear smoothing theory.*, J. Inf. Control **10**, 598-615,(1967).

[49] R. C. Merton, *Option pricing when the underlying stock returns are discontinuous.*, J. of Financial Economics **3**, 125-144, (1976)

[50] D.B. Nelson, *ARCH models as diffusion approximations.*, Journal of Econometrics, **45**, 7-38, (1990)

[51] M.J. O' Hara, *Market Microstructure Theory.*, Blackwell, (1995)

[52] T. Ozaki and M. Iino, *An Innovation Approach to Non-Gaussian Time Series Analysis.*, Journal of Applied Probability, **38A**, 78-92, (2001)

[53] T. Ozaki, *A local linearization approach to nonlinear filtering.*, International J. of Control., **57**, 75-96, (1993)

[54] J. Pan, *The jump-risk premia implicit in options: Evidence from an integrated time-series study.*, Jounal of Financial Economics, **63**, 3-50, (2002)

[55] I. Pena, G. Rubio and G. Serna, *Why Do We Smile? On the Determinants of the Implied Volatility Function*, Journal of Banking & Finance, **23**, 1151-1179, (1999)

[56] M. Rubinstein, *Implied Binominal Trees*, Journal of Finance, **49**, 771-818, (1994)

[57] A. Sahalia, P. Mykland and L. Zhang, *A Tale of Two Time Scales: Determining Integrated Volatility with Noisy High-Frequency Data.*, Journal of the American Statistical Association, **100**, 1394-1411, (2005)

[58] A. Sahalia, P. Mykland and L. Zhang, *How often to sample a continuous-time process in the presence of market microstructure noise.*, Review of Financial Studies **18**, 351-416, (2005)

[59] L.O. Scott, *Option Pricing When the Variance Changes Randomly: Theory, Estimation and an Application.*, Journal of Financial and Quantitative Analysis, **22**, 419-438, (1987)

[60] W. F. Sharpe, *Capital asset prices: A theory of market equilibrium under conditions of risk.*, Journal of Finance, **19**, (425-442), (1964)

[61] W. F. Sharpe, *Asset Allocation : Management Style and Performance Measurement.*, Journal of Portfolio Management, **18**, 7-19, (1992)

[62] R.J. Shiller, *Do Stock Prices Move Too Much to be Justified by Subsequent Changes in Dividends?*, American Economic Review, **71**, 421-436, (1981)

[63] R.J. Shiller, *Human Behavior and the Efficiency of the Financial System.*, NBER Working Papers 6375(1998)

[64] I. Shoji and T. Ozaki, *Estimation for nonlinear stochastic differential equations by a local linearization method.*, Stochastic Analysis and Applications., **16**, 733-752, (1998)

[65] R. Mantegna and H.E. Stanley, *An Introduction to Econophysics.*, Cambridge University Press, Cambrigde, (1999)

[66] E. M. Stein and J. Stain, *Stock price distributions with stochastic volatility: analytic approach.*, Review of Financial Studies, **4**, 707-752, (1991)

[67] S. Grossman and J. Stiglitz, *On the Impossibility of Informationally Efficient Markets.*, American Economic Review, **70** 393-408, (1980)

[68] G. Tauchen, *Return Volatility and Trading Volume : An Information Flow Interpretation of Stochastic Volatility.*, Econometrica, **51**, 485-506

[69] S.J. Taylor, *Modeling stochastic volatility: a review and comparative study.*, Mathematical Finance, **4**, 184-204, (1994)

[70] C.F. Van Loan, *Computing integrals involving the matrix exponential.*, IEEE Trans. Automat. Control **23** 395-404, (1978)

[71] W. Weidlich, *Br. J. Math. Statist. Psychol.*, **27**, 251-266,(1971).

[72] A. Devenow and I. Welch, *Rational herding in financial economics.*, Eur. Economic Review **40**, Apr 603(1996)

[73] N. Wiener, *Extrapolation, Interpolation and smoothing of Stationary Time Series with Engineering Applications. A classified report by MIT Radiation Lab.*, Cambridge MA, Feb.1942 Later published, (1949)

[74] H. Wold, *A Study in the Analysis of Stationary Time Series.*, Almqvist and Wiksell, Uppsala, (1938)

Appendix

A linear Kalman filter

Prediction

$$\boldsymbol{X}_{t|t-1} = \boldsymbol{F}\boldsymbol{X}_{t-1|t-1}, \tag{63a}$$
$$\boldsymbol{P}_{t|t-1} = \boldsymbol{F}\boldsymbol{P}_{t-1|t-1}\boldsymbol{F}^T, \tag{63b}$$
$$\nu_t = \boldsymbol{Z}_t - \boldsymbol{H}_t\boldsymbol{X}_t, \tag{63c}$$
$$\boldsymbol{V}_t = \boldsymbol{H}_t\boldsymbol{P}_{t|t-1}\boldsymbol{H}_t^T. \tag{63d}$$

Filtering

$$\boldsymbol{K}_t = \boldsymbol{P}_{t|t-1}\boldsymbol{H}_t^T(\boldsymbol{H}_t\boldsymbol{P}_{t|t-1})^{-1}, \tag{64a}$$
$$\boldsymbol{X}_{t|t} = \boldsymbol{X}_{t|t-1} + \boldsymbol{K}_t(\boldsymbol{Z}_t - \boldsymbol{H}_t\boldsymbol{X}_{t|t-1}), \tag{64b}$$
$$\boldsymbol{P}_{t|t} = (\boldsymbol{I} - \boldsymbol{K}_t\boldsymbol{H}_t)\boldsymbol{P}_{t|t-1}. \tag{64c}$$

B local linearlization scheme

A continuous time nonlinear state space model is represented like as Eqs. (29), where,$\boldsymbol{x}(t) \in R^d$ is the state vector at the instant of time t, $z(t) \in R^r$ is the observation vector at the instant of time t, $\boldsymbol{f}(x(t))$, $\boldsymbol{g}(x(t))$ are the nonlinear functions, and $\boldsymbol{C}\boldsymbol{x}(t)$ is the state dependent matrix described the variance feature of model. Using the local linearization method, we obtain following stochastic difference equation,

$$\boldsymbol{x}(t_{n+1}) = \boldsymbol{x}(t_n) + \boldsymbol{\psi}(\boldsymbol{x}(t_n);\Delta) + \boldsymbol{\xi}(\boldsymbol{x}(t_n);\Delta), \tag{65}$$

where $\Delta = t_{n+1} - t_n$ as sampling period,
$\boldsymbol{J}(\boldsymbol{x}_t)$:Jacobian of $\boldsymbol{f}(x(t))$,
$\boldsymbol{H}(\boldsymbol{x}_t)$:Hessian of $\boldsymbol{f}(\boldsymbol{x}(t))$,

$$\begin{aligned}
\boldsymbol{x}(t_0) &= \boldsymbol{x}_0, \\
\boldsymbol{\psi}(\boldsymbol{x}(t_n;\Delta)) &= \boldsymbol{R}_0(\boldsymbol{J}(\boldsymbol{x}(t_n)),\Delta)\boldsymbol{f}(\boldsymbol{x}(t_n)) + (\Delta\boldsymbol{R}_0(\boldsymbol{J}(\boldsymbol{x}(t_n))),\Delta) \\
&\quad - \boldsymbol{R}_1(\boldsymbol{J}(\boldsymbol{x}(t_n)),\Delta)\boldsymbol{r}(\boldsymbol{x}(t_n)), \\
\boldsymbol{R}_k(\boldsymbol{J}(\boldsymbol{x}(t_n)),\Delta) &= \int_0^\Delta \exp(u\boldsymbol{J}(\boldsymbol{x}(t_n)))u^k du, \\
\boldsymbol{R}(\boldsymbol{x}(t_n)) &= \frac{1}{2}tr\{\boldsymbol{g}(t_n)\boldsymbol{g}^T(t_n)\boldsymbol{H}(x(t_n))\}.
\end{aligned}$$

$\xi(x(t_n);\Delta)$ is a Gaussian stochastic process with zero mean and following covariance matrix

$$\boldsymbol{V}(\boldsymbol{x}(t_n)) = \int_0^\Delta \exp(\boldsymbol{x}(t_n)u)\boldsymbol{g}(t_n)\boldsymbol{g}^T(t_n)\exp(\boldsymbol{J}(\boldsymbol{x}(t_n))u)^T du. \tag{66}$$

Lemma 1[35, 36] $\psi(\boldsymbol{x}(t_n);\Delta)$ is defined in the following matrix

$$\begin{bmatrix} \boldsymbol{A}(\boldsymbol{x}(t_n);\Delta) & \boldsymbol{b}_1(\boldsymbol{x}(t_n);\Delta) & \psi(x(t_n);\Delta) \\ 0 & 1 & \boldsymbol{b}_2(\boldsymbol{x}(t_n);\Delta) \\ 0 & 0 & 1 \end{bmatrix} = \exp(\boldsymbol{M}\Delta) \tag{67}$$

where

$$\boldsymbol{M} = \begin{bmatrix} \boldsymbol{J}(\boldsymbol{x}(t_n)) & \boldsymbol{r}(\boldsymbol{x}(t_n)) & \boldsymbol{f}(\boldsymbol{x}(t_n)) \\ 0 & 0 & 0 \\ 0 & 0 & 0 \end{bmatrix}.$$

Lemma 2 [70] $\boldsymbol{V}(\boldsymbol{x}(t_n))$ in Eq.(66) is defined in the following matrix

$$\boldsymbol{V}(\boldsymbol{x}(t_n)) = \boldsymbol{F}_T^3(\Delta)\boldsymbol{G}_2(\Delta) \tag{68}$$

where

$$\exp(\begin{bmatrix} -\boldsymbol{J}(\boldsymbol{x}(t_n)) & \boldsymbol{g}(t_n)\boldsymbol{g}^T(t_n) \\ 0 & \boldsymbol{J}^T(\boldsymbol{x}(t_n)) \end{bmatrix}\Delta) = \begin{bmatrix} \boldsymbol{F}_2(\Delta) & \boldsymbol{G}_2(\Delta) \\ 0 & \boldsymbol{F}_3(\Delta) \end{bmatrix}.$$

C non linear Kalman filter

Prediction

$$\begin{aligned} \hat{x}(t_k|t_{k-1}) &= E[x(t_k)|z_{k-1}] \\ &= \hat{x}(t_{k-1}|t_{k-1}) + \psi(\hat{x}(t_{k-1}|t_{k-1});\Delta) && \text{(69a)} \\ \hat{\nu}(t_k) &= z(t_k) - C\hat{x}(t_k|t_{k-1}) && \text{(69b)} \\ S(t_k) &= E[(x(t_k) - \hat{x}(t_k|t_{k-1}))x(t_k) - \hat{x}(t_k|t_{k-1}))^T] \\ &= \exp(J(\hat{x}(t_{k-1}|t_{k-1}))\Delta)Q(t_{k-1})\exp(J(\hat{x}(t_{k-1|t_{k-1}}))\Delta)^T + V(\hat{x}(t_{k-1}|t_{k-1})), \\ & && \text{(69c)} \end{aligned}$$

where Q_{t_k} is the conditional covariance.

Filtering

$$\begin{aligned} \hat{x}(t_k|t_k) &= E[x(t_k)|z_k] \\ &= \hat{x}(t_k|t_{k-1}) + K(t_k)\hat{\nu}(t_k) && \text{(70a)} \\ Q(t_k) &= E[(x(t_k) - \hat{x}(t_k|t_k))x(t_k) - \hat{x}(t_k|t_k))^T] \\ &= (I - K(t_k)C)S(t_k) && \text{(70b)} \\ \hat{\rho}(t_k) &= E[\nu(\hat{t}_k)\nu(\hat{t}_k)^T] \\ &= CS(t_k)C^T + \sigma^2 && \text{(70c)} \\ K(t_k) &= S(t_k)C^T\rho(\hat{t_k})^{-1} && \text{(70d)} \end{aligned}$$

D jump detection technique

Here the size of the compound Poisson noise could be noticeably large, the filtering and prediction of the state space representation such as model(33), are specified in term of state variable M_t defined by

$$\hat{M}_t = \begin{cases} M_t^{(0)} \text{if } Pr(M_t = M_t^0 | Z_{t+1}) > Pr(M_t = M_t^1 | Z_{t+1}), \\ M_t^{(1)} \text{if } Pr(M_t = M_t^0 | Z_{t+1}) < Pr(M_t = M_t^1 | Z_{t+1}). \end{cases} \tag{71}$$

Here, the posterior probability of M_t^i is

$$Pr(M_t = M_t^i | Z_{t+1}) = \frac{\sum_{k=1}^{2} f_{i,k}(t+1|t) f_i(t|t-1) \pi_i \pi_k}{\sum_{k=1}^{2} \sum_{i=1}^{2} f_{i,k}(t+1|t) f_i(t|t-1) \pi_i \pi_k}, \tag{72}$$

where

$$\begin{aligned} \pi_i &= Pr(M_t = M_t^i), \\ &= \begin{cases} 1 - \vartheta & \text{if } M_t = M_t^0, \\ \vartheta & \text{if } M_t = M_t^1, \end{cases} \\ f_i(t|t-1) &= Pr(z_t | M_t^i, Z_{t-1}), \\ f_{i,k}(t+1|t) &= Pr(z_{t+1} | M_t^i, M_{t+1}^k, Z_t), \end{aligned}$$

where ϑ is a jump probability, $f_i(t|t-1)$ and $f_i(t|t+1)$ are conditional density of M_t^i and M_{t+1}^k respectively. The optimum parameters are obtained minimizing following likelihood function.

$$\begin{aligned} \{\hat{\theta}, \hat{x}_0, \hat{Q}_0\} = arg \min_{\theta, x_0, Q_0} \sum_{k=1}^{N} \{ \log | \sum_{i=0}^{1} I(M_t = M_t^{(i)}) \hat{\rho}(t_k) | \\ + \sum_{i=0}^{1} I(M_t = M_t^{(i)}) \hat{\nu}^T(t_k) \hat{\rho}^{-1}(t_k) \hat{\nu}(t_k) \} + N \log 2\pi, \end{aligned} \tag{73}$$

where,

$$I(M_t = M_t^{(i)}) = \begin{cases} 1 & \text{if } M_t = M_t^{(i)}, \\ 0 & \text{otherwise.} \end{cases}$$

	mean	standard deviation	skewness	kurtosis
S&P500	6.919×10^{-5}	1.133×10^{-2}	9.927×10^{-2}	5.245
Dow Jones	1.469×10^{-4}	1.092×10^{-2}	-4.395×10^{-2}	6.501
Nikkei225	7.590×10^{-5}	1.401×10^{-2}	-9.295×10^{-2}	4.524
Seoul comp.	6.657×10^{-4}	2.008×10^{-2}	-2.504×10^{-1}	6.080
TOYOTA	4.820×10^{-4}	1.815×10^{-2}	2.383×10^{-1}	6.712
IBM	4.021×10^{-5}	2.067×10^{-2}	1.439×10^{-1}	10.75
Microsoft	-8.595×10^{-6}	2.255×10^{-2}	-2.135×10^{-1}	10.34
Pfizer	-1.779×10^{-4}	1.936×10^{-2}	-3.646×10^{-1}	6.530
Wal-Mart	8.678×10^{-5}	1.940×10^{-2}	1.880×10^{-1}	5.812
Genral Motors	-1.747×10^{-4}	2.350×10^{-2}	7.446×10^{-1}	7.126

Table 1: Summary statistics of log-returns: over the period 31-Dec-1998 to 12-Dec-2006 for S&P500 Dow Jones IBM Microsoft Pfizer Wal-Mart and General Motors, 22-Oct-1998 to 12-Dec-2006 for Nikkei225, 23-Dec-1998 to 13-Dec-2006 for TOYOTA, 28-Oct-1998 to 12-Dec-2006 for Seoul comp.

$\times 10^{-2}$	S&P500	DJ	Nk225	Seoul Comp.	TOYOTA	IBM	Microsoft	Pfizer	Wal-Mart	GM
bottom 1	−6.005	−7.396	−7.234	−12.80	−9.8249	−16.890	−16.938	−11.815	−9.491	−15.03
2	−5.047	−5.822	−6.864	−12.37	−9.2916	−16.191	−15.633	−11.232	−8.792	−14.52
3	−4.414	−4.752	−5.226	−8.405	−6.6043	−10.671	−12.538	−11.227	−8.657	−10.85
4	−4.242	−4.470	−5.172	−7.625	−6.3893	−9.1690	−12.052	−10.662	−7.586	−10.46
5	−3.911	−4.189	−5.167	−7.441	−6.0506	−8.6660	−12.050	−9.043	−7.548	−8.598
top 5	4.625	4.468	4.584	7.363	7.5499	10.458	9.422	6.545	7.685	8.661
4	4.655	4.690	4.786	7.419	8.0707	10.651	9.470	6.716	7.725	9.146
3	4.888	4.810	4.888	7.515	8.6410	10.946	10.001	6.822	7.967	9.594
2	5.267	5.273	5.735	7.697	11.589	11.347	10.522	7.394	8.132	9.838
1	5.574	6.155	7.222	9.832	12.829	12.365	17.903	7.833	8.742	16.65

Table 2: The bottom and top 5 daily log-returns: over the period 31-Dec-1998 to 12-Dec-2006 for S&P500 and Dow Jones, IBM, Microsoft, Pfizer, Wal-Mart and General Motors. 22-Oct-1998 to 12-Dec-2006 for Nikkei225. 23-Dec-1998 to 13-Dec-2006 for TOYOTA. 28-Oct-1998 to 12-Dec-2006 for Seoul comp.

	Model VG-LS static			Model VG-LS-M static		
	Adj-R^2	-2 × LLF	AIC	Adj-R^2	-2 × LLF	AIC
FJO	0.3194	−732.8	−726.8	0.3898	−748.6	−740.7
NJO	0.0771	−721.8	−715.8	0.5009	−805.1	−797.1
VRG	0.2618	−859.0	−853.0	0.3976	−891.8	−883.8
HJF	0.4373	−714.8	−708.8	0.4346	−715.0	−707.0
FBR	0.1540	−575.3	−569.3	0.5769	−649.8	−641.8
AVO	0.3278	−663.7	−657.7	0.3230	−663.8	−655.8

Table 3: Fitting performance for six Japanese mutual funds by the linear regression model(6) and model(8) over the period Jan-1996 to Apr-2007 for FJO. Mar-1996 to Apr-2007 for NJO. May-1994 to Apr-2007 for VRG. May-1994 to Apr-2007 for HJF. Jul-1998 to Apr-2007 for FBR. Mar-1996 to Apr-2007 for AVO

	γ_{VG}	γ_{LS}	α
FJO	−3.2773(−6.33)	0.022542(0.46)	0.003920(2.72)
NJO	0.002888(0.056)	0.148279(2.99)	0.000253(0.18)
VRG	−0.27523(−5.75)	0.035308(0.79)	0.002974(2.36)
HJF	−0.81345(−10.70)	−0.26574(−3.72)	0.006821(3.40)
FBR	−0.24035(−4.56)	−0.10983(−1.78)	0.001648(1.03)
AVO	0.322558(5.01)	−0.14732(−2.39)	0.003143(1.75)

Table 4: Estimated parameters six Japanese mutual funds by the linear regression model(6), the values in () indicate student's-t value: over the period Jan-1996 to Apr-2007 for FJO. Mar-1996 to Apr-2007 for NJO. May-1994 to Apr-2007 for VRG. May-1994 to Apr-2007 for HJF. Jul-1998 to Apr-2007 for FBR. Mar-1996 to Apr-2007 for AVO.

	γ_{VG}	γ_{LS}	β_M	α
FJO	−0.3847(−7.54)	−0.0153(−0.32)	−0.1201(−4.04)	0.0043(3.15)
NJO	−0.1135(−2.86)	0.0718(1.93)	−0.2454(−10.59)	0.0011(1.00)
VRG	−0.3411(−7.64)	−0.0125(−0.30)	−0.1467(−5.96)	0.0034(3.00)
HJF	−0.8232(−10.47)	−0.2728(−3.74)	−0.0218(−0.50)	0.0069(3.42)
FBR	−0.3694(−9.39)	−0.1542(−3.51)	−0.2525(−10.20)	0.0032(2.77)
AVO	0.3178(4.73)	−0.1505(−2.39)	−0.0101(−0.26)	0.0032(1.76)

Table 5: Estimated parameters six Japanese mutual funds by the linear regression model(8),the values in () indicate student's-t value: over the period Jan-1996 to Apr-2007 for FJO. Mar-1996 to Apr-2007 for NJO. May-1994 to Apr-2007 for VRG. May-1994 to Apr-2007 for HJF. Jul-1998 to Apr-2007 for FBR. Mar-1996 to Apr-2007 for AVO.

	Model VG-LS dynamic		Model VG-LS-M dynamic		Model VG-LS-M-I dynamic	
	-2 × LLF	AIC	-2 × LLF	AIC	-2 × LLF	AIC
FJO	−1576.3	−1572.3	−1618.9	−1612.9	−1850.7	−1842.7
NJO	−1278.6	−1274.6	−1757.3	−1751.3	−2029.3	−2021.3
VRG	−1569.4	−1565.4	−2116.2	−2110.2	−2175.9	−2167.9
HJF	−1243.2	−1239.2	−1456.6	−1450.6	−1907.3	−1899.3
FBR	−1052.7	−1048.7	−1496.8	−1490.8	−1592.6	−1584.6
AVO	−1050.2	−1046.2	−1342.7	−1336.7	−1671.1	−1663.1

Table 6: Fitting performance for six Japanese mutual funds by the dynamic model(7), model(9) and model(10):over the period Jan-1996 to Apr-2007 for FJO. Mar-1996 to Apr-2007 for NJO. May-1994 to Apr-2007 for VRG. May-1994 to Apr-2007 for HJF. Jul-1998 to Apr-2007 for FBR. Mar-1996 to Apr-2007 for AVO.

	γ_{VG}	γ_{LS}	q_{VG}	q_{LS}
FJO	−1.6893	−0.5537	0.5958	0.6373
NJO	−1.4845	0.1814	1.2741	0.8201
VRG	−1.2615	0.2210	0.4731	1.3738
HJF	−0.1878	0.6679	0.1308	3.0577
FBR	−0.5861	−2.5994	1.4484	0.5357
AVO	−3.1526	−0.6510	1.2354	1.8433

Table 7: Estimated parameters for six Japanese mutual funds by the dynamic model(7):over the period Jan-1996 to Apr-2007 for FJO. Mar-1996 to Apr-2007 for NJO. May-1994 to Apr-2007 for VRG. May-1994 to Apr-2007 for HJF. Jul-1998 to Apr-2007 for FBR. Mar-1996 to Apr-2007 for AVO.

	γ_{VG}	γ_{LS}	β_M	q_{VG}	q_{LS}	q_M
FJO	−0.5091	0.4222	0.1109	0.0410	0.6103	0.1847
NJO	−0.3973	−0.0347	−0.1794	0.2841	0.4572	0.0248
VRG	−0.6827	−1.1458	0.1098	0.1381	0.2215	0.1773
HJF	0.0365	−1.1349	0.4648	0.7102	1.3402	0.0471
FBR	−0.5437	−0.5935	−0.1842	0.0638	0.1727	0.1943
AVO	−1.0736	−0.5825	−0.3678	0.6341	0.9122	0.0804

Table 8: Estimated parameters for six Japanese mutual funds by the dynamic model(9):over the period Jan-1996 to Apr-2007 for FJO. Mar-1996 to Apr-2007 for NJO. May-1994 to Apr-2007 for VRG. May-1994 to Apr-2007 for HJF. Jul-1998 to Apr-2007 for FBR. Mar-1996 to Apr-2007 for AVO.

	$\gamma_{VG,0}$	$\gamma_{LS,0}$	$\beta_{M,0}$	$\gamma_{I,0}$	q_{VG}	q_{LS}	q_M	q_I
FJO	−0.09742	0.03187	−0.04638	−0.00135	0.01873	0.03908	0.18246	0.00108
NJO	−0.07571	0.19862	−0.20017	−0.00095	0.02437	0.05832	0.10165	0.00062
VRG	−0.13996	−0.29304	−1.29545	0.00170	0.04263	0.01698	0.05406	0.00099
HJF	0.35696	−0.67803	−0.32163	0.00071	0.07981	0.11406	0.22103	0.00094
FBR	−0.32727	−0.55732	−0.56088	0.00030	0.03004	0.11884	0.03176	0.00054
AVO	−0.32311	−0.33767	0.09381	−0.00120	0.07292	0.04423	0.16598	0.00104

Table 9: Estimated parameters for six Japanese mutual funds by model(10), over the period Jan-1996 to Apr-2007 for FJO. Mar-1996 to Apr-2007 for NJO. May-1994 to Apr-2007 for VRG. May-1994 to Apr-2007 for HJF. Jul-1998 to Apr-2007 for FBR. Mar-1996 to Apr-2007 for AVO.

	$S_{0\|0}$	$\eta_{0\|0}$	α	β	θ_1	γ	θ_2	ξ_0	-2 $\times LLF$	AIC
S&P500	7.116	24.57	2.115×10^{-2}	-2.947×10^{-3}	7.124×10^{-8}	-1.992×10^{-3}	7.025×10^{-6}	-3.633×10^{-3}	-6333.4	-6323.4
Dow Jones	9.135	22.13	5.019×10^{-2}	-5.397×10^{-3}	2.417×10^{-7}	-2.197×10^{-3}	6.349×10^{-6}	-4.042×10^{-3}	-6414.5	-6409.5
Nikkei225	9.562	26.55	2.016×10^{-2}	-2.085×10^{-3}	3.757×10^{-8}	-1.987×10^{-3}	1.236×10^{-5}	-4.565×10^{-3}	-5788.6	-5778.6
Seoul comp.	5.887	23.84	1.153×10^{-2}	-1.573×10^{-3}	2.827×10^{-7}	-9.890×10^{-4}	9.974×10^{-6}	-4.286×10^{-3}	-5156.7	-5146.7
TOYOTA	3.888	13.52	2.650×10^{-2}	-4.850×10^{-4}	2.819×10^{-5}	-2.653×10^{-3}	1.314×10^{-5}	9.990×10^{-2}	-5304.9	-5294.9
Microsoft	3.402	18.05	2.235×10^{-2}	-6.887×10^{-3}	3.544×10^{-6}	-4.138×10^{-4}	3.923×10^{-6}	-4.093×10^{-3}	-5149.8	-5139.8
Pfizer	3.490	3.657	1.448×10^{-2}	-4.378×10^{-3}	4.063×10^{-3}	-7.014×10^{-3}	1.021×10^{-5}	-5.318×10^{-3}	-5320.1	-5310.1
Wal-Mart	3.639	24.54	6.413×10^{-2}	-1.641×10^{-2}	8.178×10^{-8}	-1.097×10^{-3}	1.159×10^{-5}	-4.212×10^{-3}	-5195.3	-5185.3
IBM	4.477	19.92	3.648×10^{-2}	-8.117×10^{-3}	1.626×10^{-6}	-5.971×10^{-4}	4.866×10^{-6}	1.022×10^{-1}	-6333.4	-6323.4
General Motors	3.765	2.632	1.541×10^{-2}	-4.200×10^{-3}	9.403×10^{-3}	-1.756×10^{-2}	2.095×10^{-5}	1.014×10^{-1}	-4751.5	-4741.5

Table 10: Estimated parameters and fitting performance by model(24):over the period 31-Dec-1998 to 12-Dec-2006 for S&P500, Dow Jones, IBM Microsoft, Pfizer, Wal-Mart and General Motors. 22-Oct-1998 to 12-Dec-2006 for Nikkei225. 23-Dec-1998 to 13-Dec-2006 for TOYOTA. 28-Oct-1998 to 12-Dec-2006 for Seoul comp.

	$S_{0\|0}$	$\phi_{0\|0}$	$\lambda_{0\|0}$	β	γ	θ_1	θ_2	θ_3	-2 × LLF	AIC
S&P500	7.114	1.268×10^{-4}	1.731	-8.537×10^{-1}	-3.617×10^{-3}	5.043×10^{-3}	4.032×10^{-4}	1.960×10^{-1}	−6210.4	−6200.4
TOYOTA	3.856	2.772×10^{-4}	1.858	-8.842×10^{-1}	-3.396×10^{-4}	4.833×10^{-3}	7.622×10^{-4}	1.387×10^{-2}	−5231.7	−5221.7

Table 11: Estimated parameters and fitting performance by MMS model(28):over the period 31-Dec-1998 to 12-Dec-2006 for S&P500. 23-Dec-1998 to 13-Dec-2006 for TOYOTA.

fund	-2 × LLF	AIC	strategy	improvement
FJO	−1850.9	−1840.9	LS	+1.8
NJO	−2044.0	−2034.0	VG	−12.7
VRG	−2187.8	−2177.8	IS	−9.1
HJF	−1917.3	−1907.3	IS	−8.0
FBR	−1598.5	−1588.5	VG	−3.9
AVO	−1673.0	−1663.0	IS	+0.1

Table 12: Fitting performance for six Japanese mutual funds by the Gaussian noise model(8) and mixed Gaussian-Poisson noise model(33): over the period Jan-1996 to Apr-2007 for FJO. Mar-1996 to Apr-2007 for NJO. May-1994 to Apr-2007 for VRG. May-1994 to Apr-2007 for HJF. Jul-1998 to Apr-2007 for FBR. Mar-1996 to Apr-2007 for AVO.

	$\gamma_{VG,0}$	$\gamma_{LS,0}$	$\beta_{M,0}$	$\gamma_{I,0}$	q_{VG}	q_{LS}	q_M	q_I	ι_κ
FJO	−0.09734	0.03139	−0.04976	−0.00135	0.01866	0.03937	0.1781	0.00109	0.00064
NJO	−0.08294	0.22807	−0.39157	−0.0007	0.04696	0.05023	0.06448	0.00059	0.34772
VRG	−0.16727	−0.29353	−1.30468	0.00187	0.03224	0.01761	0.05195	0.001	0.00238
HJF	0.39216	−0.70845	−0.35029	0.00067	0.08491	0.13023	0.17002	0.00092	0.00337
FBR	−0.33113	−0.54698	−0.59994	0.00024	0.03137	0.11283	0.02232	0.00053	0.12165
AVO	−0.32132	0.33820	0.07601	−0.00119	0.07035	0.04368	0.15583	0.00106	0.13254

Table 13: Estimated parameters for six Japanese mutual funds by model(33), over the period Jan-1996 to Apr-2007 for FJO. Mar-1996 to Apr-2007 for NJO. May-1994 to Apr-2007 for VRG. May-1994 to Apr-2007 for HJF. Jul-1998 to Apr-2007 for FBR. Mar-1996 to Apr-2007 for AVO.

	$S_{0\|0}$	$\eta_{0\|0}$	α	β	θ_1	γ	θ_2	ξ_0	ζ	-2 $\times LLF$	AIC	improvement
S&P500	7.116	27.25	1.468×10^{-2}	-2.025×10^{-3}	1.885×10^{-8}	-1.971×10^{-3}	7.514×10^{-6}	-3.625×10^{-3}	3.020	-6356.7	-6344.7	-21.3
Dow Jones	9.135	22.33	4.319×10^{-2}	-4.632×10^{-3}	8.053×10^{-8}	-1.953×10^{-3}	6.017×10^{-6}	-3.908×10^{-3}	3.023	-6449.3	-6437.3	-27.8
Nikkei225	9.562	22.71	1.752×10^{-2}	-1.806×10^{-3}	2.603×10^{-7}	-2.476×10^{-3}	1.274×10^{-5}	-4.520×10^{-3}	3.051	-5826.8	-5814.8	-36.2
Seoul comp.	5.887	26.65	1.798×10^{-2}	-2.483×10^{-3}	5.141×10^{-8}	-2.075×10^{-3}	2.363×10^{-5}	-4.235×10^{-3}	3.454	-5218.0	-5206.0	-59.3
TOYOTA	3.888	19.02	1.476×10^{-3}	-2.503×10^{-4}	1.811×10^{-6}	-1.826×10^{-3}	1.265×10^{-5}	9.646×10^{-2}	3.545	-5342.8	-5294.9	-35.9
Microsoft	3.402	22.73	1.420×10^{-2}	-4.246×10^{-3}	3.947×10^{-7}	-1.356×10^{-3}	1.480×10^{-5}	-5.302×10^{-3}	4.078	-5109.8	-5097.8	-133.4
Pfizer	3.490	20.80	1.878×10^{-2}	-5.565×10^{-3}	7.819×10^{-7}	-1.604×10^{-3}	1.332×10^{-5}	-3.261×10^{-3}	3.672	-5276.6	-5264.6	-124.8
Wal-Mart	3.639	24.35	6.316×10^{-2}	-1.616×10^{-2}	2.343×10^{-8}	-7.783×10^{-4}	8.408×10^{-6}	-4.212×10^{-3}	2.678	-5329.3	-5317.3	-7.2
IBM	4.477	32.00	3.695×10^{-2}	-8.154×10^{-3}	3.128×10^{-9}	-7.183×10^{-4}	9.518×10^{-6}	3.822×10^{-2}	3.583	-5292.5	-5280.5	-95.2
General Motors	3.765	19.23	1.506×10^{-2}	-4.176×10^{-3}	2.219×10^{-6}	-1.960×10^{-3}	2.279×10^{-5}	1.022×10^{-1}	3.886	-4843.9	-4831.9	-90.4

Table 14: Estimated parameters and fitting performance by model(42):over the period 31-Dec-1998 to 12-Dec-2006 for S&P500, Dow Jones, IBM, Microsoft, Pfizer, Wal-Mart and General Motors. 22-Oct-1998 to 12-Dec-2006 for Nikkei225. 23-Dec-1998 to 13-Dec-2006 for TOYOTA. 28-Oct-1998 to 12-Dec-2006 for Seoul comp.

	$S_{0\|0}$	$\phi_{0\|0}$	$\lambda_{0\|0}$	δ	β	γ	θ_1	θ_2	θ_3	-2 $\times LLF$	AIC	improvement
S&P500	7.127	-1.269×10^{-4}	2.957	-8.382×10^{-3}	-1.000	-9.550×10^{-4}	3.551×10^{-3}	3.591×10^{-4}	7.250×10^{-2}	-6246.3	-6234.3	-33.9
TOYOTA	3.867	4.417×10^{-4}	1.259	9.711×10^{-2}	-7.200×10^{-1}	5.993×10^{-3}	6.359×10^{-3}	8.510×10^{-4}	1.206×10^{-1}	-5273.6	-5261.6	-39.9

Table 15: Estimated parameters and fitting performance by HPMMS model(46):over the period 31-Dec-1998 to 12-Dec-2006 for S&P500. 23-Dec-1998 to 13-Dec-2006 for TOYOTA.

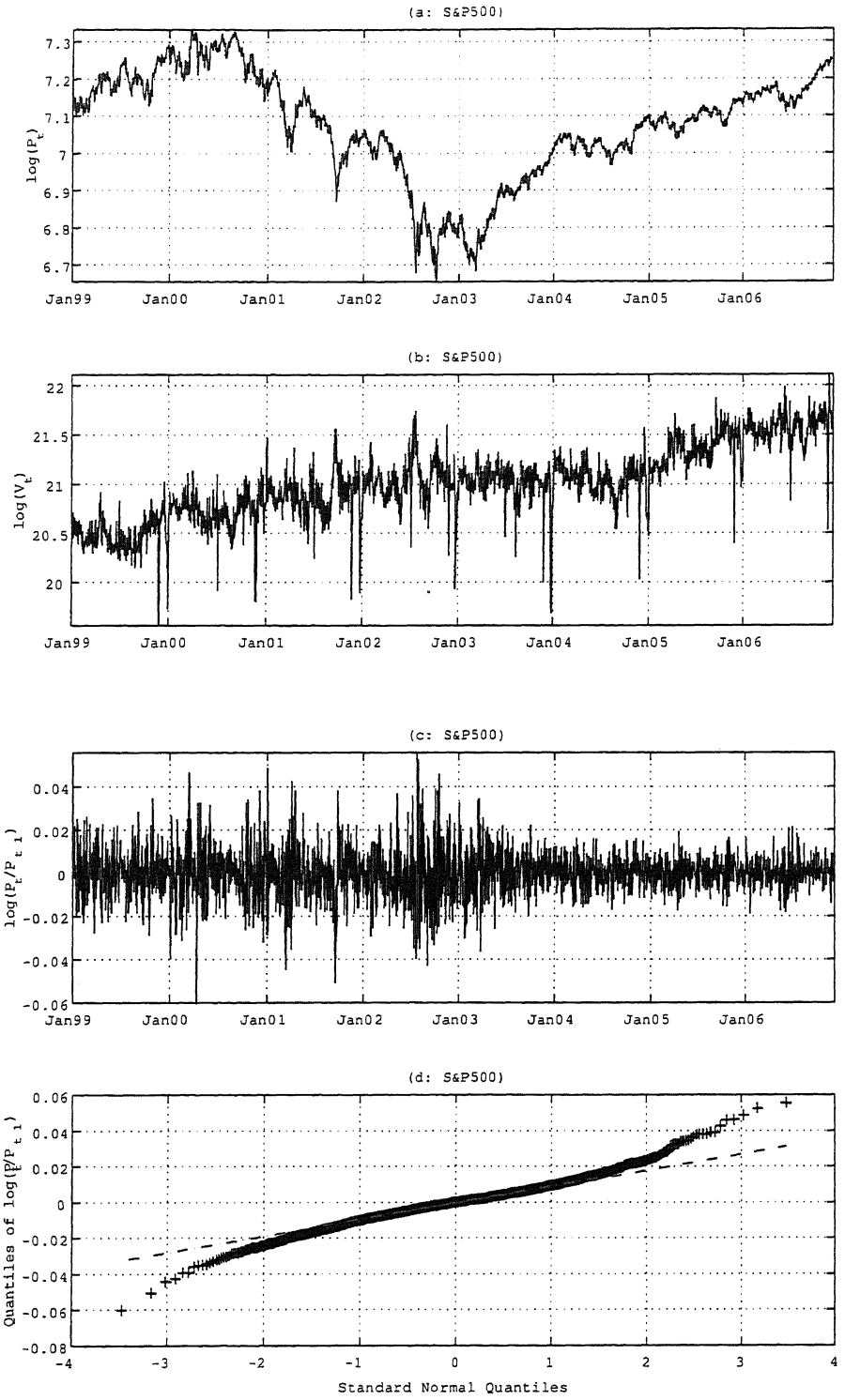

Figure 1: The daily closing log-price (a), the daily trading log-volume (b), the daily log-returns (c) and the normal-quantile log-returns plot (d)of the Standard & Poor's 500 stock index over the period 31-Dec-1998 to 12-Dec-2006.

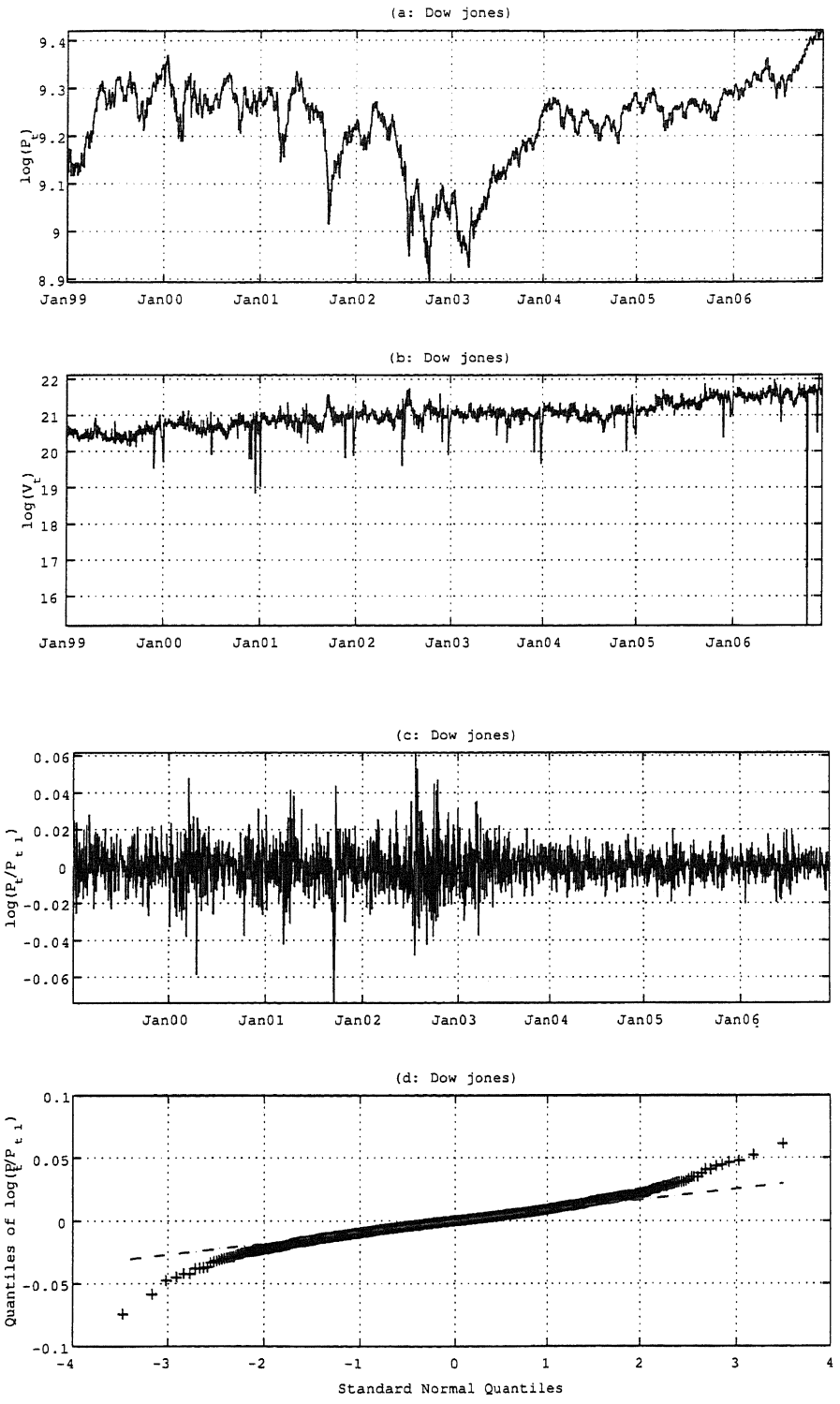

Figure 2: The daily closing log-price (a), the daily trading log-volume (b), the daily log-returns (c) and the normal-quantile log-returns plot (d)of the Dow Jones stock index over the period 31-Dec-1998 to 12-Dec-2006.

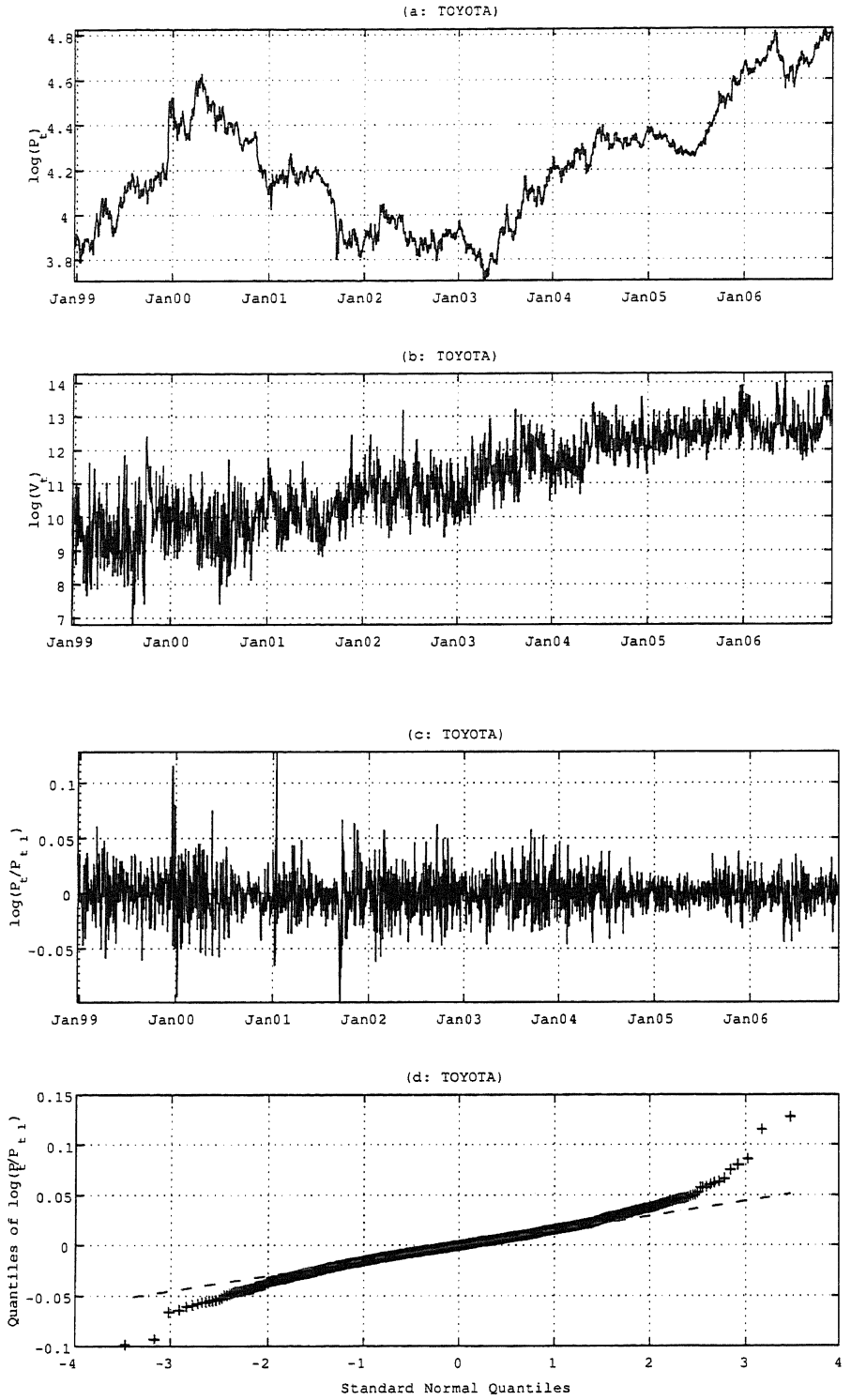

Figure 3: The daily closing log-price (a) and the daily trading log-volume (b), the daily log-returns (c) and the normal-quantile log-returns plot (d) of TOYOTA Motors stock over the period 23-Dec-1998 to 13-Dec-2006.

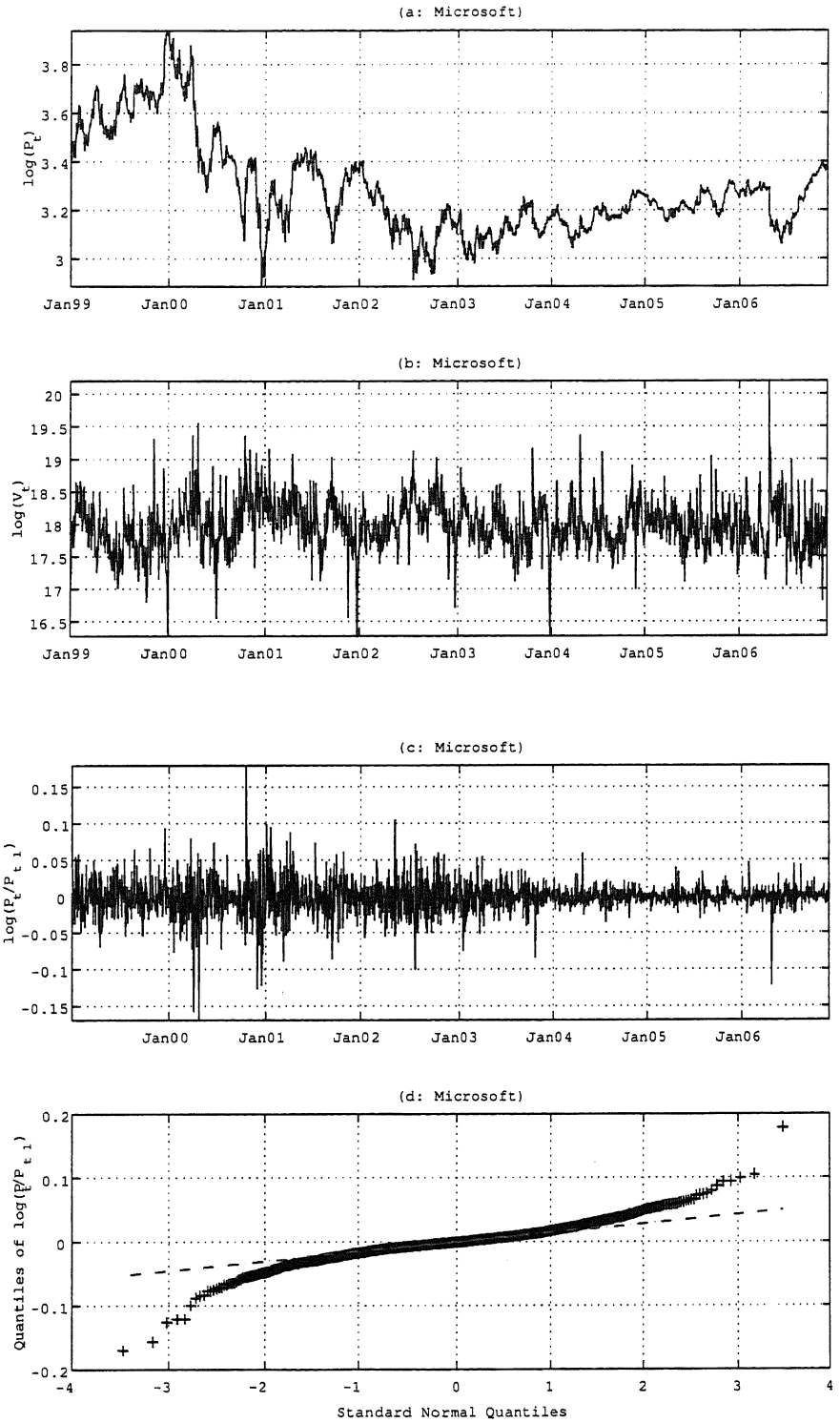

Figure 4: The daily closing log-price (a) and the daily trading log-volume (b),the daily log-returns (c) and the normal-quantile log-returns plot (d) of Microsoft Corp. stock over the period 31-Dec-1998 to 12-Dec-2006.

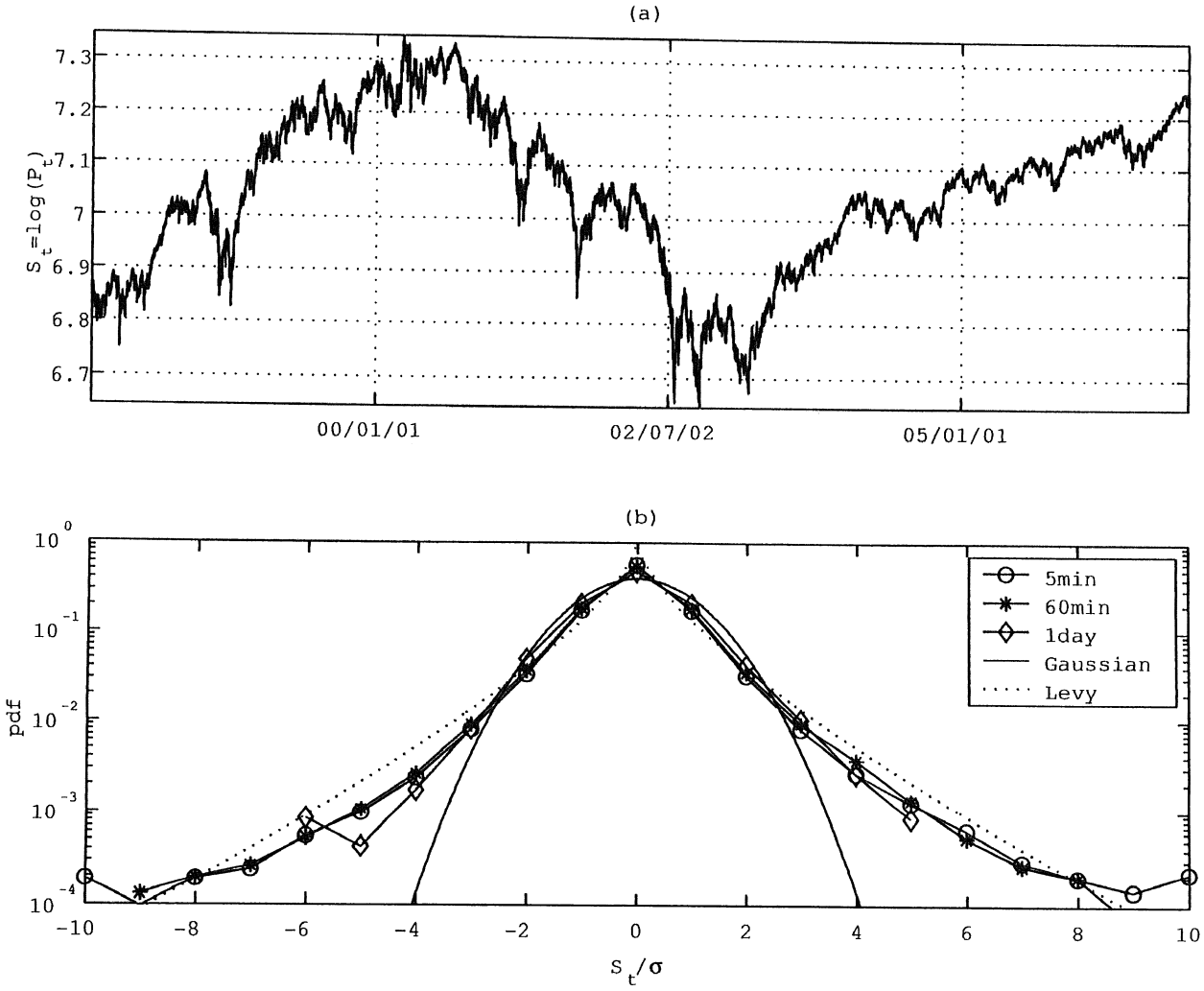

Figure 5: Time series of plot chart(a) and phenomenalistic probability density function of high frequency price data of S&P500 index over the period 31-Dec-1998 to 12-Dec-2006.

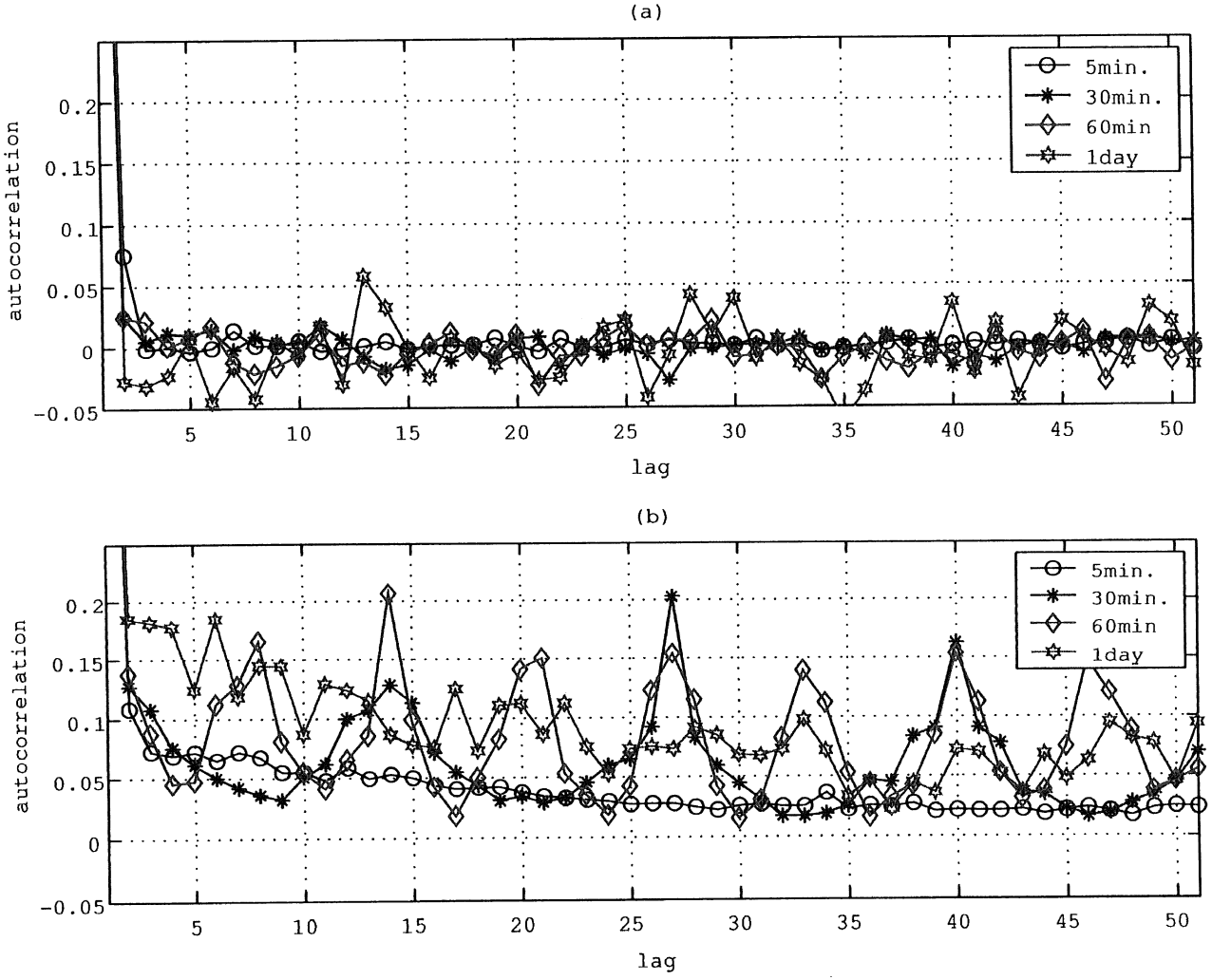

Figure 6: S&P500 index, τ=5min., 30min., 60min. and 1 day over the period 1-Apr-2006 to 31-Aug-2006. (a):autocorrelation function of log-returns. (b)autocorrelation function of squared log-returns.

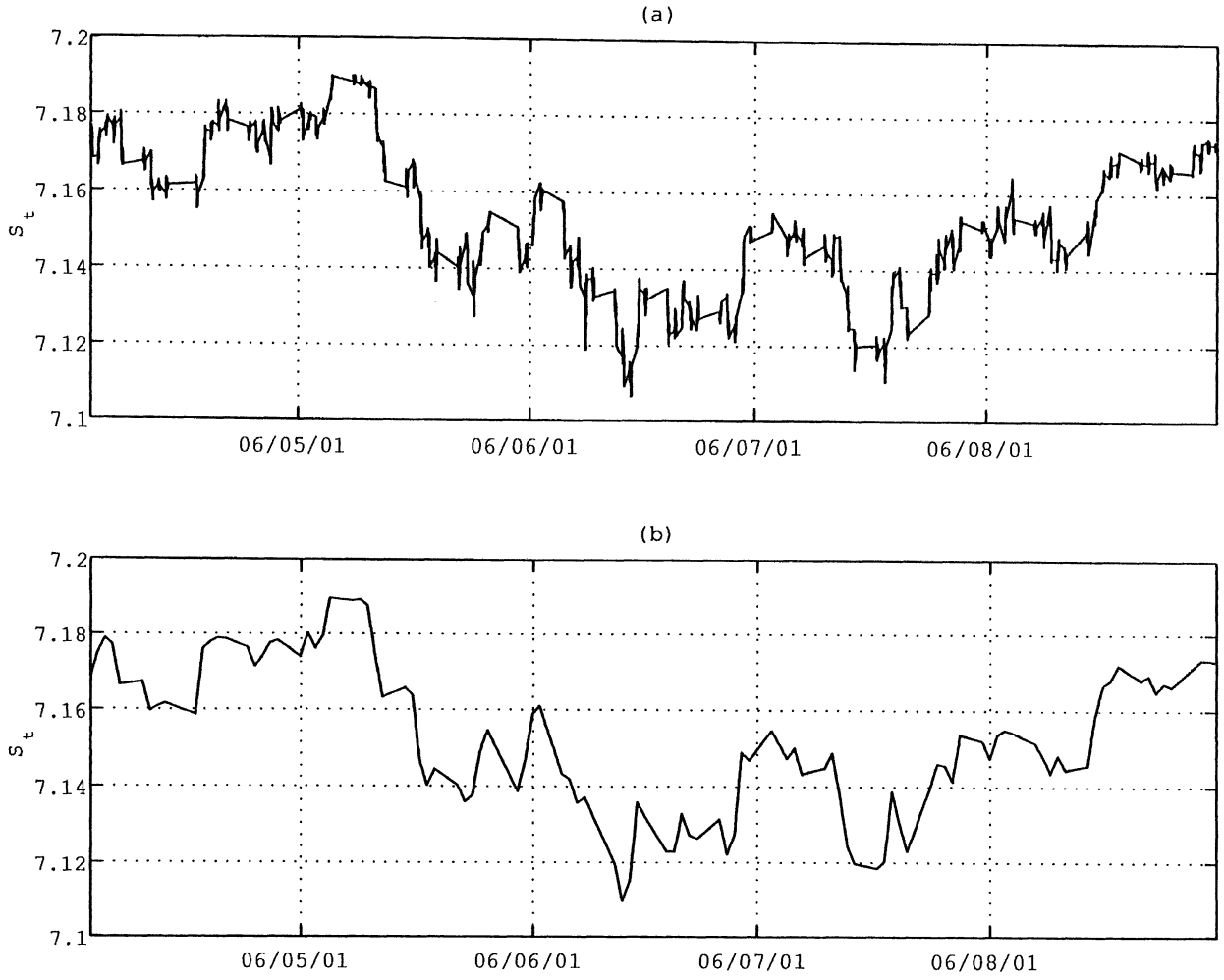

Figure 7: Time series charts of S&P500 index over the period 1-Apr-2006 to 31-Aug-2006: high frequency price data τ=5min. (a) and daily closing price data(b).

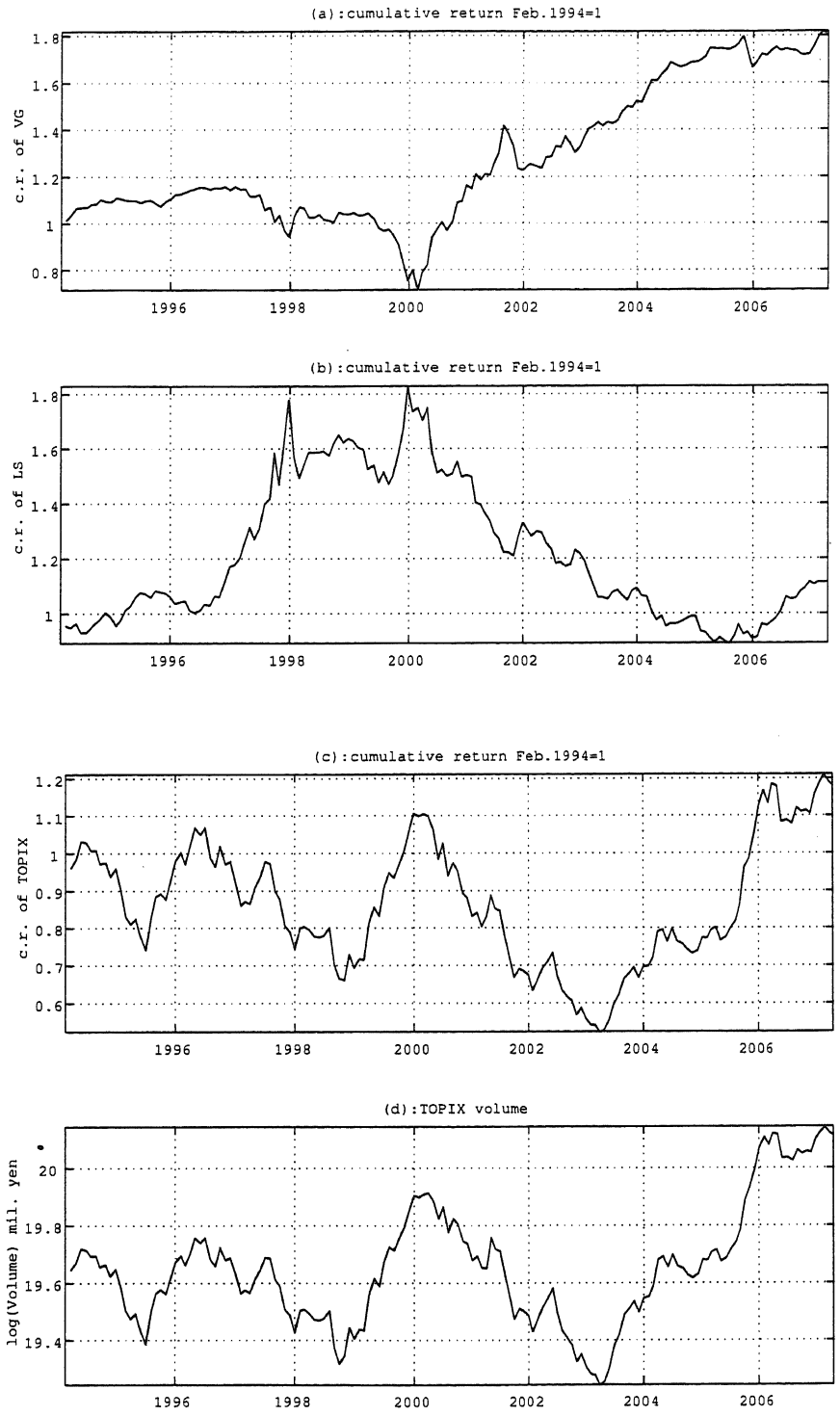

Figure 8: time series of cumulative each factor returns over the period Feb-1994 to Nov-2006, (a) VG, (b) LS, (c) TOPIX as Feb-1994 = 1, and (d) the market(TOPIX) volume.

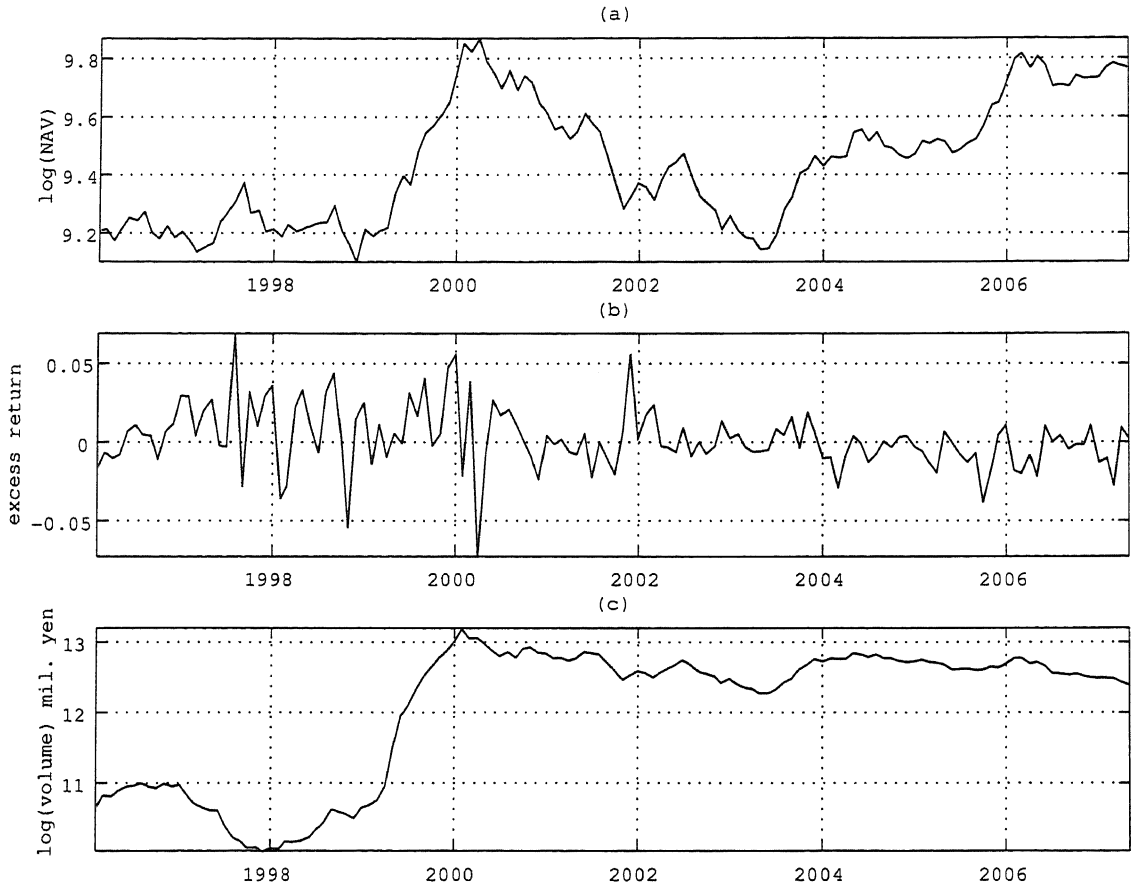

Figure 9: FJO: (a) Net Asset Value(NAV), (b) excess returns and (c) log-volume, over the period Jan-1996 to Apr-2007.

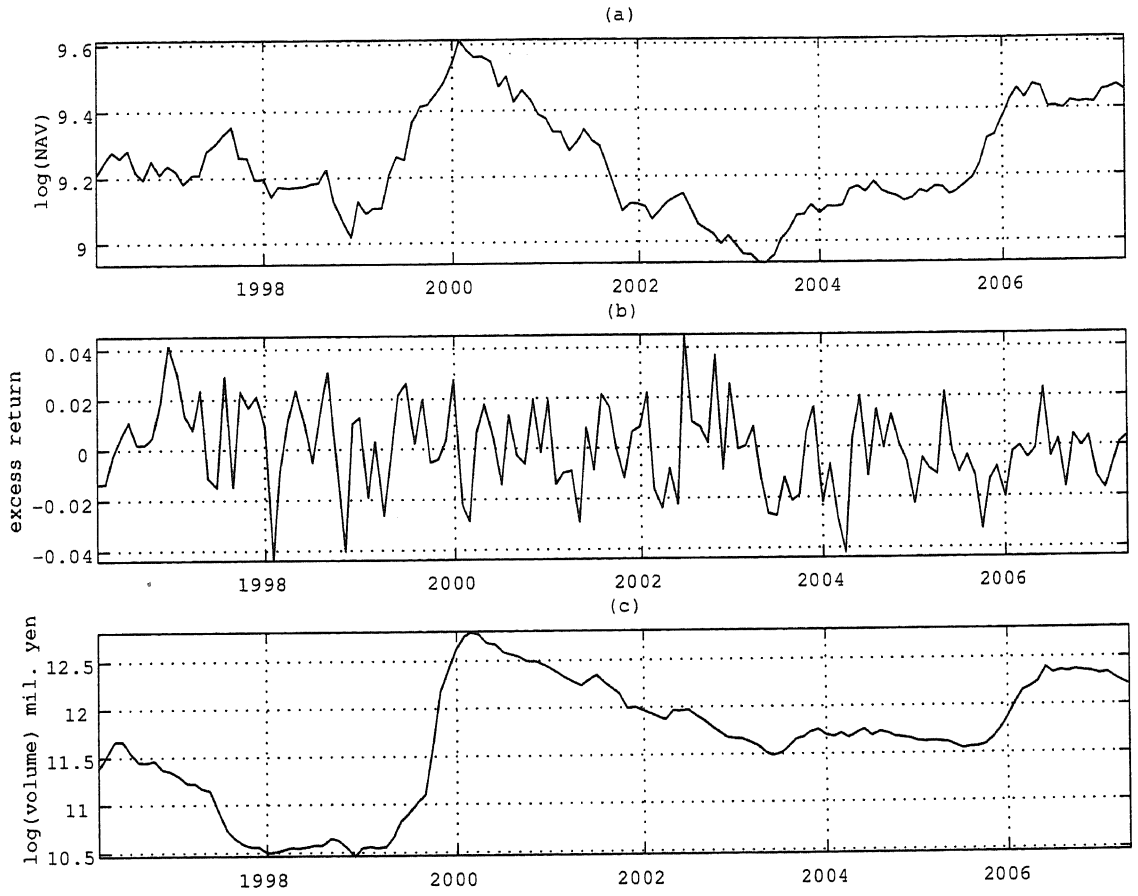

Figure 10: NJO: (a) Net Asset Value(NAV), (b) excess returns and (c) log-volume, over the period Mar-1996 to Apr-2007.

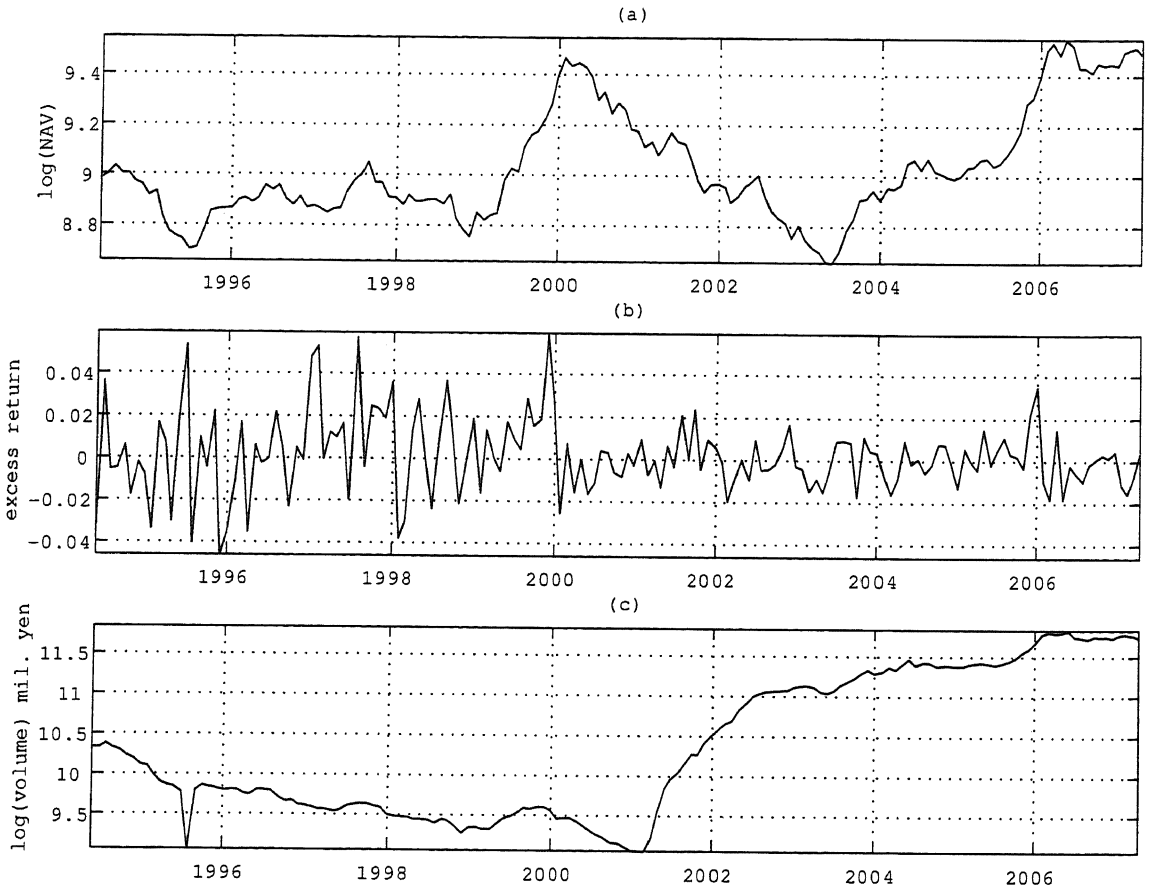

Figure 11: VRG: (a) Net Asset Value(NAV), (b) excess returns and (c) log-volume, over the period May-1994 to Apr-2007.

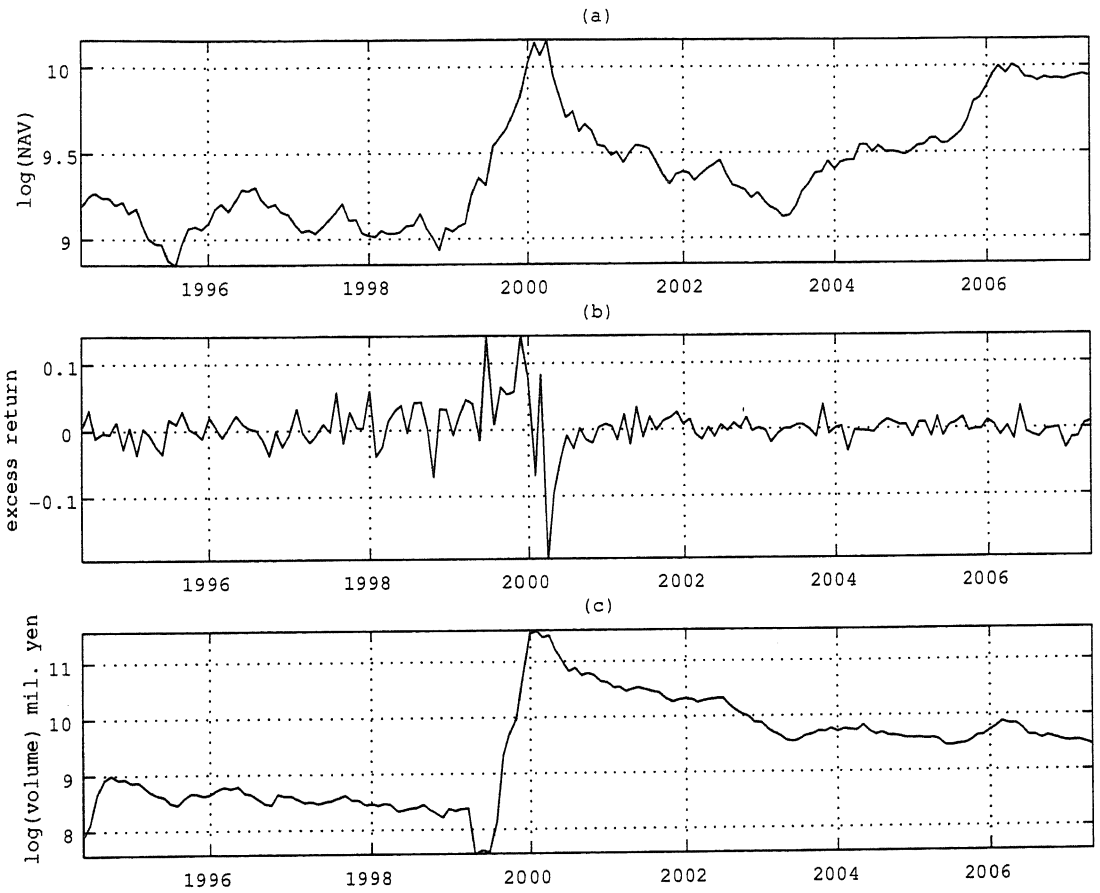

Figure 12: HJF: (a) Net Asset Value(NAV), (b) excess returns and (c) log-volume, over the period May-1994 to Apr-2007.

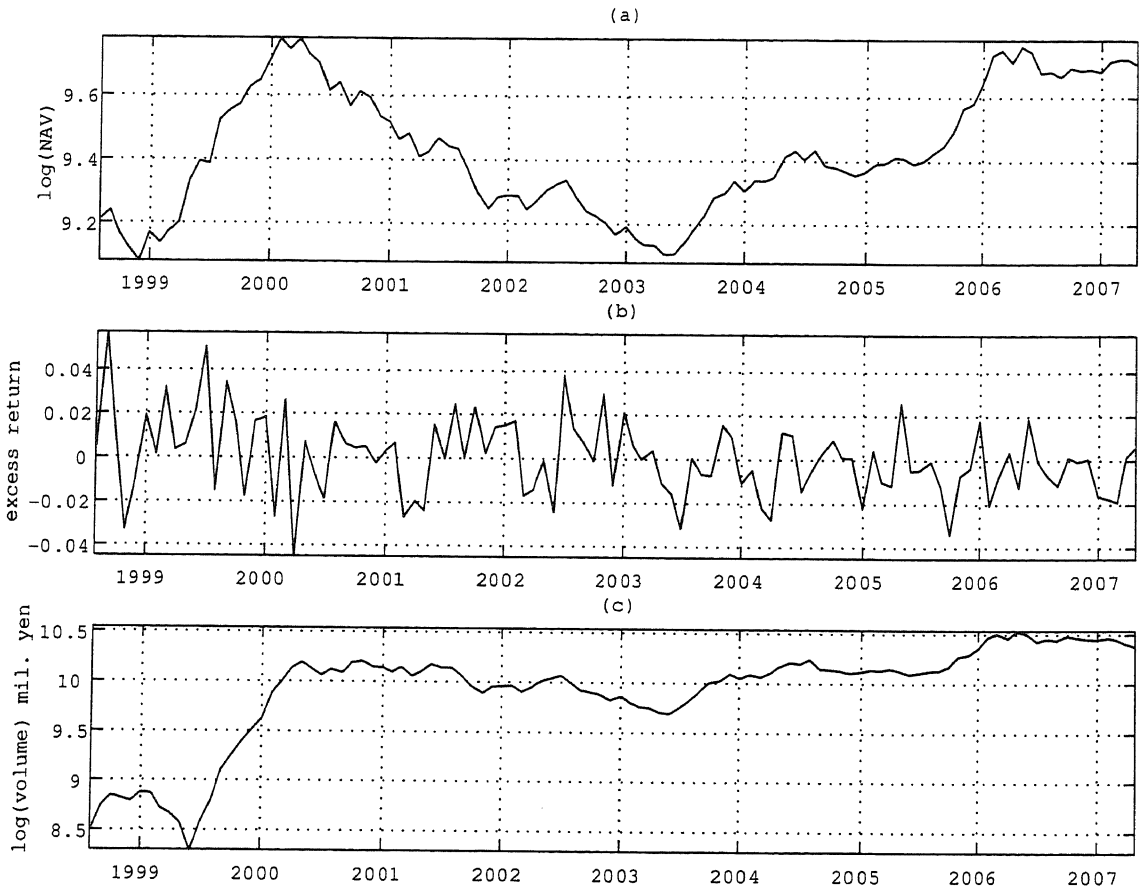

Figure 13: FBR: (a) Net Asset Value(NAV), (b) excess returns and (c) log-volume, over the period Jul-1998 to Apr-2007.

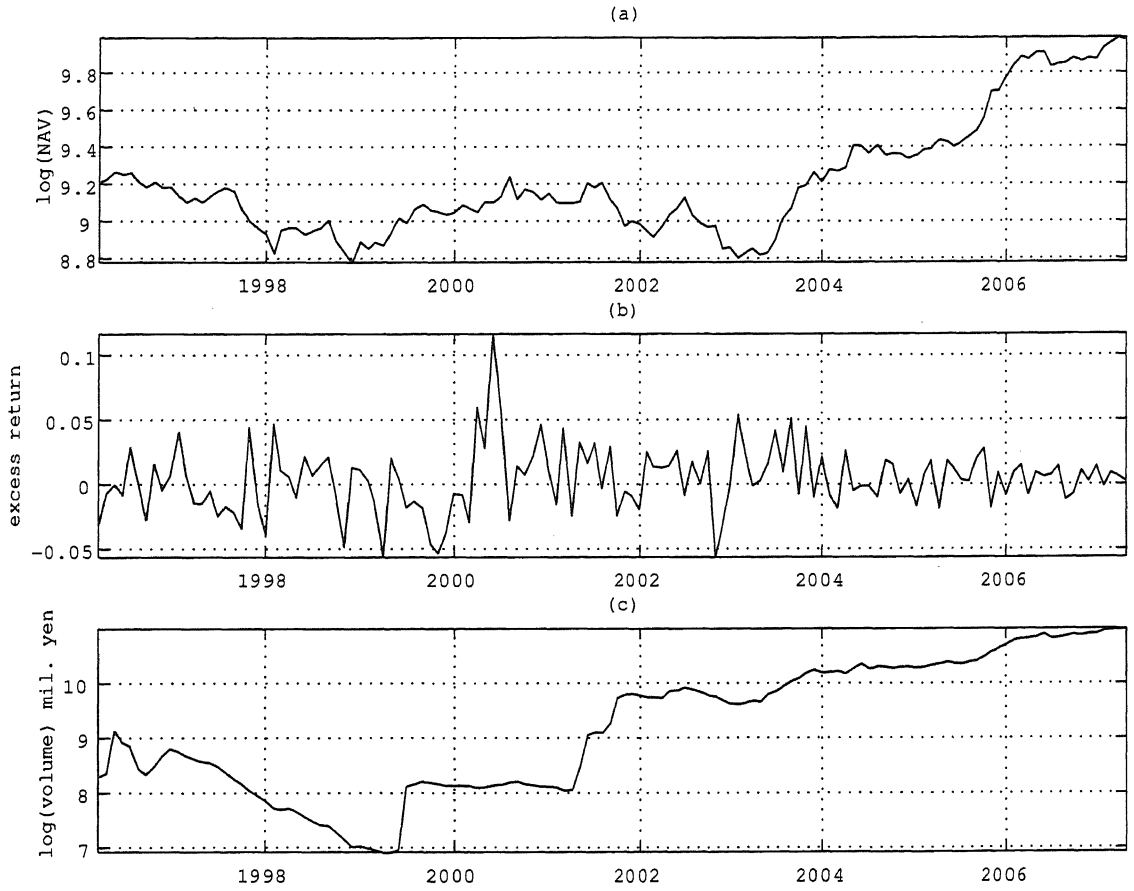

Figure 14: AVO: (a) Net Asset Value(NAV), (b) excess returns and (c) log-volume, over the period Mar-1996 to Apr-2007.

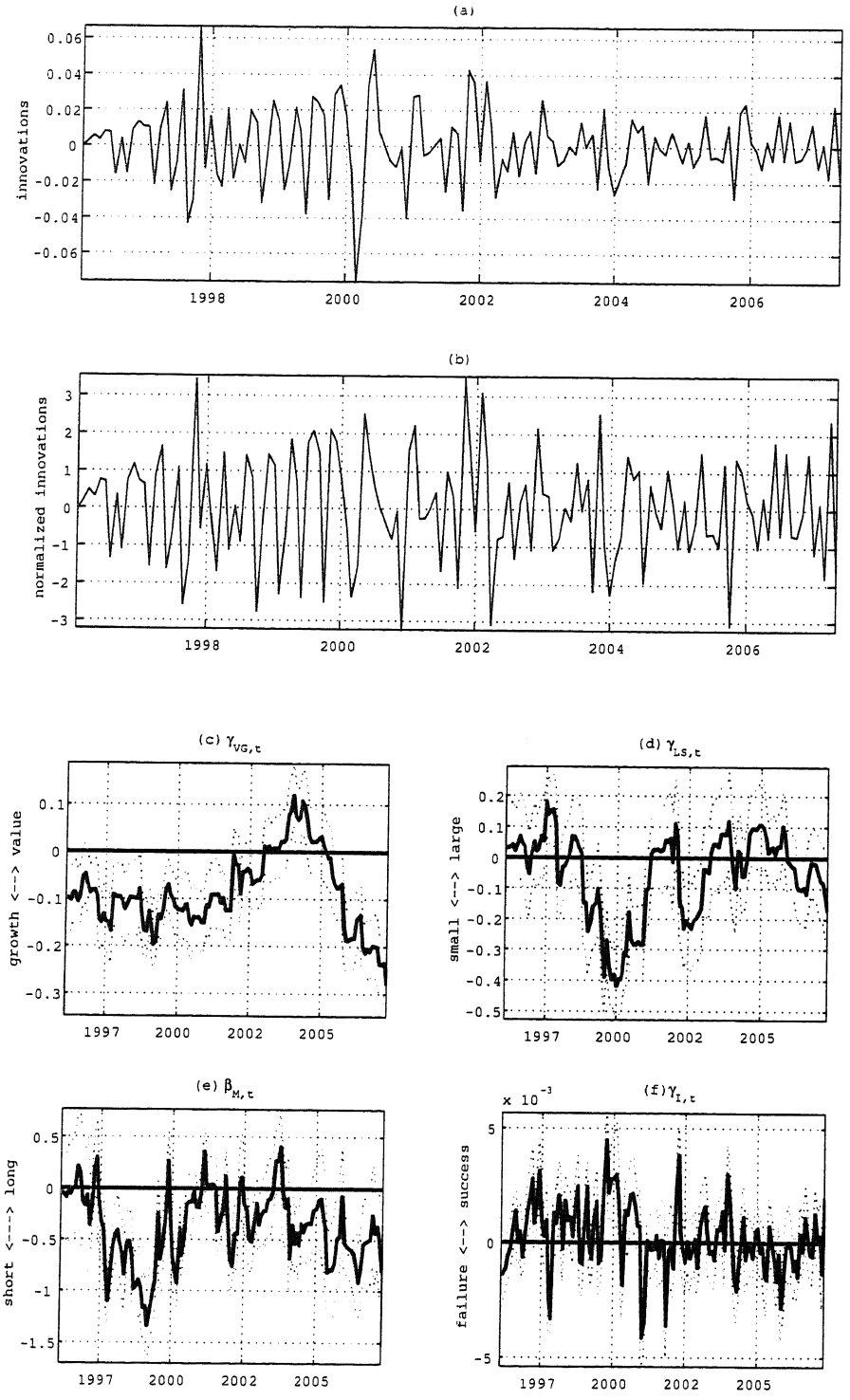

Figure 15: Estimated results of FJO (1) by model (10); (a):innovations, (b):normalized innovations, (c):$\gamma_{VG,t}$, (d):$\gamma_{LS,t}$, (e):$\beta_{M,t}$ and (f):$\gamma_{I,t}$

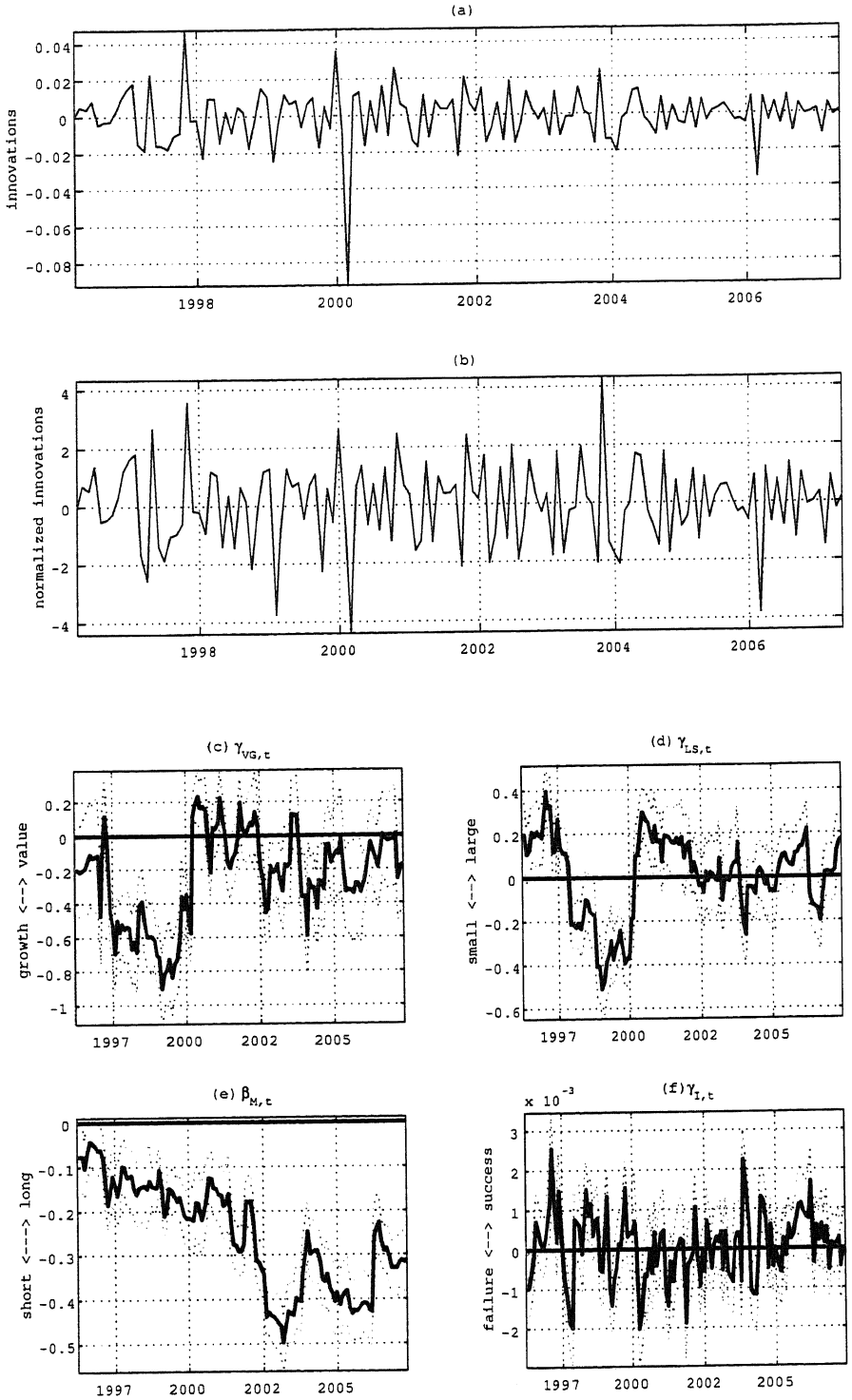

Figure 16: Estimated results of NJO (1) by model (10); (a):innovations, (b):normalized innovations, (c):$\gamma_{VG,t}$, (d):$\gamma_{LS,t}$, (e):$\beta_{M,t}$ and (f):$\gamma_{I,t}$

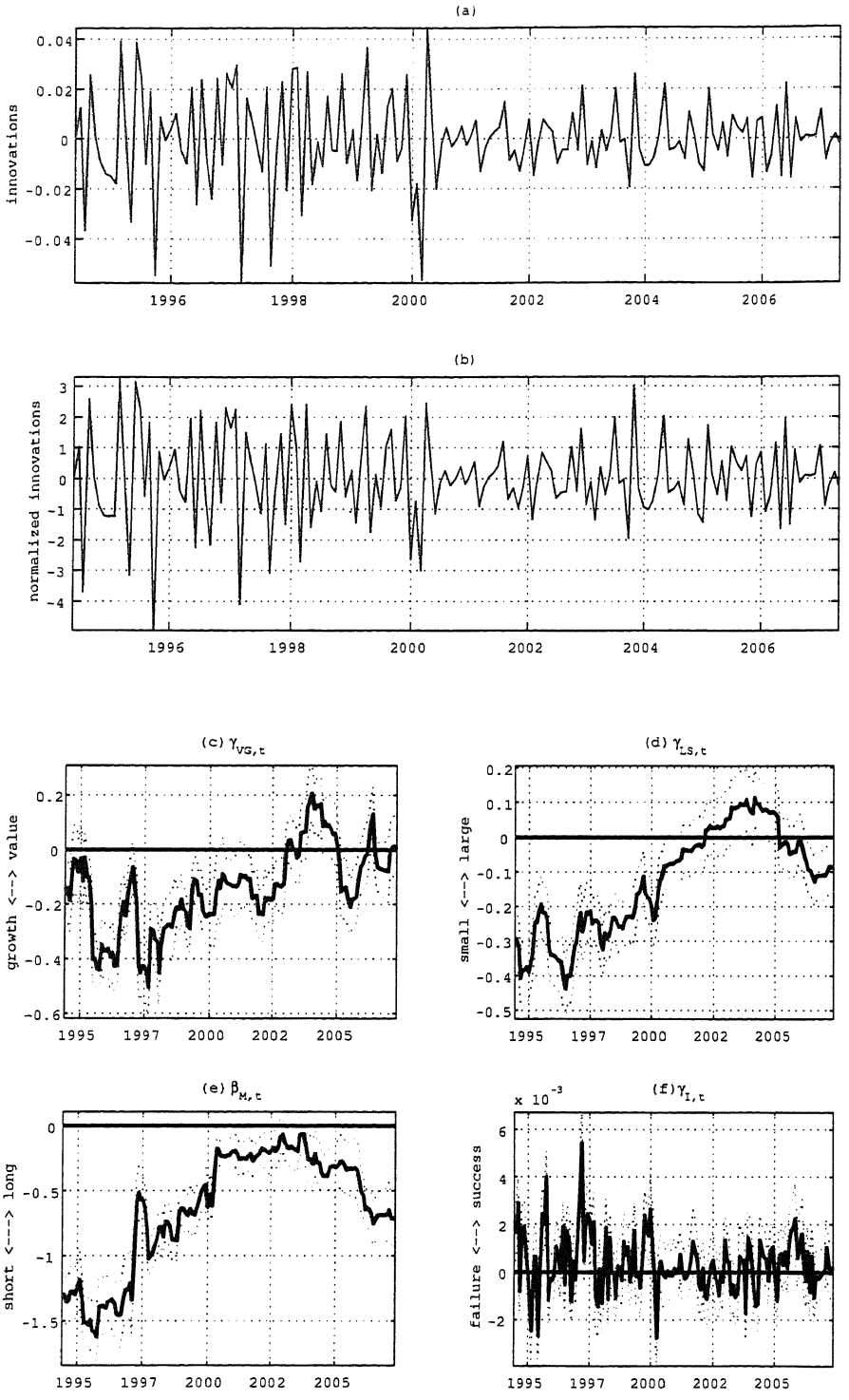

Figure 17: Estimated results of VRG (1) by model (10); (a):innovations, (b):normalized innovations, (c):$\gamma_{VG,t}$, (d):$\gamma_{LS,t}$, (e):$\beta_{M,t}$ and (f):$\gamma_{I,t}$

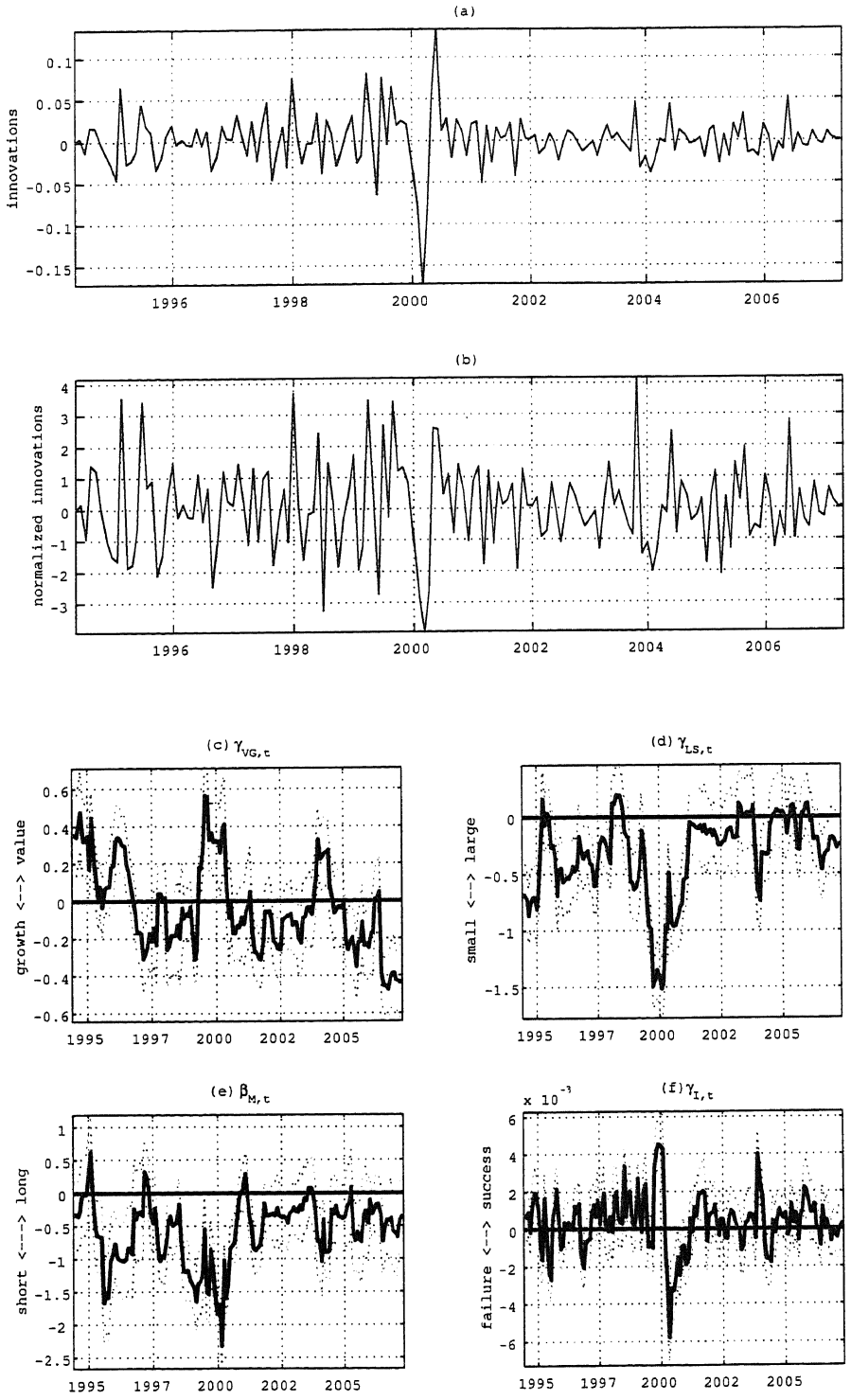

Figure 18: Estimated results of HJF (1) by model (10); (a):innovations, (b):normalized innovations, (c):$\gamma_{VG,t}$, (d):$\gamma_{LS,t}$, (e):$\beta_{M,t}$ and (f):$\gamma_{I,t}$

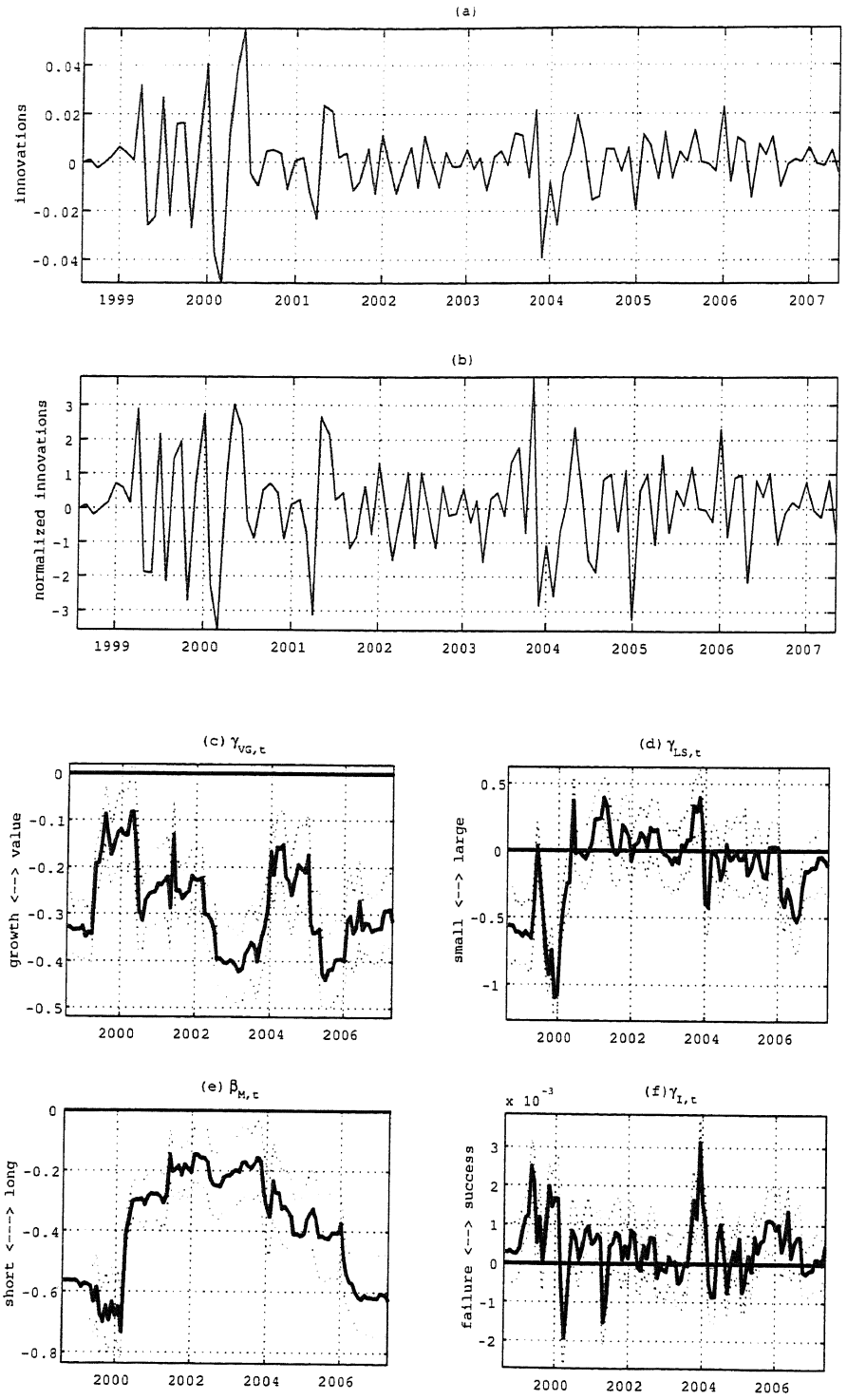

Figure 19: Estimated results of FBR (1) by model (10); (a):innovations, (b):normalized innovations, (c):$\gamma_{VG,t}$, (d):$\gamma_{LS,t}$, (e):$\beta_{M,t}$ and (f):$\gamma_{I,t}$

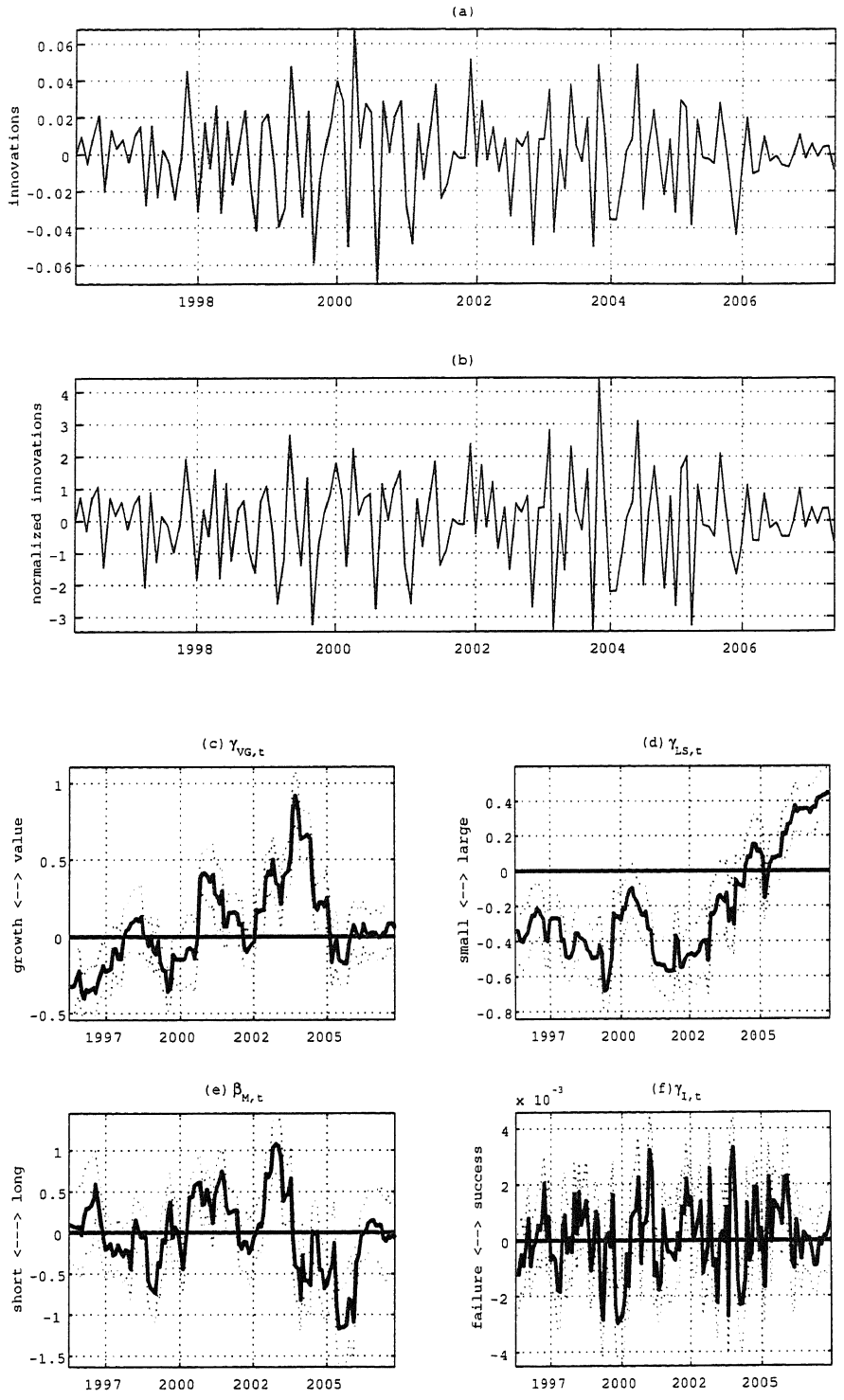

Figure 20: Estimated results of AVO (1) by model (10); (a):innovations, (b):normalized innovations, (c):$\gamma_{VG,t}$, (d):$\gamma_{LS,t}$, (e):$\beta_{M,t}$ and (f):$\gamma_{I,t}$

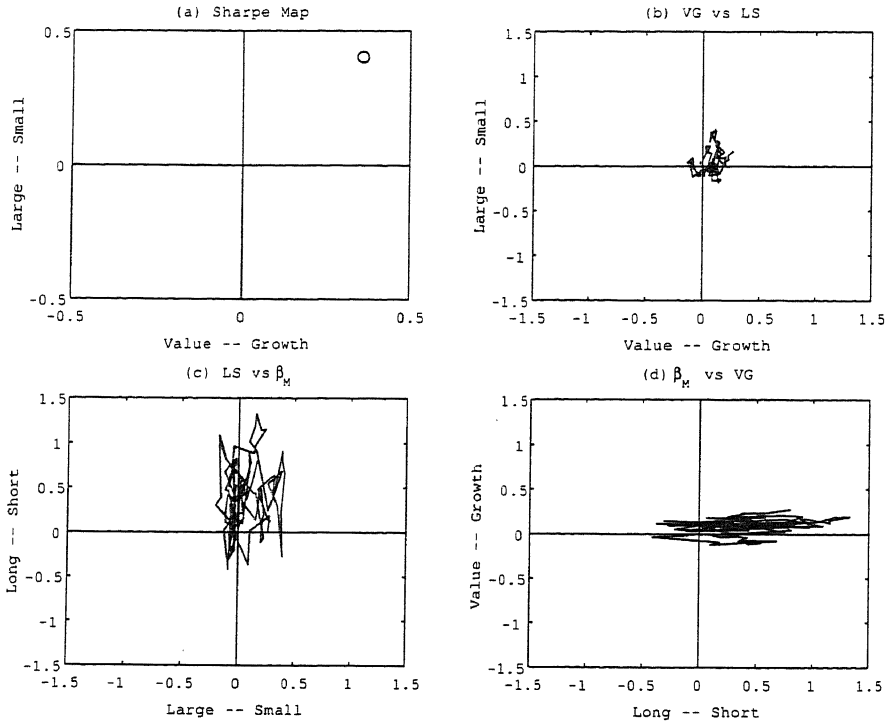

Figure 21: Estimated results of FJO (2) by model (10); (a):Sharpe(VG-LS) map, (b):VG-LS map, (c):β_M-VG map, (d):LS-β_M map, (e):cumulative return by model(10).

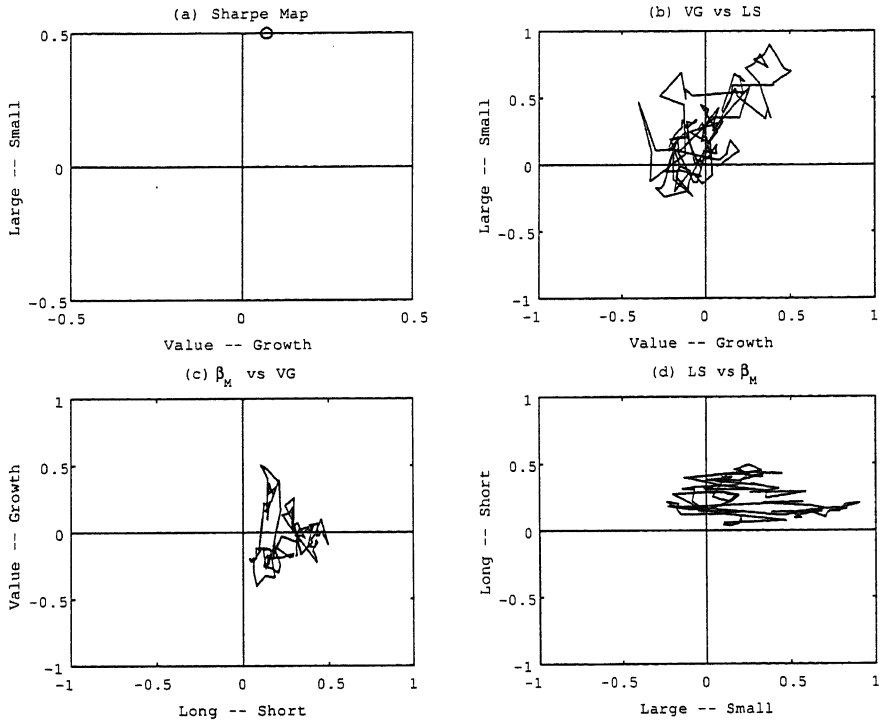

Figure 22: Estimated results of NJO (2) by model (10); (a):Sharpe(VG-LS) map, (b):VG-LS map, (c):β_M-VG map, (d):LS-β_M map, (e):cumulative return by model(10).

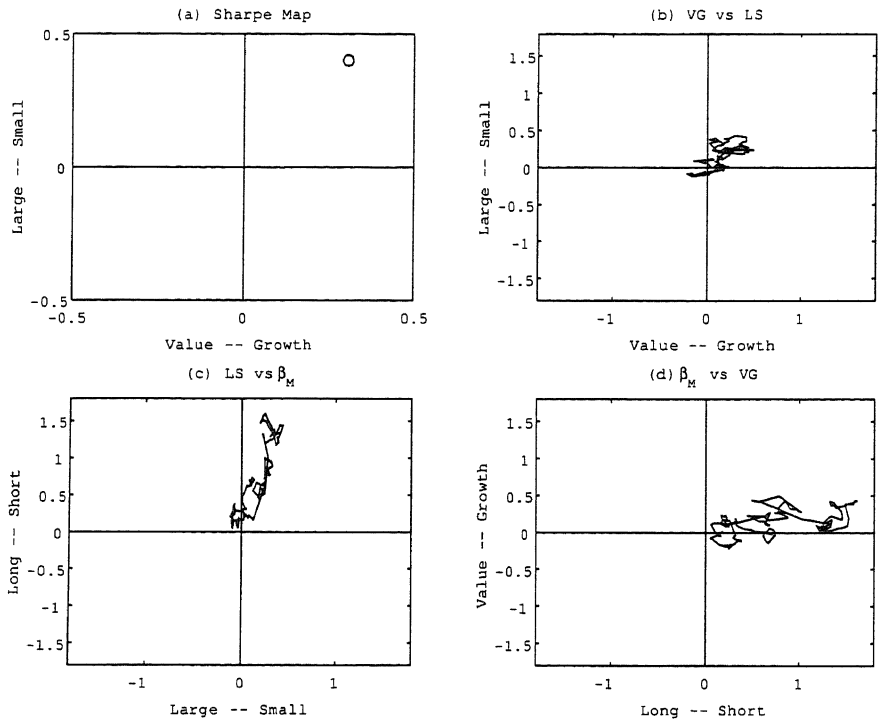

Figure 23: Estimated results of VRG (2) by model (10); (a):Sharpe(VG-LS) map, (b):VG-LS map, (c):β_M-VG map, (d):LS-β_M map, (e):cumulative return by model(10).

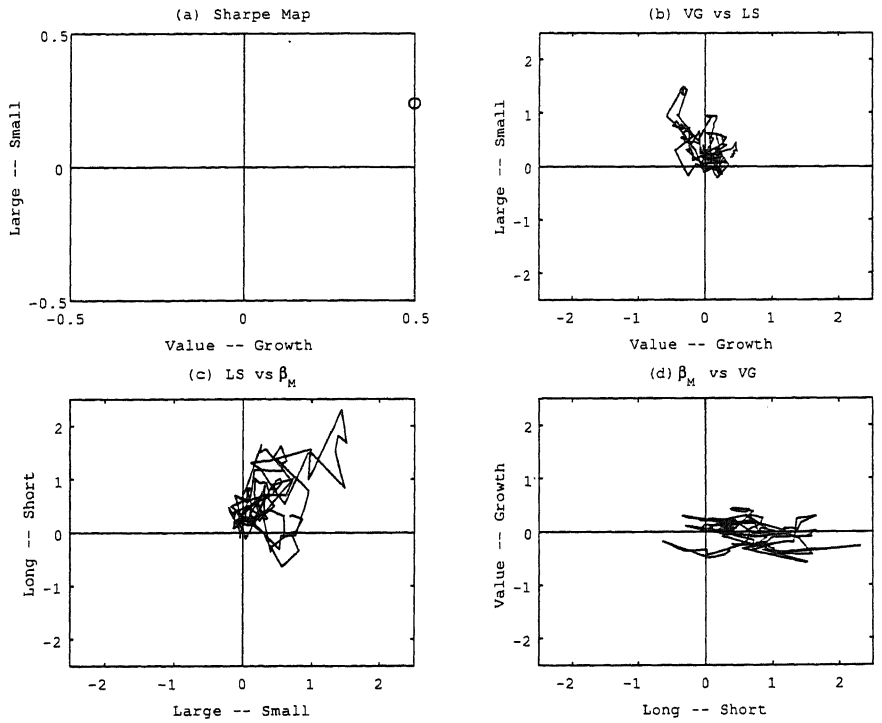

Figure 24: Estimated results of HJF (2) by model (10); (a):Sharpe(VG-LS) map, (b):VG-LS map, (c):β_M-VG map, (d):LS-β_M map, (e):cumulative return by model(10).

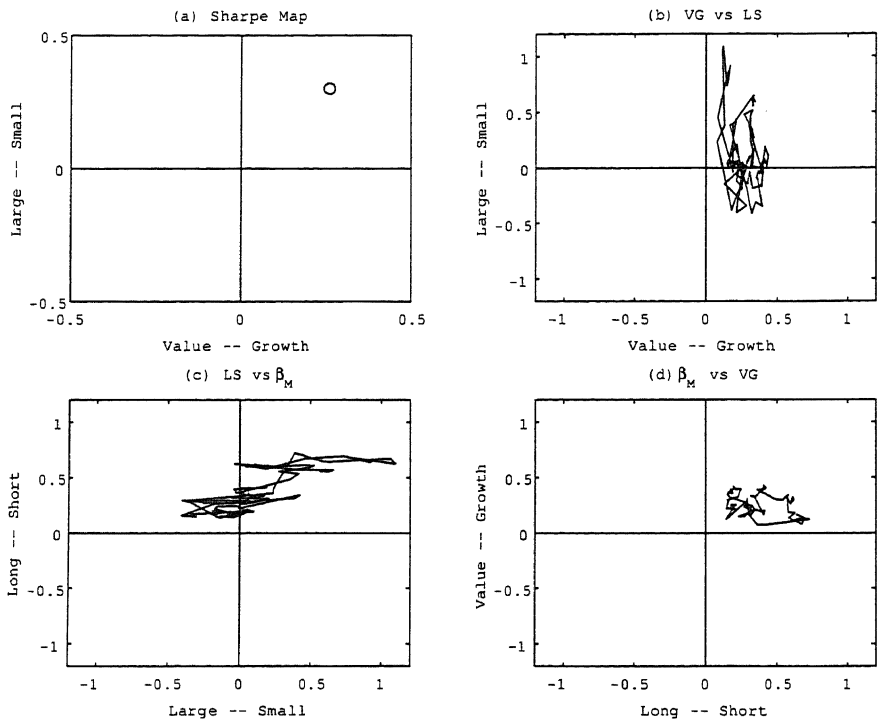

Figure 25: Estimated results of FBR (2) by model (10); (a):Sharpe(VG-LS) map, (b):VG-LS map, (c):β_M-VG map, (d):LS-β_M map, (e):cumulative return by model(10).

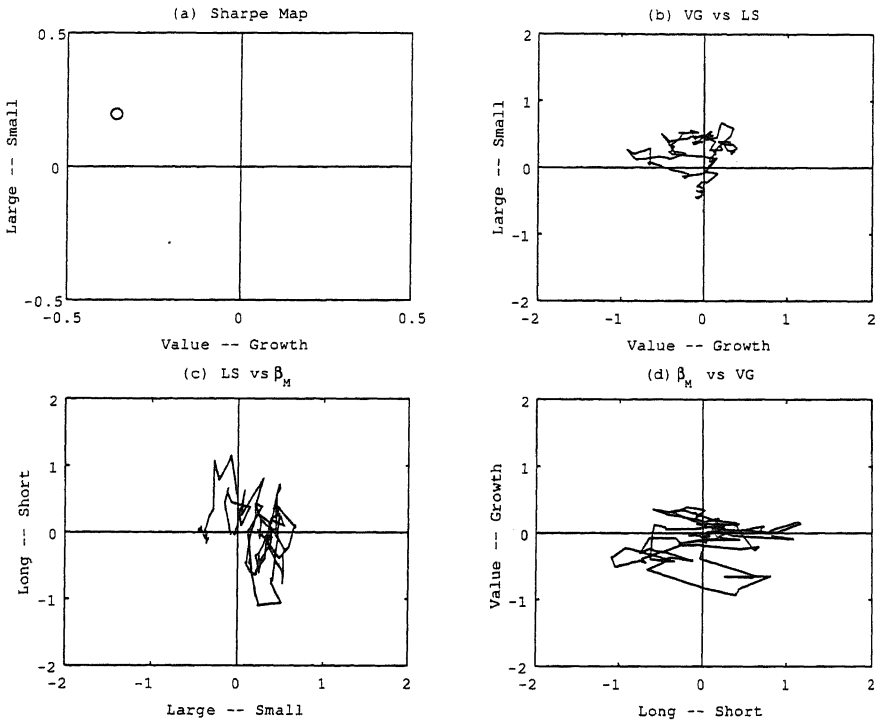

Figure 26: Estimated results of AVO (2) by model (10); (a):Sharpe(VG-LS) map, (b):VG-LS map, (c):β_M-VG map, (d):LS-β_M map, (e):cumulative return by model(10).

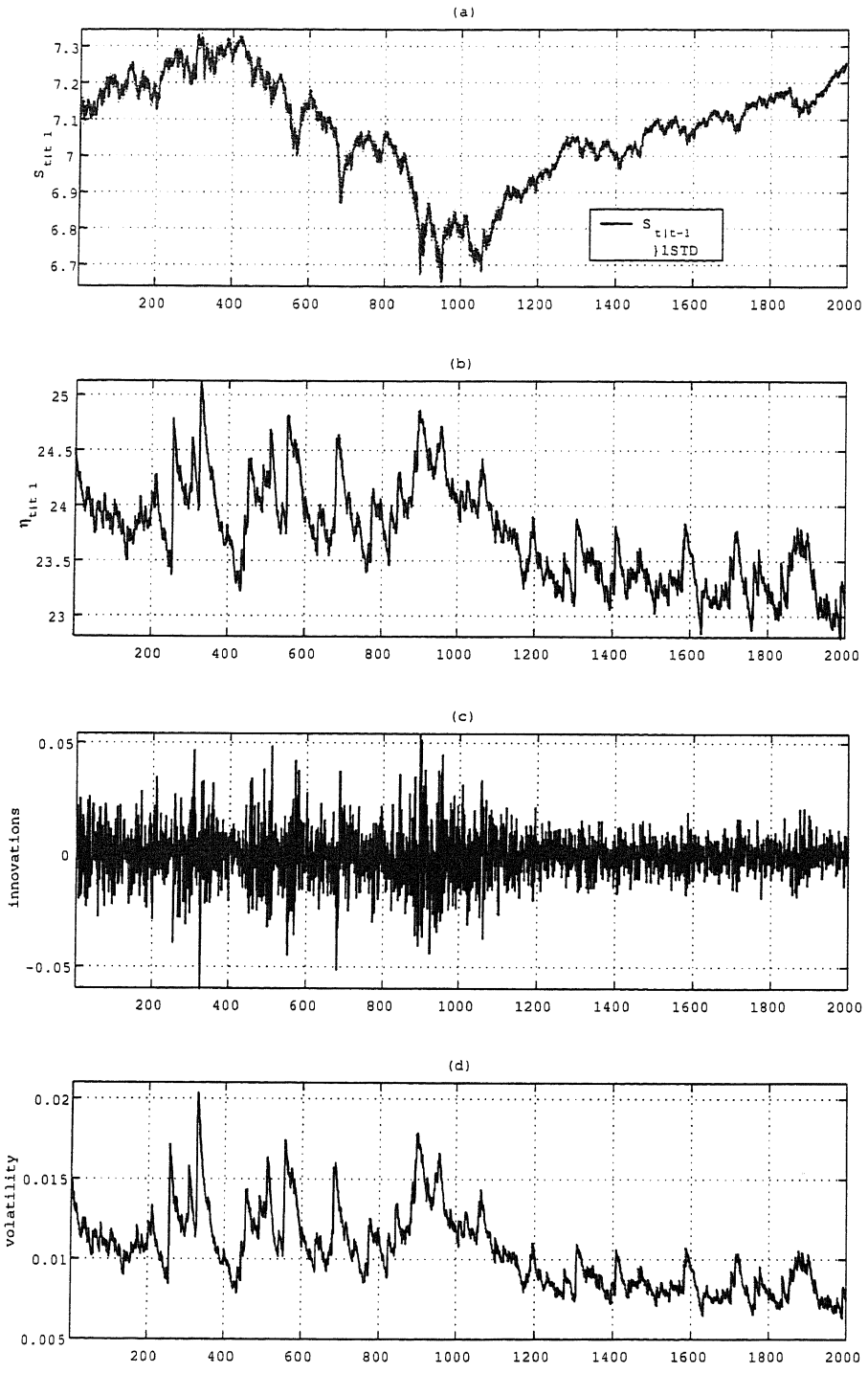

Figure 27: Estimated results of S&P500 stock index by model (24) over the period 31-Dec-1998 to 12-Dec-2006; (a):$S_{t|t-1}$, (b):$\eta_{t|t-1}$, (c):innovations and (d):volatility.

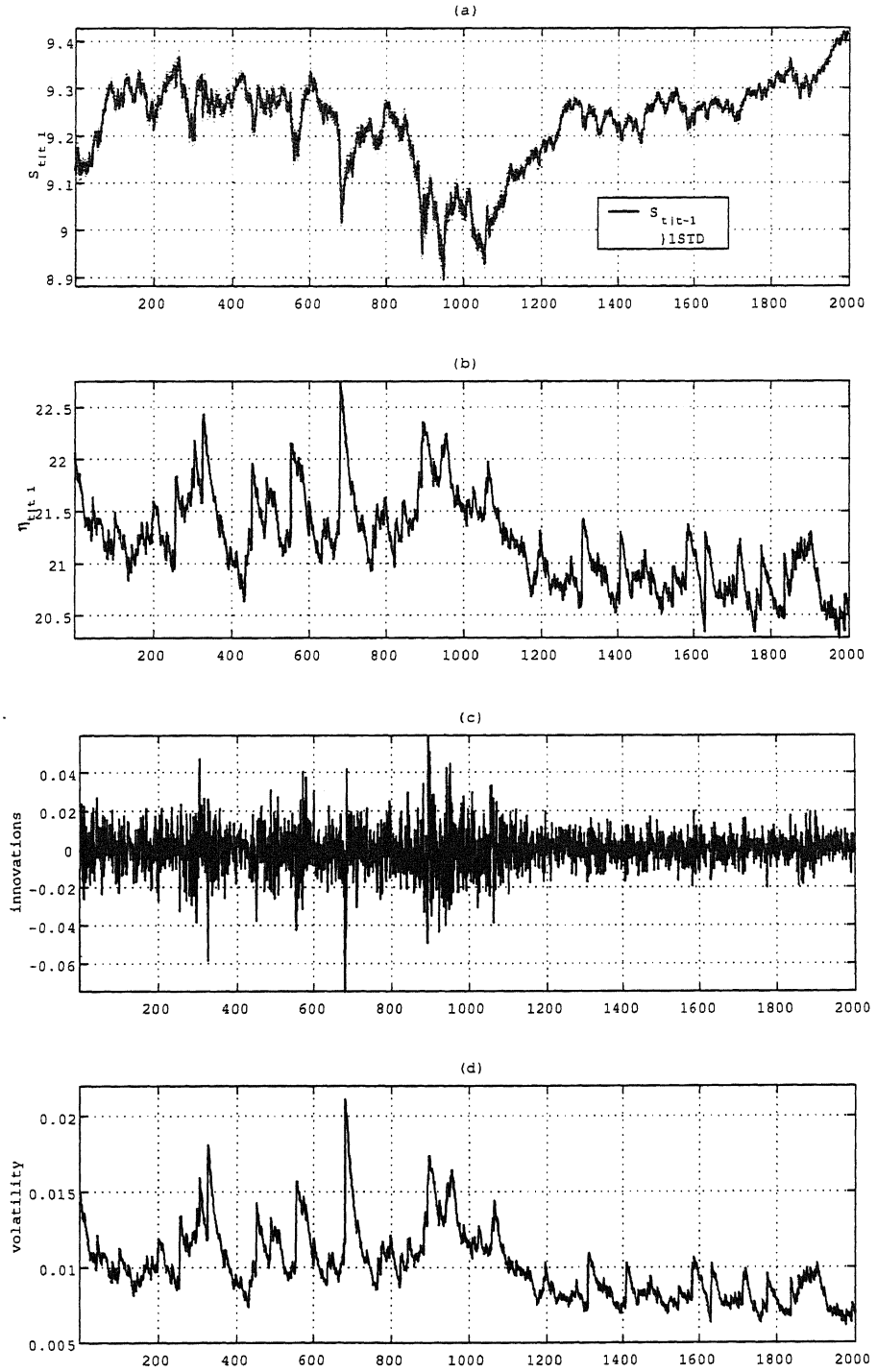

Figure 28: Estimated results of Dow Jones stock index by model (24) over the period 31-Dec-1998 to 12-Dec-2006; (a):$S_{t|t-1}$, (b):$\eta_{t|t-1}$, (c):innovations and (d):volatility.

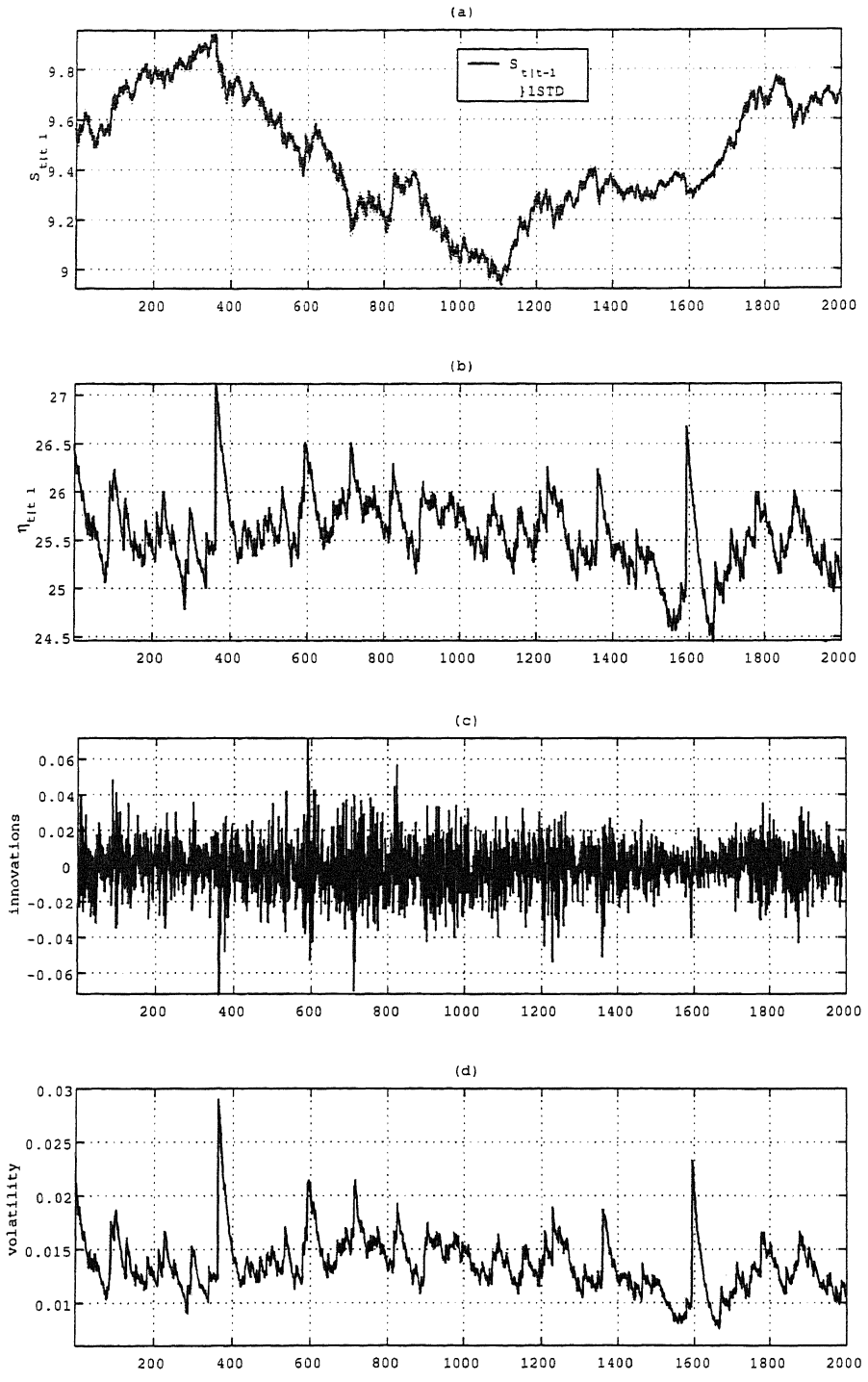

Figure 29: Estimated results of Nikkei225 stock by model (24) over the period 22-Oct-1998 to 12-Dec-2006; (a):$S_{t|t-1}$, (b):$\eta_{t|t-1}$, (c):innovations and (d):volatility.

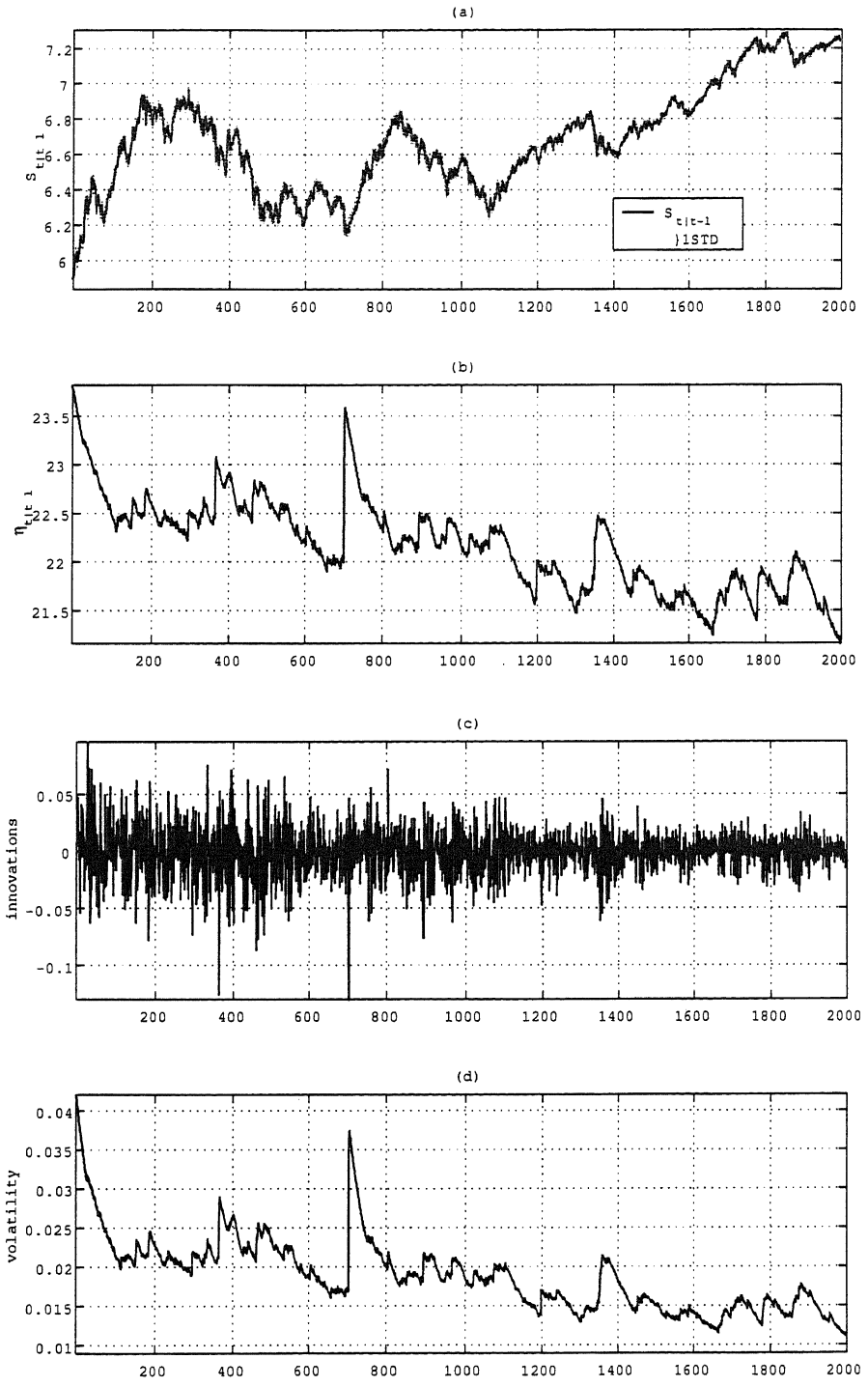

Figure 30: Estimated results of Seoul comp. stock by model (24) over the period 28-Oct-1998 to 12-Dec-2006; (a):$S_{t|t-1}$, (b):$\eta_{t|t-1}$, (c):innovations and (d):volatility.

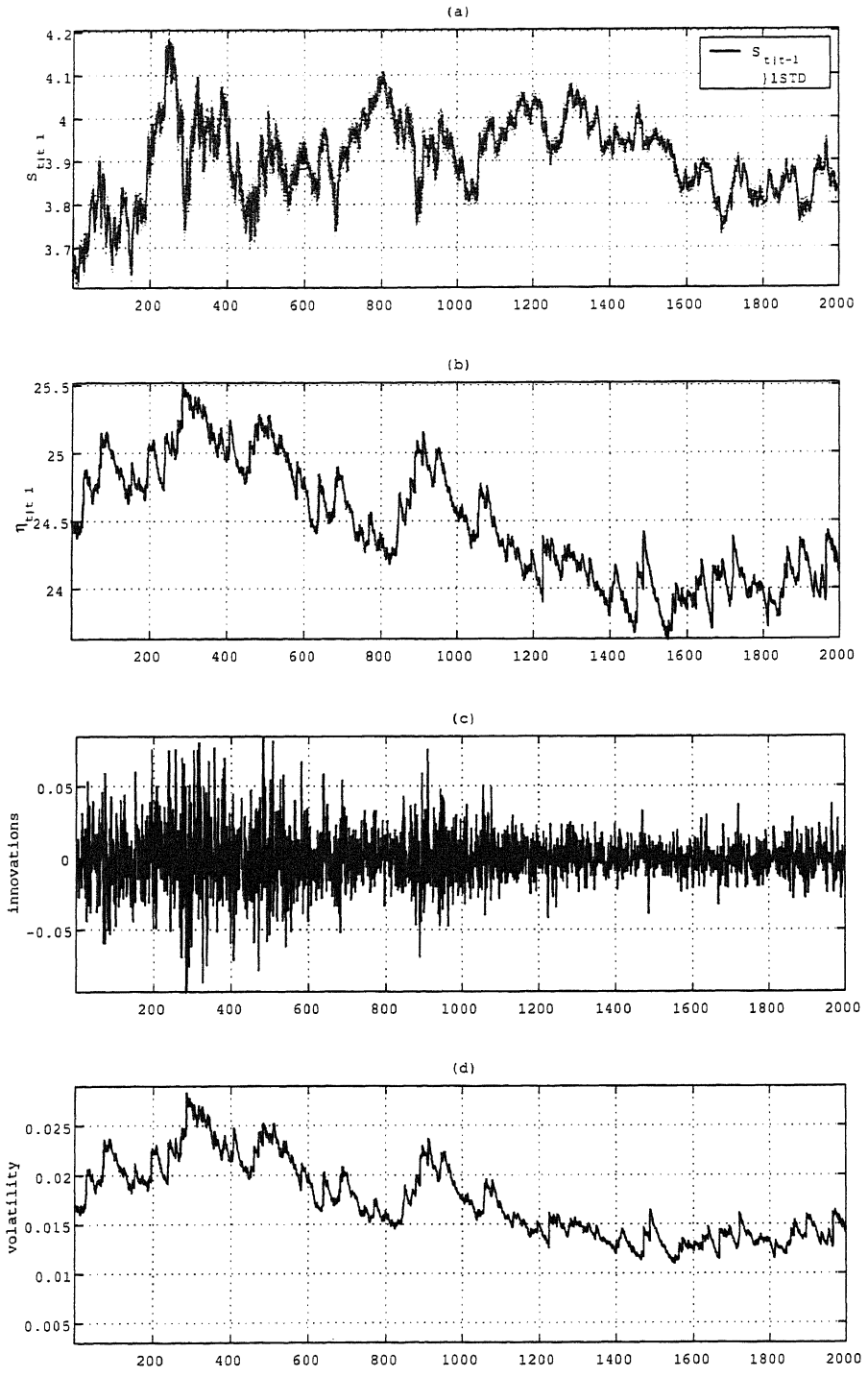

Figure 31: Estimated results of TOYOTA stock by model (24) over the period 23-Dec-1998 to 13-Dec-2006; (a):$S_{t|t-1}$, (b):$\eta_{t|t-1}$, (c):innovations and (d):volatility.

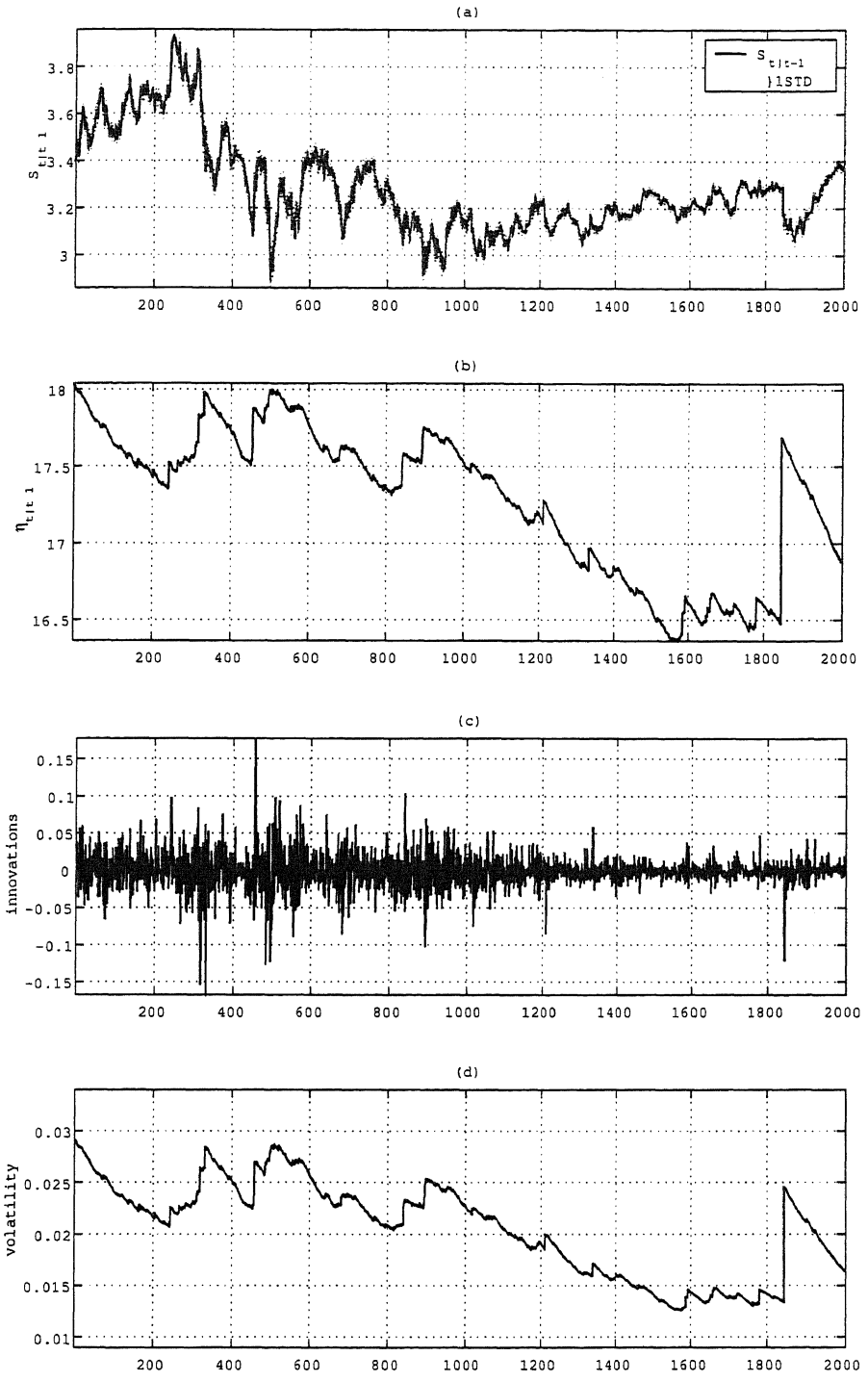

Figure 32: Estimated results of Microsoft Corp. stock by model (24) over the period 31-Dec-1998 to 12-Dec-2006; (a):$S_{t|t-1}$, (b):$\eta_{t|t-1}$, (c):innovations and (d):volatility.

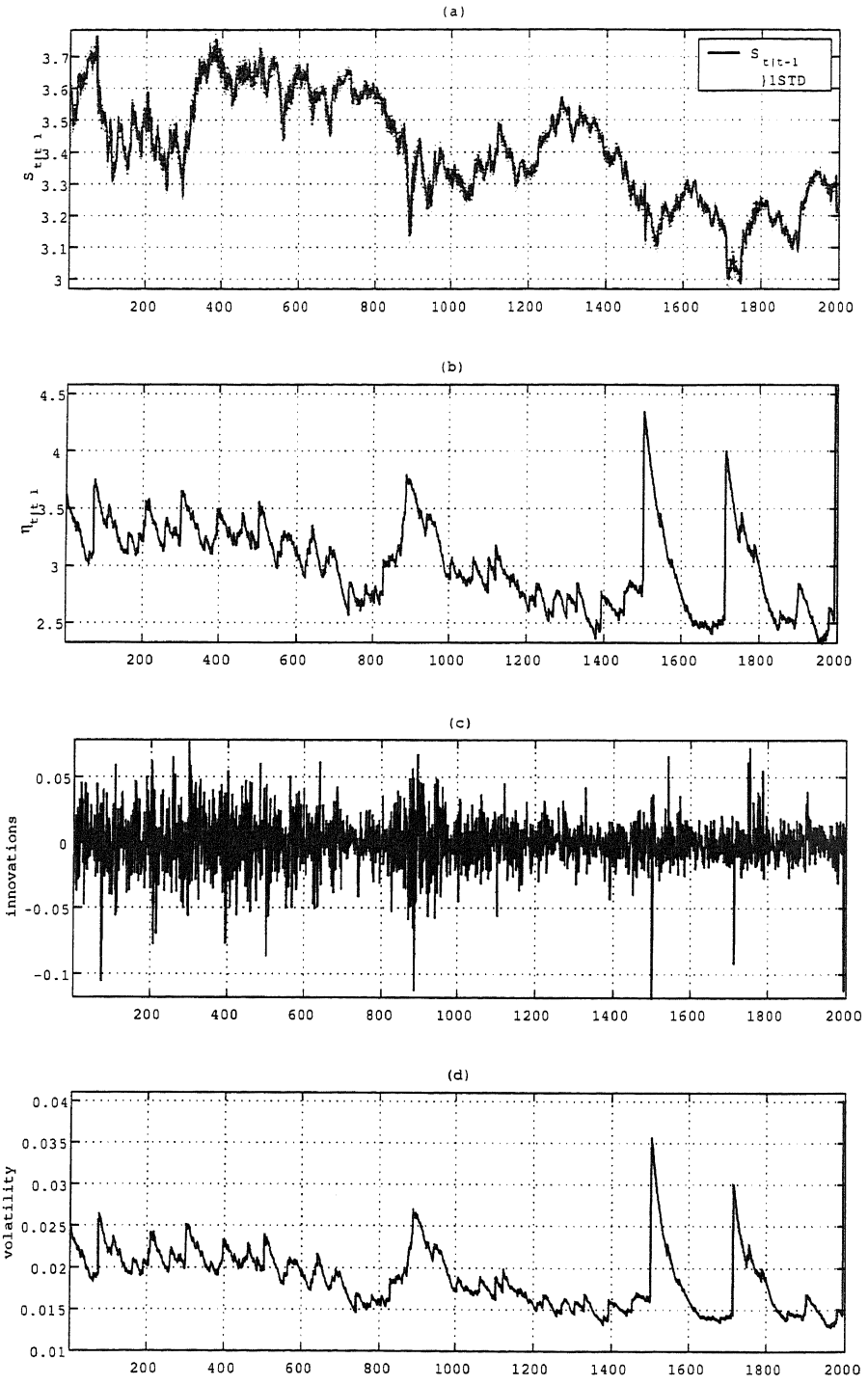

Figure 33: Estimated results of Pfizer stock by model (24) over the period 31-Dec-1998 to 12-Dec-2006; (a):$S_{t|t-1}$, (b):$\eta_{t|t-1}$, (c):innovations and (d):volatility.

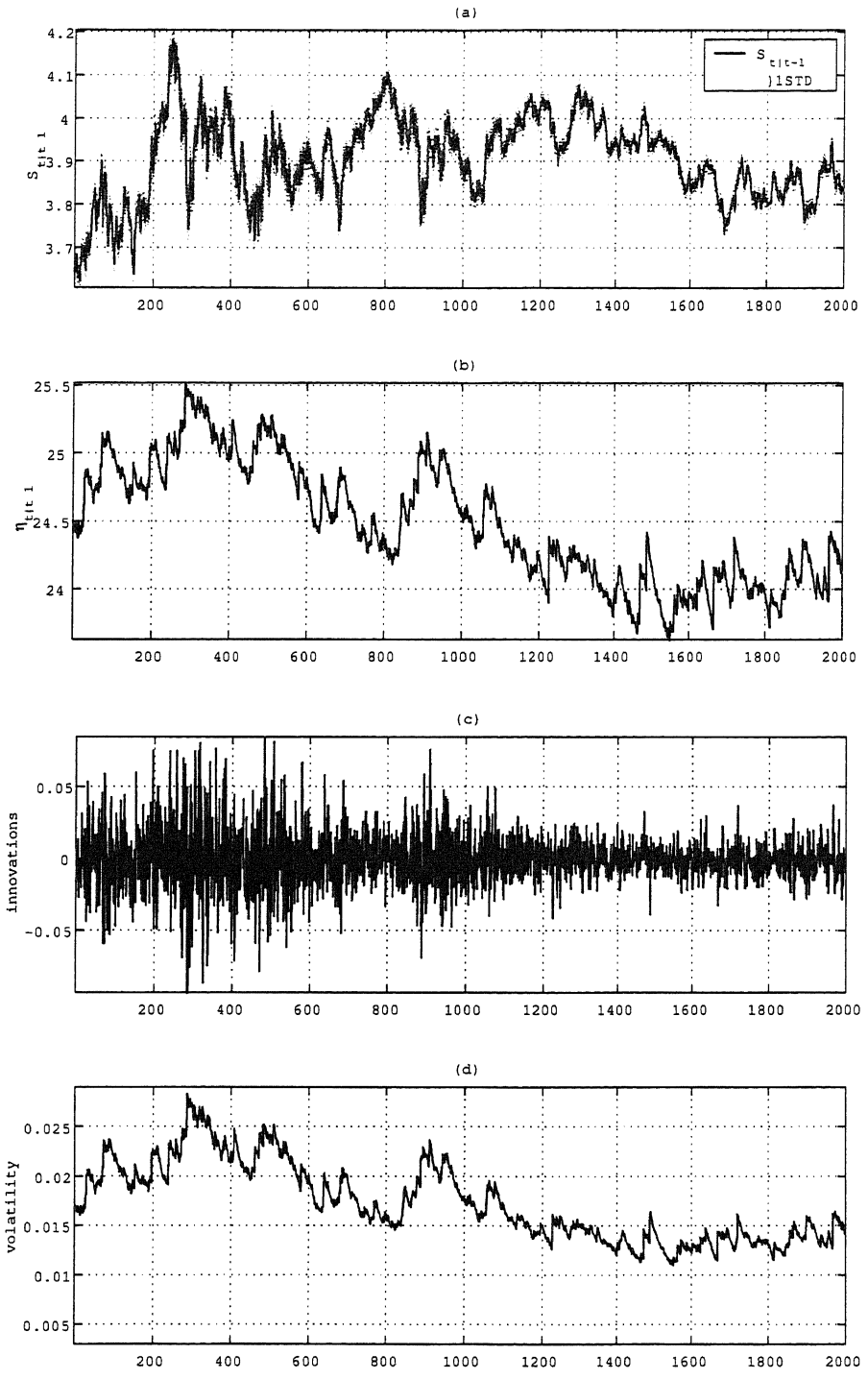

Figure 34: Estimated results of Wal-Mart stock by model (24) over the period 31-Dec-1998 to 12-Dec-2006; (a):$S_{t|t-1}$, (b):$\eta_{t|t-1}$, (c):innovations and (d):volatility.

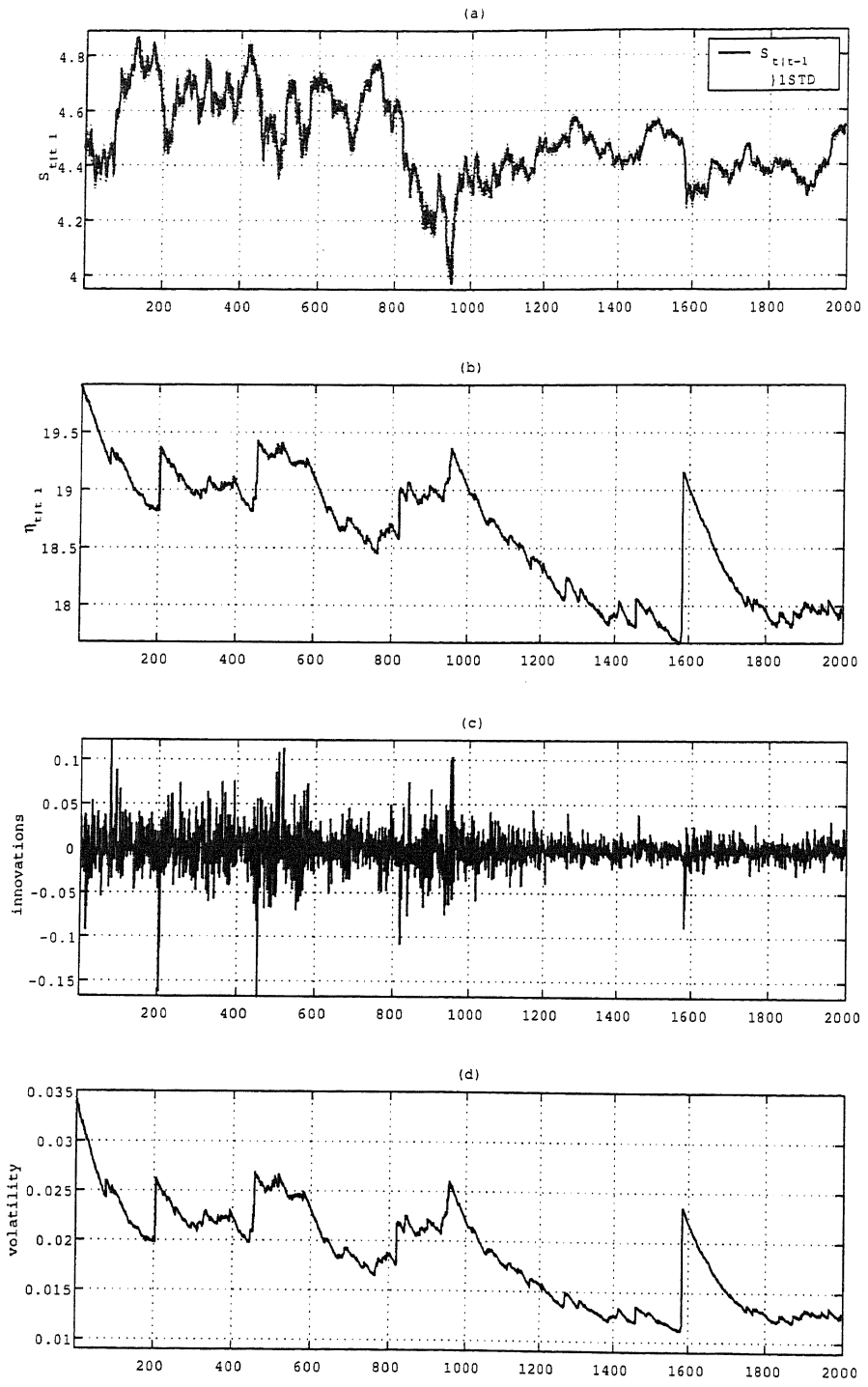

Figure 35: Estimated results of IBM stock by model (24) over the period 31-Dec-1998 to 12-Dec-2006; (a):$S_{t|t-1}$, (b):$\eta_{t|t-1}$, (c):innovations and (d):volatility.

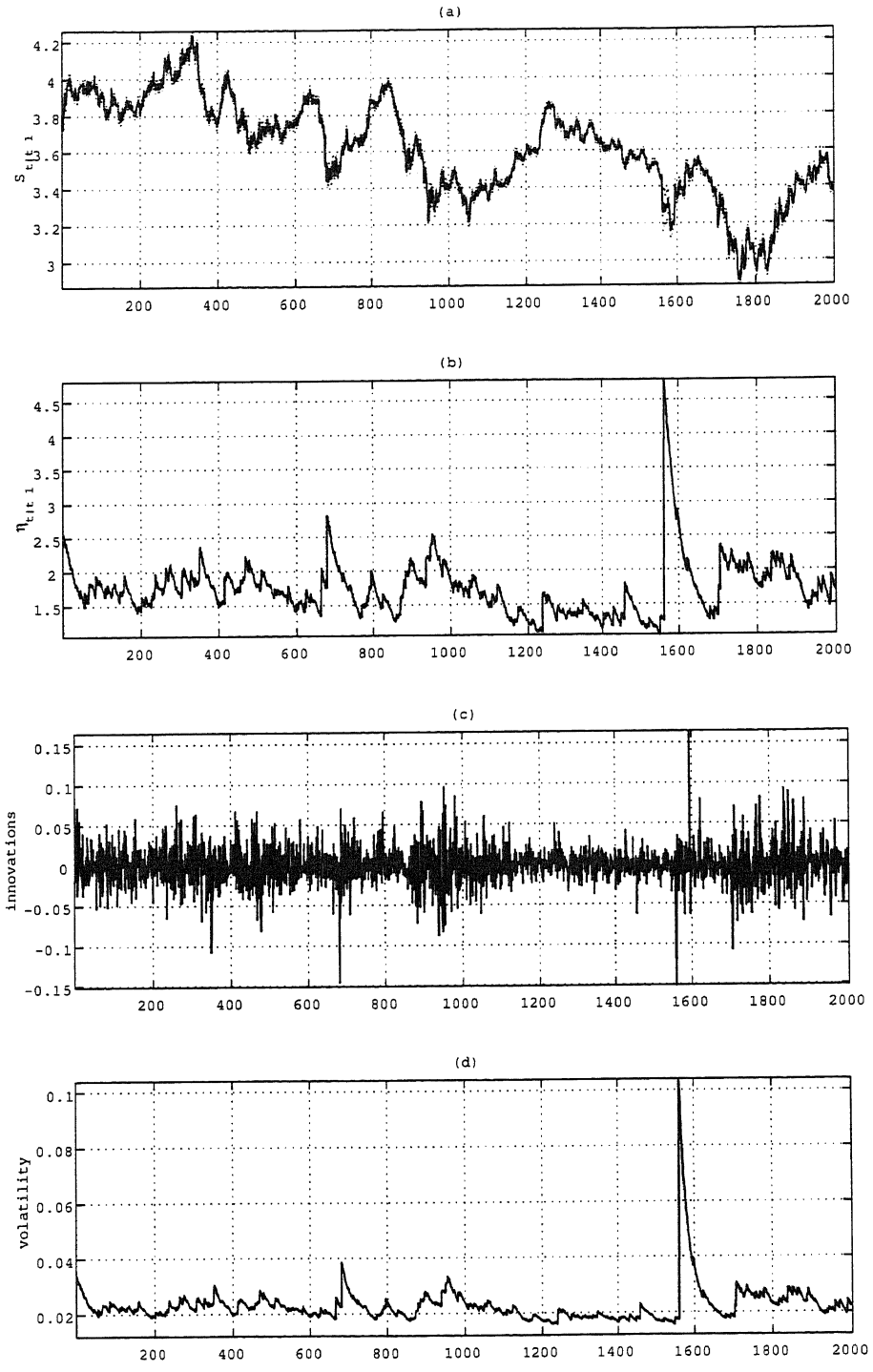

Figure 36: Estimated results of General Motors; (a):$S_{t|t-1}$, (b):$\eta_{t|t-1}$, (c):innovations and (d):volatility by model (24)

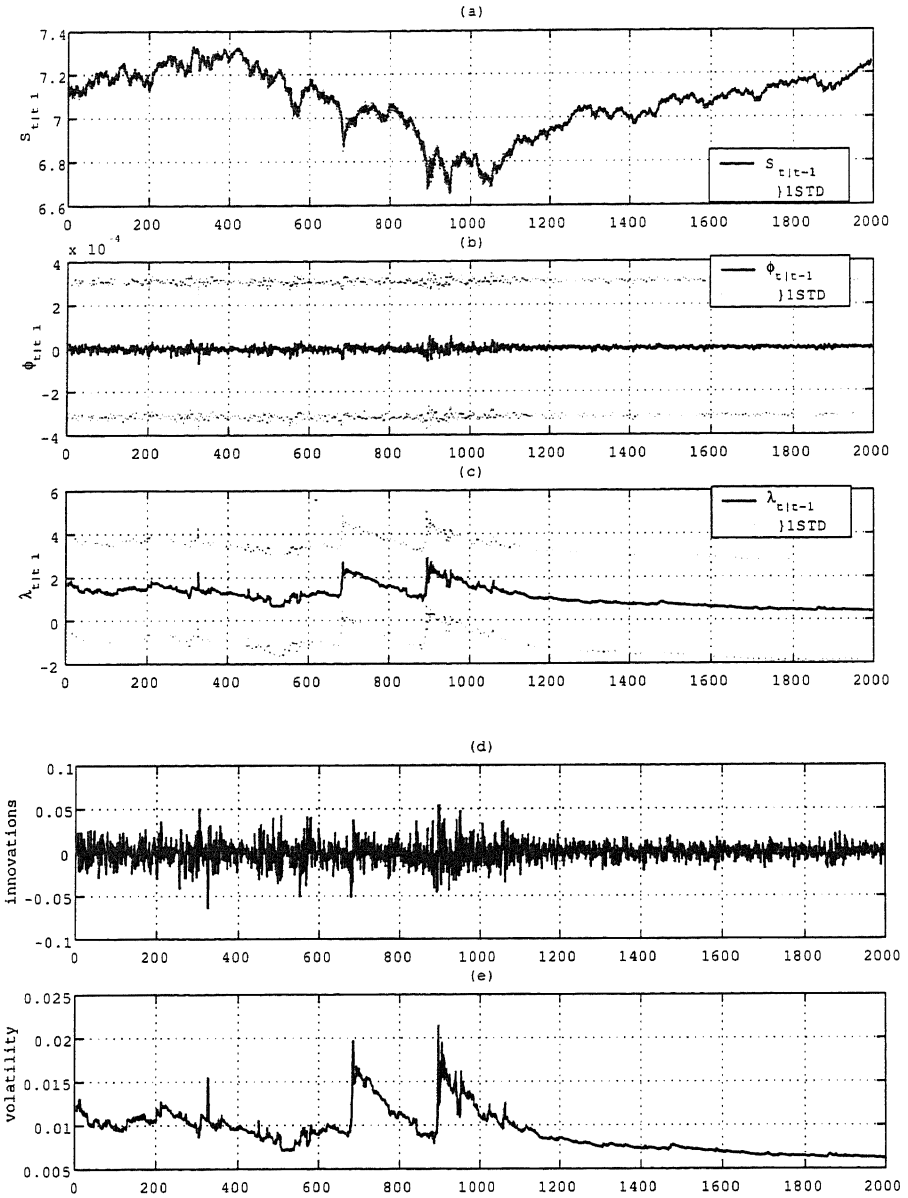

Figure 37: Estimated results of S&P500 by model (28) over the period 31-Dec-1998 to 12-Dec-2006; (a):$S_{t|t-1}$, (b):$\phi_{t|t-1}$, (c):$\lambda_{t|t-1}$, (d):innovations and (e):volatility.

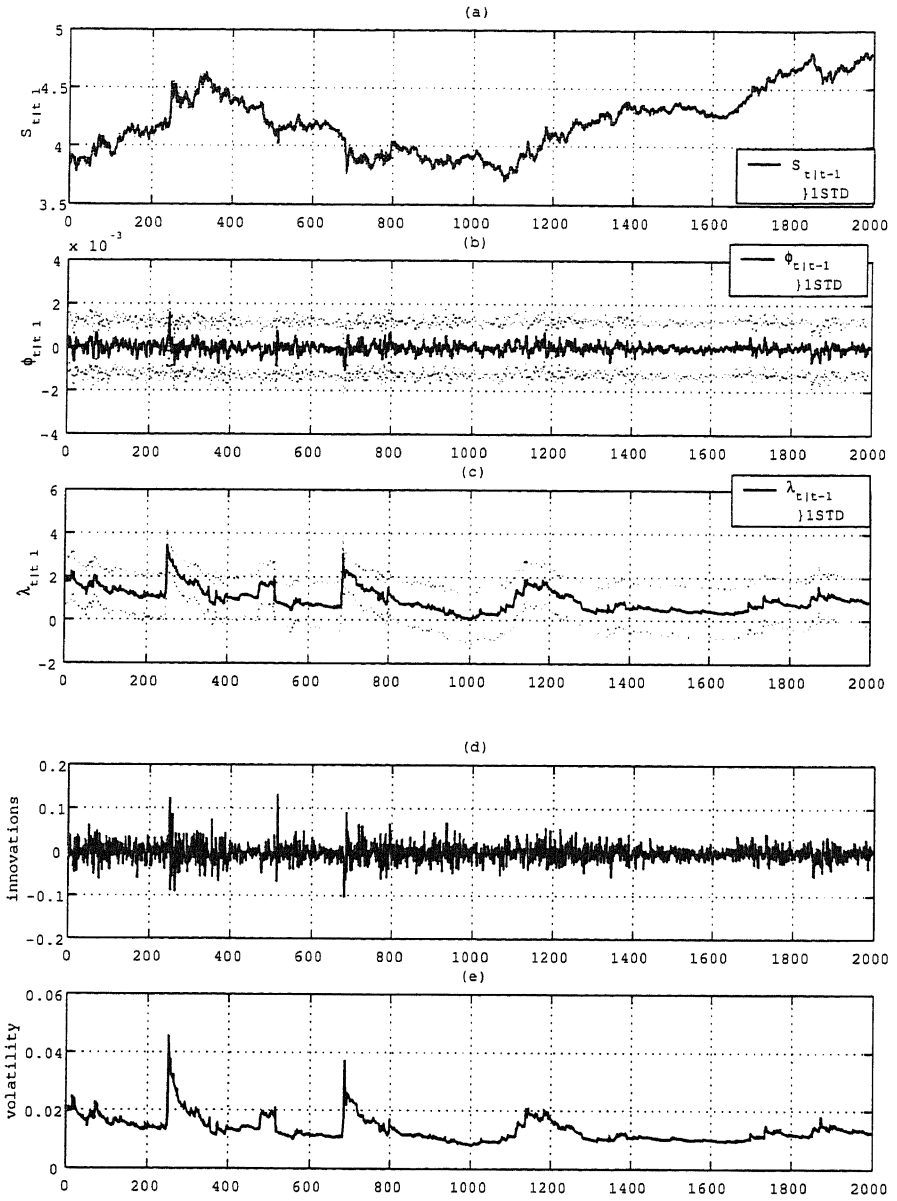

Figure 38: Estimated results of TOYOTA by model (28) over the period 23-Dec-1998 to 13-Dec-2006; (a):$S_{t|t-1}$, (b):$\phi_{t|t-1}$, (c):$\lambda_{t|t-1}$, (d):innovations and (e):volatility.

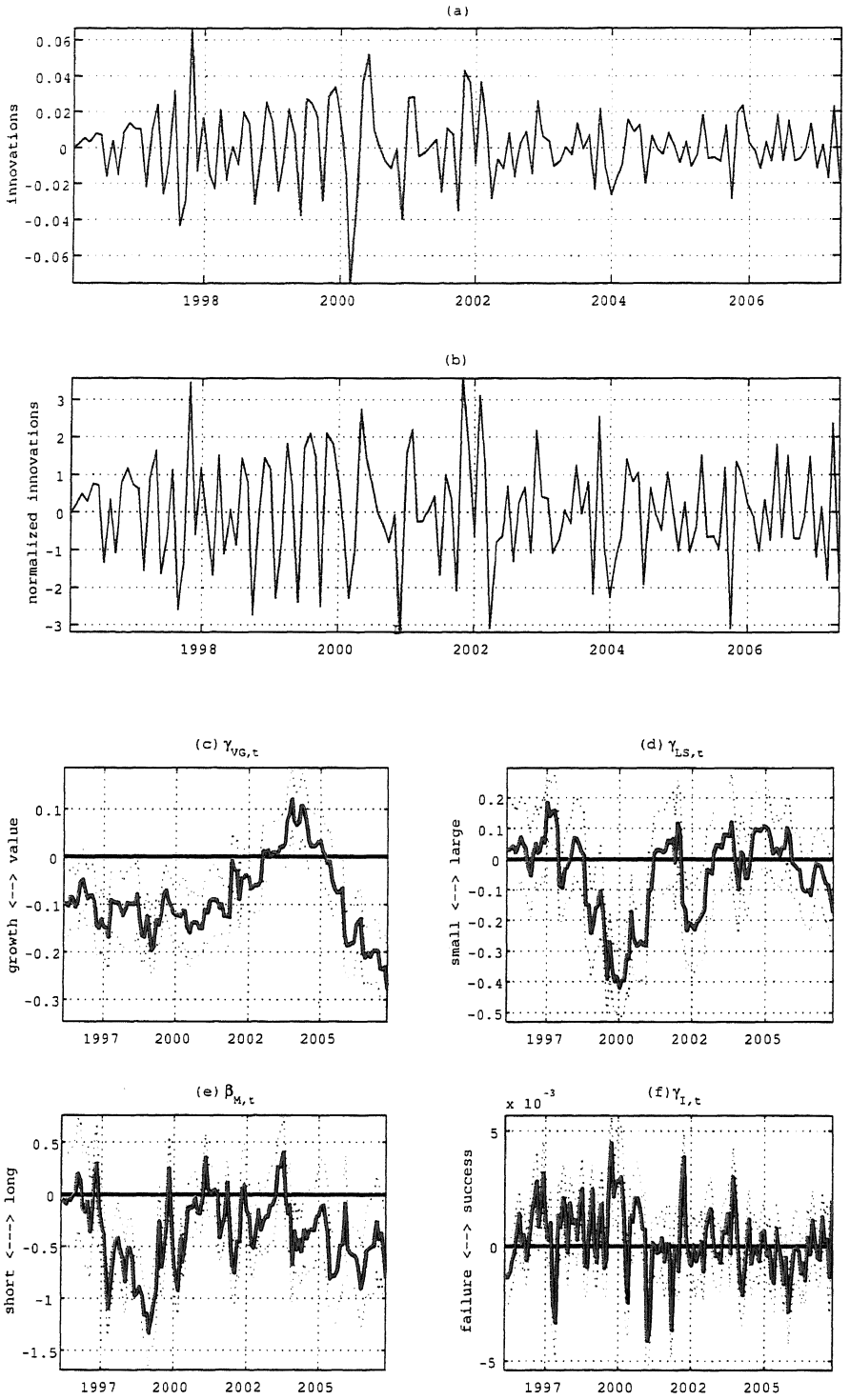

Figure 39: Estimated results of FJO (1) by mixed Gaussian-Poisson noise model (33); (a):innovations, (b):normalized innovations, (c):$\gamma_{VG,t}$, (d):$\gamma_{LS,t}$, (e):$\beta_{M,t}$ and (f):$\gamma_{I,t}$. The red solid lines indicate states obtained by Gaussian noise model (33) in graph (c)$\sim$(f).

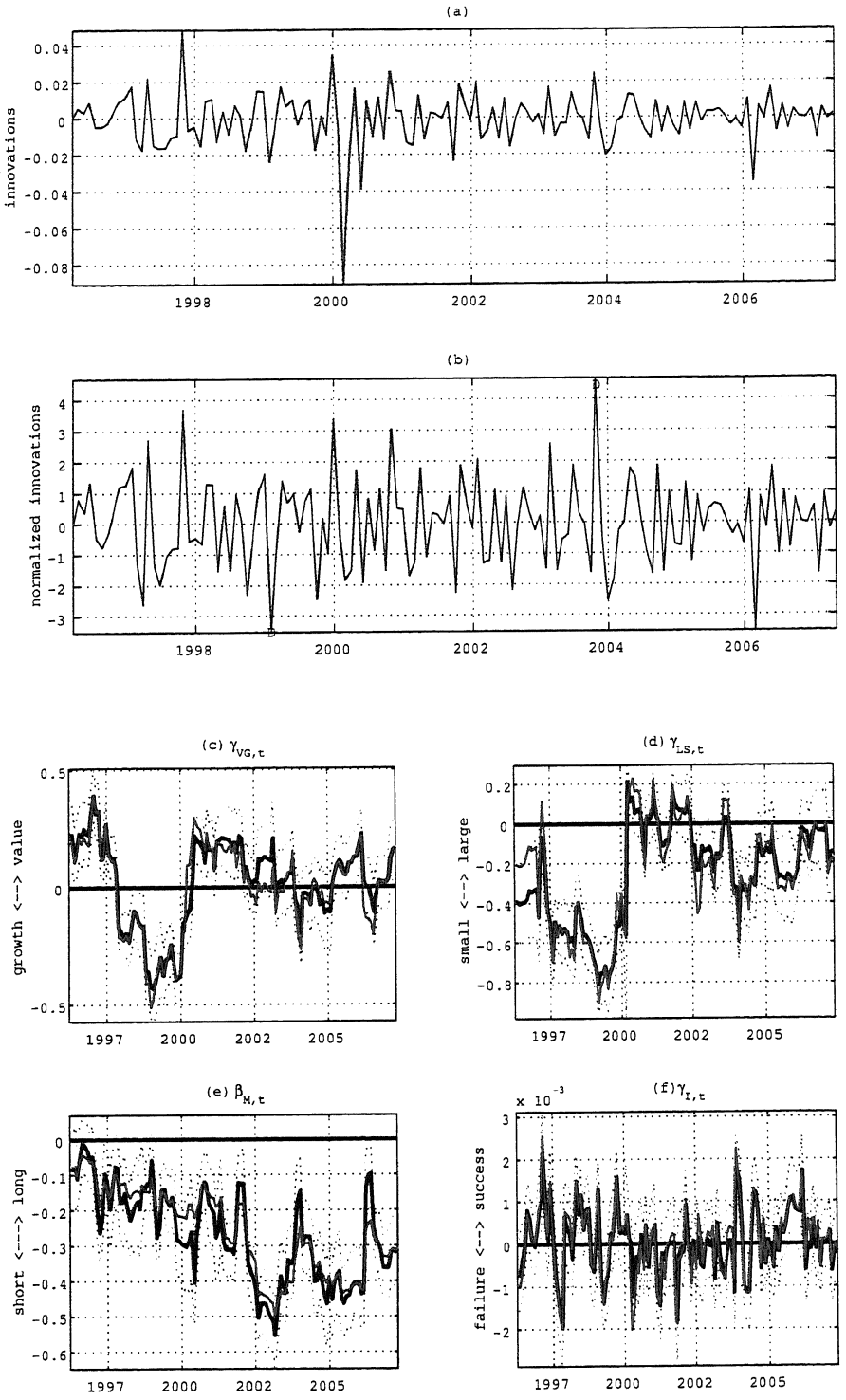

Figure 40: Estimated results of NJO (1) by mixed Gaussian-Poisson noise model (33); (a):innovations, (b):normalized innovations, (c):$\gamma_{VG,t}$, (d):$\gamma_{LS,t}$, (e):$\beta_{M,t}$ and (f):$\gamma_{I,t}$. The red solid lines indicate states obtained by Gaussian noise model (33) in graph (c)$\sim$(f).

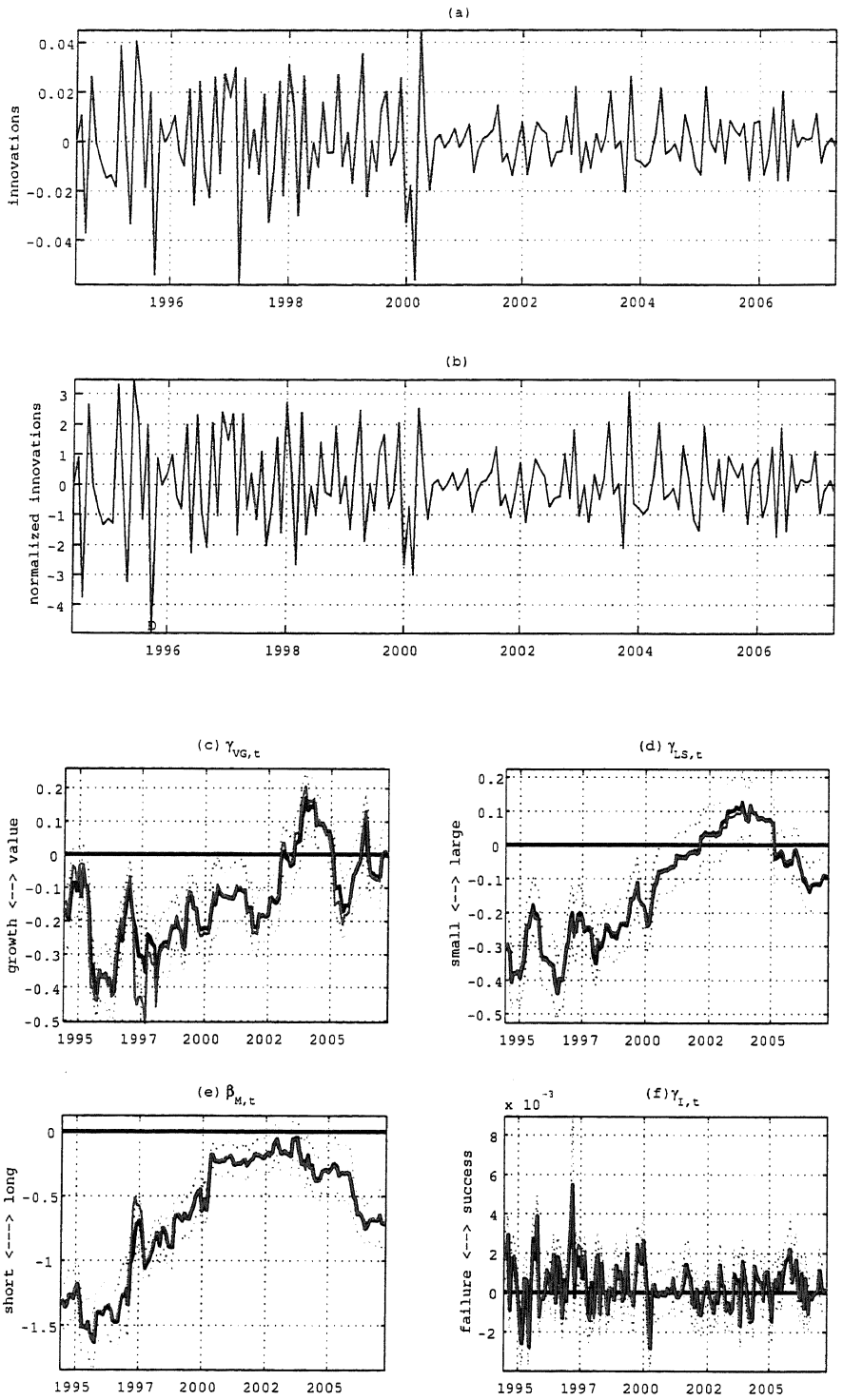

Figure 41: Estimated results of VRG (1) by mixed Gaussian-Poisson noise model (33); (a):innovations, (b):normalized innovations, (c):$\gamma_{VG,t}$, (d):$\gamma_{LS,t}$, (e):$\beta_{M,t}$ and (f):$\gamma_{I,t}$. The red solid lines indicate states obtained by Gaussian noise model (33) in graph (c)$\sim$(f).

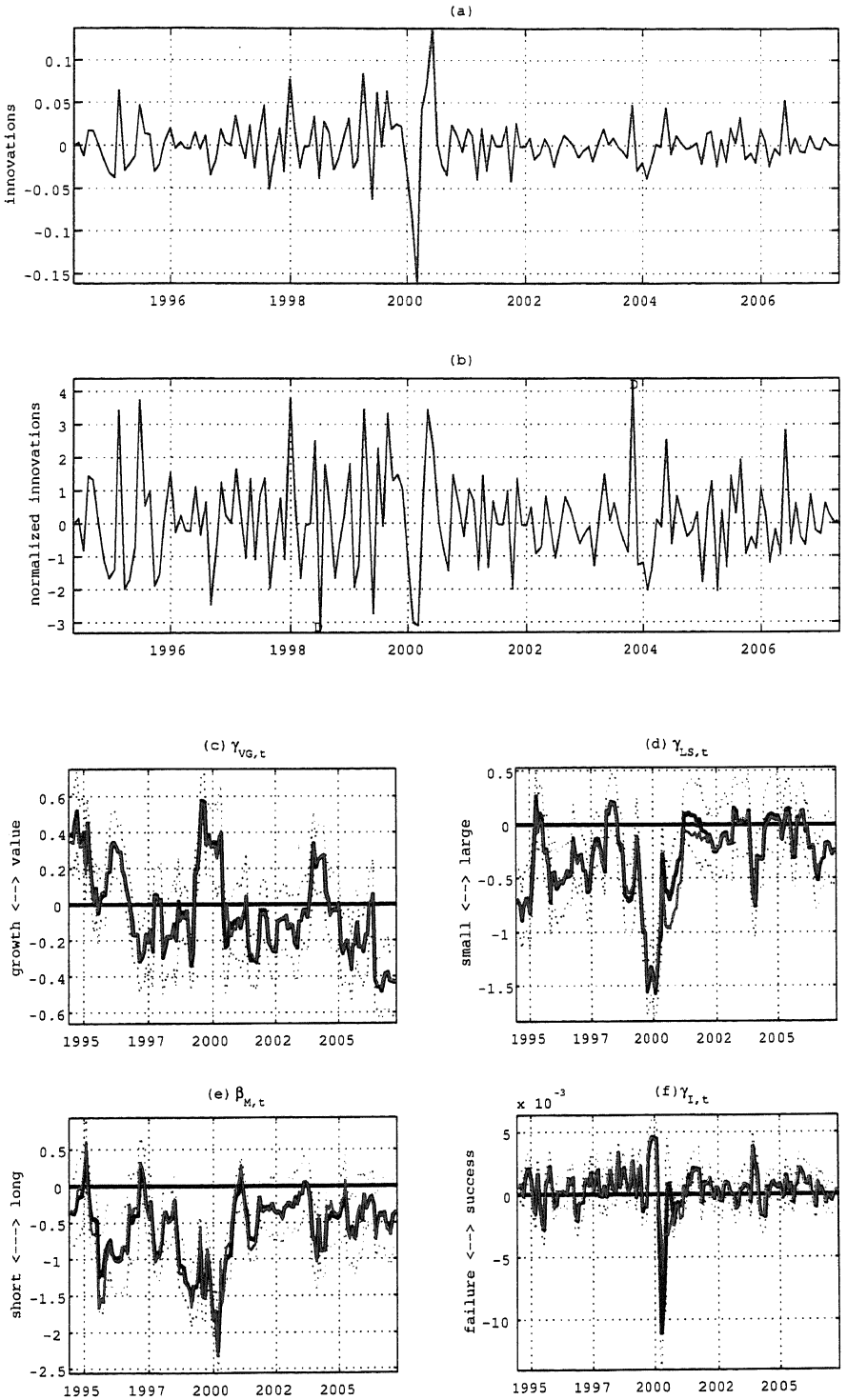

Figure 42: Estimated results of HJF (1) by mixed Gaussian-Poisson noise model (33); (a):innovations, (b):normalized innovations, (c):$\gamma_{VG,t}$, (d):$\gamma_{LS,t}$, (e):$\beta_{M,t}$ and (f):$\gamma_{I,t}$. The red solid lines indicate states obtained by Gaussian noise model (33) in graph (c)$\sim$(f).

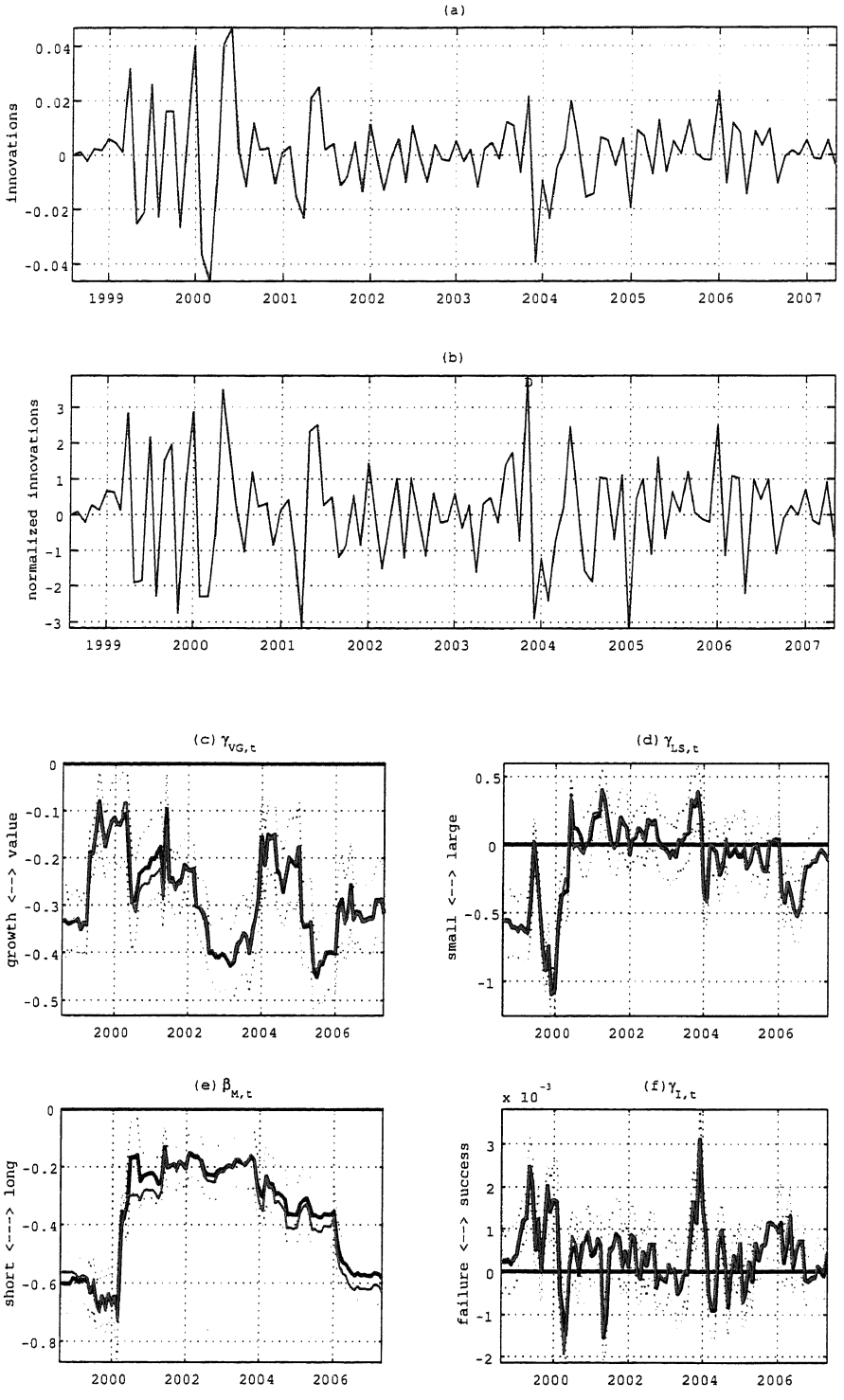

Figure 43: Estimated results of FBR (1) by mixed Gaussian-Poisson noise model (33); (a):innovations, (b):normalized innovations, (c):$\gamma_{VG,t}$, (d):$\gamma_{LS,t}$, (e):$\beta_{M,t}$ and (f):$\gamma_{I,t}$. The red solid lines indicate states obtained by Gaussian noise model (33) in graph (c)$\sim$(f).

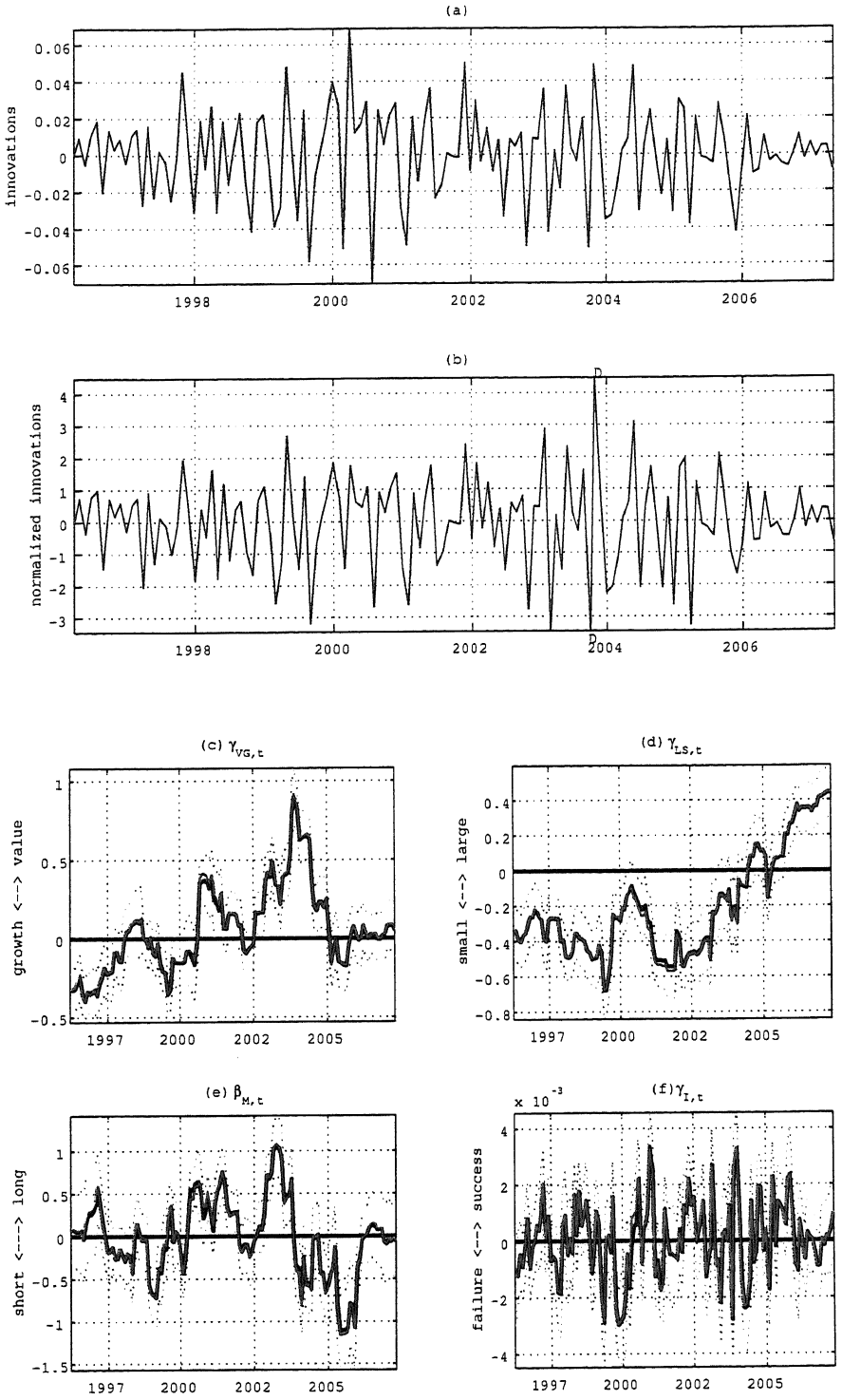

Figure 44: Estimated results of AVO (1) by mixed Gaussian-Poisson noise model (33); (a):innovations, (b):normalized innovations, (c):$\gamma_{VG,t}$, (d):$\gamma_{LS,t}$, (e):$\beta_{M,t}$ and (f):$\gamma_{I,t}$. The red solid lines indicate states obtained by Gaussian noise model (33) in graph (c)$\sim$(f).

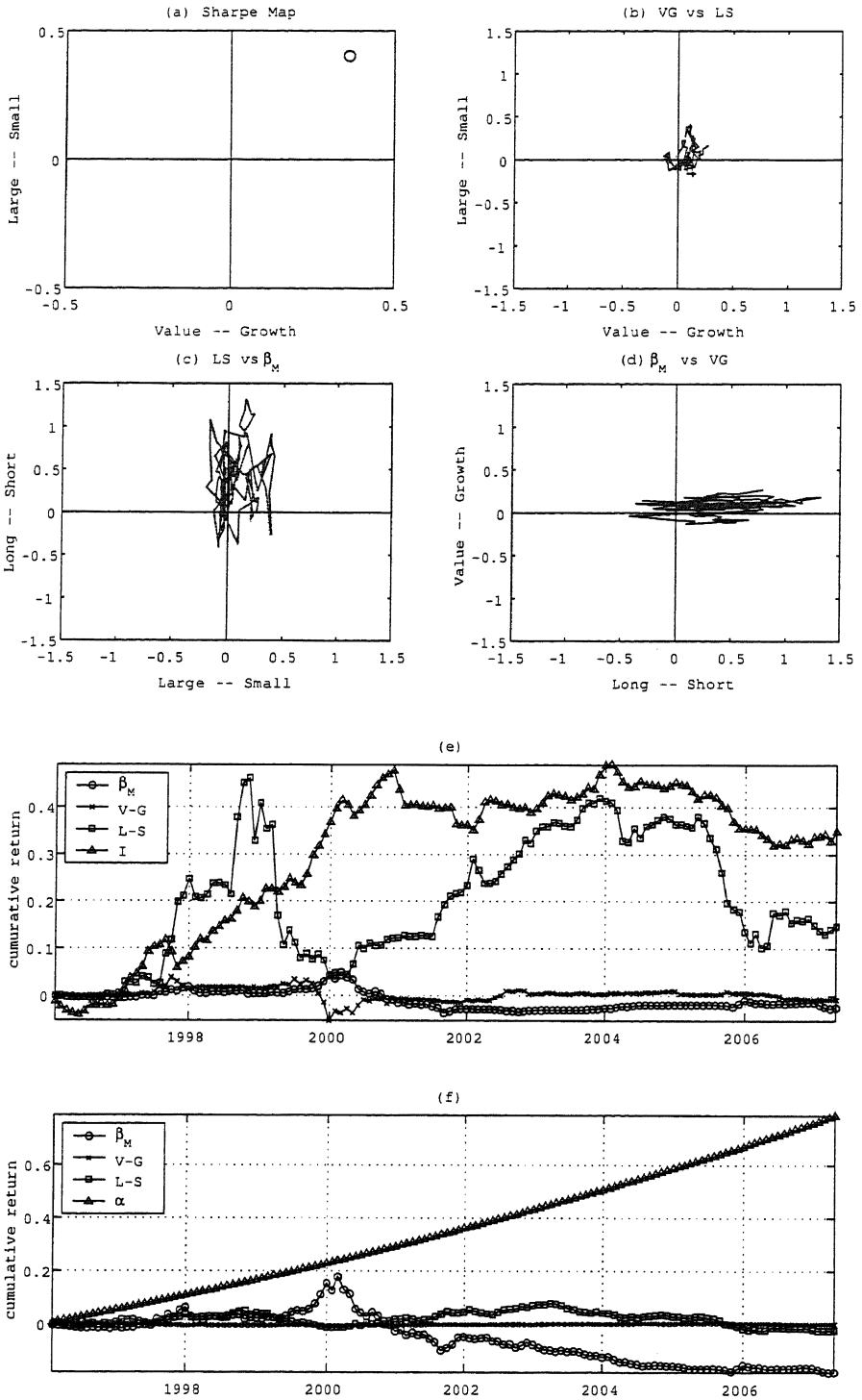

Figure 45: Estimated results of FJO (2) by mixed Gaussian-Poisson noise model (33); (a):Sharpe(VG-LS) map, (b):VG-LS map, (c):β_M-VG map, (d):LS-β_M map. The red dotted lines indicate the time-varying style estimated by Gaussian noise model (10). (e):cumulative return by system(10) and (f):cumulative return by model(4)

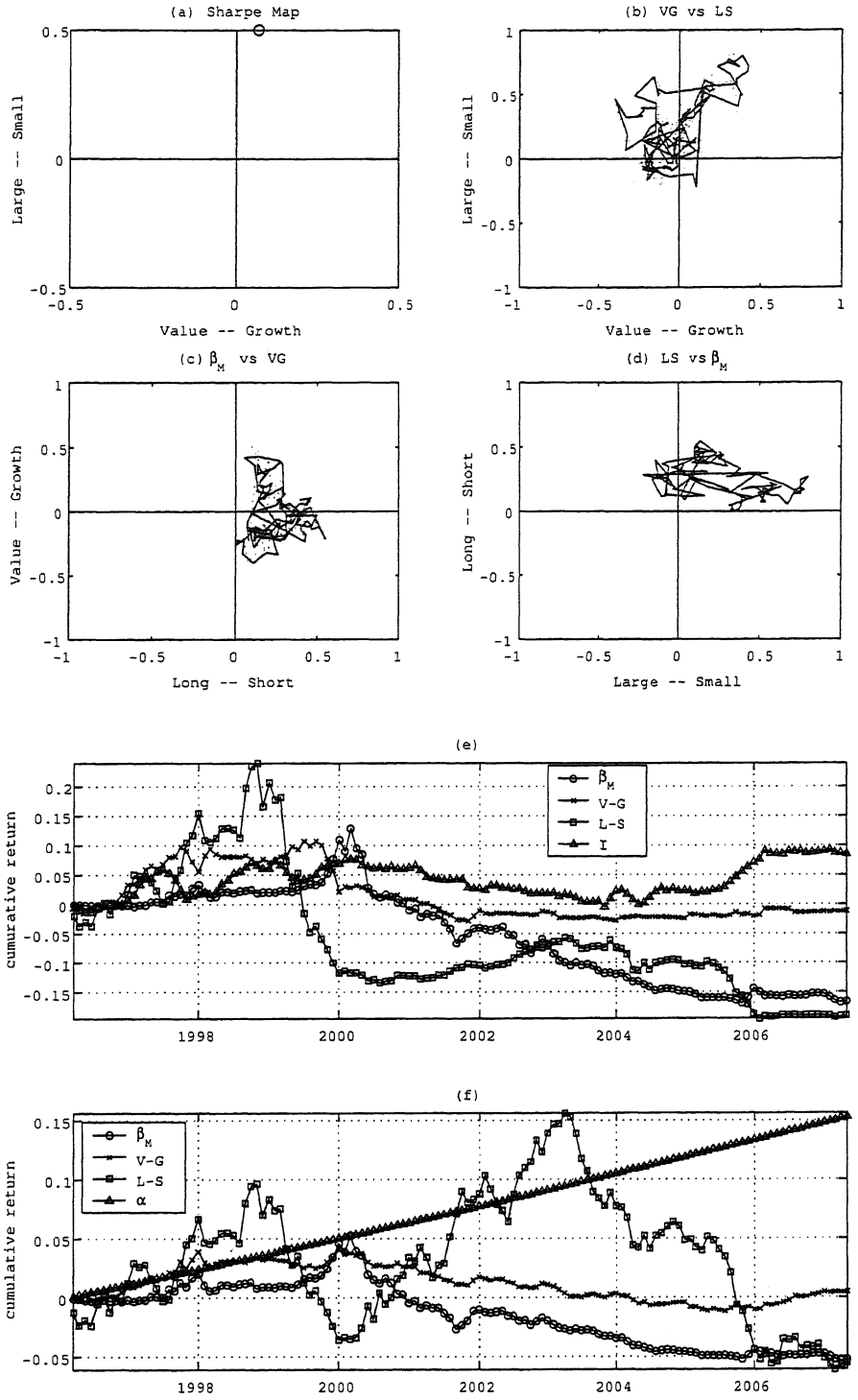

Figure 46: Estimated results of NJO (2) by mixed Gaussian-Poisson noise model (33); (a):Sharpe(VG-LS) map, (b):VG-LS map, (c):β_M-VG map, (d):LS-β_M map. The red dotted lines indicate the time-varying style estimated by Gaussian noise model (10). (e):cumulative return by system(10) and (f):cumulative return by model(4)

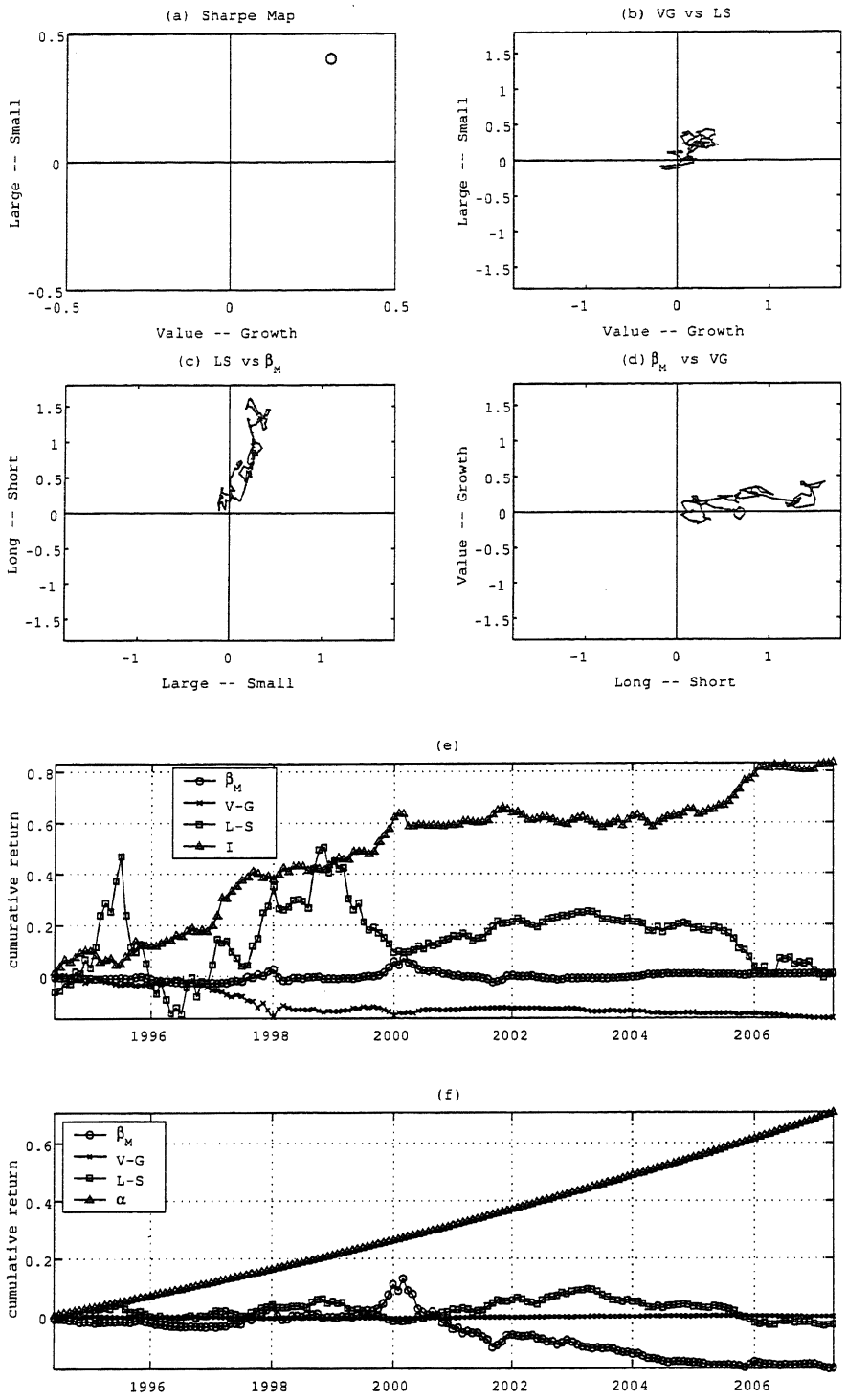

Figure 47: Estimated results of VRG (2) by mixed Gaussian-Poisson noise model (33); (a):Sharpe(VG-LS) map, (b):VG-LS map, (c):β_M-VG map, (d):LS-β_M map. The red dotted lines indicate the time-varying style estimated by Gaussian noise model (10). (e):cumulative return by system(10) and (f):cumulative return by model(4)

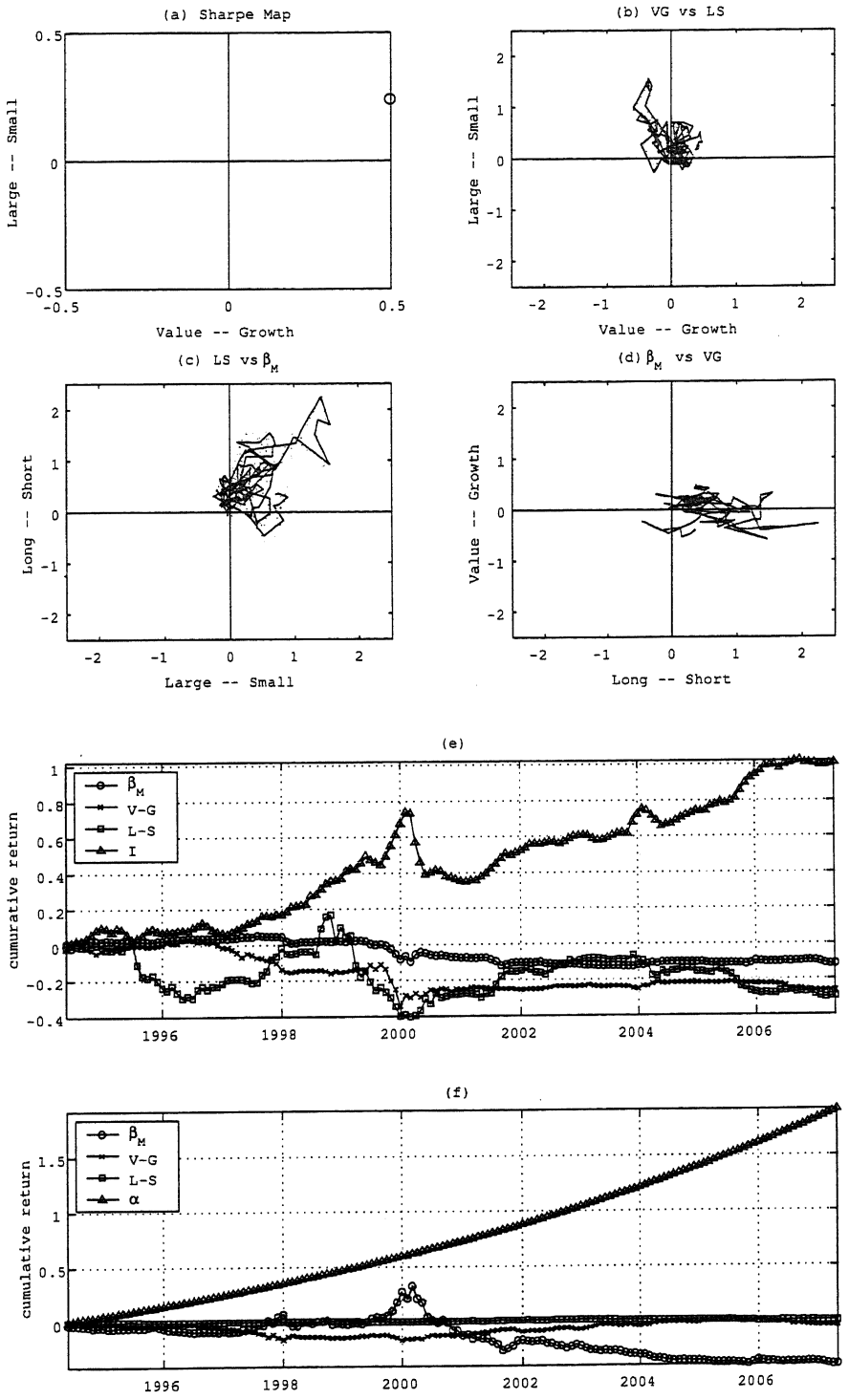

Figure 48: Estimated results of HJF (2) by mixed Gaussian-Poisson noise model (33); (a):Sharpe(VG-LS) map, (b):VG-LS map, (c):β_M-VG map, (d):LS-β_M map. The red dotted lines indicate the time-varying style estimated by Gaussian noise model (10). (e):cumulative return by system(10) and (f):cumulative return by model(4)

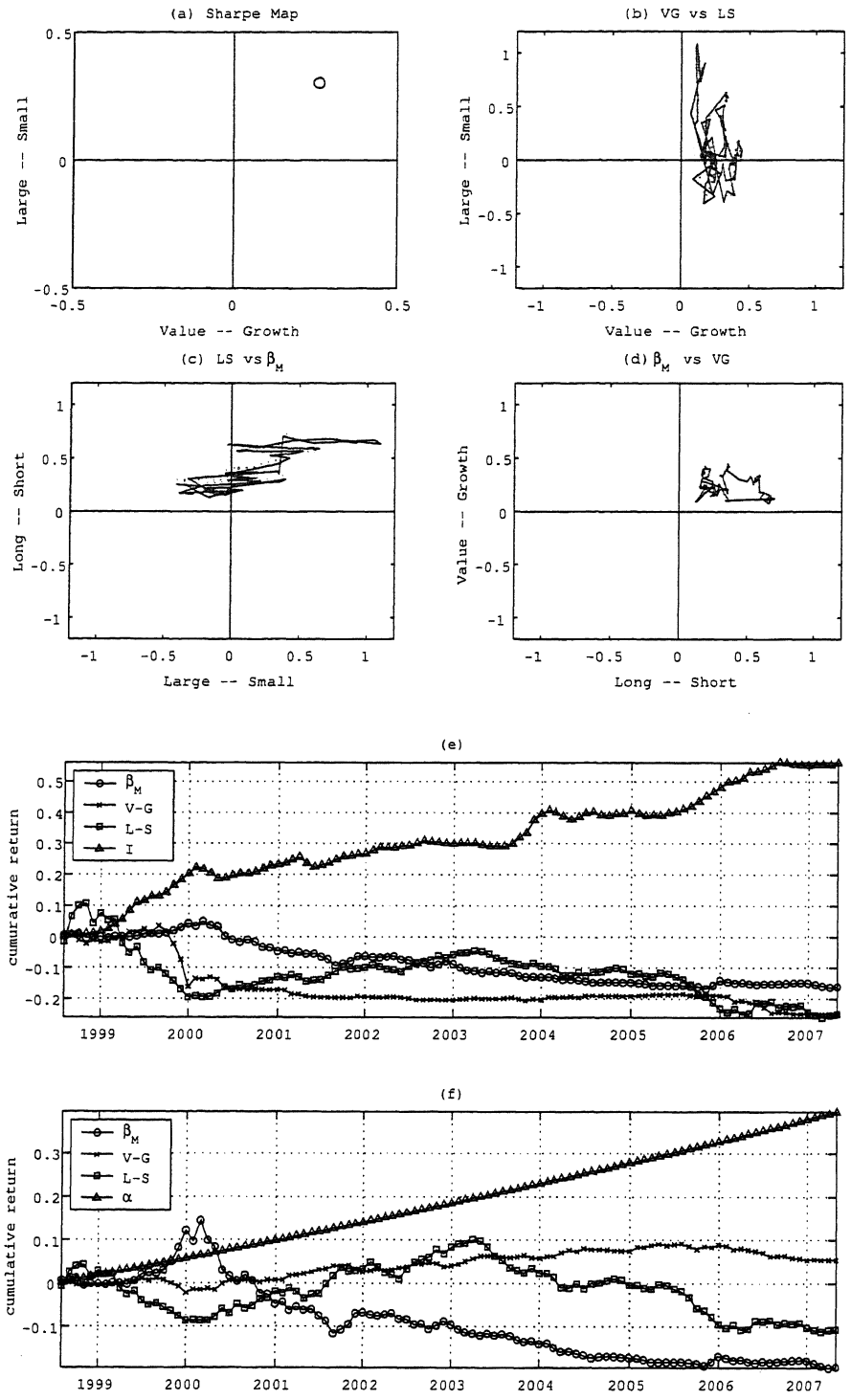

Figure 49: Estimated results of FBR (2) by mixed Gaussian-Poisson noise model (33); (a):Sharpe(VG-LS) map, (b):VG-LS map, (c):β_M-VG map, (d):LS-β_M map. The red dotted lines indicate the time-varying style estimated by Gaussian noise model (10). (e):cumulative return by system(10) and (f):cumulative return by model(4)

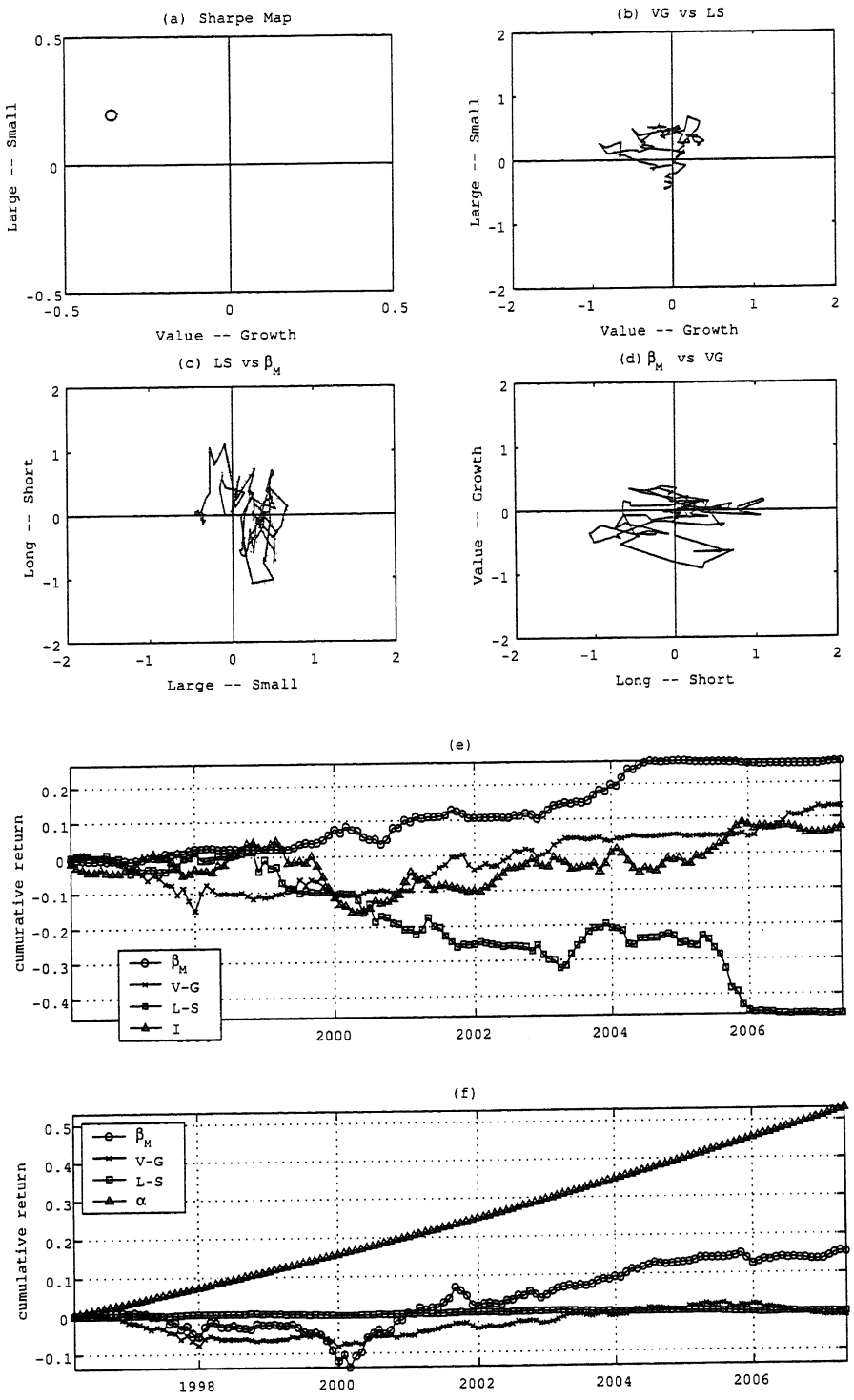

Figure 50: Estimated results of AVO (2) by mixed Gaussian-Poisson noise model (33); (a):Sharpe(VG-LS) map, (b):VG-LS map, (c):β_M-VG map, (d):LS-β_M map. The red dotted lines indicate the time-varying style estimated by Gaussian noise model (10). (e):cumulative return by system(10) and (f):cumulative return by model(4)

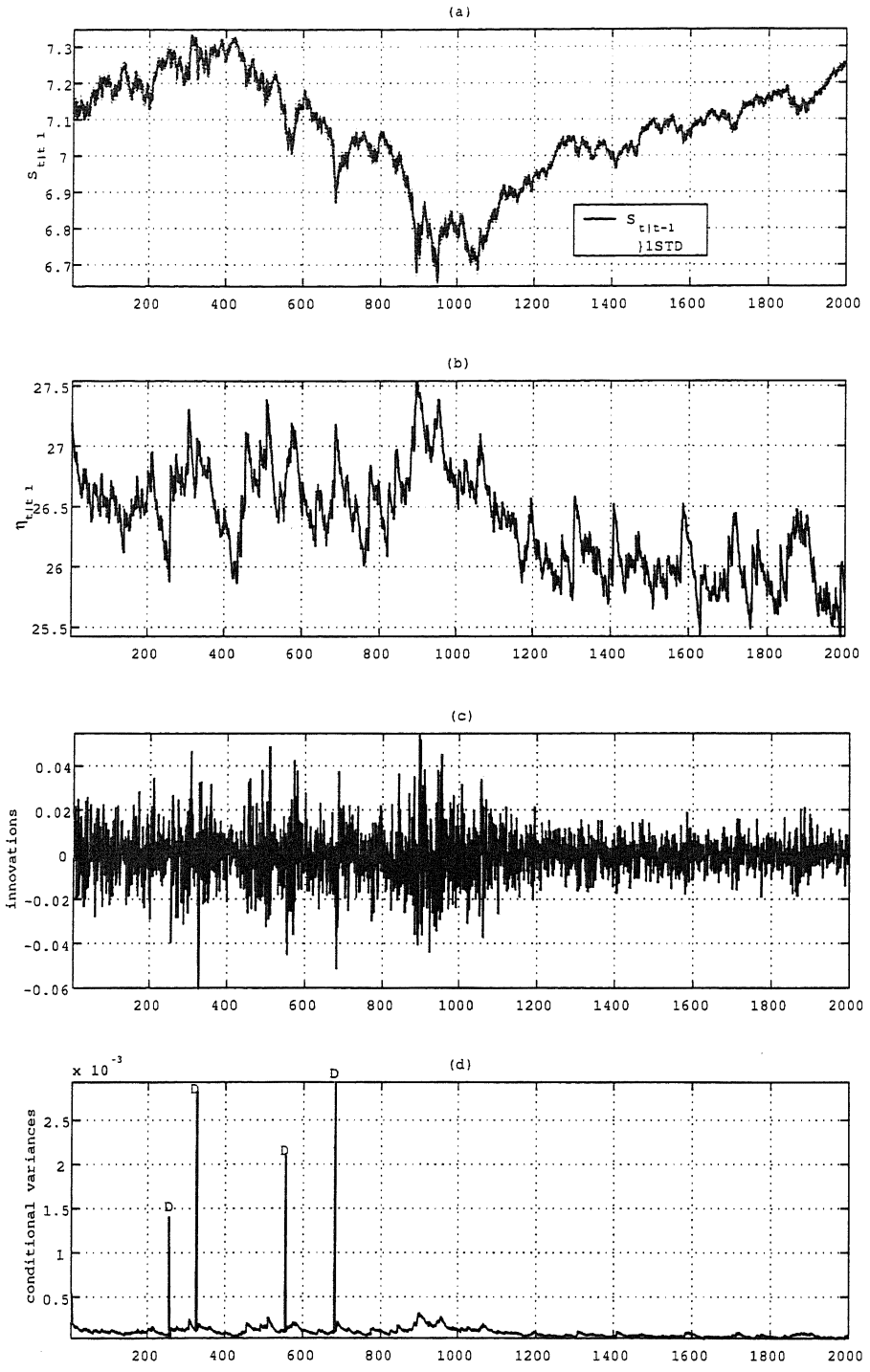

Figure 51: Estimated results of S&P500 by model (42) over the period 31-Dec-1998 to 12-Dec-2006; (a):$S_{t|t-1}$, (b):$\eta_{t|t-1}$, (c):innovations and (d):conditional variance.

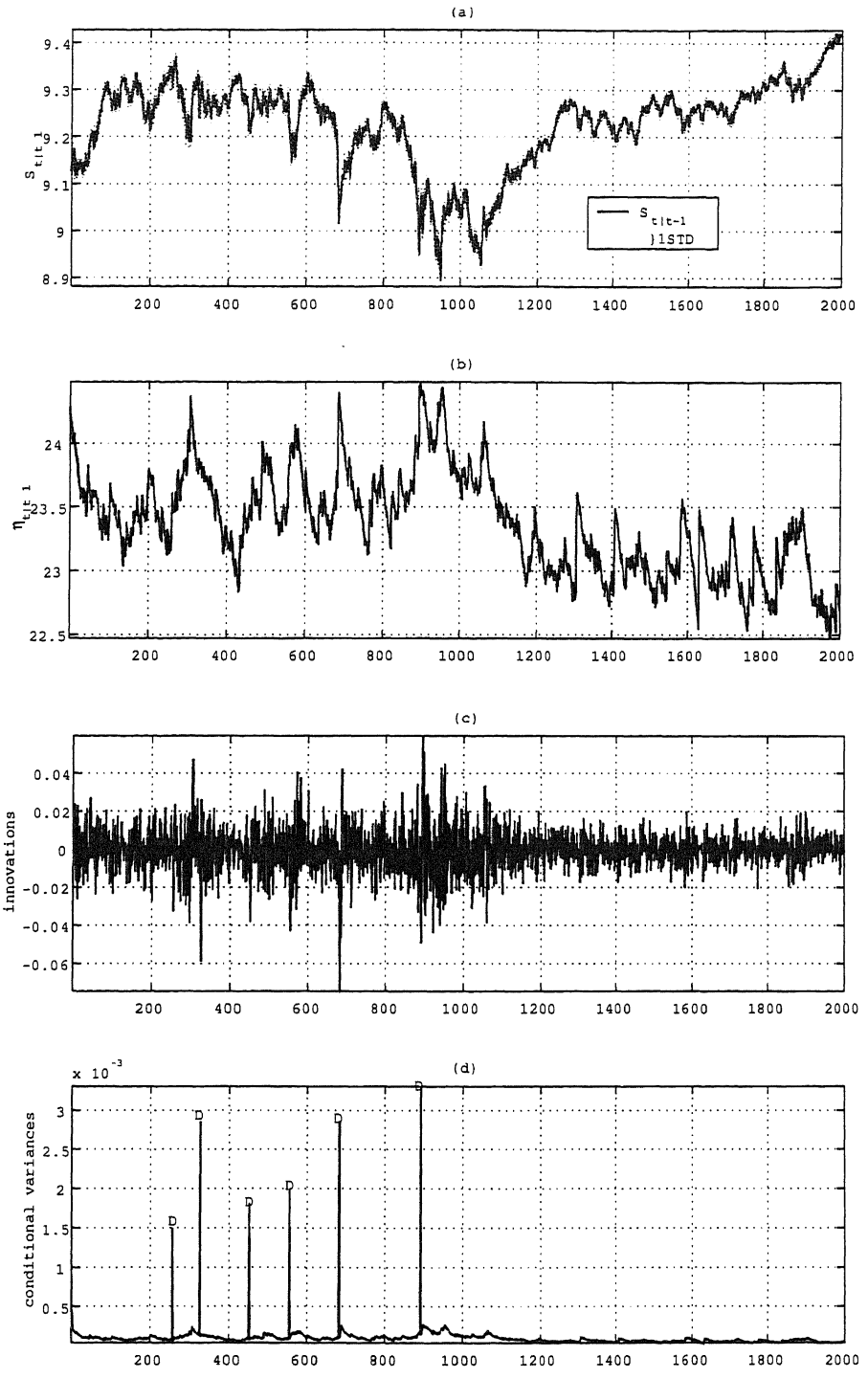

Figure 52: Estimated results of Dow Jones stock index by model (42) over the period 31-Dec-1998 to 12-Dec-2006; (a):$S_{t|t-1}$, (b):$\eta_{t|t-1}$, (c):innovations and (d):conditional variance.

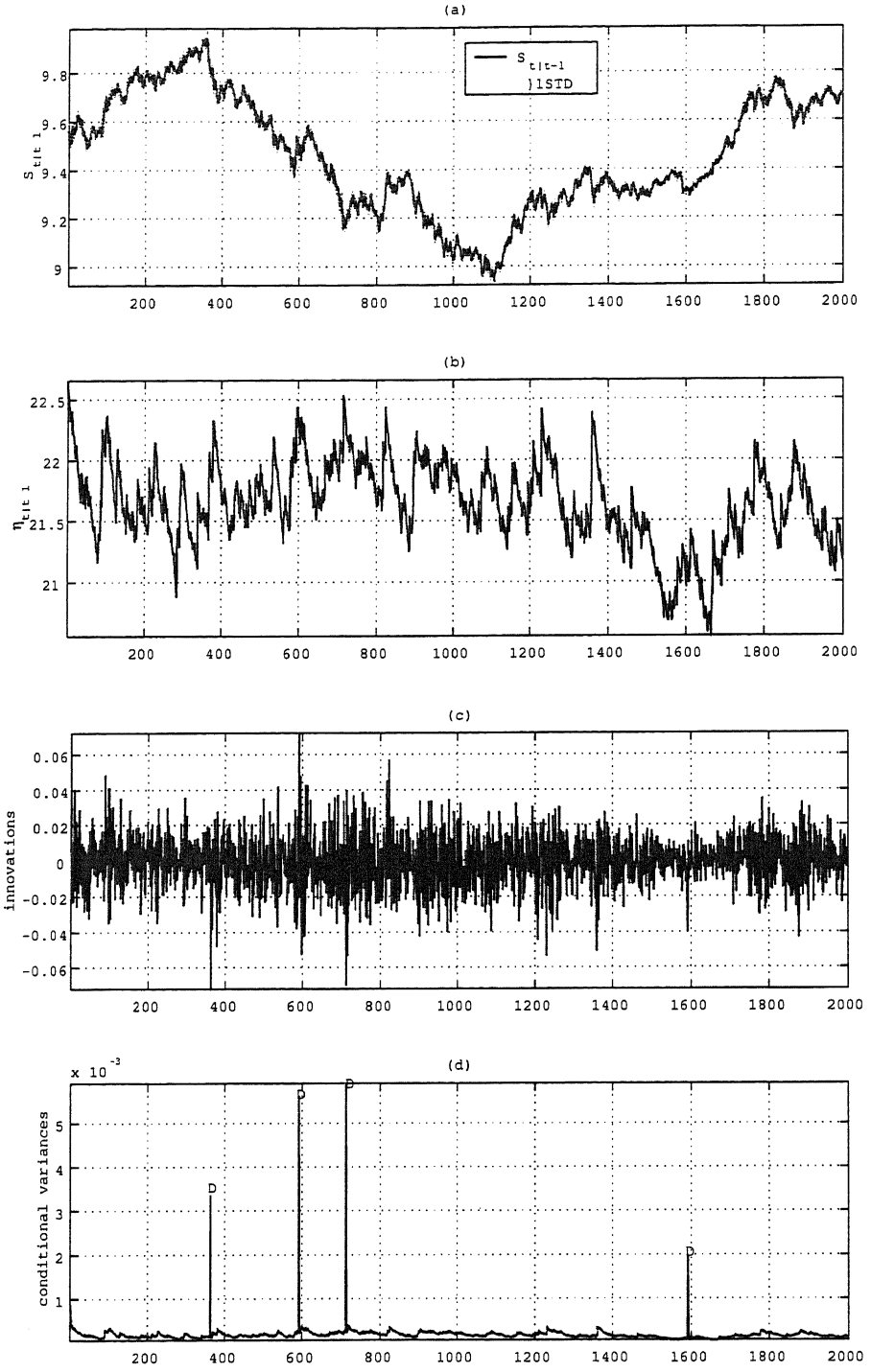

Figure 53: Estimated results of Nikkei225 by model (42) over the period 22-Oct-1998 to 12-Dec-2006 ; (a):$S_{t|t-1}$, (b):$\eta_{t|t-1}$, (c):innovations and (d):conditional variance.

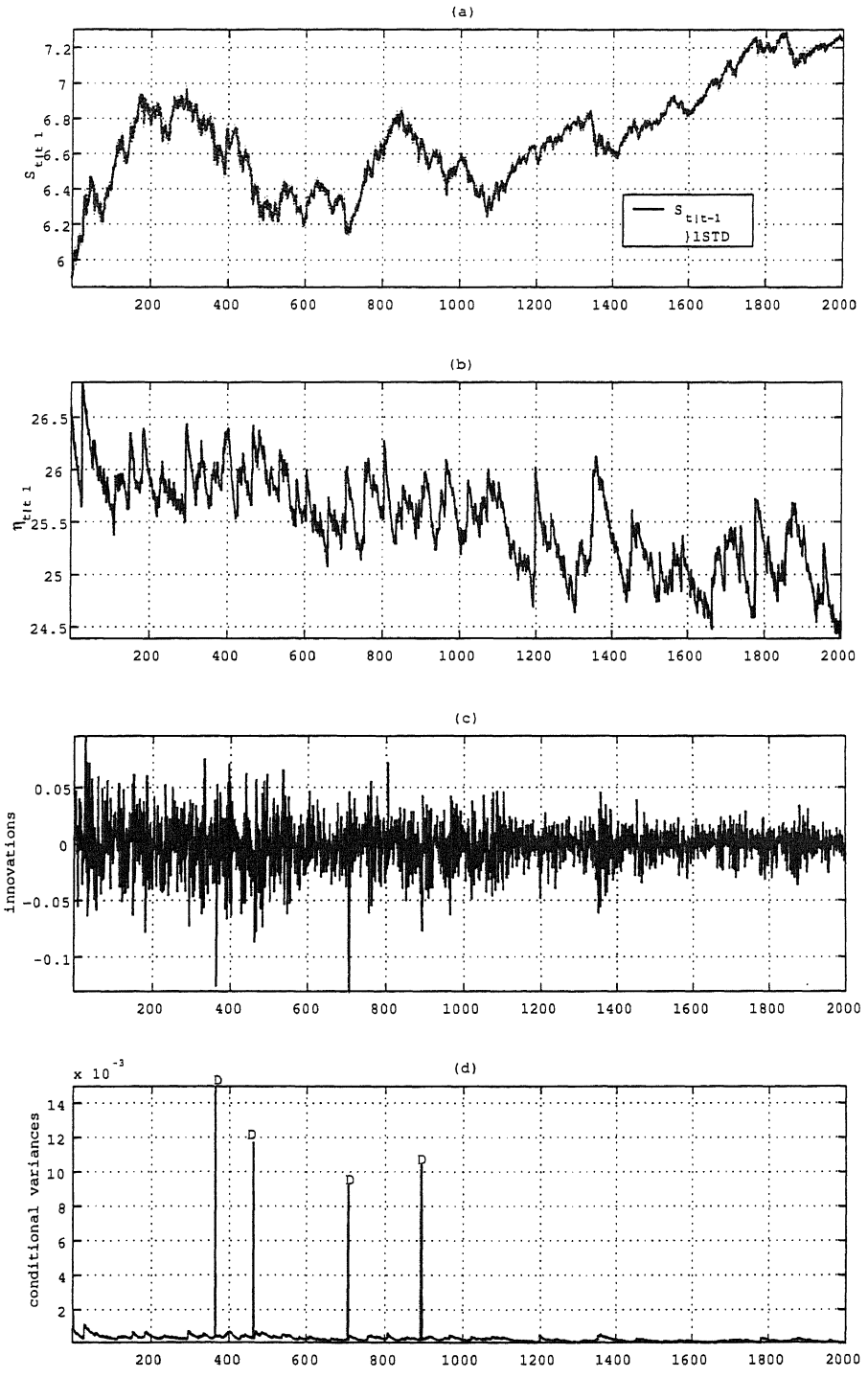

Figure 54: Estimated results of Seoul comp. by model (42) over the period 28-Oct-1998 to 12-Dec-2006; (a):$S_{t|t-1}$, (b):$\eta_{t|t-1}$, (c):innovations and (d):conditional variance.

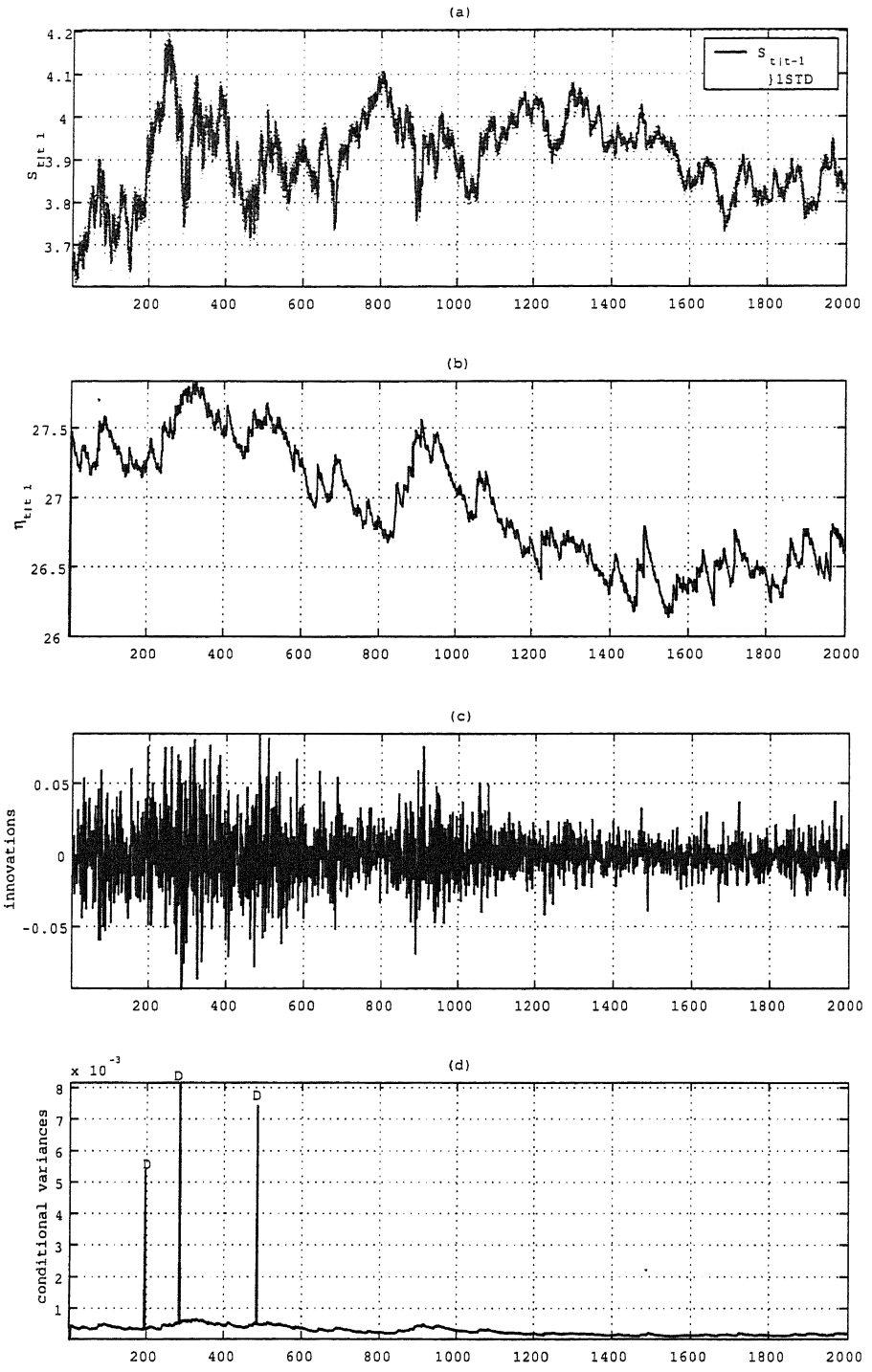

Figure 55: Estimated results of TOYOTA by model (42) over the period 23-Dec-1998 to 13-Dec-2006; (a):$S_{t|t-1}$, (b):$\eta_{t|t-1}$, (c):innovations and (d):conditional variance.

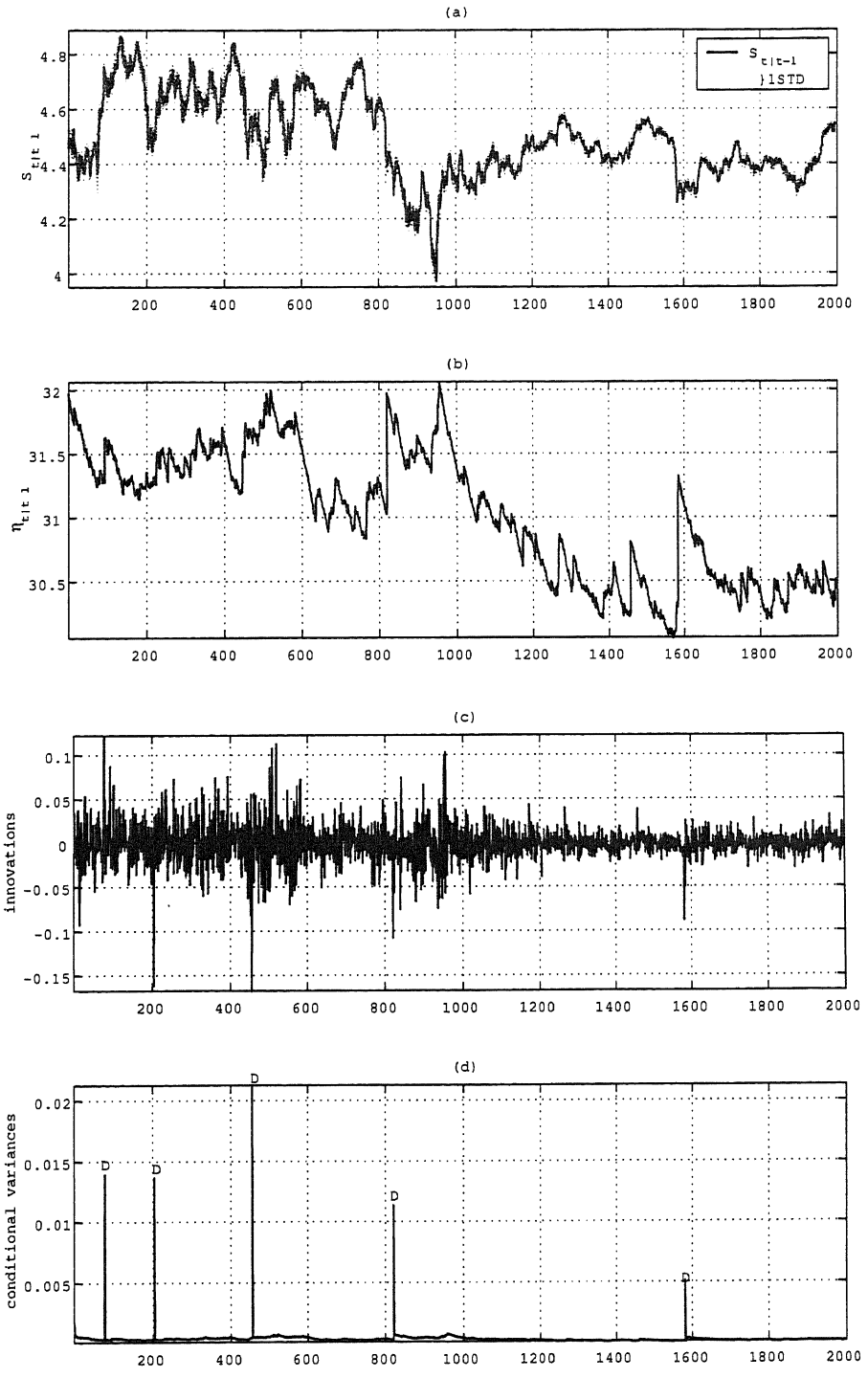

Figure 56: Estimated results of IBM by model (42) over the period 31-Dec-1998 to 12-Dec-2006; (a):$S_{t|t-1}$, (b):$\eta_{t|t-1}$, (c):innovations and (d):conditional variance.

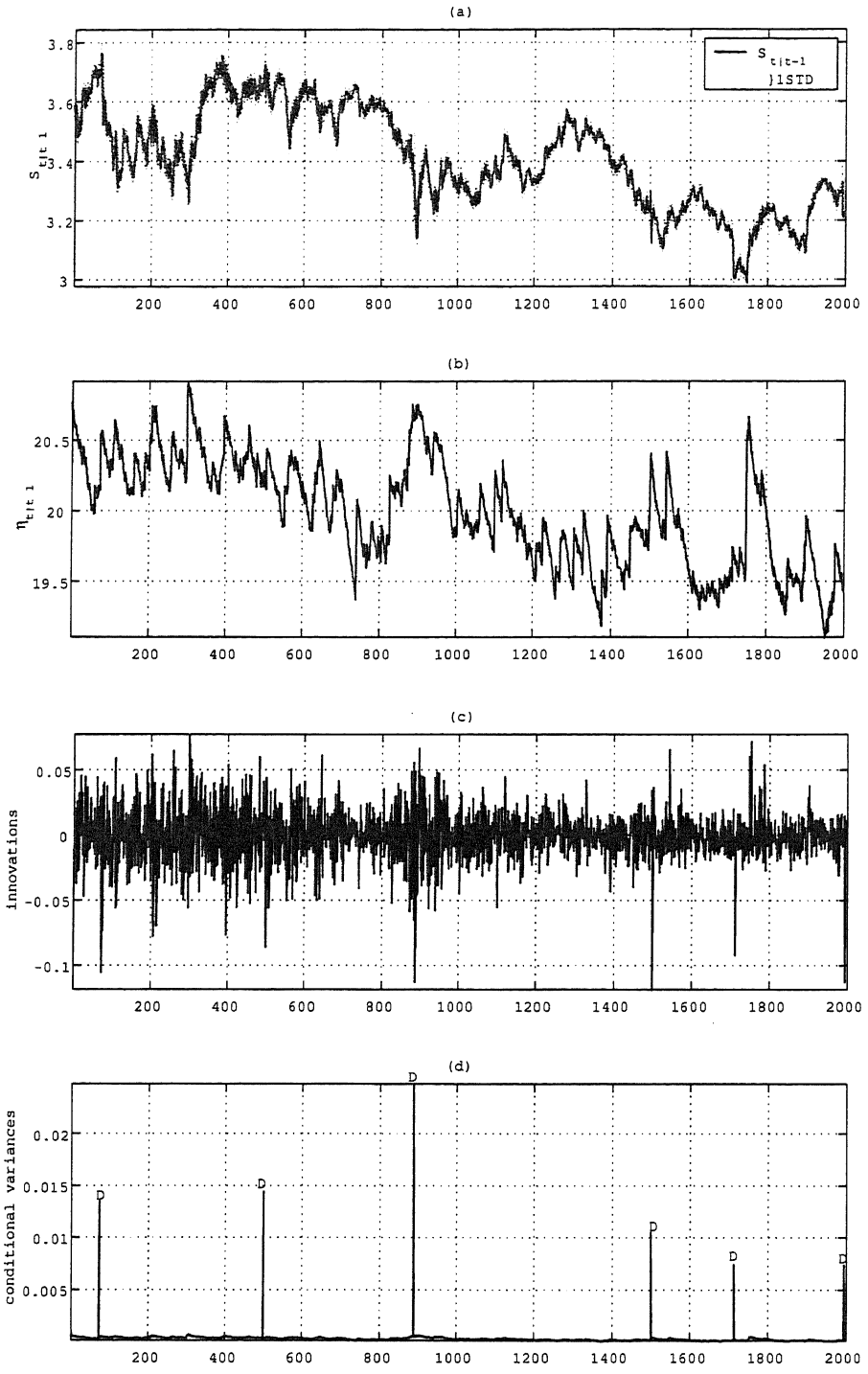

Figure 57: Estimated results of Pfizer by model (42) over the period 31-Dec-1998 to 12-Dec-2006; (a):$S_{t|t-1}$, (b):$\eta_{t|t-1}$, (c):innovations and (d):conditional variance.

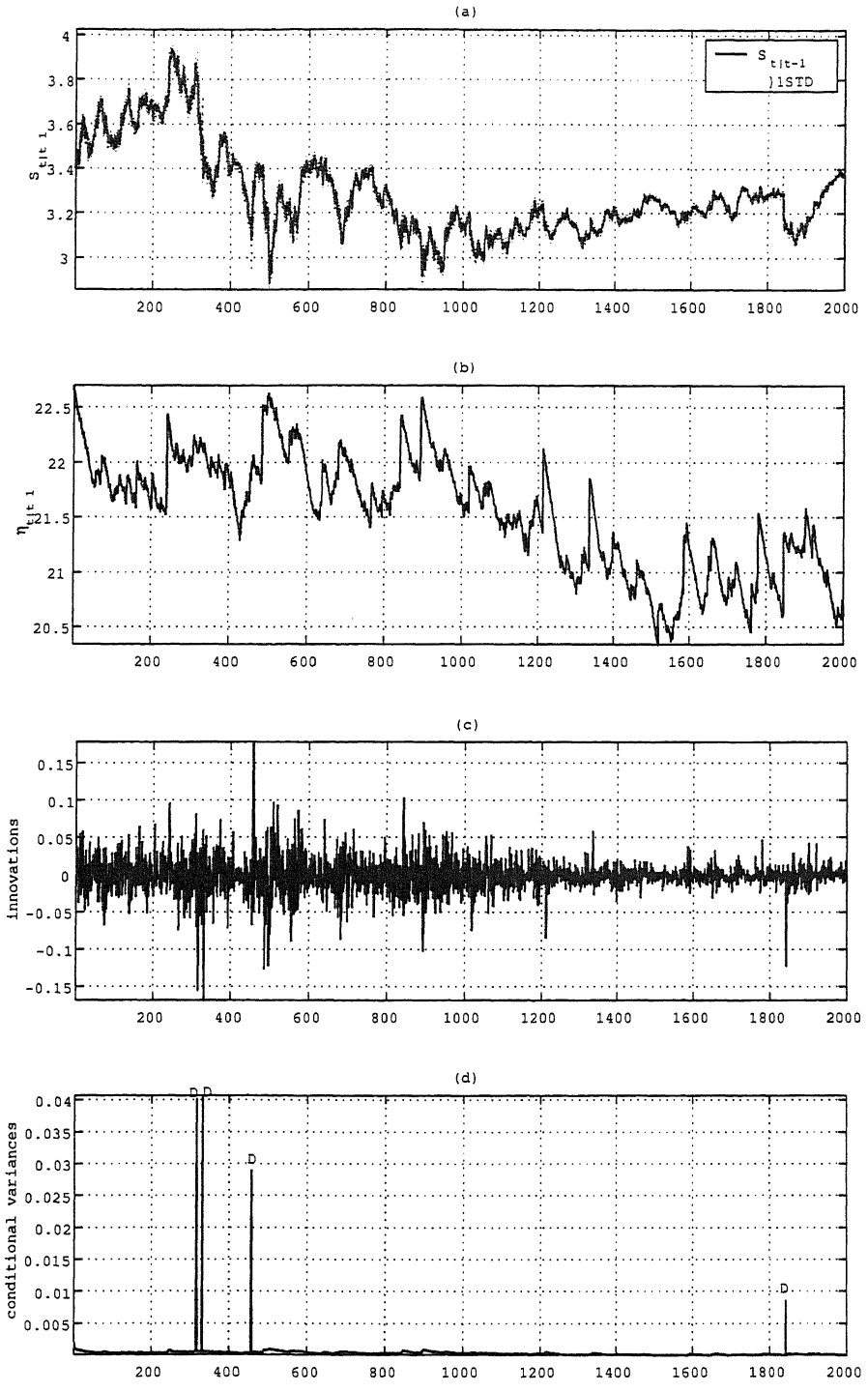

Figure 58: Estimated results of Microsoft by model (42) over the period 31-Dec-1998 to 12-Dec-2006; (a):$S_{t|t-1}$, (b):$\eta_{t|t-1}$, (c):innovations and (d):conditional variance.

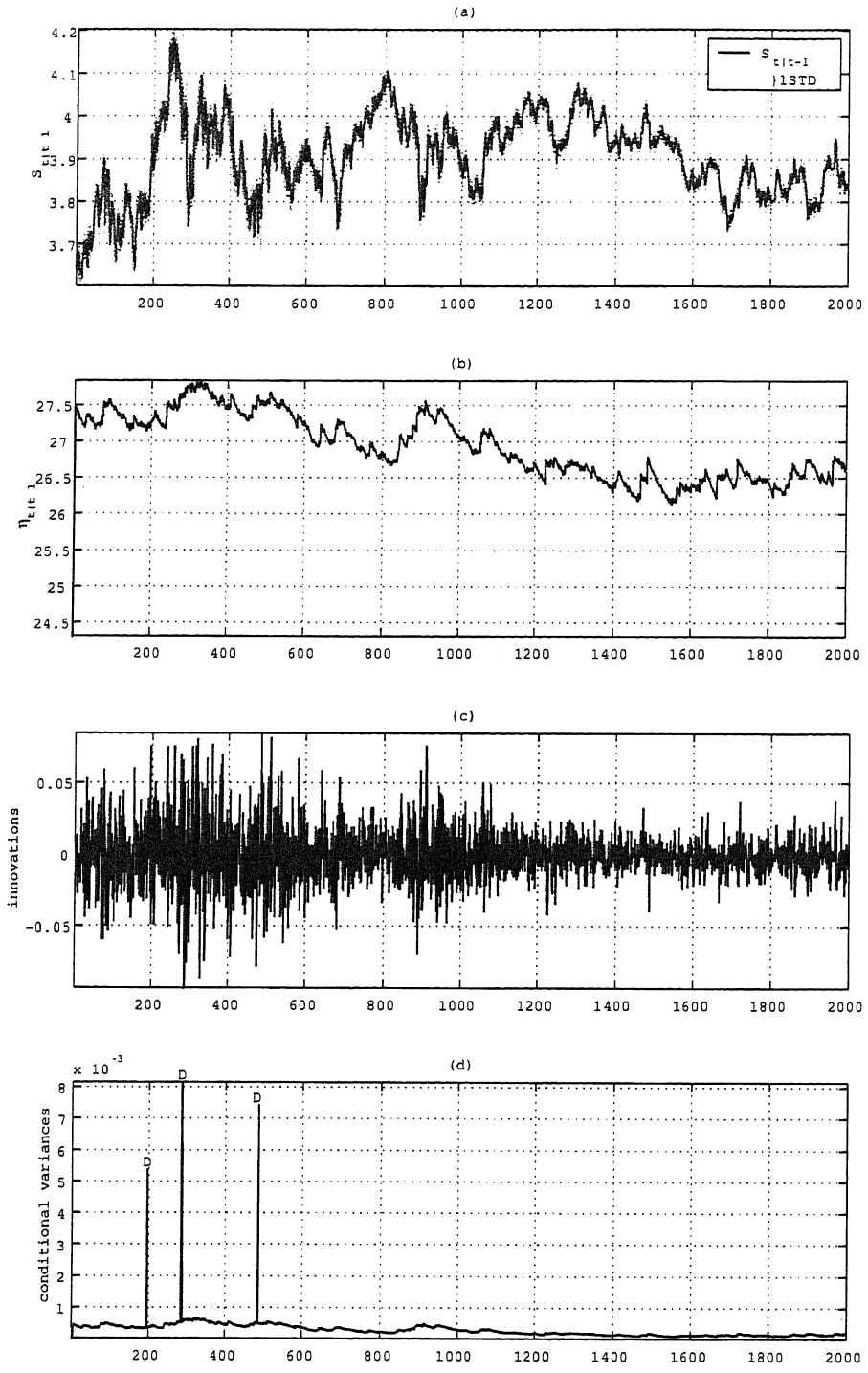

Figure 59: Estimated results of Wal-Mart by model (42) over the period 31-Dec-1998 to 12-Dec-2006; (a):$S_{t|t-1}$, (b):$\eta_{t|t-1}$, (c):innovations and (d):conditional variance.

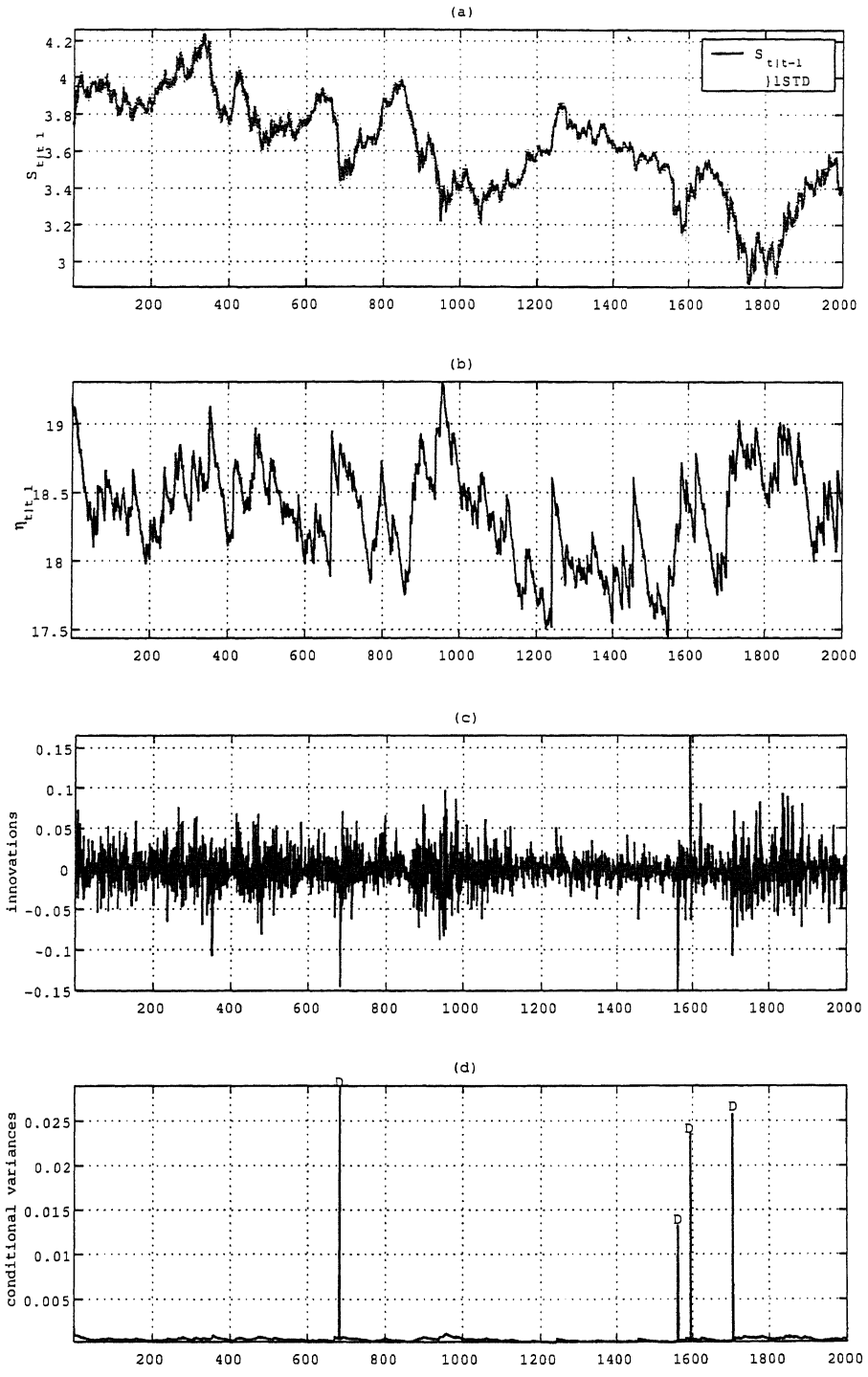

Figure 60: Estimated results of General Motors by model (42) over the period 31-Dec-1998 to 12-Dec-2006; (a):$S_{t|t-1}$, (b):$\eta_{t|t-1}$, (c):innovations and (d):conditional variance.

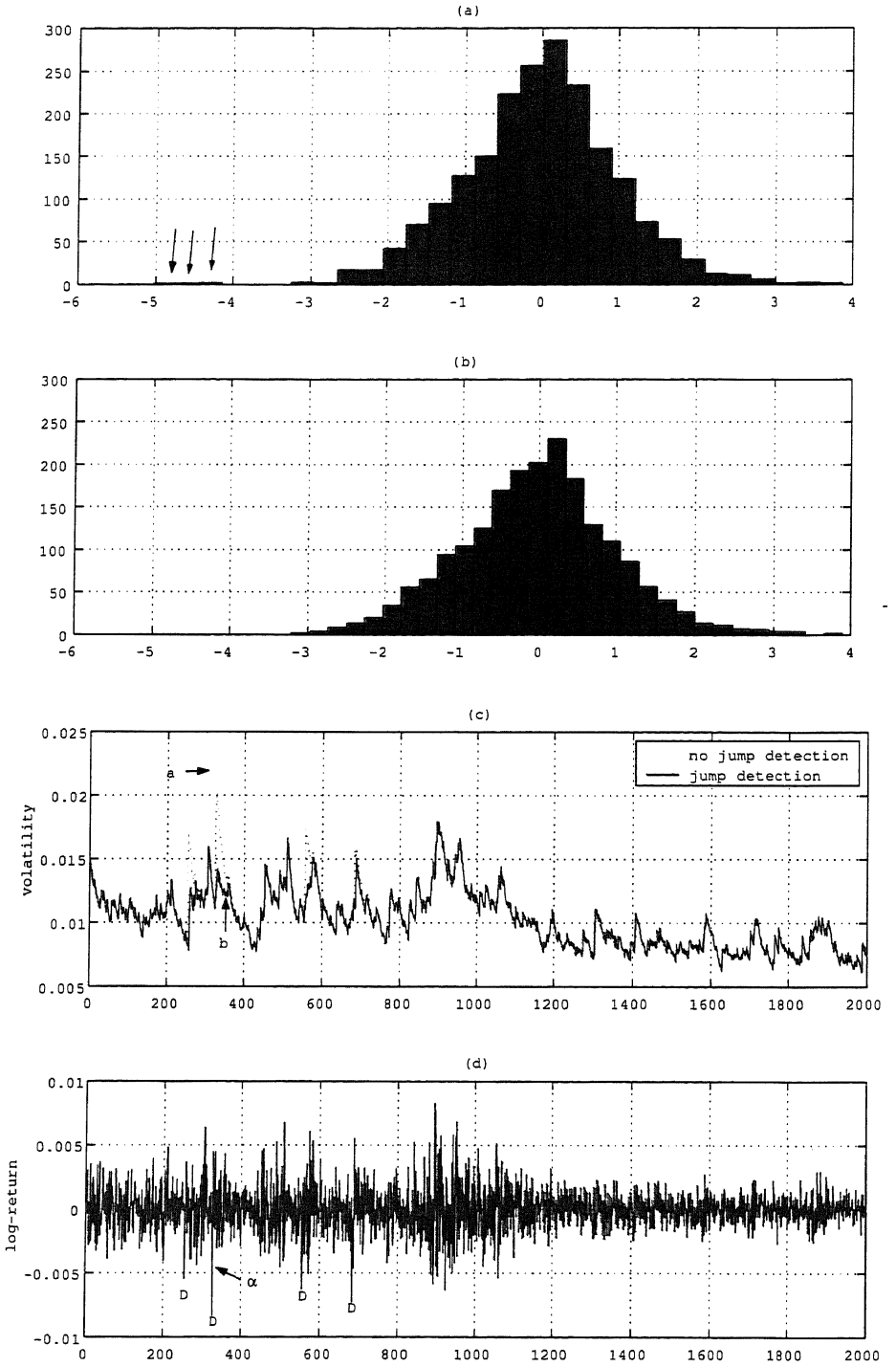

Figure 61: Estimated results of S&P500 over the period 31-Dec-1998 to 12-Dec-2006; (a):histogram of normalized innovation by model (24), (b):by model (42), (c): estimated volatility by model (42) and (d) log-return of the data.

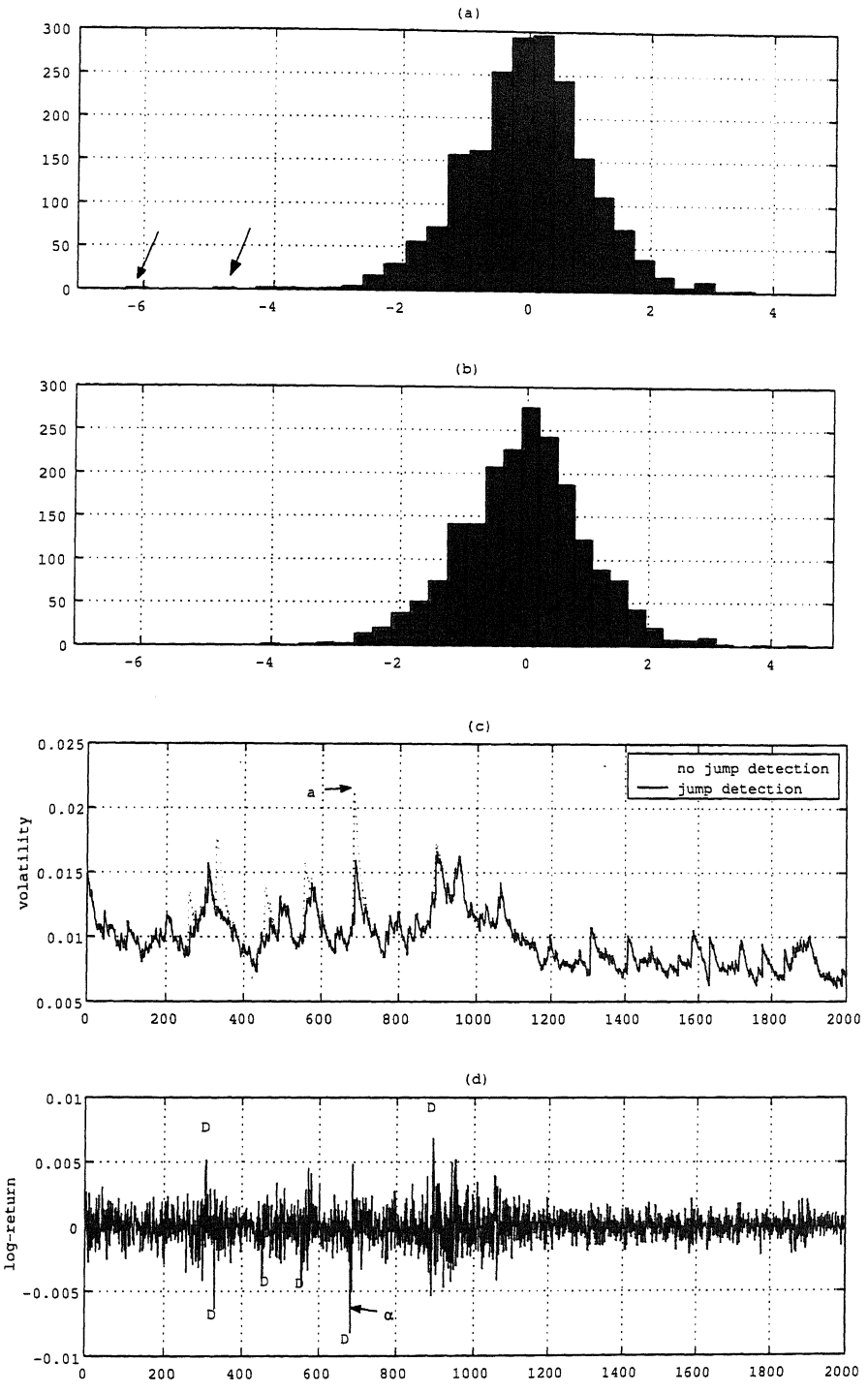

Figure 62: Estimated results of Dow Jones stock index over the period 31-Dec-1998 to 12-Dec-2006; (a):histogram of normalized innovation by model (24), (b):by model (42), (c): estimated volatility by model (42) and (d) log-return of the data.

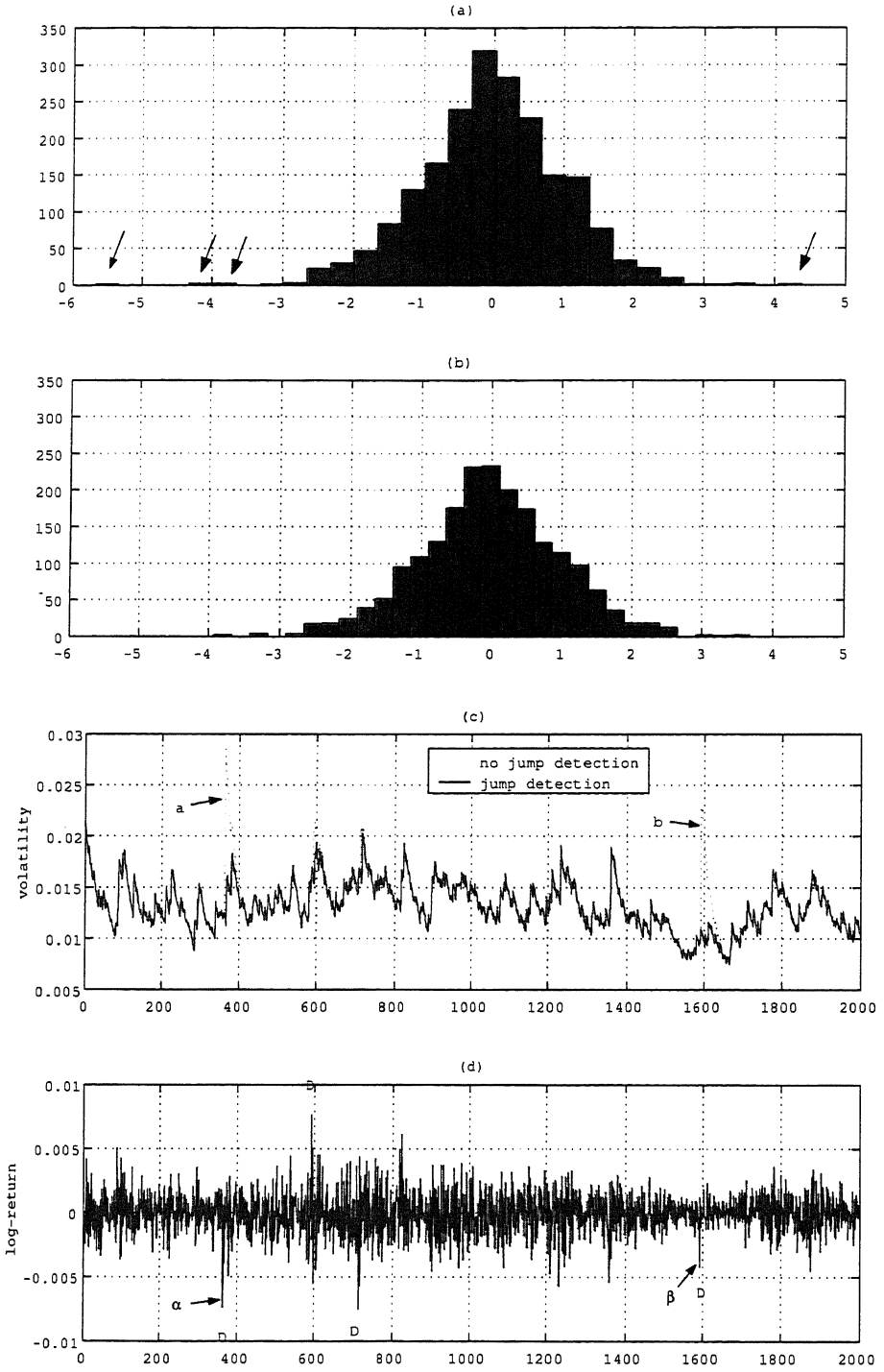

Figure 63: Estimated results of Nikkei225 over the period 22-Oct-1998 to 12-Dec-2006 ; (a):histogram of normalized innovation by model (24), (b):by model (42), (c): estimated volatility by model (42) and (d) log-return of the data.

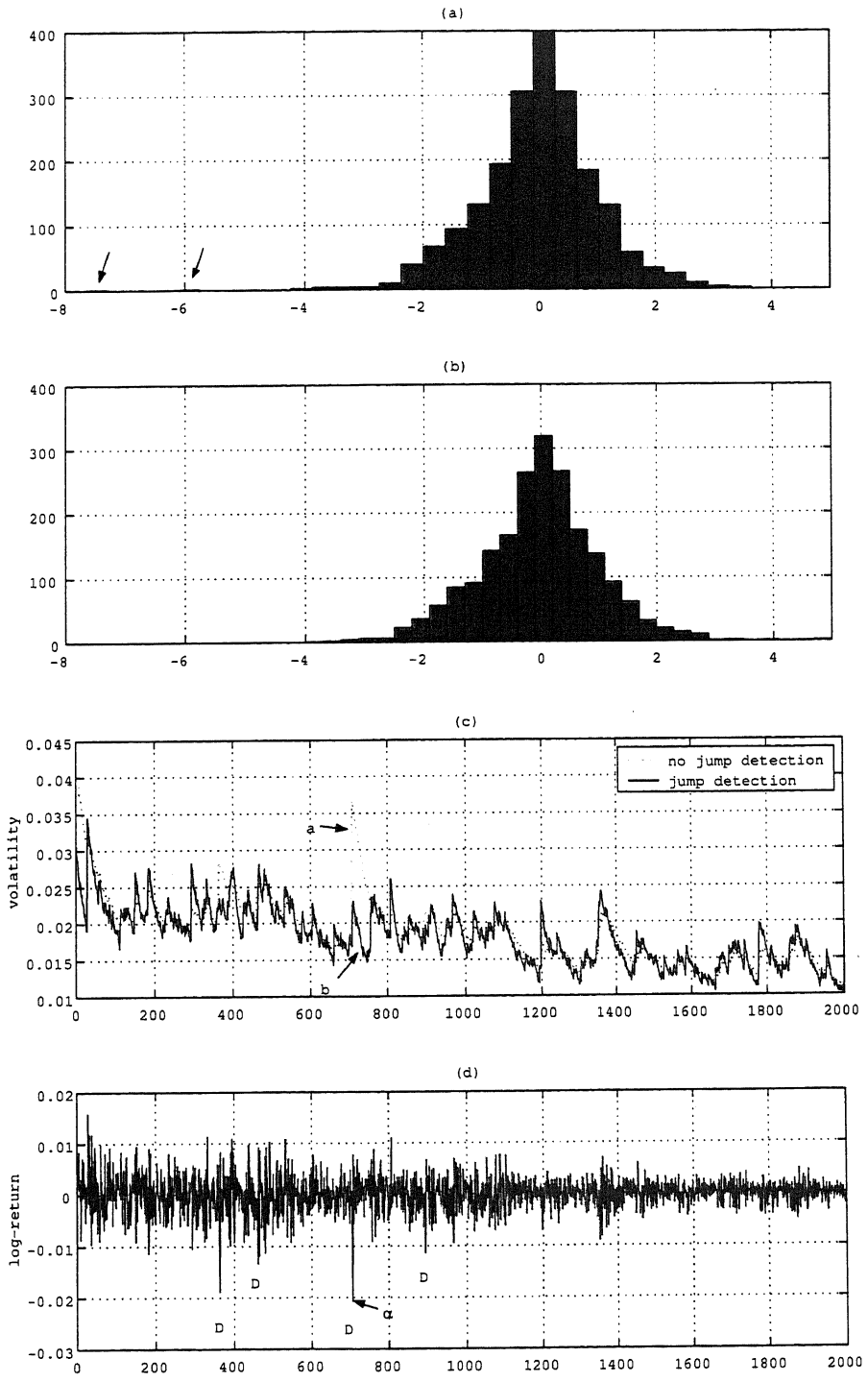

Figure 64: Estimated results of Seoul comp. over the period 28-Oct-1998 to 12-Dec-2006; (a):histogram of normalized innovation by model (24), (b):by model (42), (c): estimated volatility by model (42) and (d) log-return of the data.

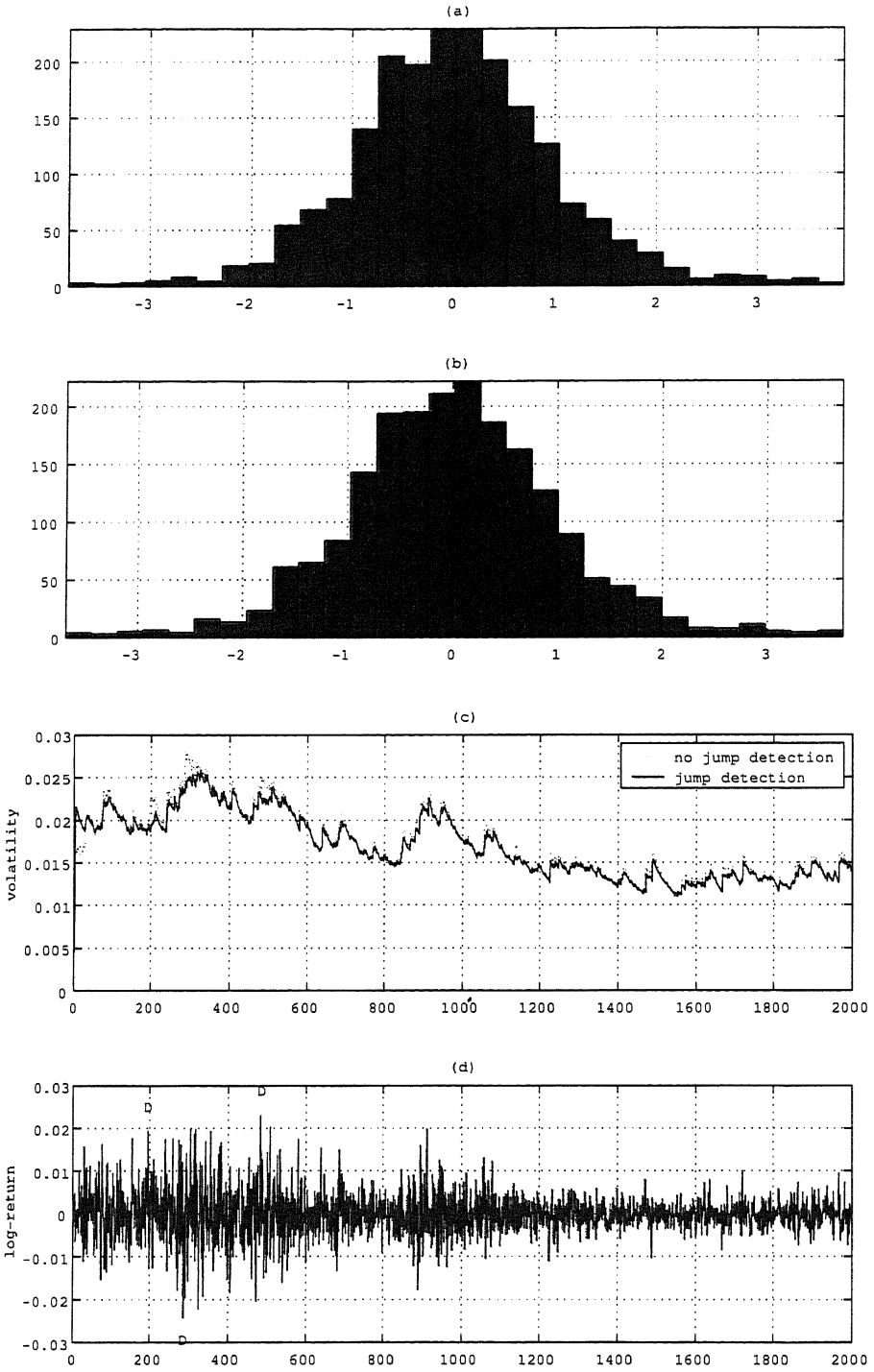

Figure 65: Estimated results of TOYOTA over the period 23-Dec-1998 to 13-Dec-2006 ; (a):histogram of normalized innovation by model (24), (b):by model (42), (c): estimated volatility by model (42) and (d) log-return of the data.

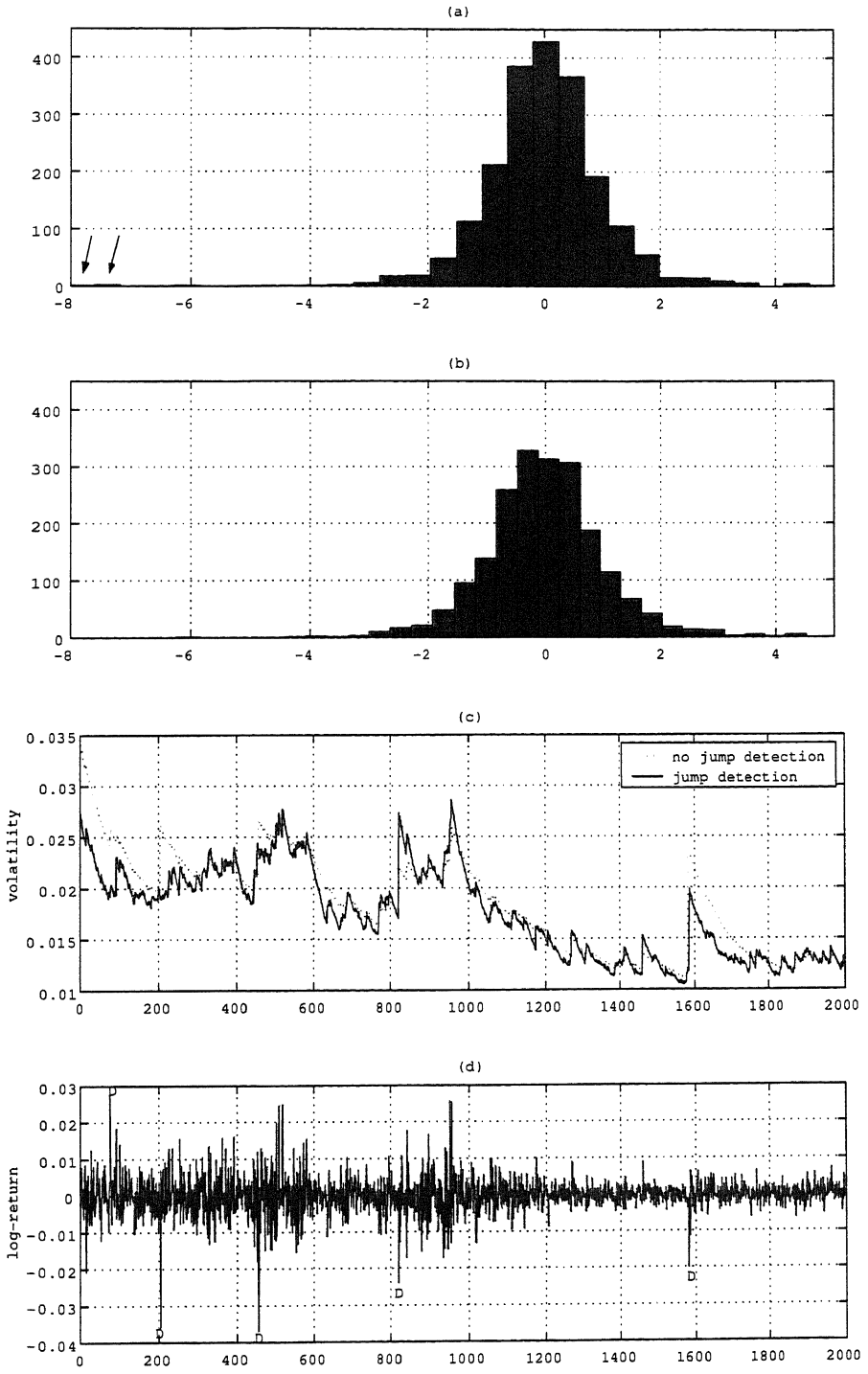

Figure 66: Estimated results of IBM over the period 31-Dec-1998 to 12-Dec-2006; (a):histogram of normalized innovation by model (24), (b):by model (42), (c): estimated volatility by model (42) and (d) log-return of the data.

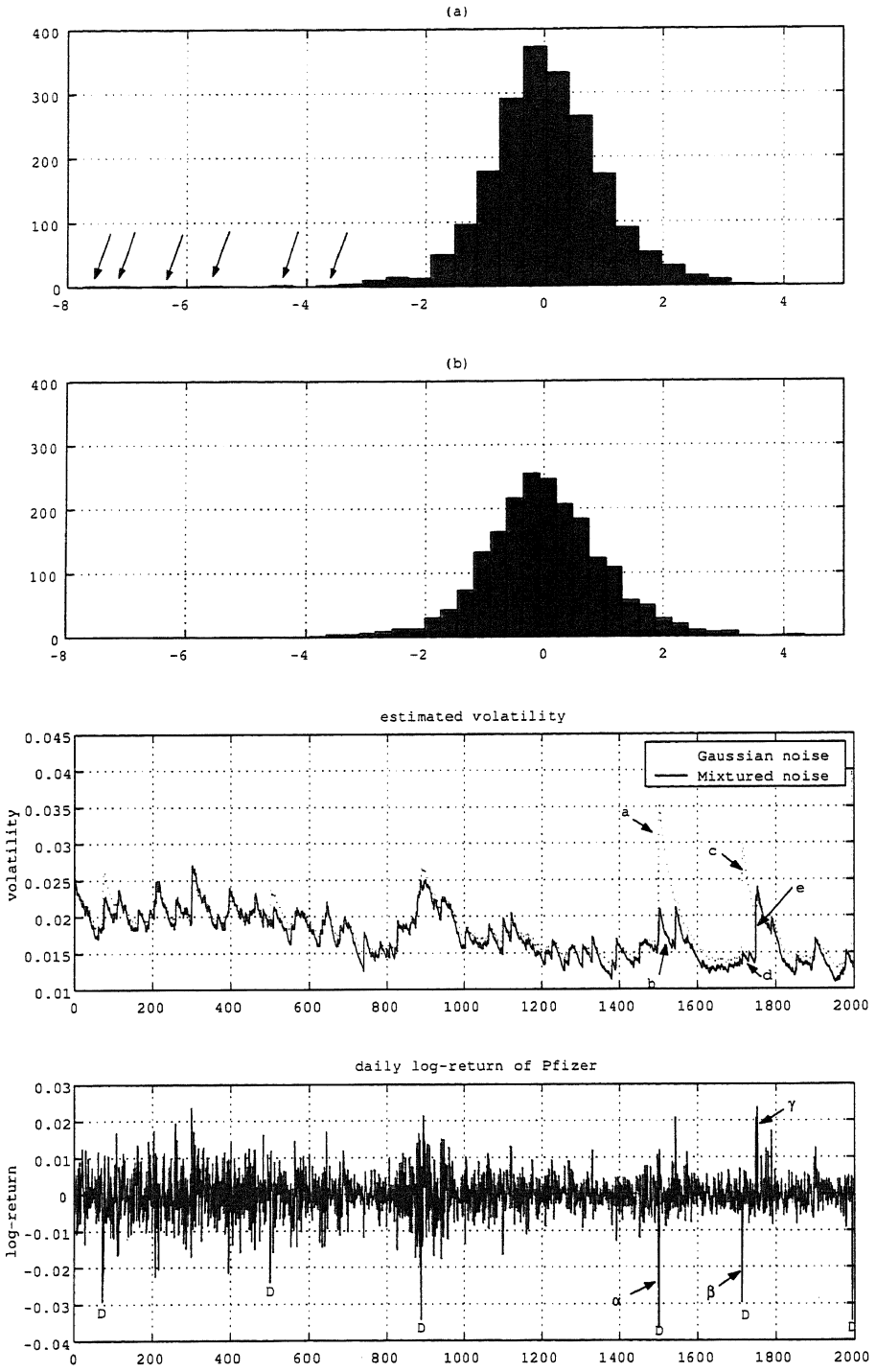

Figure 67: Estimated results of Pfizer over the period 31-Dec-1998 to 12-Dec-2006; (a):histogram of normalized innovation by model (24), (b):by model (42), (c): estimated volatility by model (42) and (d) log-return of the data.

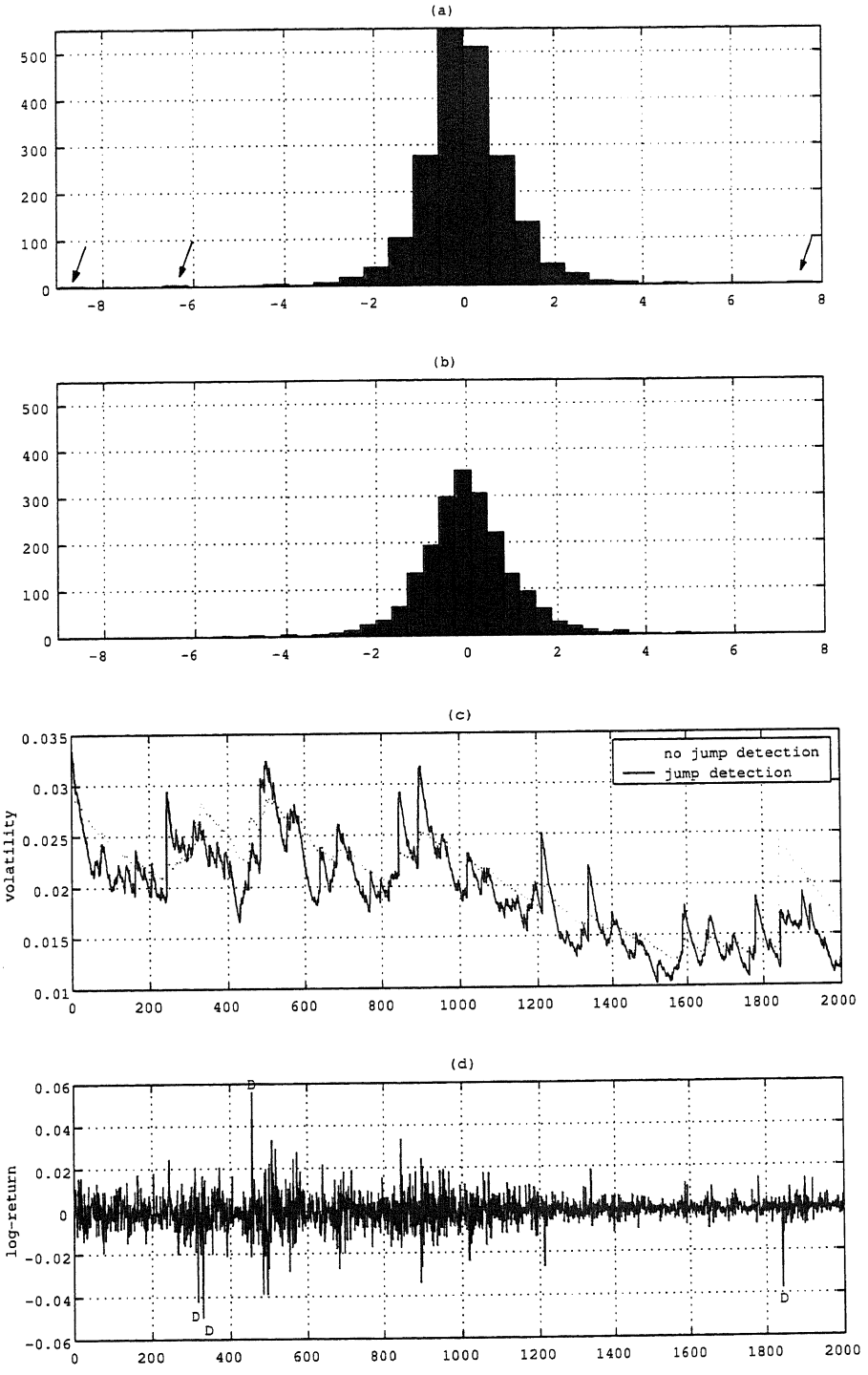

Figure 68: Estimated results of Microsoft over the period 31-Dec-1998 to 12-Dec-2006; (a):histogram of normalized innovation by model (24), (b):by model (42), (c): estimated volatility by model (42) and (d) log-return of the data.

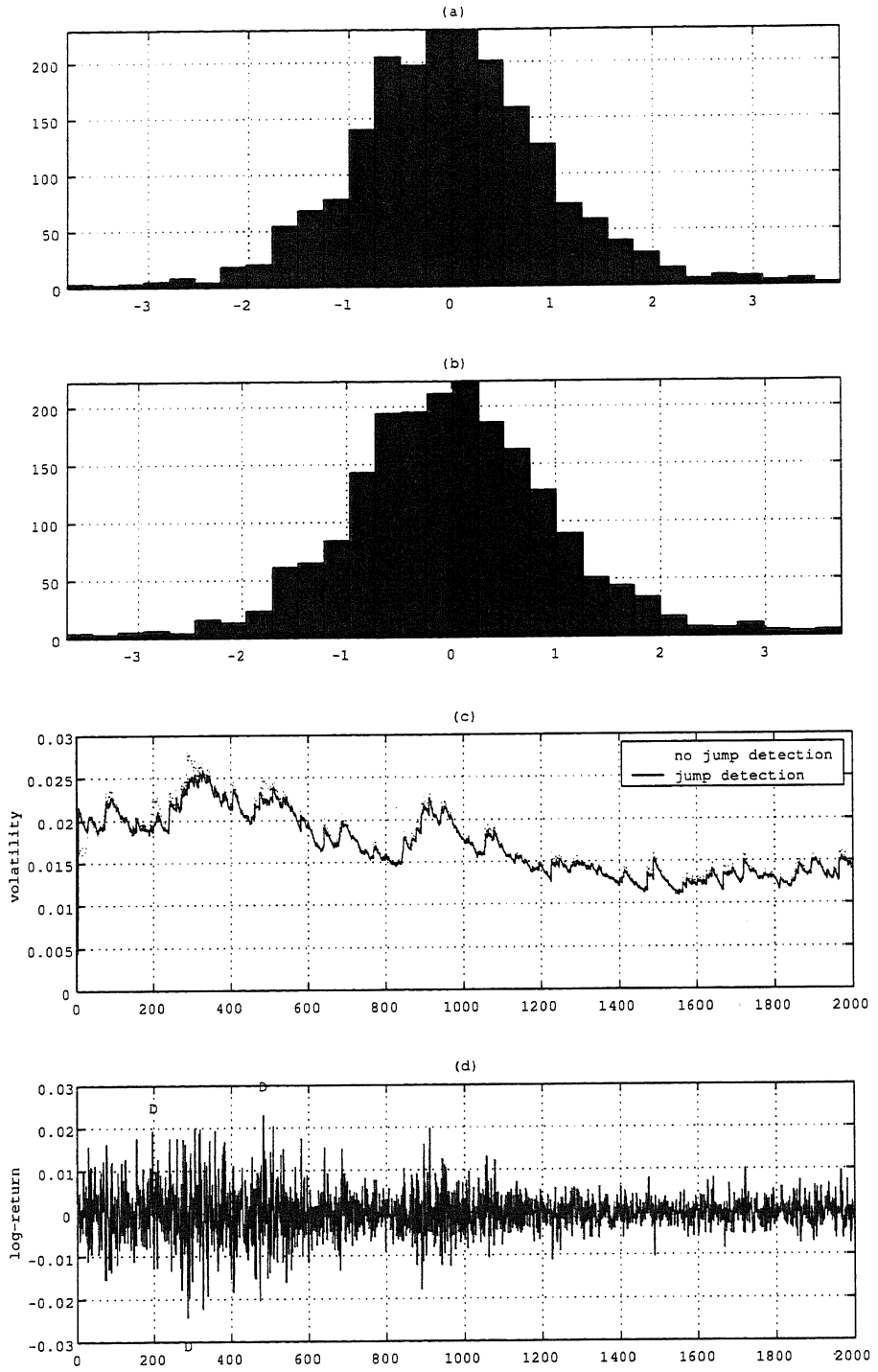

Figure 69: Estimated results of Wal-Mart over the period 31-Dec-1998 to 12-Dec-2006; (a):histogram of normalized innovation by model (24), (b):by model (42), (c): estimated volatility by model (42) and (d) log-return of the data.

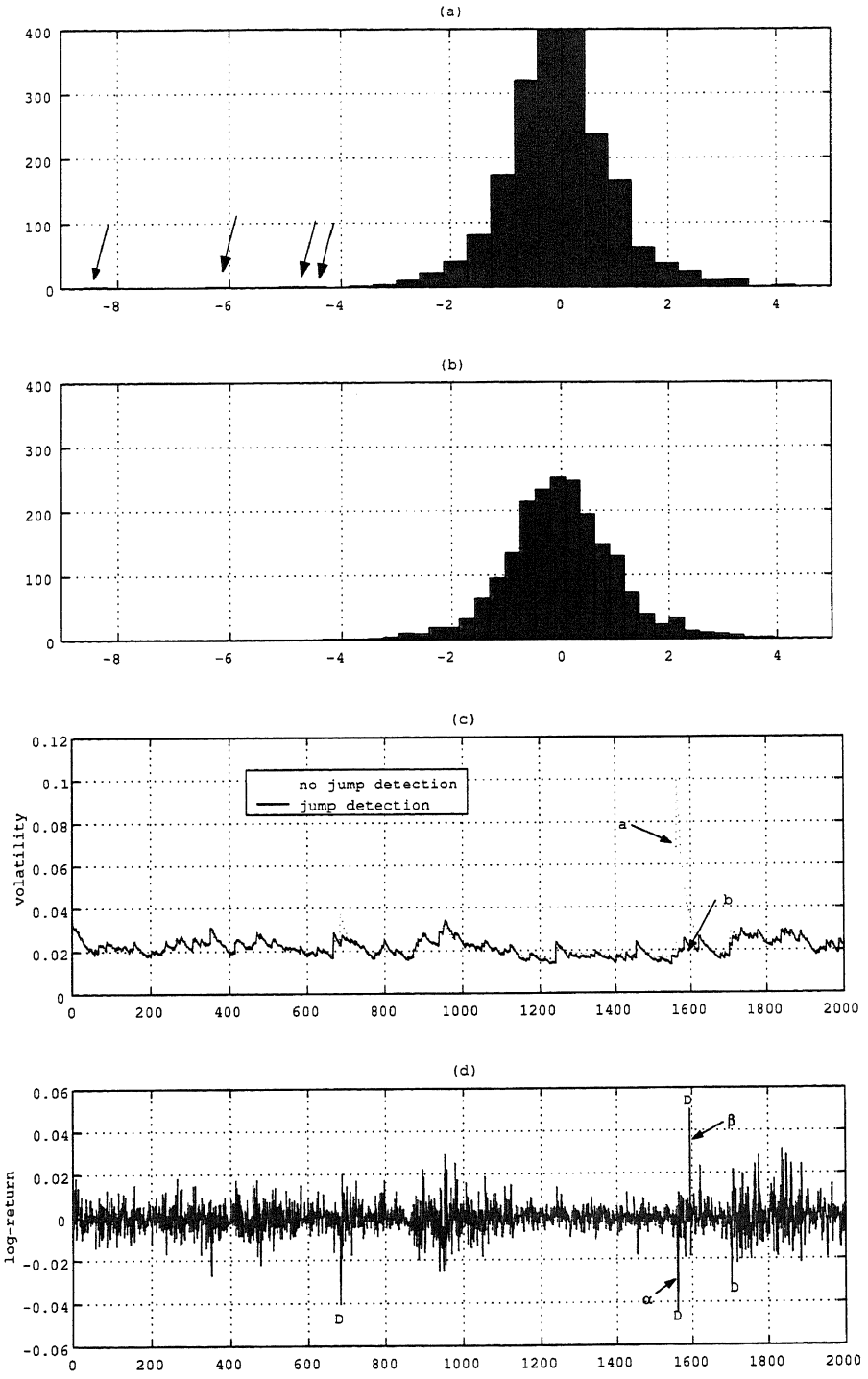

Figure 70: Estimated results of General motors over the period 31-Dec-1998 to 12-Dec-2006; (a):histogram of normalized innovation by model (24), (b):by model (42), (c): estimated volatility by model (42) and (d) log-return of the data.

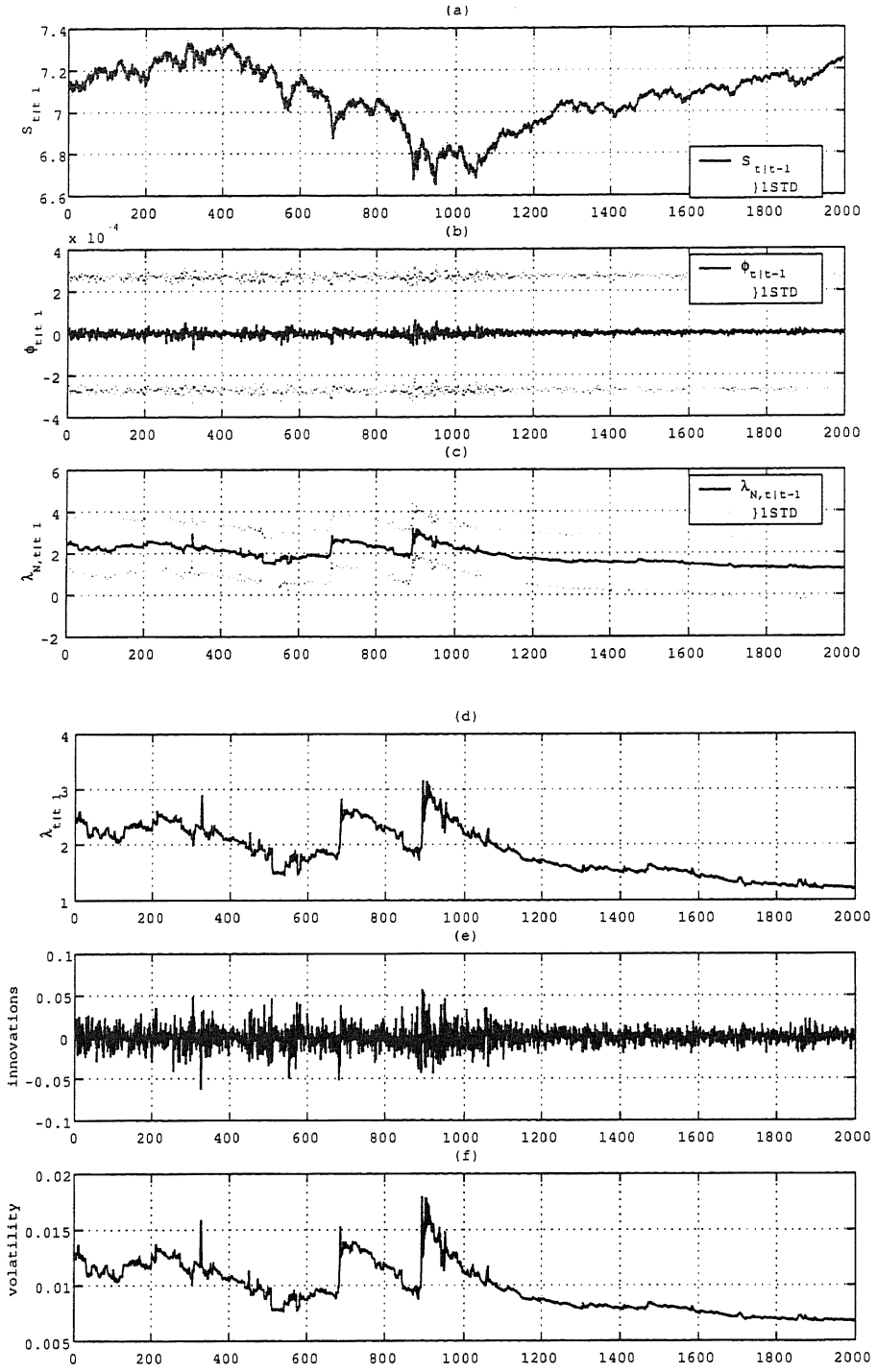

Figure 71: Estimated results of S&P500 by model (28) over the period 31-Dec-1998 to 12-Dec-2006; (a):$S_{t|t-1}$, (b):$\phi_{t|t-1}$, (c):$\lambda_{N,t|t-1}$, (d):$\lambda_{N,t|t-1}$, (e):innovations and (f):volatility.

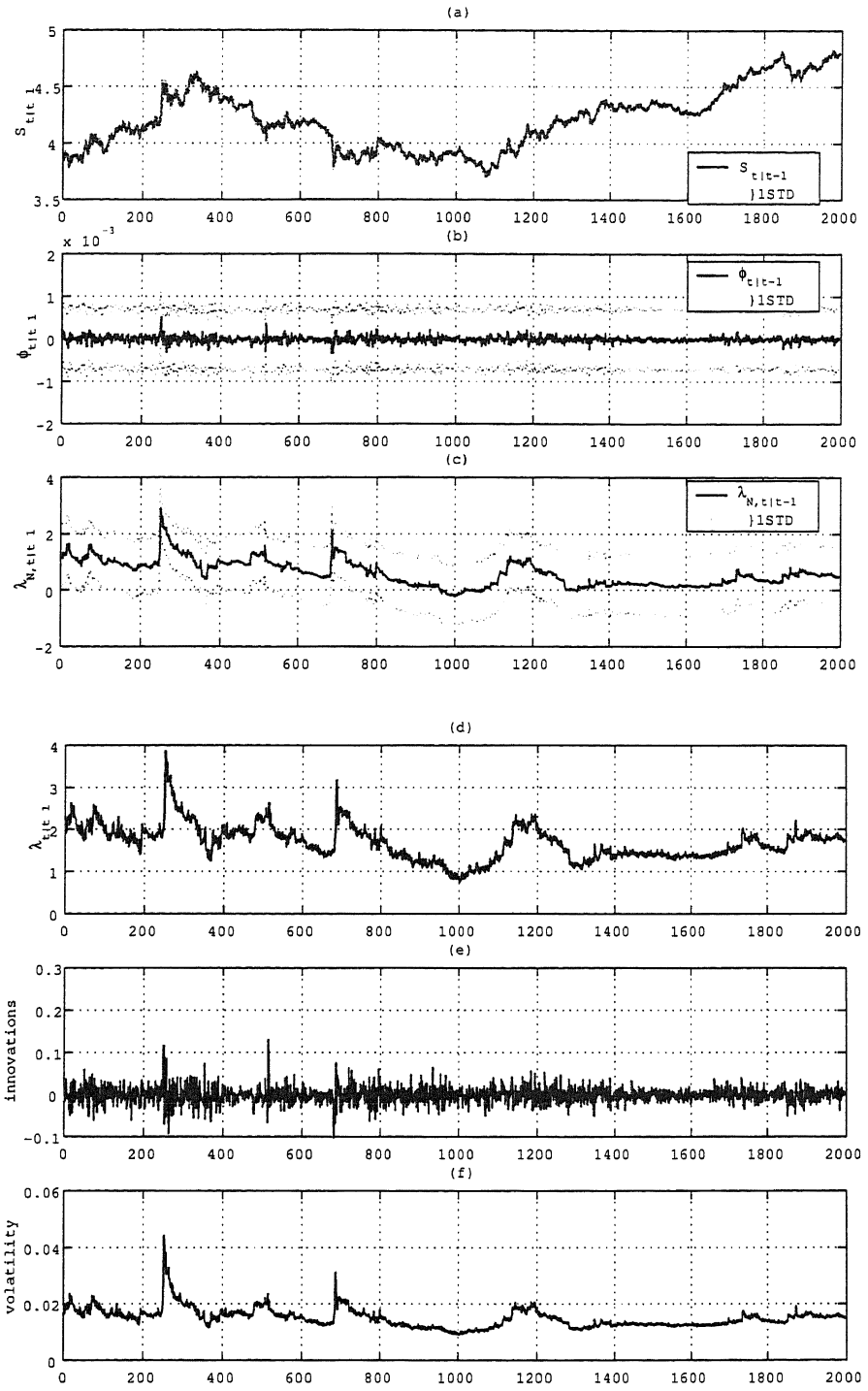

Figure 72: Estimated results of TOYOTA by model (28) over the period 23-Dec-1998 to 13-Dec-2006 ; (a):$S_{t|t-1}$, (b):$\phi_{t|t-1}$, (c):$\lambda_{N,t|t-1}$, (d):$\lambda_{N,t|t-1}$, (e):innovations and (f):volatility.

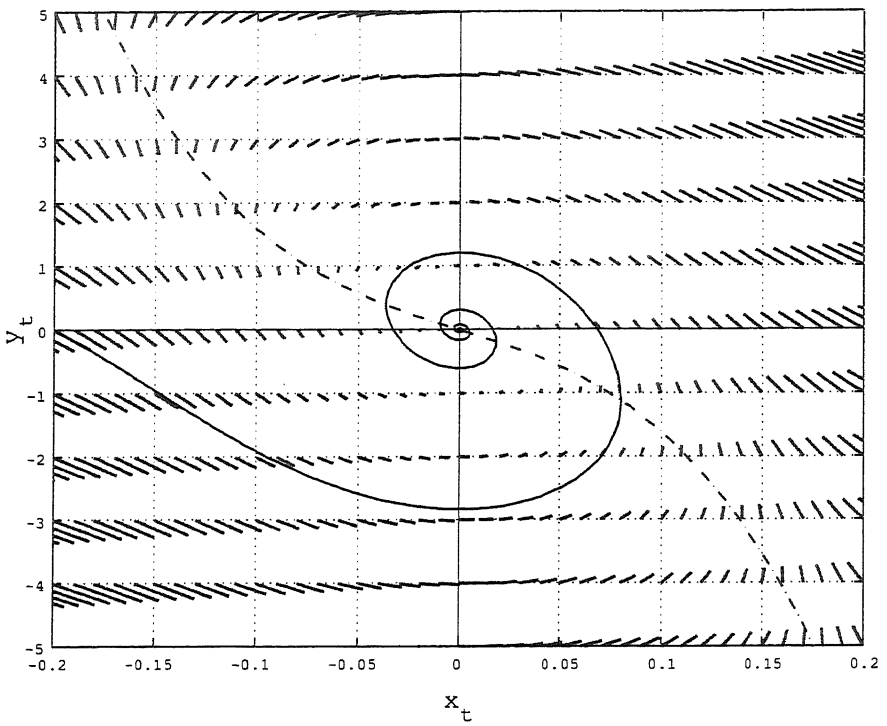

(a) Phase chart and solution flow

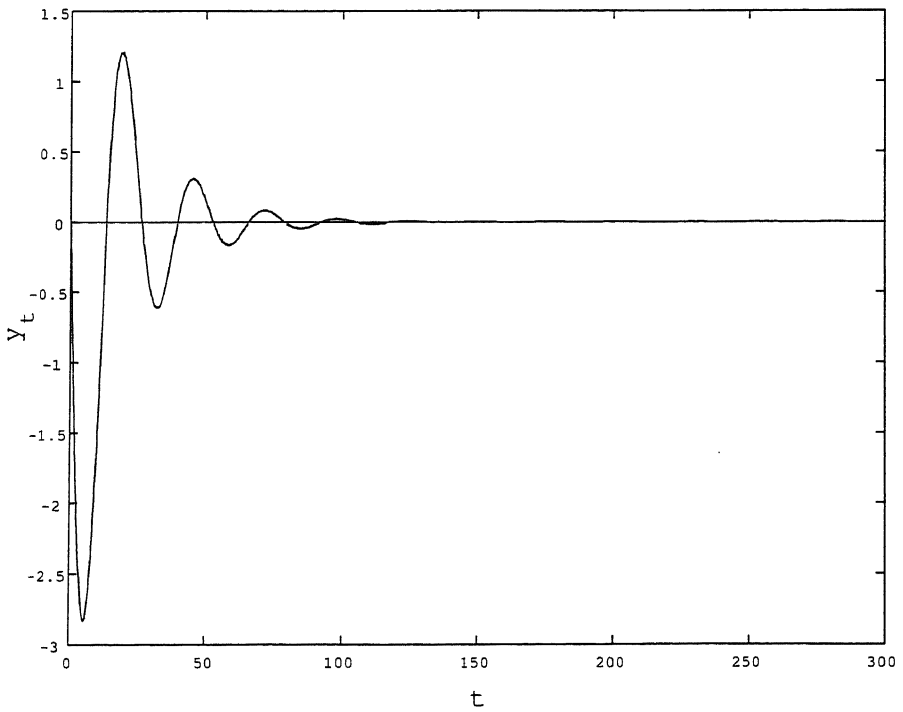

(b) Price orbit

Figure 73: Numerical simulations of the van der Pol equation by the 4th Runge-Kutta method $t = 300$, $x_0 = -0.2$, $y_0 = 0$, $m = 0.8$, $\nu = 0.01$

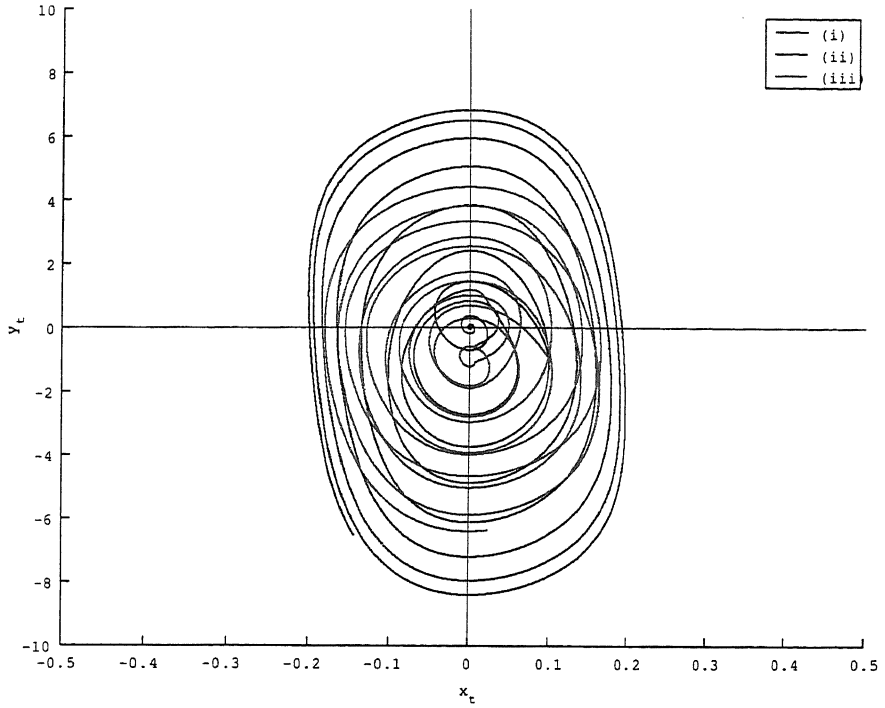

(a) Phase chart and orbit at changing delay

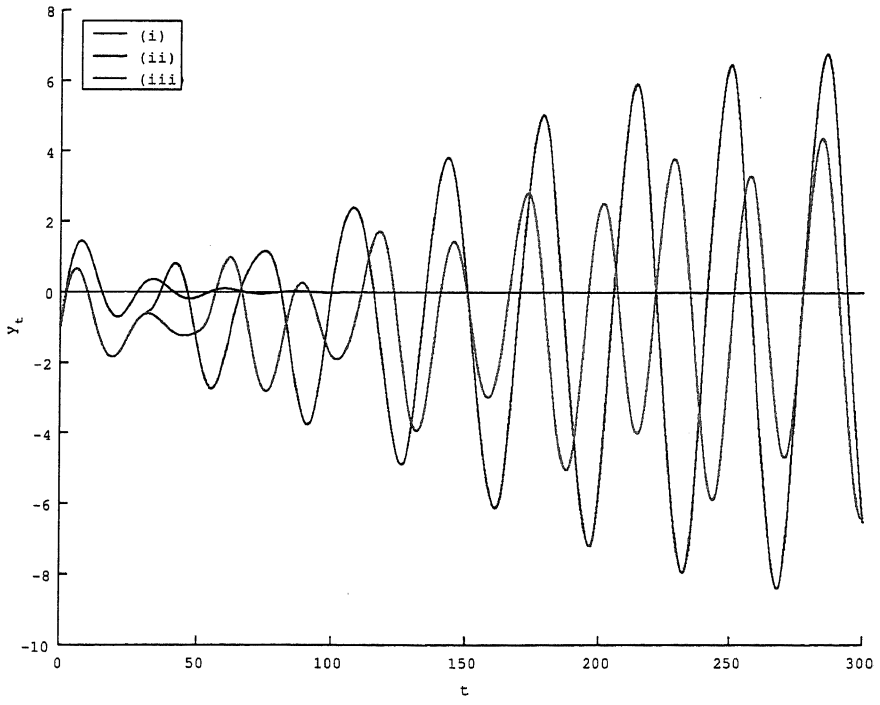

(b) Price orbit at changing delay

Figure 74: Numerical simulations of the delayed van der Pol equation and the van der Pol equation by the 4th Runge-Kutta method $t = 300$, $x_0 = -0.2$, $y_0 = 0$, $m = 0.8$, $\nu = 0.01$, (i):$u = 0$ (no delay) (ii):$u = 30$ (iii):$u = 50$

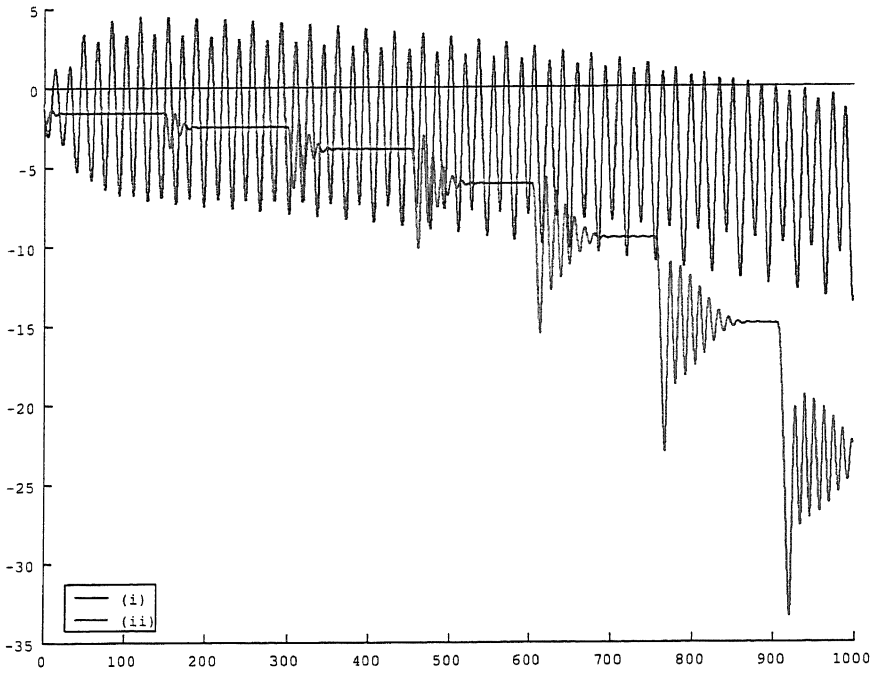

Figure 75: Numerical simulations of the delayed van der Pol equation considering demand cost by the 4th Runge-Kutta method $t = 1000$, $x_0 = -0.1$, $y_0 = -1$, (i):$m = 0.7$, $\nu = 0.02$, $u = 30$, $g = 0.002$, (ii):$m = 0.8$, $\nu = 0.01$, $u = 150$, $g = 0.003$

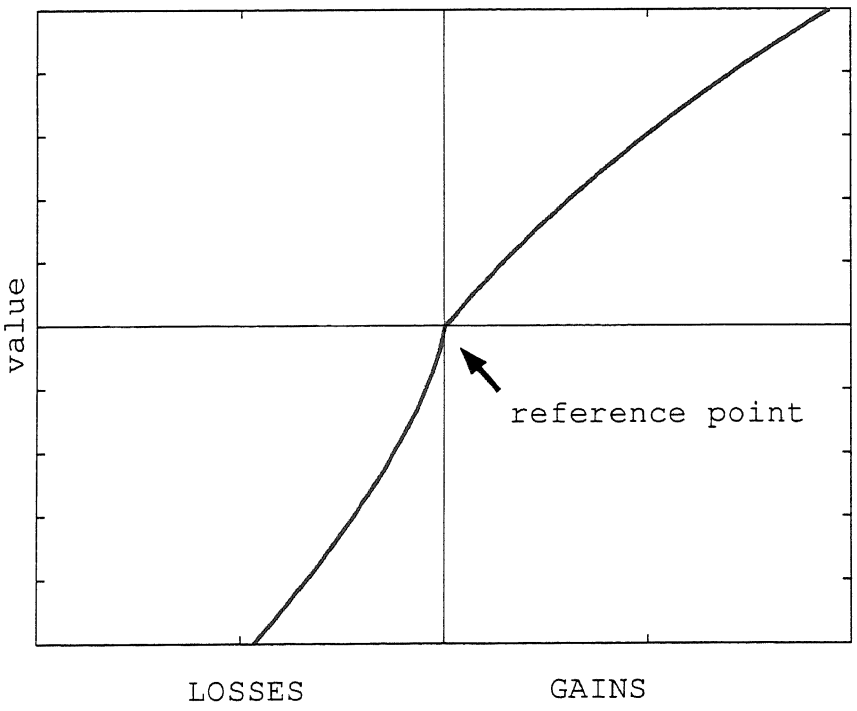

Figure 76: Value Function

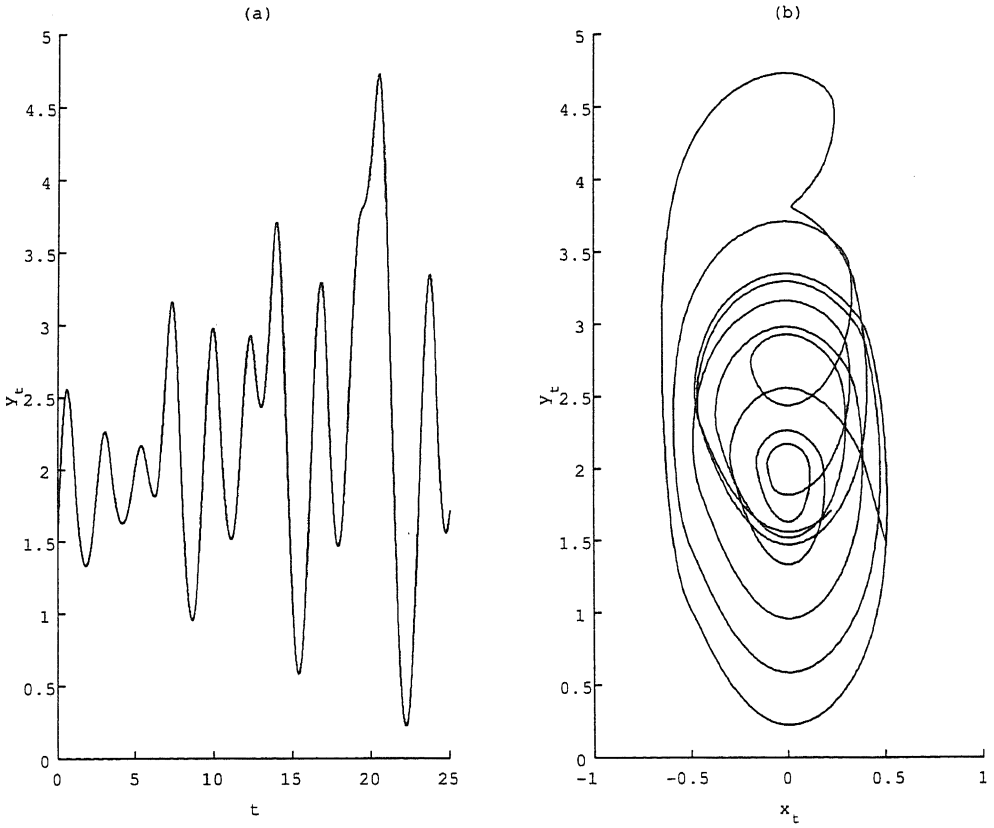

Figure 77: Numerical simulations of the delayed van der Pol equation for nonlinear value function by the 4th Runge-Kutta method. a)Price orbit and b)Phase chart and orbit nonlinear value function: for $y_t \geq 0 := \nu \times log(y_t \times 5 + 1)$, for $y_t < 0 := \nu \times -log(-y_t + 1)$ $t = 25$, $x_0 = 0.5$, $y_0 = 1.5$, $m = 0.95$, $\nu = 0.8$, $u = 6$, $g = 0.05$